INFORMATION TO USERS

This manuscript has been reproduced from the microfilm master. UMI films the text directly from the original or copy submitted. Thus, some thesis and dissertation copies are in typewriter face, while others may be from any type of computer printer.

The quality of this reproduction is dependent upon the quality of the copy submitted. Broken or indistinct print, colored or poor quality illustrations and photographs, print bleedthrough, substandard margins, and improper alignment can adversely affect reproduction.

In the unlikely event that the author did not send UMI a complete manuscript and there are missing pages, these will be noted. Also, if unauthorized copyright material had to be removed, a note will indicate the deletion.

Oversize materials (e.g., maps, drawings, charts) are reproduced by sectioning the original, beginning at the upper left-hand corner and continuing from left to right in equal sections with small overlaps.

ProQuest Information and Learning
300 North Zeeb Road, Ann Arbor, MI 48106-1346 USA
800-521-0600

Université d'Ottawa · University of Ottawa

Université d'Ottawa · University of Ottawa

FACULTÉ DES ÉTUDES SUPÉRIEURES ET POSTDOCTORALES

FACULTY OF GRADUATE AND POSTDOCTORAL STUDIES

André Myles KOLADICH

AUTEUR DE LA THÈSE - AUTHOR OF THESIS

M. Sc. (Earth Sciences)

GRADE - DEGREE

Department of Earth Sciences

FACULTÉ, ÉCOLE, DÉPARTEMENT - FACULTY, SCHOOL, DEPARTMENT

TITRE DE LA THÈSE - TITLE OF THE THESIS

Sedimentology, Sequence Stratigraphy and Reservoir Quality of the Lower Cretaceous Glauconitic Sandstone, Southeastern Alberta

W. Arnott

DIRECTEUR DE LA THÈSE - THESIS SUPERVISOR

CO-DIRECTEUR DE LA THÈSE - THESIS CO-SUPERVISOR

EXAMINATEURS DE LA THÈSE - THESIS EXAMINERS

A. Fowler

D. Leckie

C. Schroder-Adams

J.-M. De Koninck, Ph.D.

LE DOYEN DE LA FACULTÉ DES ÉTUDES SUPÉRIEURES ET POSTDOCTORALES

DEAN OF THE FACULTY OF GRADUATE AND POSTDOCTORAL STUDIES

SEDIMENTOLOGY, SEQUENCE STRATIGRAPHY, AND RESERVOIR QUALITY OF THE LOWER CRETACEOUS GLAUCONITIC SANDSTONE, SOUTHEASTERN ALBERTA

By

André Myles Koladich

A thesis submitted to the School of Graduate Studies and Research in partial fulfillment of the requirements for the degree of M.Sc. in Earth Sciences

OTTAWA-CARLETON GEOSCIENCE CENTRE
AND
UNIVERSITY OF OTTAWA
OTTAWA, CANADA

Abstract

The Lower Cretaceous (Albian) Glauconitic Sandstone is the lowermost stratigraphic unit of the Upper Mannville interval in southern Alberta. It overlies calcareous and fossiliferous strata of the Ostracode Limestone and is unconformably overlain by feldspathic and lithic-rich fluvial sandstone of the undifferentiated Upper Mannville. In the study area, Glauconitic Sandstone strata comprise three facies associations consisting of prograding shoreface to shallow shelf (FA1), upper estuary channel fill (FA2) and tidally-influenced abandoned channel fill/interchannel (FA3) deposits.

The Jenner Upper Mannville E Pool is a 10 km long by 2 km wide north-south trending conventional oil pool located in Townships 19-20, Range 9W4 in southeastern Alberta. Since its discovery in 1963, the pool has produced 7.3 million barrels of 21.1° API oil and 6.7 billion cubic feet of gas from the Glauconitic Sandstone. The original oil in place is 28.6 mmbbl and estimated remaining reserves are of the order of 700 mbbl.

Résumé

Dans le sud de l'Alberta, le Grès Glauconitique du Crétacé inférieur est l'unité stratigraphique la plus profonde du Group Mannville supérieur. Le grès superpose les strates du Calcaire Ostracode. Il est à son tour superposé par des stratifications discordantes du grès fluvial du Mannville supérieur. Dans cette région d'étude, les strates de Grès Glauconitique sont constituées par trois associations des faciès comprenant des dépôts d'une progradation de l'avant-côte à un plateau peu profond (FA1), d'un chenal estuaire intérieur (FA2), et d'un chenal abandonné/interchenal influencé par les marées.

Le « Jenner Upper Mannville E Pool », un réservoir d'huile de 10 km de longueur par 2 km de largeur du nord au sud, est situé dans les canton 19-20, rangées 9W4 au sud-est de l'Alberta. Depuis sa découverte en 1963, le réservoir a produit 7.3 millions de barils d'huile et 6.7 billions de pieds carrés de gaz du Grès Glauconitique. La quantité d'huile présente au moment de la découverte était de 28.6 millions de barils et on estime qu'il en reste approximativement 700 mille barils.

Acknowledgements

Financial and logistical support for this research was provided by ConocoPhillips Canada and is gratefully acknowledged. I want to thank everyone on the Alsask-Jenner team who contributed to the success of this project, particularly Paul Bushell, Phil Handcock, Ron Jackson, Jeff Kiernan, Hans Speelman, and Mike Wilson. Additional funding was supplied by the Canadian Society of Petroleum Geologists (CSPG) Education Trust Fund, American Association of Petroleum Geologists (AAPG) Foundation, Ontario Ministry of Training, Colleges and Universities, and Natural Sciences and Engineering Research Council of Canada (NSERC). Whole core photographs were generously provided by AGAT Laboratories. I sincerely appreciate the invaluable assistance provided by the staff of the Alberta and Energy Utilities Board (AEUB) Core Research Centre during several months of core logging.

Many thanks go to the Department of Earth Sciences for making my graduate years at the University of Ottawa a most memorable experience. It was a pleasure to serve as a graduate student representative and I extend my heartfelt appreciation to all the grads, in particular to the SITE lunch crew: Kristal Dubois, Juraj Farkaš, Paul Ferguson, Guillaume Girouard, and Janet Kingsley. Special thanks go to Hélène DeGouffe and Sylvie Thériault for their tireless administrative assistance and to George Mrazek for his prompt delivery of thin section samples. During my studies, I have had the excellent fortune to meet with many knowledgeable and enthusiastic geologists representing a wide cross-section of sedimentological sub-disciplines. Discussions with these individuals, whether it was in a classroom, at an outcrop, or over a pint, greatly benefited the ideas and concepts presented in this thesis. Thanks to Bart Blakney, Erin Crerar, Don Cummings, Simone Dumas, Cheryl Hanson, Mike Hearn, Mike Johnson, Zishann Kahn, André Lalonde, Suzanne Leclair, John Lerrete, Marianne Molgat, Lilian Navarro, Hazen Russell, Mark Smith, and Art Sweet for their constructive input and advice.

This thesis would not have been completed without the supervision of Bill Arnott. His vast sedimentological knowledge and superb editing skills contributed greatly to the material presented herein. But in addition to, and more importantly than, his technical guidance was his undying enthusiasm and dedication to the teaching and understanding

of geology. Despite his many commitments and responsibilities, Bill always found time to review concepts and discuss any problems with his students. This devotion to science and education was infectious and served as a major source of inspiration towards completing my research. The energy he infused into his teaching and supervision is very much appreciated.

Throughout my university career, I have enjoyed the constant support and encouragement from my family in Alberta and Ontario/Quebec. From taxiing me to airports to helping translate my abstract to providing a place to stay when I was away from home, their generosity has been a tremendous help and for that I am extremely grateful. Finally, I want to thank my mom, dad, and brother for their unconditional love and support. They have always been my biggest sponsors and their contributions to my academic achievements cannot be overstated.

Table of Contents

List of Figures

List of Plates

List of Tables

1. INTRODUCTION

1.1 Introductory Statement

The Glauconitic Sandstone of the Lower Cretaceous Mannville Group has been an important target for oil exploration across southern Alberta for many years (Workman, 1958; Herbaly, 1974). Because of its economic significance, the Glauconitic Sandstone has been the subject of many sedimentological investigations. Previous paleogeographic reconstructions of the Glauconitic Sandstone in southern Alberta include: 1) barrier island, off-shore bar and related environments (Holmes and Rivard, 1976; Tilley and Longstaffe, 1984); and 2) fluvial or deltaic channels and related environments (Hopkins *et al.*, 1982; Farshori, 1983). In other studies, however, estuarine deposits (Banerjee, 1989; Reinson, 1989) and incised valley fills (Hradsky and Griffin, 1984; Karvonen and Pemberton, 1997) have been recognized, suggesting that in parts of southern Alberta the Glauconitic Sandstone accumulated in a marginal-marine setting where fluctuations of relative sea level would have had an important effect on the stratigraphic record. This thesis represents a combined sedimentological and sequence stratigraphic investigation of the Glauconitic Sandstone in order to better understand its depositional history and assess the relationship between stratal architecture and reservoir distribution and performance in an area of southeastern Alberta where closely spaced wells and cores have been drilled in the vicinity of a conventional oil pool.

1.2 Western Canada Sedimentary Basin

The Western Canada Sedimentary Basin is a northeastward-thinning wedge of supracrustal rocks that overlap Precambrian crystalline rocks forming the core of the North American craton (Figure 1.1). The thickness of the supracrustal wedge increases gradually southwestward and over a distance of between 600 and 1200 km thickens from a zero edge along the exposed margin of the Canadian Shield to between 3 and 6 km at the northeastern margin of the foreland fold and thrust belt (Masters, 1984; Wright *et al.*, 1994). Deposition in the Western Canada Sedimentary Basin persisted from the Middle

Figure 1.1: Schematic cross-section of the Western Canada Sedimentary Basin across central Alberta. Maximum sedimentary thickness is 6 km at the western margin of the basin. The sedimentary wedge tapers to the northeast where it pinches out onto Precambrian crystalline rocks of the North American craton. Dev = Devonian, Miss = Mississippian, Penn = Pennsylvanian, Perm = Permian, Trias = Triassic, Jur = Jurassic, T = Tertiary (modified from Masters, 1984).

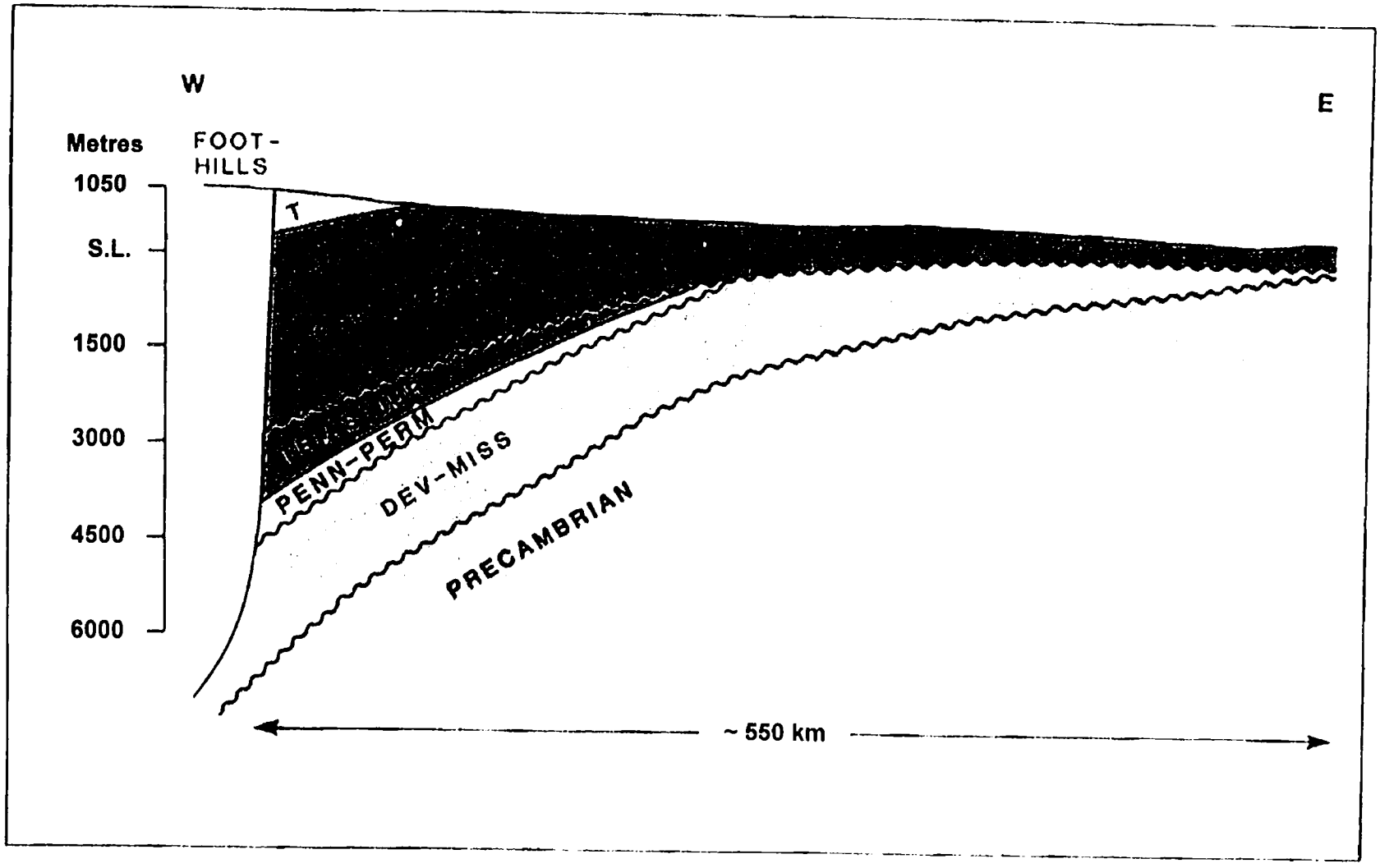
W
E
Metres
1050
S.L.
1500
3000
4500
6000
FOOT-
HILLS
T
PENN-PERM
DEV-MISS
PRECAMBRIAN
~ 550 km

Proterozoic to the Tertiary and the resulting sedimentary succession records changes from a stable passive margin to an actively subsiding foreland basin. Early evolution of the basin involved the development of a passive continental margin terrace wedge that existed from the Early Paleozoic to the Middle Jurassic. This passive continental margin comprised eugeoclinal, miogeoclinal and platformal sediments that may have reached thicknesses in excess of 20 km (Price, 1981). Oblique collision of exotic terranes during the Late Jurassic to Late Cretaceous/Early Tertiary resulted in eastward thrusting of supracrustal rocks and substantial thickening of the western continental margin (Monger *et al.*, 1982). Subsequent lithospheric flexure caused the area adjacent to the fold and thrust belt to subside, forming the asymmetric-shaped Western Canada foreland basin (Cant and Stockmal, 1989; Stockmal *et al.*, 1992). The foreland basin was repeatedly inundated by marine waters from the southern Gulfian and northern Boreal seaways, at times forming a continuous north-south trending body of water, the Western Interior Seaway, which occupied different parts of the foreland basin from the Late Jurassic to the Tertiary.

1.3 Structural Elements

The Western Canada Sedimentary Basin is characterized by several major tectonic and physiographic elements that were present during the evolution of the foreland basin. Major structural elements include: 1) Peace River Arch; 2) Sweetgrass Arch; 3) Punnichy Arch; 4) Williston Basin; and 5) Alberta Syncline (Figure 1.2). Of these structural features, the Sweetgrass Arch most strongly affected marine circulation and sedimentation patterns in southeastern Alberta (Hayes *et al.*, 1994). The Sweetgrass Arch separates the Williston Basin from the Alberta Basin and comprises several subarches, domes and northwest-trending, north-plunging faulted folds (Tovell, 1958; Podruski, 1988). The arch was a positive structural feature during the Jurassic (Podruski, 1988). During the Cretaceous, the arch appears to have been inactive, but subsequently was uplifted during the Laramide orogeny. Eocene plutonic intrusions forming the Sweetgrass Hills in northern Montana occur along the axis of the Sweetgrass Arch and have produced the consistent dip toward the northeast of strata in southeastern Alberta.

Figure 1.2: Location of major tectonic and physiographic elements that affected sedimentation patterns of Lower Cretaceous strata within the Western Canada foreland basin (from Leckie and Smith, 1992).

AREA OF DEVONIAN SALT SOLUTION
PUNNICHY ARCH
WILLISTON BASIN
SALT SOLUTION
SWEET GRASS ARCH
PEACE RIVER ARCH
ALBERTA SYNCLINE
FOOTHILLS
ROCKY MOUNTAIN TRENCH
ROCKY MOUNTAIN
NORTHERN ROCKY MOUNTAIN TRENCH
FRASER FAULT
LIARD SUBBASIN

1.4 Mannville Group Paleogeography and Stratigraphy

Sedimentary rocks of the Western Canada foreland basin have been informally subdivided into several discrete clastic wedges (Cant and Stockmal, 1989; Leckie and Smith, 1992). Each wedge is bounded above and below by unconformities or major lithological changes interpreted to correlate with major tectonic events and/or changes in relative sea level (Stockmal *et al.*, 1992). The Lower Cretaceous Mannville Group (Aptian-Albian) makes up part of the second clastic wedge (Wood and Hopkins, 1989). Prior to Mannville deposition, major northwest-southeast trending alluvial valley systems incised Upper Paleozoic to Jurassic strata (Williams, 1963; Christopher, 1975) on a mature land surface with several hundred metres of erosional relief, forming the sub-Cretaceous unconformity. The sub-Cretaceous unconformity has been dated to have formed between: 1) Berriasian (~ 135 Ma) and Tithonian (~ 140 Ma) in the southern foothills (Leckie *et al.*, 1996); or 2) Kimmeridgian (~ 143 Ma) and Hauterivian (~ 126 Ma) in south-central Saskatchewan (Leckie *et al.*, 1997). The hiatus across the basal unconformity in southern Alberta therefore is of the order of 5-17 My. Mannville Group sediments were deposited above the sub-Cretaceous unconformity and below the post-Ostracode unconformity (Zaitlin *et al.*, 2002).

The Mannville Group of southeastern Alberta records a major third-order transgressive-regressive cycle of the Boreal Sea (Figure 1.3) with superimposed cycles of smaller magnitude (Jackson, 1984). It thins from 460 m in western Alberta to 60 m at the Saskatchewan border (Glaister, 1959) and is unconformably overlain by predominantly marine strata of the Colorado Group (Jackson, 1984). Lower Mannville sediment accumulated in fluvial, marginal-marine and shallow-marine environments as the Boreal Sea transgressed southward during the Aptian (MacLean and Wall, 1981). Strata of the Ostracode Limestone accumulated in diverse shallow water environments including freshwater to brackish water lakes, bays, estuaries, lagoon/tidal-flat complexes and shallow-marine environments during maximum transgression (Finger, 1983; James, 1985; Banerjee and Davies, 1988). In the early Albian, an increase in sediment influx from the Cordillera resulted in northward migration of Upper Mannville coastal and continental environments. Overall regression of the paleoshoreline was punctuated by

Figure 1.3: North American paleogeography during the Lower Albian showing the distribution of the Boreal Sea (modified from Williams and Stelck, 1975).

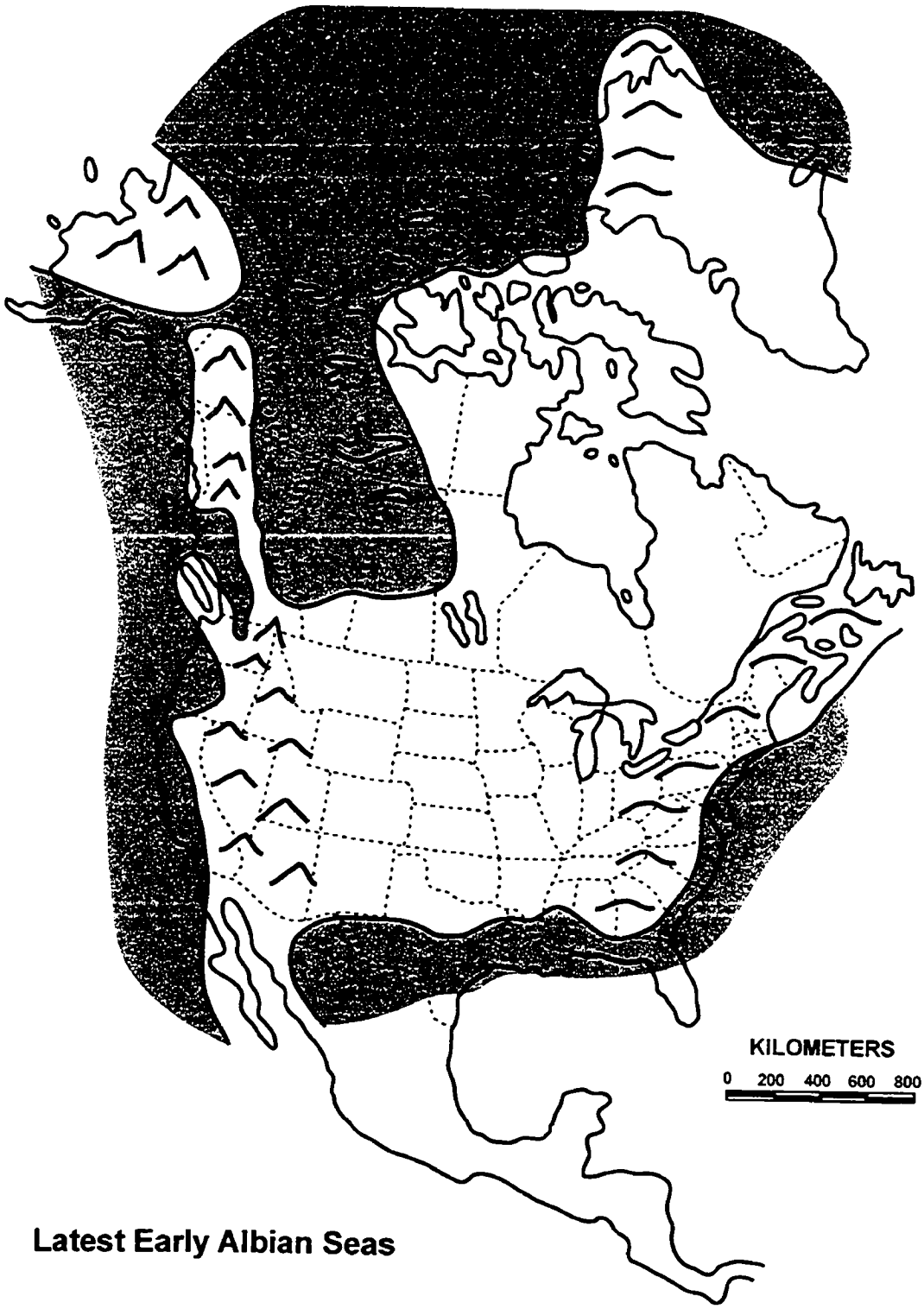

Latest Early Albian Seas

cycles of retreat and advance that at least in part were tectonically controlled (Rosenthal, 1988). Wave-dominated, siliciclastic shoreline complexes in west-central Alberta separated open-marine environments to the northwest from coastal plain environments to the southeast (Chiang, 1984; Jackson, 1984; Strobl, 1988). The broad coastal plain consisted of a mosaic of fluvial, deltaic and marginal-marine environments (Hopkins *et al.*, 1982; Farshori, 1983; Hradsky and Griffin, 1984; James, 1985). Coastal plain channel systems generally flowed toward the northwest, although local variations, including southward flow (see Chapter 4), resulted from local embayments and ridges of northwest-southeast trending Paleozoic highlands along the Boreal Sea shoreline (Figure 1.4).

Glaister (1959, p. 611) divided the Mannville Group into lower and upper units and placed the contact between them at a marine flooding surface that marks the top of the calcareous and fossiliferous Ostracode Limestone. In southern Alberta the Lower Mannville, therefore, includes the informal "Basal Quartz" sandstone (Ellerslie Formation and equivalents) and the Ostracode Limestone. The Upper Mannville comprises the Glauconitic Sandstone unconformably overlain by a thick succession of undifferentiated strata (Figure 1.5). The unconformity between the Glauconitic Sandstone and undifferentiated Upper Mannville strata is marked by a change of sandstone composition from quartzarenite of the Glauconitic Sandstone to lithic arkose and sublitharenite in the undifferentiated Upper Mannville. This unconformity indicates a change in provenance from cratonic to Cordilleran, respectively, and most probably formed in response to regional tectonism (Wood, 1994).

1.5 Glauconitic Sandstone

The early Albian Glauconitic Sandstone, so named due to the presence of glauconite in marine sandstones of central Alberta, was assigned by Glaister (1959) to the lowermost portion of the Upper Mannville. Subsequently, the term "Glauconitic" or "Glauconite" was extended to include correlative sandstones and associated strata in southern Alberta, even though glauconite is rare to absent within these predominantly freshwater to brackish water deposits. The term "Glauconitic Sandstone" conforms to the existing

Figure 1.4: Paleogeographic reconstruction of the Upper Mannville in southern Alberta during deposition of the Glauconitic Sandstone. Note the location of correlative shoreface complexes, northwest-southeast trending Paleozoic highlands, and the study area. Toothed line indicates eastern limit of Cordilleran deformed belt (modified from Sherwin, 1996).

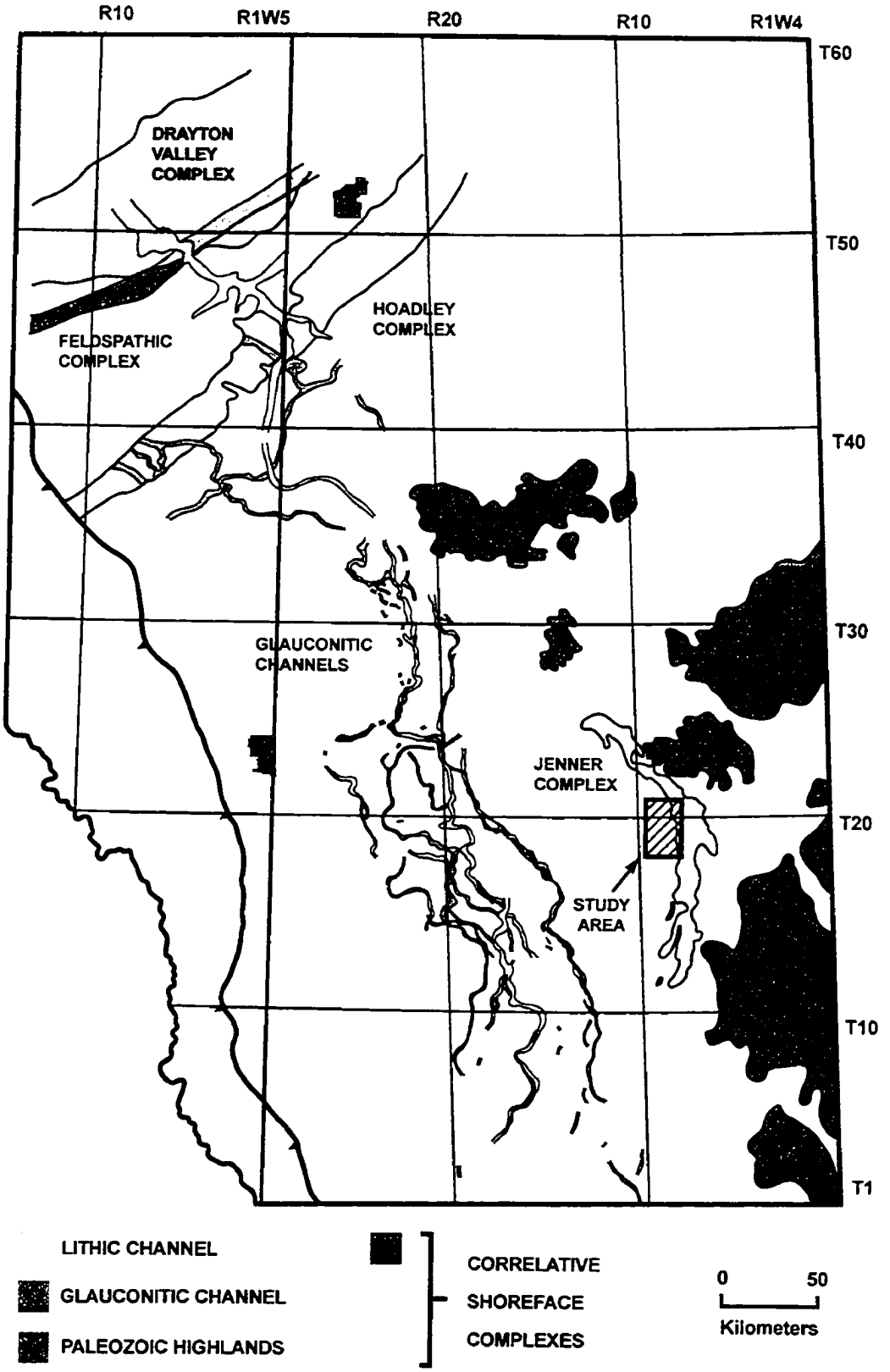
R10
R1W5
R20
R10
R1W4
T60
T50
T40
T30
T20
T10
T1
DRAYTON VALLEY COMPLEX
HOADLEY COMPLEX
FELDSPATHIC COMPLEX
GLAUCONITIC CHANNELS
JENNER COMPLEX
STUDY AREA
LITHIC CHANNEL
GLAUCONITIC CHANNEL
PALEOZOIC HIGHLANDS
CORRELATIVE SHOREFACE COMPLEXES
0
50
Kilometers

Figure 1.5: Stratigraphic nomenclature for the Lower Cretaceous Mannville Group in southeastern Alberta. Asterisk highlights early Albian Glauconitic Sandstone and associated Glauconitic and Lithic channels (modified from Sherwin, 1996).

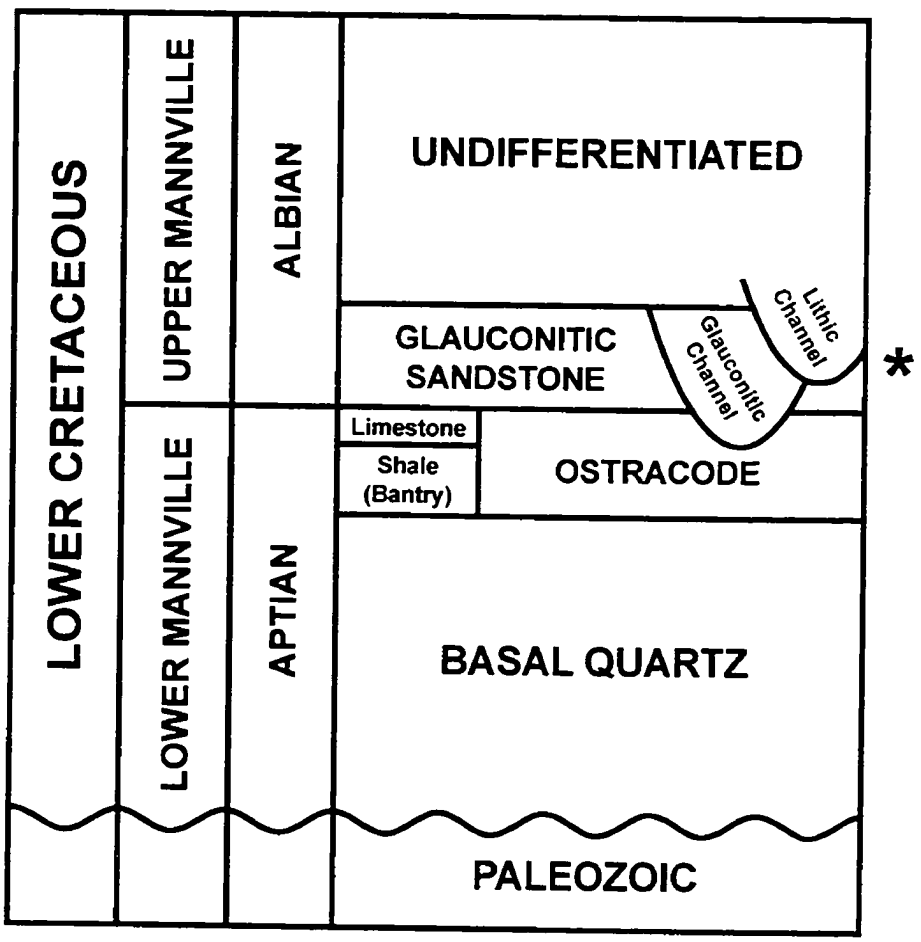
LOWER CRETACEOUS
UPPER MANNVILLE
LOWER MANNVILLE
ALBIAN
APTIAN
UNDIFFERENTIATED
GLAUCONITIC SANDSTONE
Lithic Channel
Glauconitic Channel
*
Limestone
Shale (Bantry)
OSTRACODE
BASAL QUARTZ
PALEOZOIC

North American Stratigraphic Code and is formally recognized in the Lexicon of Canadian Stratigraphy (1990). For these reasons, the name "Glauconitic Sandstone" is used in this thesis. Following Glaister (1959), the base of the Glauconitic Sandstone is defined here to be the top of the Ostracode Limestone, an easily recognized and readily correlatable marker horizon throughout southeastern Alberta. The top of the Glauconitic Sandstone is placed at the base of the first feldspathic to lithic-rich fluvial sandstone of the undifferentiated Upper Mannville (Figure 1.5). The Glauconitic Sandstone correlates with the Bluesky Formation in northwestern Alberta, the Wabiskaw Member of the Clearwater Formation in northeastern Alberta, and the upper part of the Cummings Sandstone in east-central Alberta (Rudkin, 1964). Published regional studies indicate that the Glauconitic Sandstone is predominantly marine in the Edmonton area and becomes progressively more continental towards the south, with the abundance of glauconite decreasing east of the 5th meridian and south of Edmonton (Glaister, 1959).

Much has been published in the geological literature on the Glauconitic Sandstone. The Glauconitic sand series was first described by Layer *et al.* (1949) who divided Lower Cretaceous Mannville sandstone, shale and coal of the Edmonton-Stettler area into 3 zones: 1) the Coaly series; 2) the Glauconitic sand series; and 3) the Quartz sand series. Workman (1958) was the first to point out that the "Glauconitic sandstone" represented a widespread mappable unit in Alberta. Subsequent discovery of oil and gas in the Glauconitic Sandstone led to a rapid increase in the number of sedimentological and stratigraphic studies in order to maximize production efficiency of existing pools and aid in the exploration for new pools. In the Jenner-Suffield area of southeastern Alberta, Herbaly (1974) interpreted thick reservoir sandstones (up to 45 m thick) of the Glauconitic Sandstone as a dune deposit cut by silt-filled channels. Alternatively, Holmes and Rivard (1976) and Tilley and Longstaffe (1984) interpreted the Glauconitic Sandstone in the Jenner-Suffield area as a marine barrier-island complex that represented the termination of marine deposition in the Upper Mannville section. Glauconitic paleovalleys in the southern Alberta plains have been interpreted as meandering river channels (Hopkins *et al.*, 1982; Farshori, 1983), estuarine channels (Wood and Hopkins, 1989), alluvial valley fills (Hradsky and Griffin, 1984) and estuarine valley fills (James, 1985; Wood, 1994; Karvonen and Pemberton, 1997). In addition, Glauconitic sandstone

channel-fills have been reported from many areas of the province (Farshori, 1983; James, 1985; Strobl; 1988). For example, Rosenthal (1988) described the correlative quartzose and lithic shoreface successions and associated channels in the Hoadley-Drayton Valley area. Later, Wood and Hopkins (1992) mapped and described a series of quartzose "Glauconitic" channels and a series of slightly younger feldspathic or "lithic" channels in the Little Bow-Turin area. Later still, Sherwin (1996) illustrated the regional distribution and continuity of the main Lithic and Glauconitic channel systems in southern Alberta and linked them northward with correlative shoreface complexes.

1.6 Study Area and Methodology

The study area is located in southeastern Alberta, south of the northwest-southeast trending Jenner shoreface complex and comprises the area between portions of townships 19-21 and from ranges 8-10W4 (Figure 1.6). In this area, over 1400 wells penetrate Lower Cretaceous strata, due mostly to local concentrations of closely-spaced horizontal wells along the Jenner shoreface trend. Of these, 264 were selected for stratigraphic correlation in this study. In addition, 26 cores (420 m total; 14 cores from E pool) were examined and described in bed-by-bed detail (Appendix 1), and used to calibrate geophysical well-log profiles. Additional whole core photographs provided by AGAT Laboratories were studied to help refine stratigraphic correlations. Also, 29 samples were selected for petrographic examination (Appendix 2) and 20 additional samples were processed and analyzed for palynology by Dr. A.R. Sweet of the Geological Survey of Canada (Appendix 3).

1.7 Objectives

The principal objective of this thesis was to develop a detailed depositional model for the Glauconitic Sandstone in the study area. Specifically, the objectives were:

1) Provide a comprehensive sedimentological and stratigraphic model of the Glauconitic Sandstone in the Jenner Upper Mannville E Pool.

Figure 1.6: Location map of the study area in southeastern Alberta and distribution of well and core control.

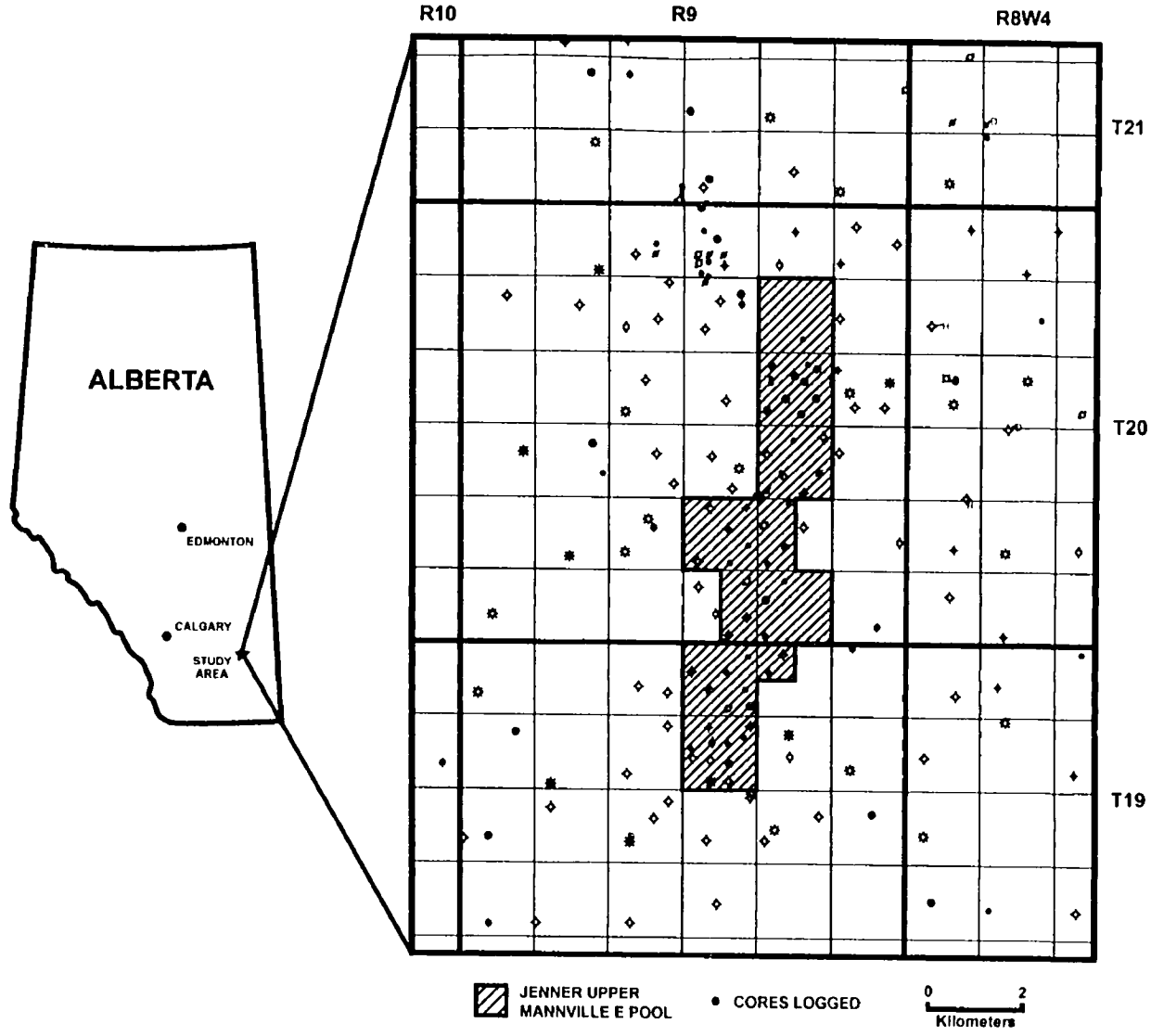
R10
R9
R8W4
T21
T20
T19
ALBERTA
EDMONTON
CALGARY
STUDY AREA
JENNER UPPER MANNVILLE E POOL
CORES LOGGED
0
2
Kilometers

2) Determine the control of primary and authigenic attributes on reservoir quality (porosity and permeability), distribution, and production.

2. SEDIMENTARY FACIES

2.1 Introduction

The modern geological usage of the term facies was introduced by Gressly (1838), who used it to describe marked changes in lithology and paleontology of a stratigraphic unit. A facies is defined as the sum total of all primary characteristics of a sedimentary unit detectable in the field (de Raaf *et al.*, 1965). However, the term facies has been used in many different senses: 1) in a strictly observational sense, e.g. 'sandstone facies'; 2) in a genetic sense, e.g. 'turbidite facies'; 3) in an environmental sense, e.g. 'fluvial facies' or 'shallow marine facies'; and 4) as a tectofacies, e.g. 'post-orogenic facies' or 'molasse facies' (Reading, 1986). Succinct discussions outlining the various definitions of the facies concept have been given by Teichert (1958), Krumbein and Sloss (1963), Middleton (1978) and Walker (1992). A facies is a body of rock with specified characteristics: it is defined on the basis of colour, bedding, composition, texture, fossils and sedimentary structures. A facies is a result of deposition in a given environment, and thus possesses characteristics indicative of that specific environment. It is understood that facies are units that will ultimately be given an environmental interpretation: but the facies definition itself is quite objective and based on the total field aspect of the rocks themselves. Facies designations such as 'continental facies' and 'delta facies' arise on the basis of assumed depositional environments. Reineck and Singh (1973) cautioned that a stratigraphic unit may be assigned an environment only after studying its various characteristics and describing it as a facies. This sentiment was echoed by Middleton (1978) who noted that "the key to the interpretation of facies is to combine observations made on their spatial relations and internal characteristics (lithology and sedimentary structures) with comparative information from other well-studied stratigraphic units, and particularly from studies of modern sedimentary environments". In this study, strata of the Glauconitic Sandstone have been divided into seven sedimentary facies (Table 2.1).

Table 2.1: Summary of description and interpretation of the seven sedimentary facies and three facies associations of the Glauconitic Sandstone identified in the study area. Ar: *Arenicolites*, As: *Asterosoma*, Be: *Bergaueria*, Ch: *Chondrites*, Co: *Conichnus*, Cy: *Cylindrichnus*, Di: *Diplocraterion*, Op: *Ophiomorpha*, Pa: *Palaeophycus*, Pl: *Planolites*, Rh: *Rhizocorallium*, Sc: *Scolicia*, Sk: *Skolithos*, Tb: *Terebellina*, Te: *Teichichnus*, Th: *Thalassinoides*, Zo: *Zoophycos*.

Facies	Lithology	Sedimentary Structures	Trace Fossils	Interpretation	Facies Association
F1	interstratified fine siltstone and silty mudstone	graded bedding, planar- to wave ripple cross-lamination, soft-sediment deformation	low to moderate, locally intense; Ar, As, Be, Ch, Co, Cy, Di, Op, Pa, Pl, Rh, Sc, Sk, Tb, Te, Th, Zo	storm-influenced transitional offshore	FA1
F2	coarse siltstone to very-fine grained sandstone	hummocky cross-stratification, normal grading, wave ripple to pinstripe lamination, synaeresis cracks	low; Ar, As, Ch, Di, Op, Pl, Sk, Te, escape traces	storm-dominated lower shoreface	
F3	fine- to medium-grained sandstone	dune cross-stratification, sharp-based granular to pebbly interbeds, upward-fining silty mudstone interbeds	low; Op, Pa, Pl, Sk, Th	migration of subaqueous dunes	FA2
F4	very fine- to medium-grained sandstone and muddy siltstone	massive to contorted, faint horizontal to low-angle cross-lamination, soft-sediment deformation	moderate; Pl, Sk, Te, Th	channel bank collapse	
F5	chert pebble conglomerate	matrix- and clast-supported, dune cross-stratification, graded bedding	absent	migration of subaqueous dunes in heterogeneous sediment	
F6	very fine- to fine-grained sandstone, sandy siltstone and mudstone	flaser to lenticular bedding, graded bedding, wave ripple lamination, horizontal stratification, soft-sediment deformation	low to moderate, locally high; As, Ch, Cy, Pl, Sk, Te, Th, Zo, escape traces	tidally-influenced abandoned channel-fill	FA3
F7	carbonaceous mudstone and coal	blocky to fissile, graded bedding, rooted sandstone interbeds, slickensides, local small-scale cross-stratification	low, locally high; As, Ch, Pl, Th	floodbasin	

2.2 Facies 1: Interstratified Fine Siltstone and Silty Mudstone

Description

Facies 1 (F1) consists of interstratified fine siltstone and silty mudstone with rare silty sandstone interbeds. F1 ranges in thickness from 10 cm to 5.8 m and averages 1.1 m. The base of F1 strata is commonly sharp and inclined at angles between 5-10° (Plate 2.1a); rarely, basal contacts are obscured or completely obliterated by bioturbation. Relief on lower bounding surfaces is typically 1-2 cm. Interstratified layers of fine siltstone and silty mudstone range in thickness from millimetre-scale to 25 cm and average 1-2 cm (Plate 2.1b). Fine siltstone is characterized by low-angle, small-scale cross-stratification and horizontal stratification. Siltstone layers commonly grade to massive or thinly horizontal-laminated silty mudstone (Plate 2.2a). Soft-sediment deformation structures are common and include load structures, convolute lamination, slump structures and microfaults (Plate 2.2b). Rare gutter casts and scour-fills up to 10 cm wide and 3 cm deep are present at the base of interstratified fine siltstone and silty mudstone beds. Silty sandstone interbeds are 9-60 cm thick and are characterized by moderately sorted siltstone and very fine- to fine-grained sandstone. Carbonaceous material and chert granules are locally dispersed within silty sandstone. Silty sandstone interbeds are variably oil-stained. Bed sets of F1 are commonly arranged in stacked successions of sharp-based lenticular beds gradationally overlain by wavy-bedded strata. Also, grain size and bed thickness gradationally increase upward in sequences that range from 50-60 cm thick.

The trace fossil assemblage of F1 consists of three distinctive ichnocoenoses. The first is a low- to moderate-diversity, moderate-abundance suite of primarily horizontal structures. Ichnotaxonomic diversity is dominated by diminutive forms of *Asterosoma*, *Planolites*, *Chondrites* and *Teichichnus* with lower abundances of slightly more robust *Rhizocorallium*, *Palaeophycus*, *Thalassinoides*, *Terebellina* and *Zoophycos* (Plate 2.3a). Locally, primary stratification of silty mudstone beds 5-35 cm thick has been completely destroyed by a monospecific assemblage of *Asterosoma* burrows (Plate 2.3b). These intensely bioturbated fine-grained zones commonly occur at the top of upward-fining

Plate 2.1: Interstratified Fine Siltstone and Silty Mudstone (F1)

a) Sharp, curvilinear contact (arrow) between low-angle, medium-scale cross-stratified coarse siltstone to very fine-grained sandstone (F2) and overlying thoroughly bioturbated silty mudstone (F1). Well 02/14-11-020-09W4/0, 968.4 m.

b) Interstratified low-angle, small-scale cross-stratified fine siltstone and massive to faintly horizontal-laminated silty mudstone. Well 02/06-11-020-09W4/0, 966.6 m.

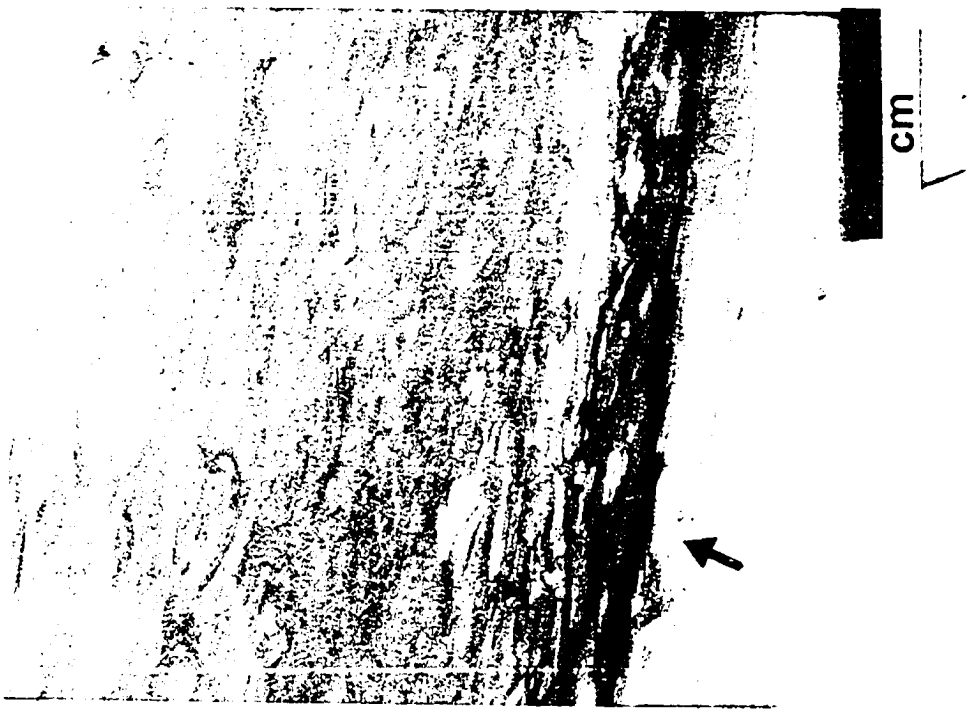

a)

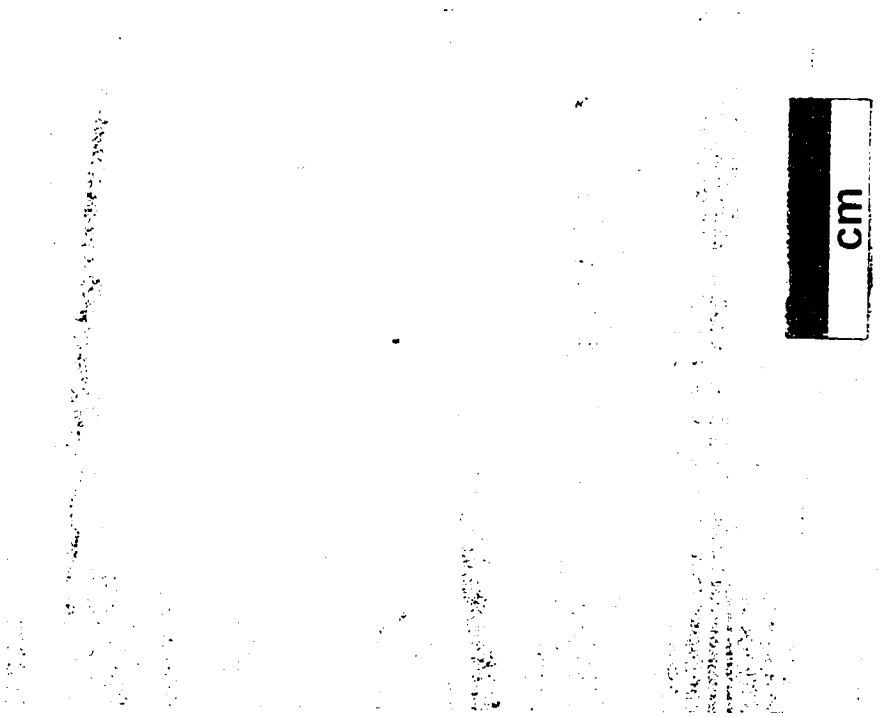

b)

Plate 2.2: Interstratified Fine Siltstone and Silty Mudstone (F1)

a) Normally graded bed of horizontal-laminated siltstone passing upwards into massive mudstone. Well 02/16-23-020-09W4/0, 951.5 m.

b) Overturned convolute lamination within interstratified fine siltstone and silty mudstone. Note the absence of bioturbation. Well 02/10-23-020-09W4/0, 954.9 m.

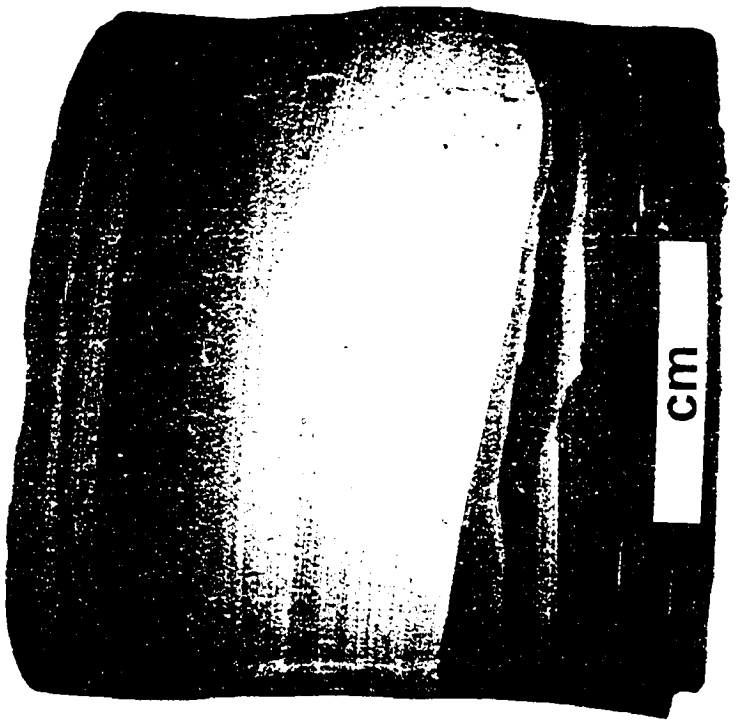

a)

b)

Plate 2.3: Interstratified Fine Siltstone and Silty Mudstone (F1)

a) *Planolites* (Pl), *Thalassinoides* (Th) and *Zoophycos* (Zo) trace fossils in low-angle, wavy-laminated interstratified fine siltstone to silty mudstone. Some of the larger structures are *Chondrites* (Ch) re-burrowed. Well 00/06-34-019-09W4/0, 3289.5'.

b) 6 cm thick silty mudstone bed burrowed by an assemblage dominated by *Asterosoma*. Trace fossil suites dominated by a single ichnogenus are characteristic of brackish water conditions. The top and base of the bioturbated interval abut sharply with cross-laminated siltstone beds; this configuration defines a 'laminated-to-burrowed' bedding fabric and is indicative of rhythmic storm deposition. Well 00/06-23-020-09W4/0, 963.8 m.

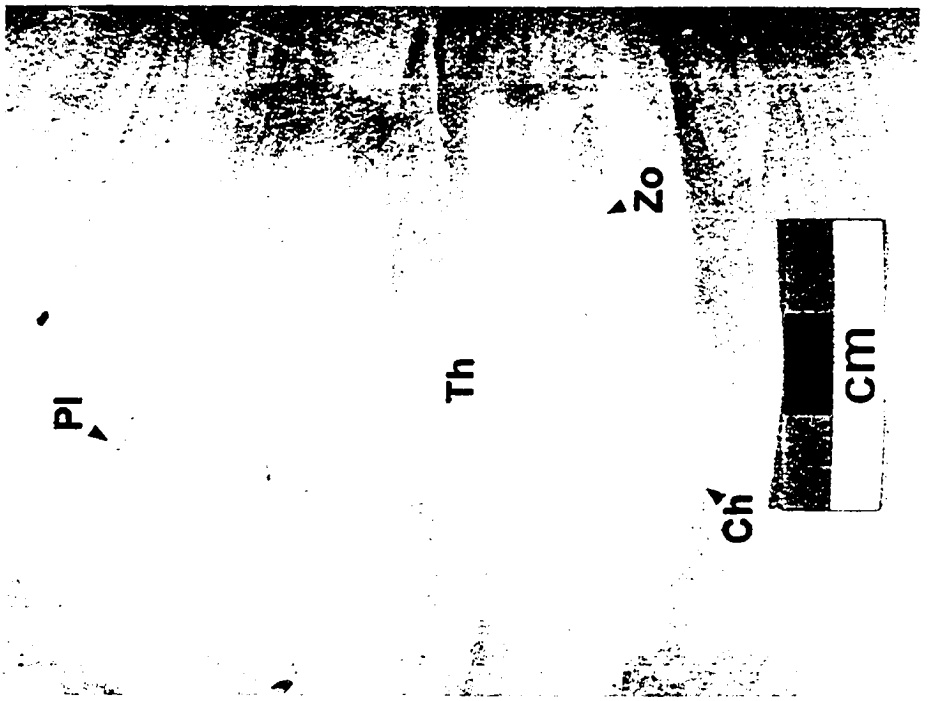

a)

b)

planar- to cross-laminated fine siltstone to silty mudstone interbeds. This ichnocoenosis dominates the overall trace fossil assemblage. The second ichnocoenosis consists of a subordinate moderate-diversity, low-abundance suite characterized by vertical and inclined structures. Trace fossils include *Skolithos*, *Diplocraterion*, *Arenicolites*, *Teichichnus*, *Cylindrichnus*, *Ophiomorpha*, *Palaeophycus* and *Conichnus* (Plate 2.4). Trace fossils of this second ichnocoenosis occur mostly in planar- to low-angle cross-laminated siltstone beds. The third ichnocoenosis is a low-diversity, low- to moderate-abundance suite of robust vertical, inclined and branched horizontal structures. Ichnogenera include *Skolithos*, *Thalassinoides*, *Scolicia*, *Teichichnus*, *Bergaueria* and escape traces (Plate 2.5). Vertical structures are commonly unlined or concentrically laminated thin shafts that are up to 10 cm long. Horizontal to gently inclined burrows are typically unlined with sharply defined walls and a meniscate fill. Trace fossils of this suite commonly occur within interstratified mudstone, fine to coarse siltstone and silty sandstone at the top of F1 successions.

Interpretation

Upward thickening and coarsening strata of F1 are interpreted to represent deposition in the transitional offshore of a prograding storm-influenced shoreline. Sharp-based interstratified cross-laminated fine siltstone overlain gradationally by massive or thinly horizontal-laminated silty mudstone is interpreted to represent the tractive and suspension sediment-transporting processes of storm and fairweather conditions, respectively (Reineck and Singh, 1972; Dott, 1981). Silty mudstone interbeds of F1 are commonly thoroughly bioturbated; sharp-based planar- to low-angle cross-stratified fine siltstone gradationally overlain by burrowed silty mudstone produces 'laminated-to-burrowed' bedding and is indicative of rhythmic storm deposition (Bourgeois, 1980; Figure 2.1). Low-angle, small-scale cross-stratified fine siltstone beds are interpreted as wave ripple cross-stratification. Differences in sedimentological characteristics between cross-stratified event beds of F1 and F2 (see next) imply differences in bathymetry, storm frequency, duration and magnitude (Clifton *et al.*, 1971; Duke, 1985). The fine grain-size, small-scale structures, low sand/mud ratio and abundance of bioturbation of F1

Plate 2.4: Interstratified Fine Siltstone and Silty Mudstone (F1)

a) Bioturbated interstratified fine siltstone and silty mudstone. Mudstone laminae contain a comparatively denser population of *Planolites* (Pl) and *Asterosoma* (As) trace fossils; vertical to inclined *Skolithos* (Sk) and *Cylindrichnus* (Cy) burrows appear to originate within mudstone laminae and penetrate downwards into horizontal- to cross-laminated siltstone layers. This may reflect different behavioral strategies of a single genus responding to variable substrate and energy conditions over time. Well 02/06-11-020-09W4/0, 968.1 m.

b) *Skolithos* (Sk) and *Conichnus* (Co) trace fossils within horizontal- to cross-laminated fine siltstone to silty mudstone. Inclined structures of suspension-feeders have locally cross-cut a thin mudstone bed containing a resident *Cruziana* assemblage consisting of *Planolites* and *Chondrites* traces. Well 00/16-08-021-09W4/0, 946.5 m.

a)

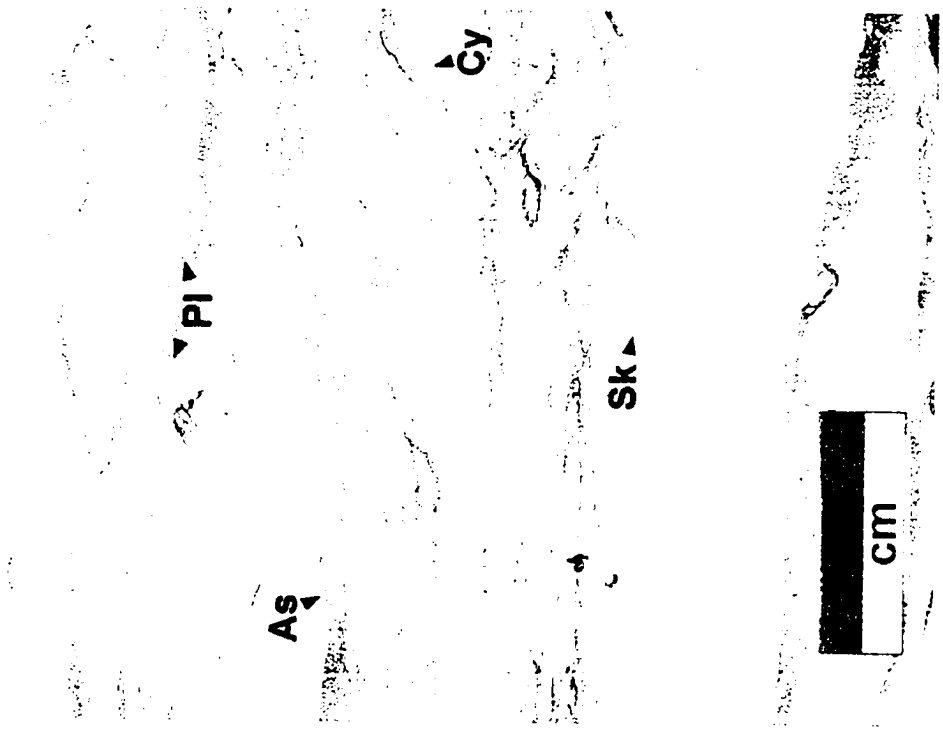

b)

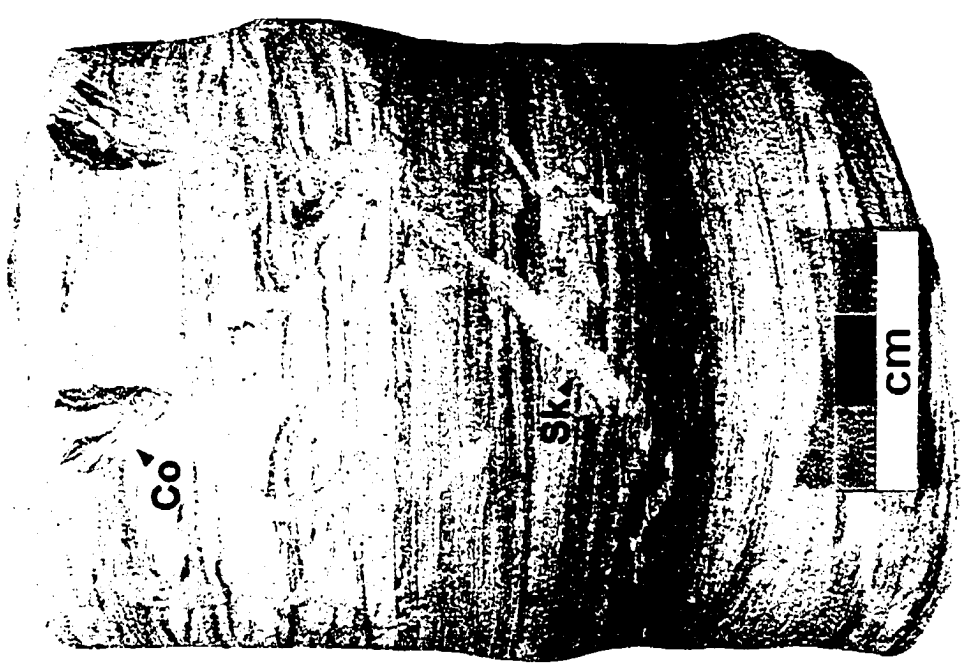

Plate 2.5: Interstratified Fine Siltstone and Silty Mudstone (F1)

a) Unlined, sharp-walled *Skolithos* (Sk) and *Thalassinoides* (Th) trace fossils in sandy mudstone interbed. Burrows are passively filled with fine-grained sandstone from overlying strata and represent the *Glossifungites* ichnofacies, a substrate-controlled ichnocoenosis. Well 00/05-10-021-09W4/0, 957.2 m.

b) Robust *Bergaueria* (Be), the resting trace of a sea anemone, passively filled with fine-grained sandstone from overlying strata. Well 00/06-23-020-09W4/0, 959.9 m.

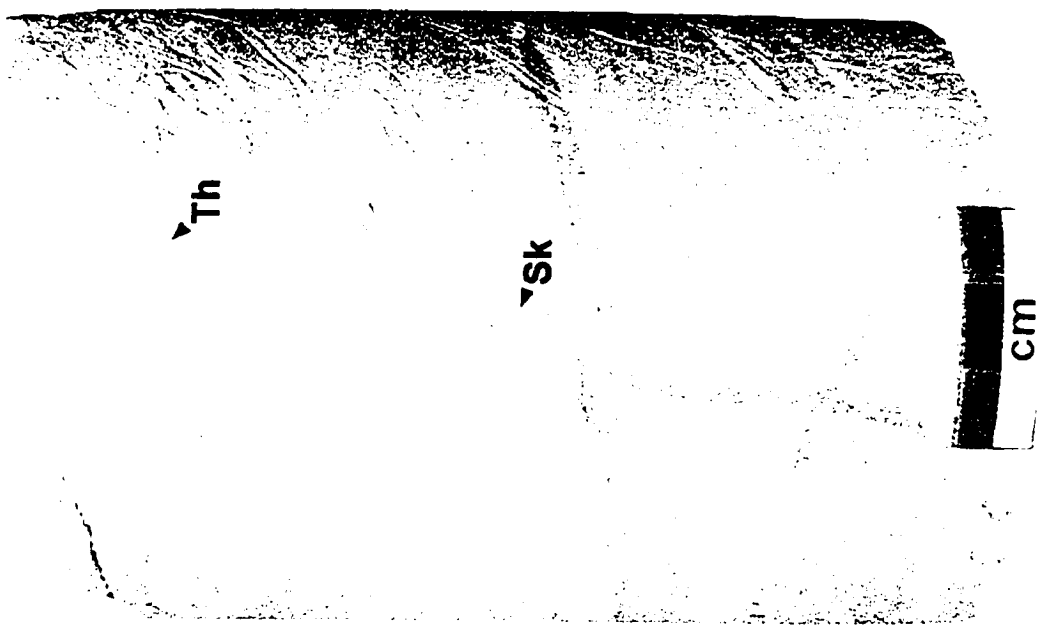

a)

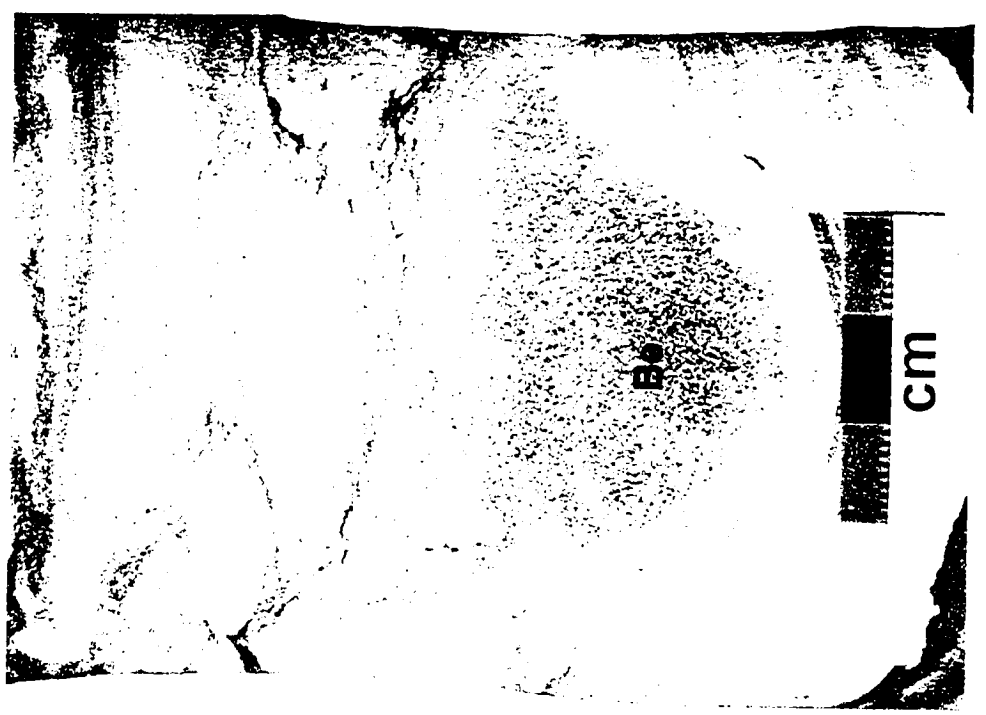

b)

Figure 2.1: Progressive colonization of storm-event beds. Following emplacement (1), the event bed is initially colonized under post-storm conditions (2). This suite is dominated by the dwelling structures of deeply tiered opportunistic organisms. The return of fairweather conditions marks the re-establishment of the resident equilibrium community (3). Subsequent storms may result in erosional amalgamation of event beds and preservation of both the opportunistic storm and fairweather suites, producing 'laminated-to-burrowed' bedding (4) (modified from Dott, 1983).

1) Storm Event

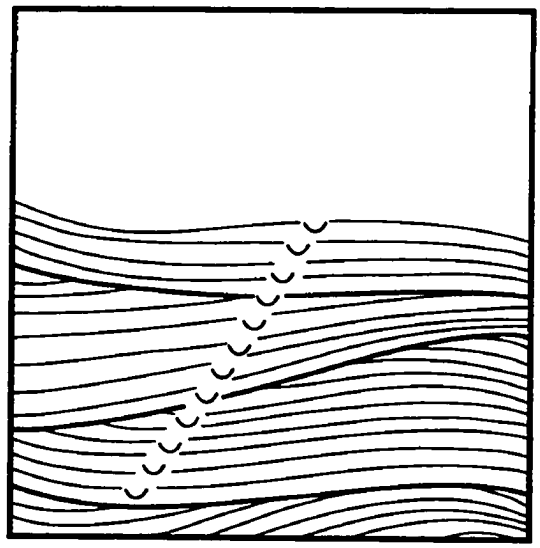

2) Post-Storm Colonization

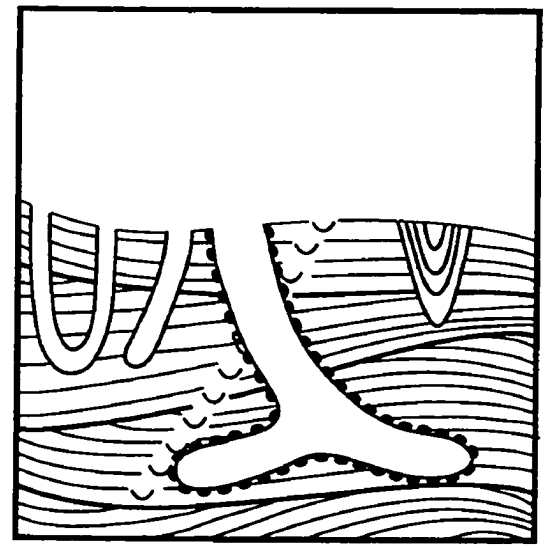

3) Fairweather Colonization

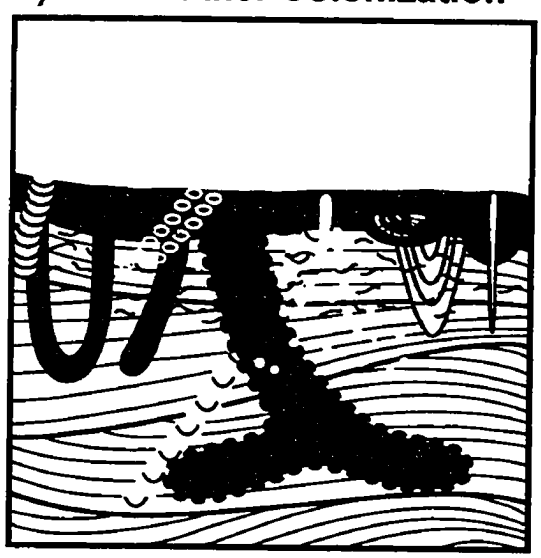

4) Storm Event

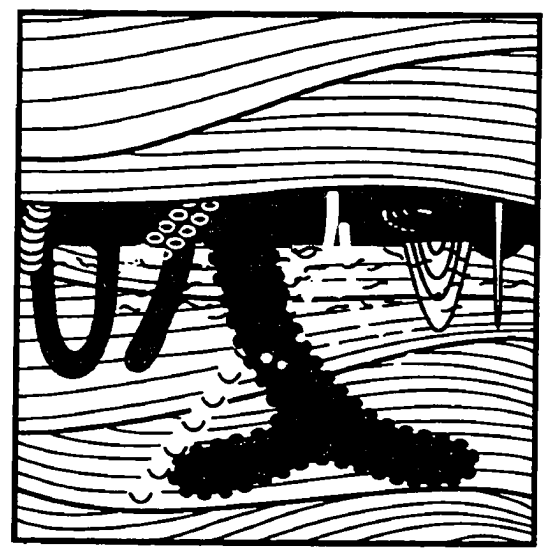

imply deeper-water conditions; F1 is interpreted to occur slightly basinward of F2 from a distal lower shoreface to a transitional offshore marginal-marine environment (Figure 2.2). Low sand/mud ratios and lenticular- and wavy-bedded strata of F1 resemble transitional offshore storm sands observed in the tide- and storm-influenced German Bight, SE North Sea (Aigner and Reineck, 1982). Furthermore, Allen (1982) theoretically positioned storm layers with similar sedimentological characteristics to have been deposited along a shallow marine sandy shoreline passing gradationally onto a muddy shelf as offshore thinning and fining sand and silt sheets in response to reduced bottom current velocities and sediment flux.

F1 contains a low- to moderate-diversity, moderate-abundance mixed *Skolithos-Cruziana* trace fossil assemblage dominated by horizontal structures of the *Cruziana* ichnofacies. The predominance of horizontal, deposit-feeding burrows suggests a transitional offshore environment located basinward of the lower shoreface (Frey *et al.*, 1990; Figure 2.2). Periodic generation of elements of the *Skolithos* ichnofacies in cross-laminated siltstone event beds represents the invasion and proliferation of a community of opportunistic organisms responding to a temporary environmental change (Pemberton *et al.*, 1992b). Intensely reworked silty mudstone beds characterized by monospecific *Asterosoma* assemblages represent a return of the resident ichnocoenosis (i.e. elements of the *Cruziana* ichnofacies). Trace fossil diversity gradually increases upwards from the tops of storm-generated cross-laminated siltstone beds, indicating the re-establishment of fairweather, open marine conditions.

A second trace fossil assemblage recognized within F1 consists of robust vertical, inclined and branched horizontal structures and is interpreted as elements of the *Glossifungites* ichnofacies, a substrate-controlled ichnocoenosis (Ekdale *et al.*, 1984). The *Glossifungites* ichnofacies represents the colonization of a firm muddy substrate during a hiatus between the erosional exhumation of an initially deposited softground facies and deposition of the overlying unit (Pemberton and Frey, 1985; Figure 2.3). The post-depositional origin of the *Glossifungites* suite in F1 is demonstrated by the cross-cutting relationships with the previous softground *Skolithos-Cruziana* assemblage. Sharp-walled, unlined and passively filled firmground trace fossils reflect the stable, cohesive nature of the substrate at the time of colonization and burrow excavation. This

Figure 2.2: Idealized model for ichnofacies distribution in a nearshore to offshore shallow-marine transect. For ichnofacies, dashed intervals reflect a presence, whereas solid lines indicate a dominance. Deposit-feeding strategies of the *Cruziana* ichnofacies are characteristic of distal lower shoreface to offshore settings; suspension-feeders and passive carnivores of the *Skolithos* ichnofacies reflect shallower water depths and increased energy levels of the middle shoreface to foreshore (modified from Frey *et al.*, 1990; and Walker and Plint, 1992).

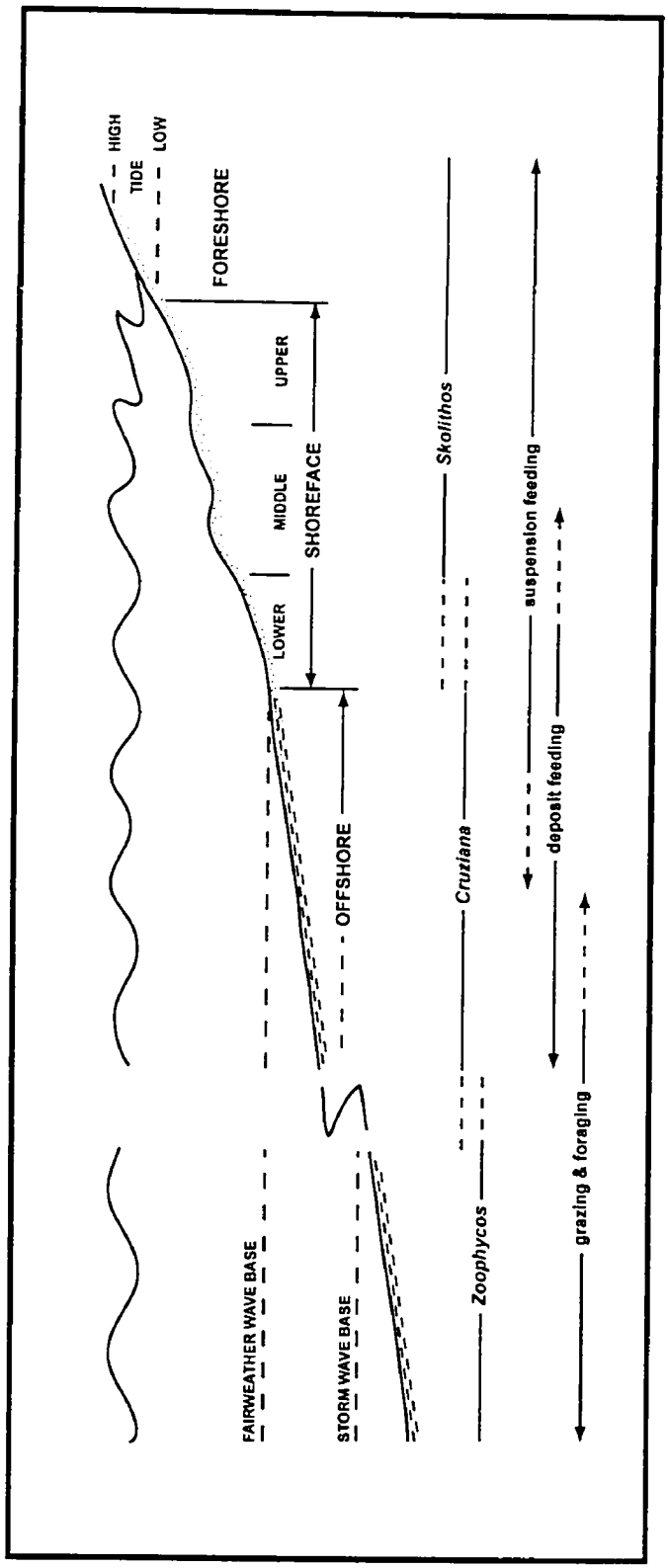
HIGH
TIDE
LOW
FORESHORE
UPPER
MIDDLE
LOWER
SHOREFACE
OFFSHORE
FAIRWEATHER WAVE BASE
STORM WAVE BASE
Skolithos
Cruziana
Zoophycos
suspension feeding
deposit feeding
grazing & foraging

Figure 2.3: Schematic development of a *Glossifungites* surface. A muddy substrate is initially rendered semi-consolidated through burial and dewatering. The shaly bed is then erosionally exhumed, resulting in an exposed, firm substrate. During a depositional hiatus, the discontinuity surface is colonized by tracemakers of the *Glossifungites* ichnofacies under marine conditions. Finally, the structures are passively infilled during a succeeding depositional episode (modified from Pemberton and Frey, 1985).

Stage Development of *Glossifungites* Ichnofacies

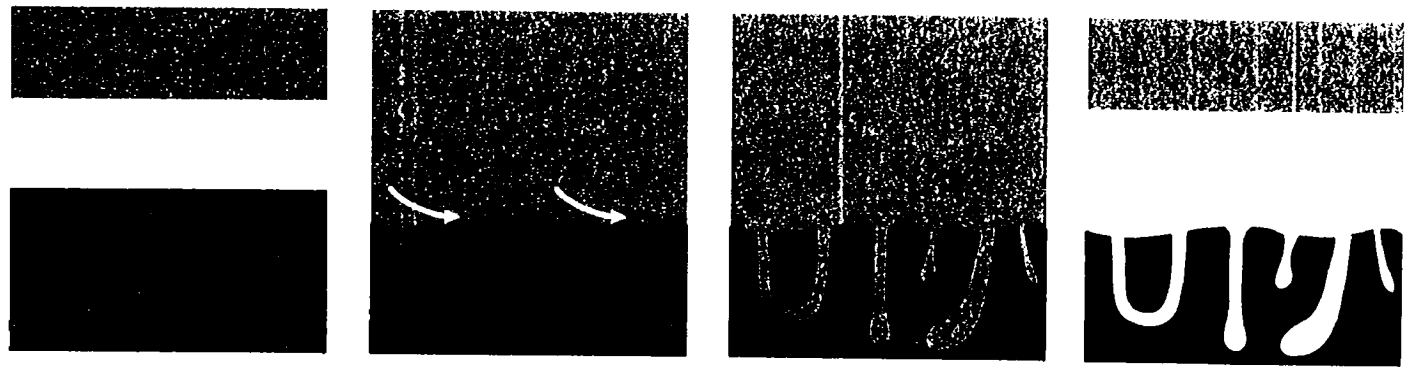

assemblage demarcates an erosional discontinuity and its importance with respect to the depositional history of the study area will be discussed in Chapter 4. The significance of the *Glossifungites* ichnofacies to the identification and interpretation of stratigraphic discontinuities has been recognized in numerous other deposits (e.g. Savrda, 1991; MacEachern *et al.*, 1992; Pemberton *et al.*, 1992a; Pemberton and MacEachern, 1995).

Soft-sediment deformation structures observed in silty mudstone strata of F1 suggest rapid deposition and substrate instability (Moslow and Pemberton, 1988). Localized occurrences of soft-sediment deformation structures are interpreted to be distal delta front deposits that formed along an otherwise prograding marginal-marine strandline system. Episodes of high precipitation resulted in high local flood discharge through rivers, and basinward, local deltaic distributary networks that locally deposited sediment faster than it could be reworked, and thereby stabilized, by basinal processes (cf. Pemberton *et al.*, 2001). Thus, although in general event beds of F1 are typical of storm-induced deposition rather than delta front sediment gravity-flows, the preservation of distal delta front deposits within storm event beds is not extraordinary. Transitional offshore to distal delta front sediments of F1 show remarkable similarity to the distal facies in allomembers D and E of the Upper Cretaceous Dunvegan Formation of Alberta, interpreted to be wave-dominated deltaic deposits (Bhattacharya and Walker, 1991; Gingras *et al.*, 1998). Furthermore, the paucity of bioturbation in distal delta front deposits of F1 (bioturbation is limited to a low-diversity *Cruziana* ichnofossil assemblage containing diminutive *Asterosoma*, *Planolites*, *Chondrites* and *Teichichnus* traces) is inconsistent with ecologically-stressed conditions commonly associated with deltaic sedimentation (Moslow and Pemberton, 1988).

2.3 Facies 2: Cross-Stratified Coarse Siltstone to Very Fine-Grained Sandstone

Description

Facies 2 (F2) is characterized by coarse siltstone to very fine-grained sandstone with rare mudstone interbeds. F2 ranges from 15 cm to 1.5 m and averages 75 cm in thickness. Lower bounding surfaces are sharp, curvilinear, rarely with sole marks, and commonly slope at angles less than 10° (Plate 2.6a). Strata are well sorted with low-angle, medium-scale cross-laminae separated by shallow-dipping second-order truncation surfaces (Plate 2.6b). Relief on lower bounding surfaces and internal second-order truncation surfaces is commonly 1-3 cm. Laminae overlying set boundaries are typically nearly parallel to that surface and commonly onlap onto the lower set boundary. Laminae are upward-fanning with a progressively diminishing angle of dip until they become nearly horizontal or slightly convex-upward in form (Plate 2.7a). Dip directions of set boundaries and overlying laminae are variable. Stacked cosets of low-angle, medium-scale cross-stratified coarse siltstone to very fine-grained sandstone are locally up to 45 cm thick.

The tops of F2 are commonly small-scale cross-laminated to gently undulating laminated coarse siltstone with interstratified mudstones 1-20 cm thick (Plate 2.7b). Cross-stratification of this upper interval is characterized by troughs 3-5 cm in width overlain by low-angle cross-laminated siltstone. Undulating pinstripe-laminated siltstone beds 6-8 cm thick are commonly preserved above cosets of low-angle cross-stratified coarse siltstone to very fine-grained sandstone. These finely laminated siltstones are low-angle, small-scale cross-stratified and are generally shallowly inclined sub-parallel to an underlying bounding surface (Plate 2.8a). Where form sets of laminated siltstones have been preserved, crest profiles are slightly asymmetrical with internal cross-laminae dipping consistently in one direction. Mudstone interbeds are commonly normally graded and fine upwards from fine siltstone to massive mudstone beds. Crenulated cracks, filled with coarse siltstone to very fine-grained sandstone from overlying cross-stratified units, are uncommonly preserved within mudstone interbeds (Plate 2.8b).

Plate 2.6: Cross-Stratified Coarse Siltstone to Very Fine-Grained Sandstone (F2)

a) Sharp, low-angle contact (arrow) between bioturbated silty mudstone (F1) and overlying medium-scale cross-stratified coarse siltstone to very fine-grained sandstone (F2). Note the onlap of laminae onto the lower set boundary and the J-shaped *Arenicolites* burrow (Ar) in the upper half of the photograph. Well 02/06-11-020-09W4/0, 965.8 m.

b) Low-angle, medium-scale cross-stratified coarse siltstone to very fine-grained sandstone. Note the curved laminae, variable dip directions and onlap of laminae onto lower set boundaries. Well 02/06-11-020-09W4/0, 967.8 m.

a)

b)

Plate 2.7: Cross-Stratified Coarse Siltstone to Very Fine-Grained Sandstone (F2)

a) Second-order truncation surface (arrow) within upward-fanning, medium-scale cross-laminated coarse siltstone to very fine-grained sandstone bed set. Well 00/06-23-020-09W4/0, 962.9 m.

b) Medium- to small-scale cross-laminated coarse siltstone with interstratified burrowed mudstone laminae. Note the upward decrease in the scale of cross-stratification and the presence of mudstone at the top of the sample. This transition from medium- to small-scale cross-stratification is commonly found at the tops of F2 cosets and is indicative of an upward decrease in energy conditions associated with waning storm deposition. Well 00/06-34-019-09W4/0, 3299.8'.

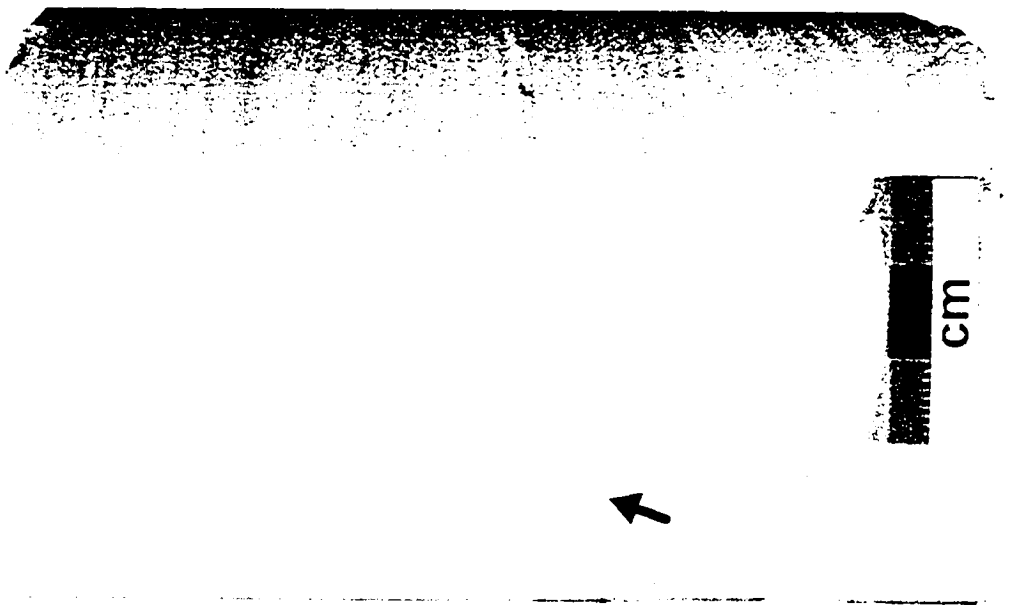

a)

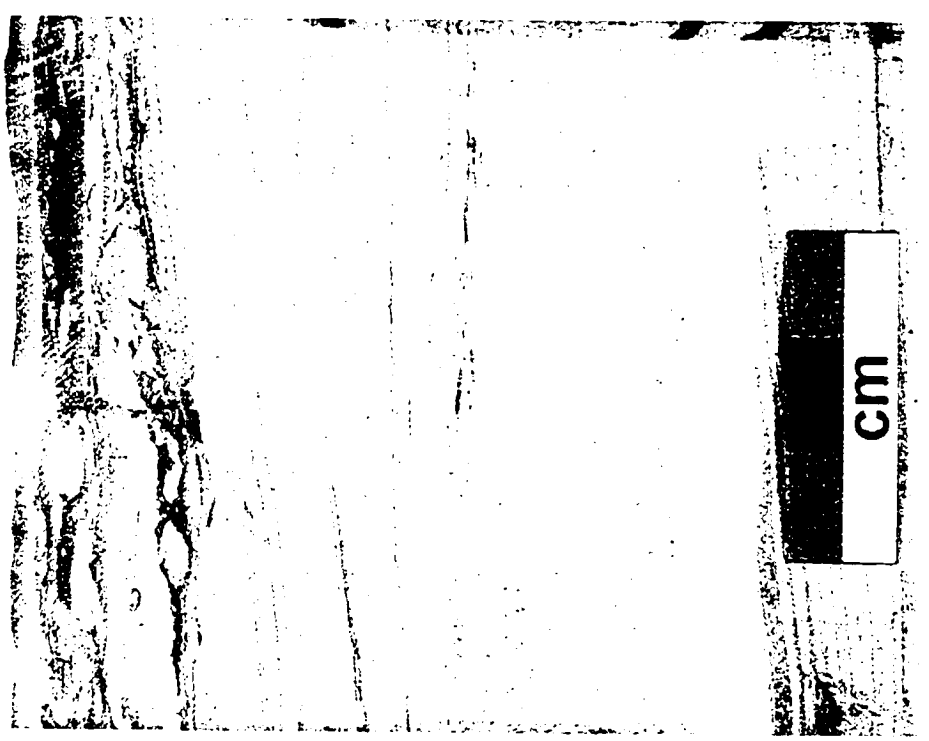

b)

Plate 2.8: Cross-Stratified Coarse Siltstone to Very Fine-Grained Sandstone (F2)

a) Gently undulating pinstripe-laminated siltstone. The shallow inclination of the bed is sub-parallel to an underlying bounding surface. Well 00/04-23-020-09W4/0, 973.8 m.

b) Crenulated cracks within graded mudstone interlaminae. Cracks are filled with coarse siltstone to very-fine grained sandstone of overlying low-angle, small- to medium-scale cross-stratified beds. Well 02/10-23-020-09W4/0, 956.0 m.

a)

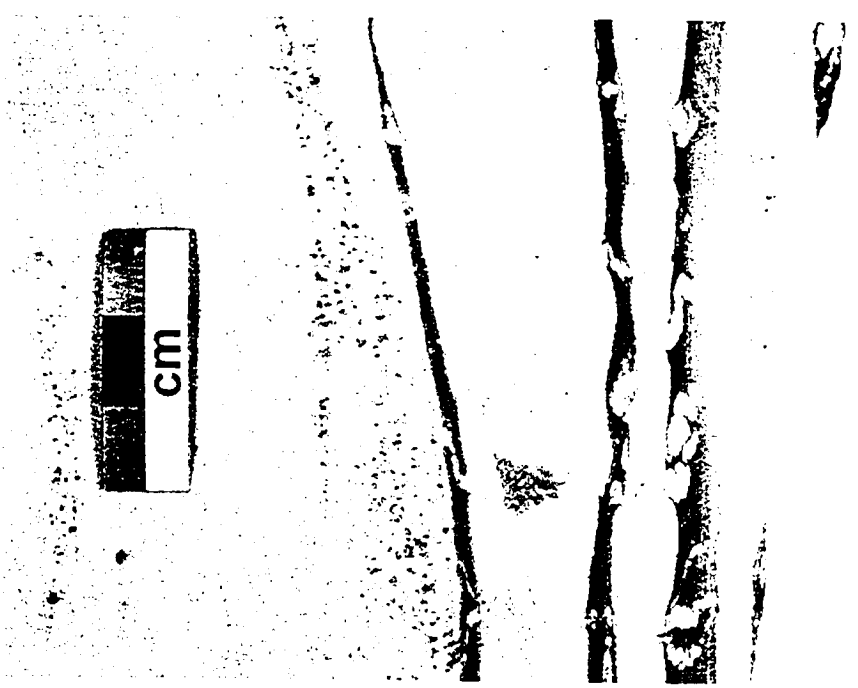

b)

Trace fossil diversity and abundance within strata of F2 is low with the majority of individual forms displaying diminutive morphologies. Trace fossil suites are composed of bedding-plane-parallel structures within interbedded mudstones and vertical structures within cosets of low-angle cross-stratified siltstone to very fine-grained sandstone. Bioturbation within mudstone interbeds is slightly more abundant and includes *Planolites*, *Chondrites* and *Teichichnus* (Plate 2.9a). Ichnogenera within cosets of cross-stratified siltstone to very fine-grained sandstone include *Diplocraterion*, *Arenicolites*, *Skolithos*, *Ophiomorpha* and escape structures (Plate 2.10). Small-scale cross-laminated siltstone cosets are characterized by circular to oblate *Asterosoma* burrows (Plate 2.9b).

Interpretation

F2 is interpreted to represent a storm-dominated succession composed of lower shoreface deposits. Cosets of low-angle, medium-scale cross-stratified coarse siltstone to very fine-grained sandstone are interpreted as hummocky cross-stratification (*sensu* Harms *et al.*, 1975; Figure 2.4). The origin of hummocky cross-stratification has long been the subject of considerable debate among researchers (e.g. Walker *et al.*, 1983; Duke *et al.*, 1991). A main point of controversy concerns the bed configuration(s) required to produce hummocky cross-stratification. Dott and Bourgeois (1982) have suggested formation by the aggradation and tractive transport of fine-grained sediment over a basal erosion surface moulded into roughly circular, unoriented hummocks and swales by large waves. Experimental observations by Southard *et al.* (1990) and Arnott and Southard (1990), by contrast, emphasize the development of hummocky cross-stratification by an equilibrium bed form generated in very fine sand by long-period oscillatory and/or very strongly oscillatory-dominated combined flows. The low-angle erosional bounding surfaces, onlap of laminae onto lower set boundaries and upward-fanning of laminae of F2 appear to support a scour and drape interpretation; however, hummocky cross-stratification is a polygenetic phenomenon (Southard *et al.*, 1990) and likely involves a combination of the aforementioned formative mechanisms. Regardless of the physical constraints that govern its development, hummocky cross-stratified coarse

Plate 2.9: Cross-Stratified Coarse Siltstone to Very Fine-Grained Sandstone (F2)

a) Diminutive *Planolites* (Pl) and *Chondrites* (Ch) burrows within intercalated mudstone and small-scale cross-stratified coarse siltstone. Well 04/06-03-021-09W4/0, 958.4 m.

b) Tapered, shallowly-inclined *Asterosoma* (As) and *Cylindrichnus* (Cy) burrows in small- to medium-scale cross-stratified coarse siltstone to very fine-grained sandstone. Well 00/13-23-020-09W4/0, 953.6 m.

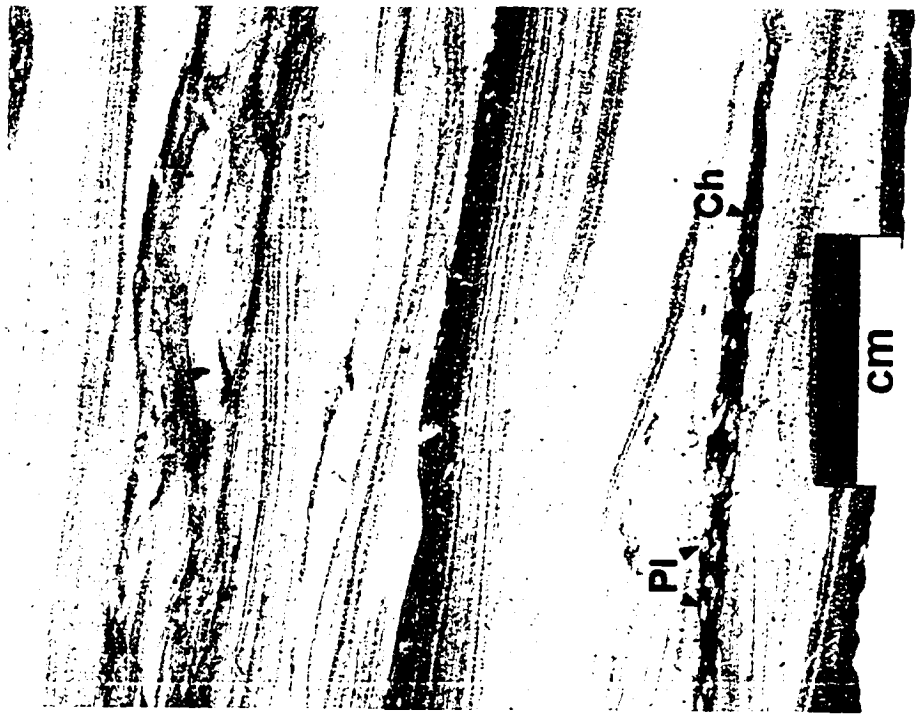

a)

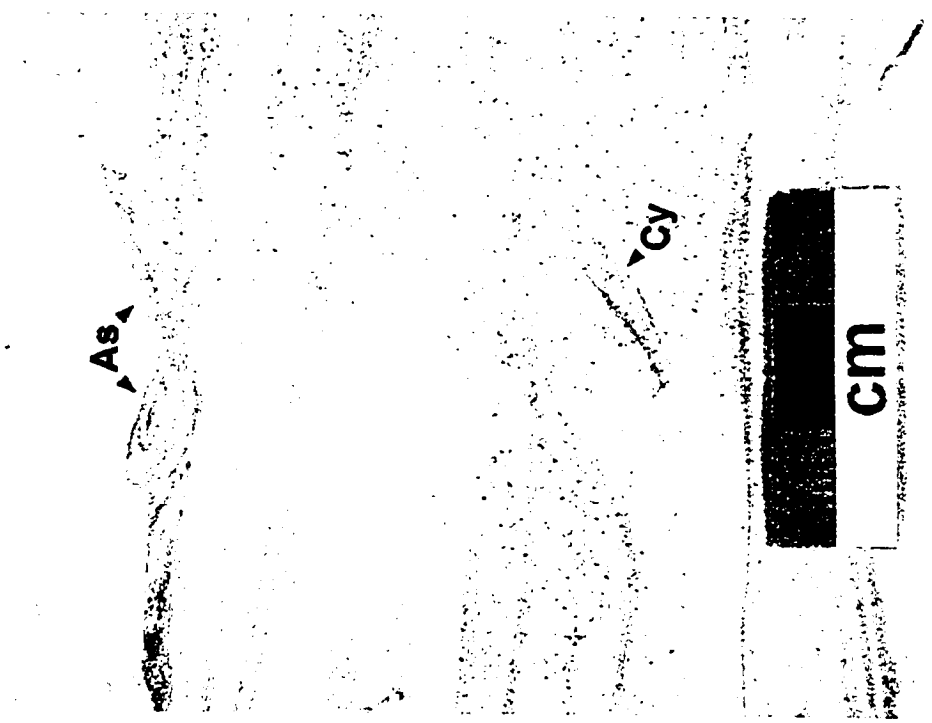

b)

Plate 2.10: Cross-Stratified Coarse Siltstone to Very Fine-Grained Sandstone (F2)

a) *Skolithos* (Sk), *Diplocraterion* (Di) and escape structures (esc) in small- to medium-scale cross-stratified coarse siltstone to very fine-grained sandstone. Elements of the *Skolithos* ichnofacies associated with an endemic *Cruziana* trace fossil assemblage represent the proliferation of opportunists in response to increased levels of sedimentation. Well 02/10-23-020-09W4/0, 956.3 m.

b) *Ophiomorpha* burrows (arrows) in medium-scale cross-stratified coarse siltstone to very fine-grained sandstone. Note the thin, vaguely mammalated wall linings of the burrows, suggestive of a distal lower shoreface depositional setting. Well 00/01-34-019-09W4/0, 1012.8 m.

a)

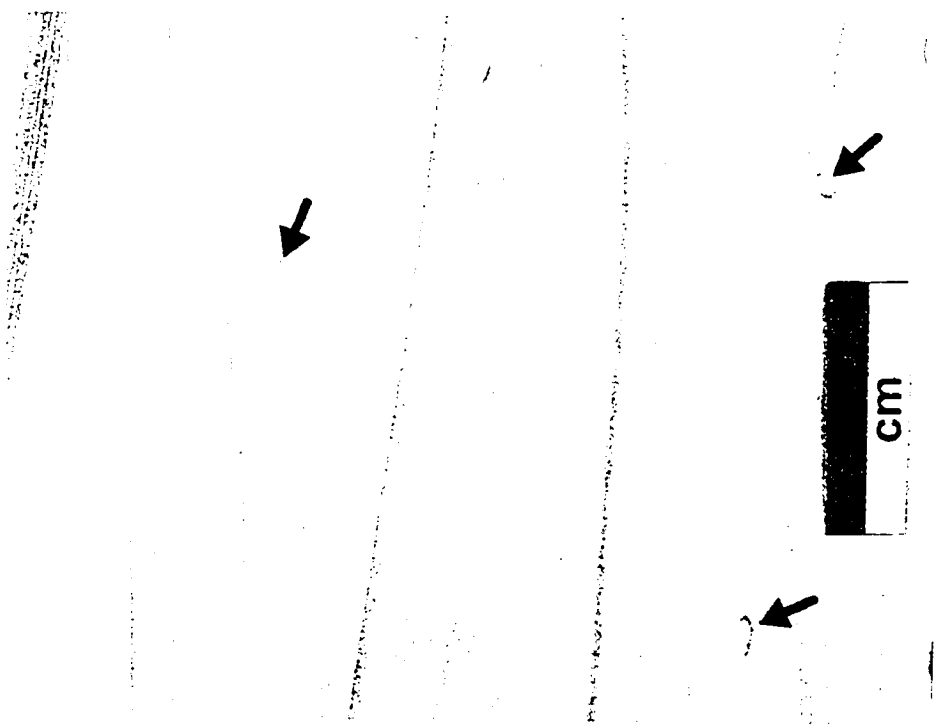

b)

Figure 2.4: Block diagram showing major morphological features of hummocky cross-stratification (modified from Harms *et al.*, 1975).

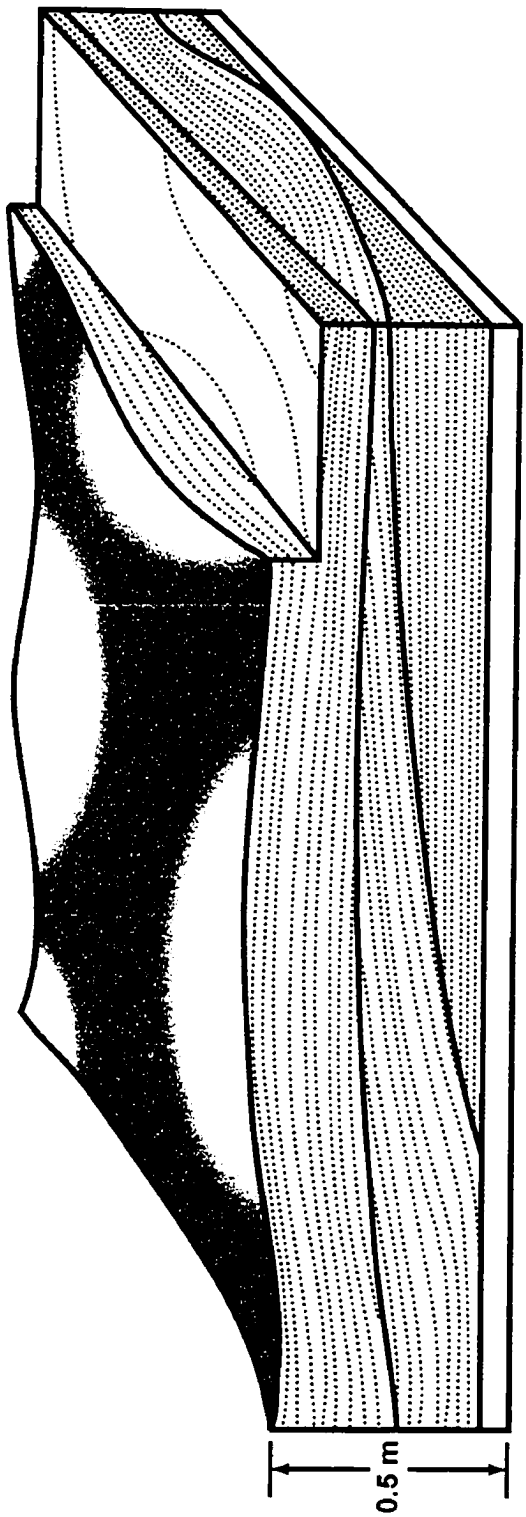
0.5 m

siltstone to very fine-grained sandstone of F2 indicate deposition in a lower shoreface environment during storms that formed high-energy, long period waves.

The superposition of small-scale ripple cross-laminated to undulating ripple-laminated coarse siltstone above hummocky cross-stratified coarse siltstone to very fine-grained sandstone cosets is interpreted to represent waning storm deposition, indicating a progressive return to lower energy conditions (Johnson and Baldwin, 1986). Asymmetric form sets and homoclinal internal stratification of ripple-laminated siltstone cosets suggests sedimentation under low-energy combined flows (cf. Arnott and Southard, 1990; Figure 2.5). An interpretation of small-scale cross-laminated siltstone cosets as asymmetric wave ripples produced by purely oscillatory flows is incompatible with a lower shoreface depositional environment; asymmetric wave ripples are produced in the upper shoreface where shoaling water waves develop a disharmonic oscillation at the bed (de Raaf *et al.*, 1977). Normally graded fine siltstone to massive or bioturbated mudstone interbeds represent post-storm deposition and reflect either the final suspension fall-out of storm derived sediment or the return to normal background sedimentation (Johnson and Baldwin, 1986). Mudstone interbeds are commonly erosively overlain by hummocky cross-stratified coarse siltstone to very fine-grained sandstone cosets associated with the next storm event.

Strata of F2 contain a low-diversity, low-abundance mixed *Skolithos-Cruziana* trace fossil assemblage. Horizontal burrows of the endemic *Cruziana* ichnofacies are consistent with an interpreted distal lower shoreface depositional setting (Frey *et al.*, 1990; Figure 2.2). Vertical structures within hummocky cross-stratified cosets represent the activities of opportunistic organisms of the *Skolithos* ichnofacies. Juxtaposition of elements of the *Skolithos* and *Cruziana* ichnofacies within a single depositional cycle has been previously interpreted by Pemberton and Frey (1984) as the alternation of sand and silty substrates caused by changing hydrodynamic energy conditions, specifically storm and fairweather conditions, respectively. A lower shoreface interpretation is further supported by the presence of *Ophiomorpha* burrows with thin, vaguely mammalated wall linings that are typically associated with distal lower shoreface to offshore sediments (Frey *et al.*, 1978). The low diversity, abundance and overall diminutive morphologies of trace fossils within strata of F2 are suggestive of growth in a

Figure 2.5: Some idealized types of cross-stratification produced by oscillatory wave ripples; migration of ripples results from the influence of a weak unidirectional component of flow. Preserved form sets of ripple-laminated siltstone cosets of F2 resemble cross-stratification types 3 and 4, suggesting sedimentation under combined flow conditions (modified from Harms *et al.*, 1982).

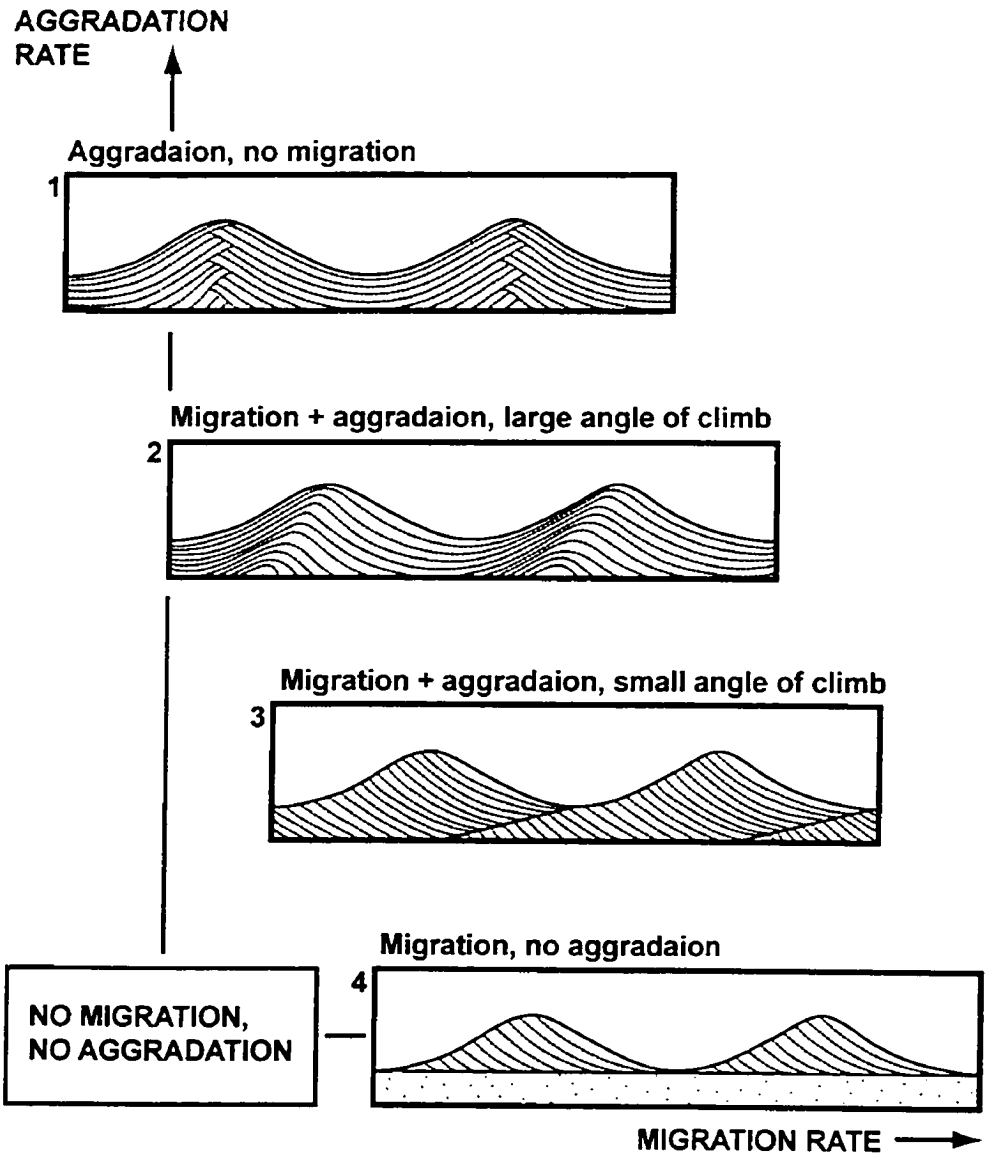
AGGRADATION
RATE
Aggradaion, no migration
1
Migration + aggradaion, large angle of climb
2
Migration + aggradaion, small angle of climb
3
Migration, no aggradaion
4
NO MIGRATION,
NO AGGRADATION
MIGRATION RATE

stressed environment (Frey and Seilacher, 1980). The presence of escape structures in hummocky cross-stratified siltstone supports an interpretation of episodic high rates of sedimentation associated with storm deposition (Pemberton *et al.*, 1992c). Furthermore, the presence of crenulated crack-fills, which are most likely synaeresis shrinkage structures, may suggest that F2 was deposited in an area that underwent periodic fluctuations of salinity (Wightman *et al.*, 1987; Paik and Kim, 1998).

2.4 Facies 3: Medium-Scale Cross-Stratified Sandstone

Description

Facies 3 (F3) is characterized by medium-scale cross-stratified fine- to medium-grained sandstone with rare granular to pebbly sandstone and silty mudstone interbeds. F3 ranges from 75 cm to 4 m and averages 2 m in thickness. Lower bounding surfaces of F3 vary depending on the nature of underlying strata. Where overlying strata of F1 and F2, lower contacts of F3 are commonly gradational, interbedded or obscured by bioturbation (Plate 2.11a). In contrast, where F3 overlies strata of Facies 4 and 5 (see below), the lower contact is commonly sharp and either horizontal to faintly inclined or undulating. Locally, F3 sandstones gradationally overlie thin conglomerate units of F5 (Plate 2.11b).

Cross-stratified sandstone beds are 10 cm to over 1 m thick. Sandstones are typically well to very well sorted with an average grain size ranging from lower fine to upper medium. Where cross-bedded sandstones are associated with pebbly sandstone and silty mudstone interbeds the sandstone is more poorly sorted and the average grain size ranges from lower very fine to very coarse. There is typically a slight upward-fining or, locally, upward-coarsening trend within F3 successions. The base of sandstone beds is sharp and uncommonly overlain by a 1-3 cm thick layer of subrounded to rounded chert granules and pebbles 2 mm to 1 cm in width (Plate 2.12a). Chert pebbles are commonly arranged *en echelon*, parallel to medium-scale cross-stratified sandstone bed sets. Sandstones are trough and planar cross-stratified (Plate 2.12b). Foreset laminae are inclined at angles ranging between 10-29° but more commonly are between 15-18°. Cross-stratification is

Plate 2.11: Medium-Scale Cross-Stratified Sandstone (F3)

a) Interstratified siltstone and mudstone (F2) overlain by medium-scale cross-stratified fine-grained sandstone (F3). Note the partial blurring of the contact by bioturbation associated with the underlying facies. Well 04/06-03-021-09W4/0, 955.5 m.

b) Gradational contact between matrix-supported chert pebble conglomerate (F5) and overlying medium-scale cross-stratified medium- to coarse-grained sandstone (F3). Well 00/04-23-020-09W4/0, 965.0 m.

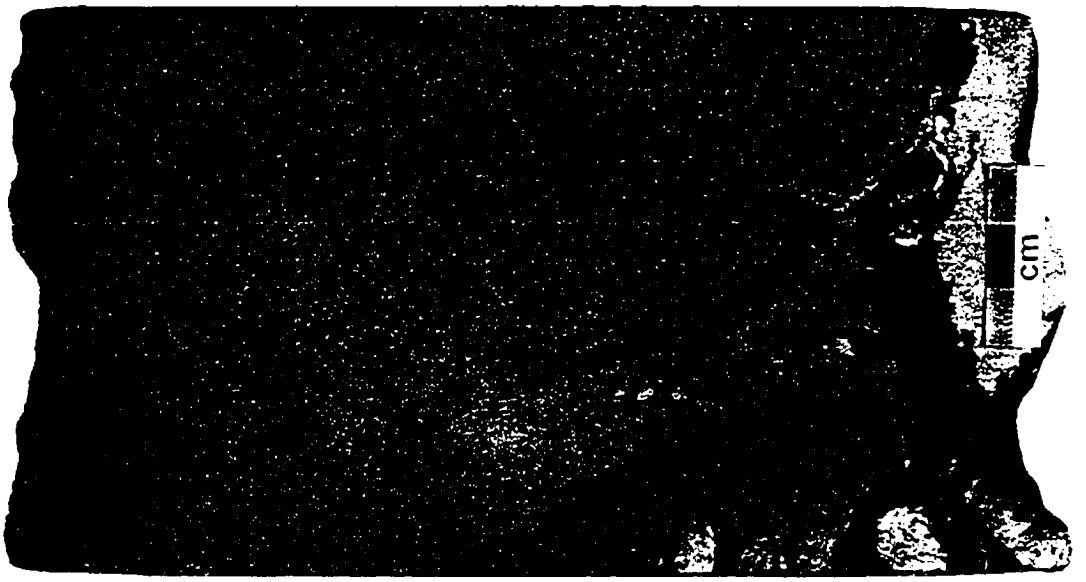

a)

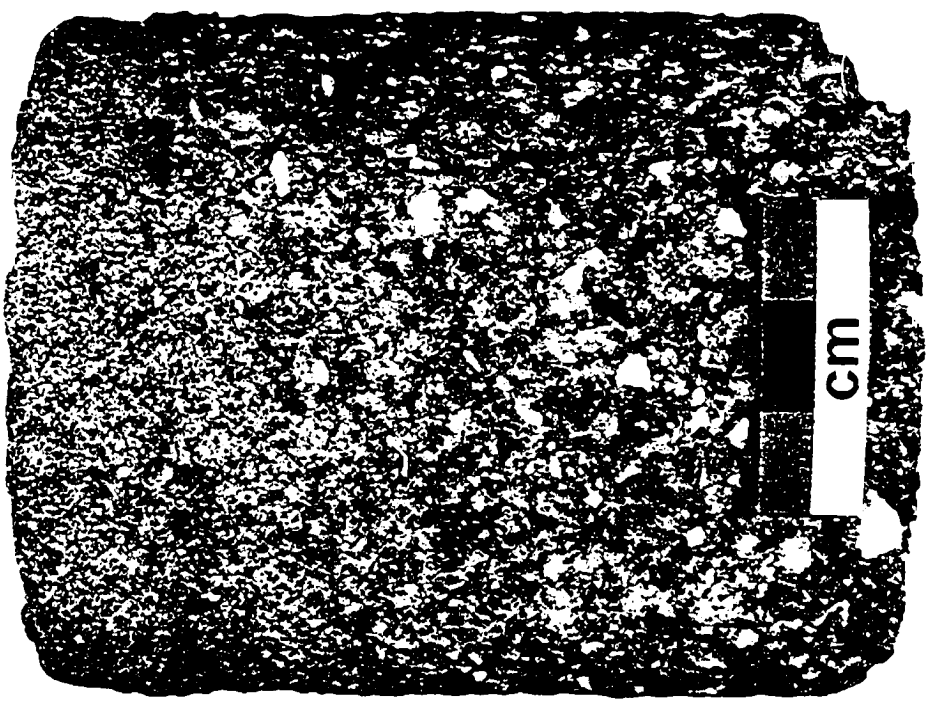

b)

Plate 2.12: Medium-Scale Cross-Stratified Sandstone (F3)

a) Planar-tabular cross-stratification. The base of the upper, horizontally to low-angle planar-stratified sandstone bed is overlain by a 2 cm thick layer of rounded chert granules and pebbles aligned parallel to stratification. Well 04/06-03-021-09W4/0, 955.1 m.

b) Planar cross-stratified medium-grained sandstone. Note the imbrication of elongate chert granules and their alignment parallel to medium-scale cross-stratification along the base of bed sets. Well 04/06-03-021-09W4/0, 953.6 m.

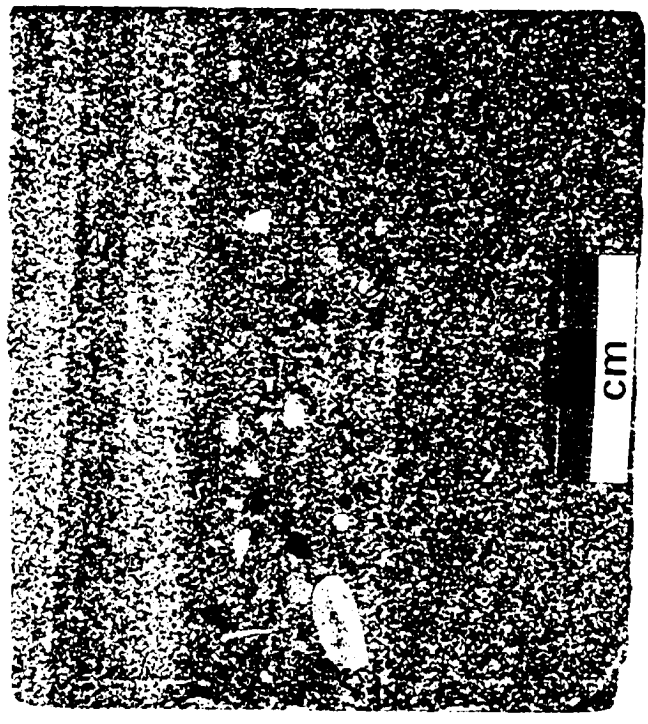

a)

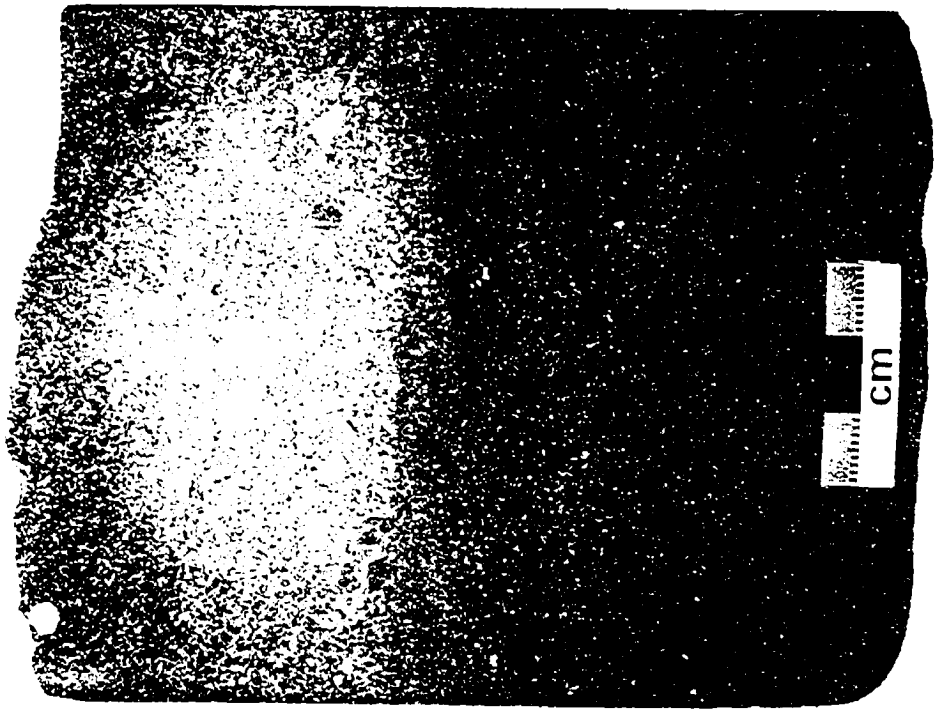

b)

accentuated by alternating quartz-rich (light) and chert-rich (dark) laminae and a slight grain size variation between laminae (Plate 2.13a). Thin-walled *Skolithos* and vaguely mammalated *Ophiomorpha* trace fossils are present locally within fine-grained, medium-scale cross-stratified sandstone units (Plate 2.13b). Silty mudstone interbeds range from 1 to 30 cm thick and contain small-scale cross-stratification, carbonaceous material and mud clasts. Mudstone interbeds contain a low-diversity, low-abundance trace fossil assemblage consisting of *Planolites*, *Thalassinoides*, and *Palaeophycus*. The abundance and thickness of silty mudstone interbeds commonly increases gradationally upwards within F3 successions.

Sandstones of F3 are quartzarenites (McBride, 1963) composed of 75-90% quartz, 5-20% chert, 3-4% rock fragments and less than 2% accessory minerals including epidote, feldspar and mica (Appendix 2). In thin section, quartz grains of F3 sandstones are moderately to well rounded; syntaxial overgrowths impart a diagenetic angularity. Quartz grains have low undulosity, going completely extinct within less than 1-2°, and contain rare acicular accessory inclusions of rutile (A.E. Lalonde, pers. comm., 2003). Many quartz grains have a dark coating of oil or hematite rimming their margins. Chert grains tend to be larger, darker and more angular than quartz grains. Elongated grains are commonly faintly to strongly imbricated.

Interpretation

Medium-scale cross-stratified sandstones of F3 are interpreted to represent the migration of two- and three-dimensional subaqueous dunes. Dunes are lower flow-regime bedforms that occur between ripple and plane bed stability fields in sediment greater than ~ 0.12 mm (Harms *et al.*, 1982). Dunes scale to the physical conditions of the flow, specifically the scale of organized macroturbulence structures in the boundary layer. Ideally, dune height is ~ 17% of water depth and on average approximately one third of the dune height is preserved in ancient fluvial deposits (Leclair, 2002). Two-dimensional dunes are formed at somewhat moderate current velocities, intermediate between those of ripples and three-dimensional dunes. Traces of laminae viewed on horizontal surfaces of two-dimensional dunes are straight or sinuous (Figure 2.6a). In

Plate 2.13: Medium-Scale Cross-Stratified Sandstone (F3)

a) Moderate-angle, medium-scale cross-stratified sandstone. Stratification is made visible by the alternation of thin quartz-rich laminae (light) and thicker, chert-rich laminae (dark) composed of slightly coarser grains. Well 00/05-10-021-09W4/0, 953.9 m.

b) Inclined *Skolithos* (Sk) and vaguely mammalated *Ophiomorpha* (Op) trace fossils within medium-scale cross-stratified fine-grained sandstone. Well 00/04-23-020-09W4/0, 967.8 m.

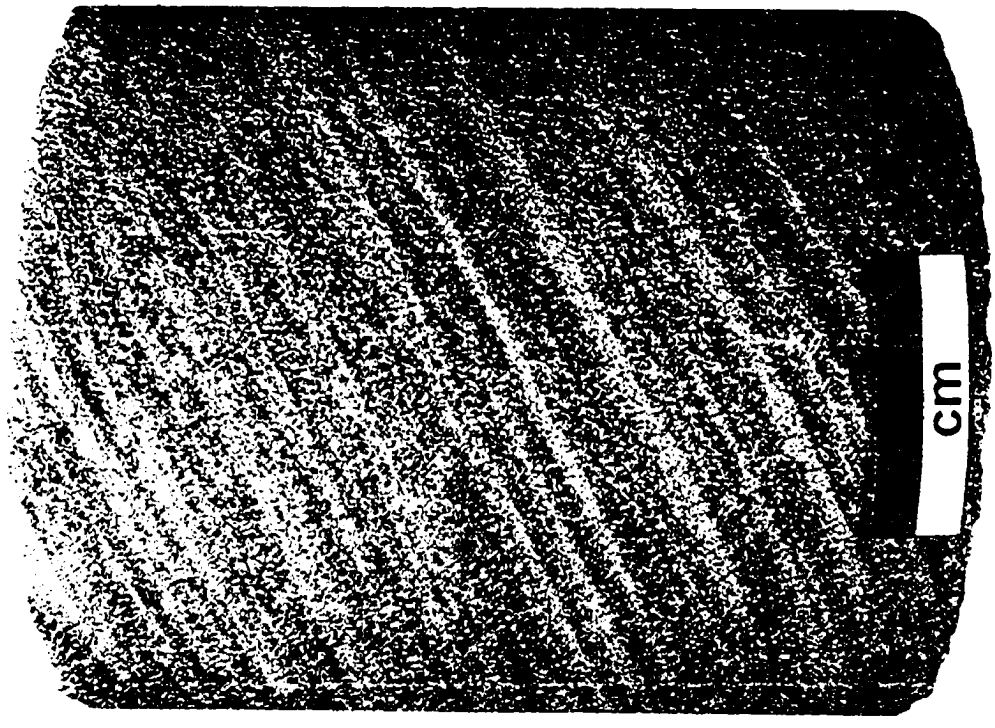

a)

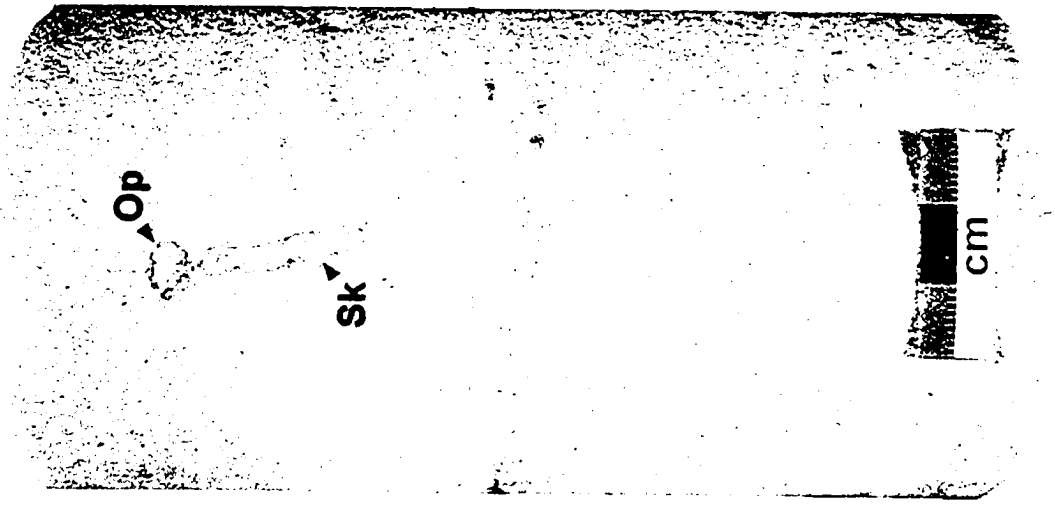

b)

cross-section, laminae are planar-tabular and truncate abruptly and at a high angle on the lower bounding surface; the average angle of dip is close to the angle of repose, that is, 30° or more. Thus, two-dimensional dunes appear as steeply dipping medium-scale planar-tabular cross-stratified sandstone in core. Three-dimensional dunes have curved crests with deeper, trough-shaped slipfaces formed by a centralized eddy that deeply scours the toeset of the dune; this manifests as radiating and upward-steepening cross-stratification (Figure 2.6b). The expression of three-dimensional dunes in core is trough cross-stratified and tangentially cross-bedded fine- or coarser-grained sandstone. The alternation of fine and coarse laminae within cross-stratified sets is caused by the segregation of quartz and coarser, more angular chert grains along the slipface of migrating dunes during avalanching. Locally preserved small-scale cross-stratified silty mudstone interbeds are related to the migration of current ripples (Harms *et al.*, 1975). The presence of small- and medium-scale cross-stratification within the same facies sequence suggests that subtle variations in flow velocity juxtaposed bedforms of different scale and genesis. Sedimentation was rapid enough to bury these bedforms relatively quickly and preserve their association in the stratigraphic record.

Strata of F3 contain a low-diversity, low-abundance mixed *Skolithos-Cruziana* trace fossil assemblage comprising diminutive simple forms. The low diversity, small size and simple structures of vertical and horizontal ichnofossils suggest that strata of F3 were deposited in an ecologically-stressed, possibly brackish water environment (Pemberton and Wightman, 1992). Modern examples of estuarine point bar successions containing a similar mixed *Skolithos-Cruziana* trace fossil assemblage have been reported from the Georgian coast (Howard and Frey, 1973) and Willapa Bay, Washington state (Gingras *et al.*, 1999). From these examples, admixtures of traces from both the *Skolithos* and *Cruziana* ichnofacies within point bar successions have been interpreted as variations in the colonization strategies of organisms in sandy versus muddy substrates. Because of the physical similarities between modern fluvial and tidally-influenced meandering streams (e.g. Jackson, 1981), ichnology is a useful criterion to differentiate these two deposits in the ancient record (cf. Barwis, 1978; de Mowbray, 1983). Unlike fluvial systems, biogenic structures are abundant in estuarine point bar deposits (Ekdale *et al.*,

Figure 2.6: Types of cross-bedding produced by migrating subaqueous dunes (from Reineck and Singh, 1973).

a) Block diagram showing planar cross-bedding formed by migrating two-dimensional dunes as seen in horizontal, transverse and longitudinal sections. Units are tabular to wedge-shaped; bedding surfaces are planar.

b) Block diagram showing trough cross-bedding formed by migrating three-dimensional dunes as seen in horizontal, transverse and longitudinal sections. Units are festoon- or trough-shaped. In transverse section troughs are well developed, with strongly curved bedding surfaces.

a)

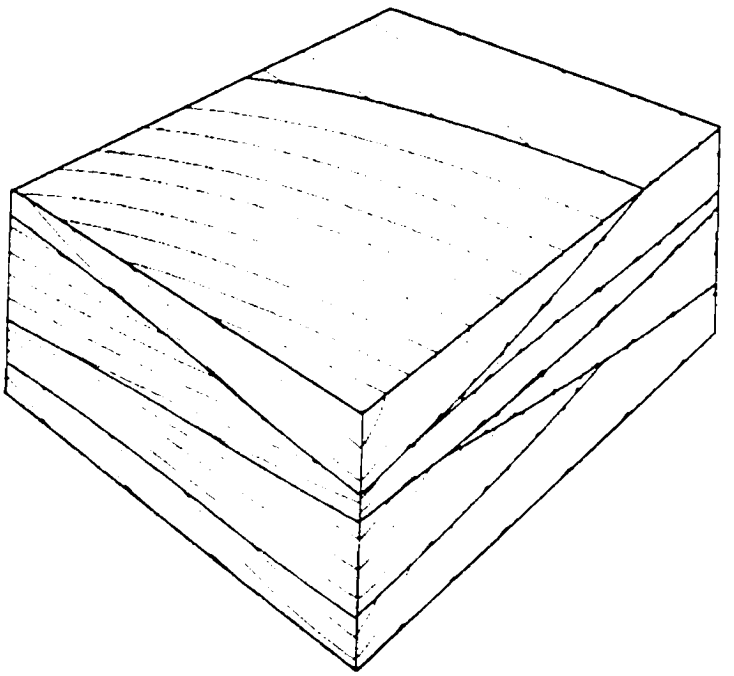

b)

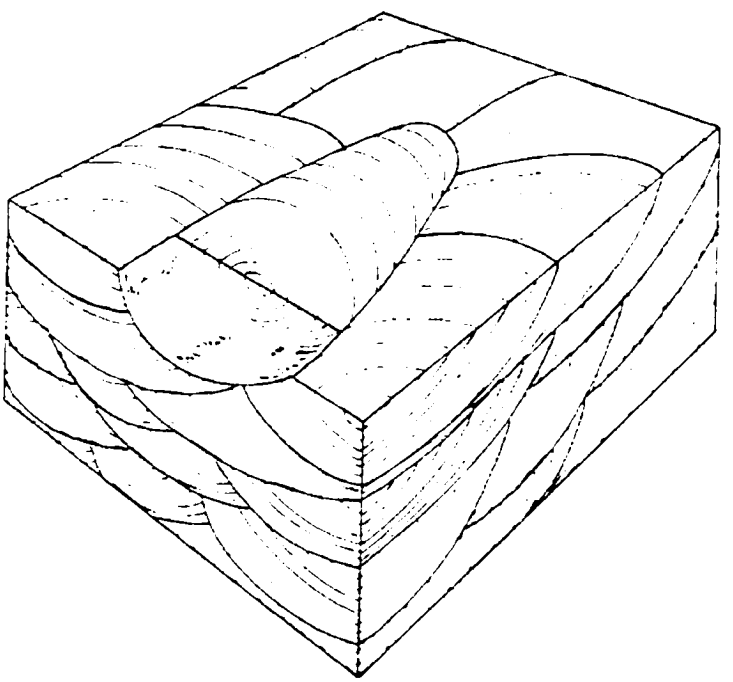

1984). Furthermore, within coastal environments, there exists an increase in the diversity, abundance and size of biogenic structures in a seaward direction (Wightman *et al.*, 1987; Gingras *et al.*, 1999). Thus, the presence of subaqueous dunes combined with a low-abundance, ecologically-stressed *Skolithos-Cruziana* ichnofossil assemblage within strata of F3 suggests predominantly fluvial or highly stressed tidal-fluvial deposition within the upper reaches of a tide-dominated estuary.

2.5 Facies 4: Interstratified Massive Sandstone and Contorted Muddy Siltstone

Description

Interstratified massive, moderately to well sorted, very fine- to medium-grained sandstone and contorted muddy siltstone characterize strata of Facies 4 (F4). F4 ranges from 25 cm to 3 m in thickness and averages 1.5 m. Beds of massive sandstone range from 3 to 30 cm thick, averaging 10-15 cm. Muddy siltstone laminae/beds are typically several mm to a few cm thick but are locally up to 10 cm. Basal contacts are sharp and approximately planar-horizontal or highly irregular. Where basal successions of F4 are composed of thickly bedded massive sandstone, lower bounding surfaces are sharp, shallowly-inclined and slightly undulating with less than 1 cm of relief (Plate 2.14a). Alternatively, basal successions composed of thinly interstratified massive sandstone and contorted muddy siltstone have highly irregular, jagged lower contacts with up to 8 cm of relief that truncate underlying strata (Plate 2.14b).

Massive sandstone beds are quartzarenites (McBride, 1963) composed of over 95% quartz and chert with trace amounts of feldspar, mica, epidote and rock fragments (Appendix 2). A light brown-coloured mud matrix locally fills pores between framework grains and can represent as much as 5-15% of the rock, by volume. Massive sandstones are ubiquitously oil-stained, making the recognition of sedimentary and biogenic structures difficult (Plate 2.16a). Although F4 sandstones are generally devoid of primary structures, faint horizontal and low-angle cross-lamination is observed locally (Plate 2.15). Laminae are spaced 3 to 30 mm apart and are discerned by slightly higher concentrations of coarser grains along discrete horizons or by alignment of organic

Plate 2.14: Interstratified Massive Sandstone and Contorted Muddy Siltstone (F4)

a) Sharp, low-angle and slightly undulating lower contact (arrow) of massive fine-grained sandstone (F4) overlying bioturbated and wavy-laminated interstratified fine siltstone and silty mudstone (F2). Relief on contact is 1 cm. Well 00/07-27-019-09W4/0, 1015.6 m.

b) Highly irregular lower bounding surface (arrow) of interstratified massive sandstone and contorted muddy siltstone (F4). Note the truncation of underlying thoroughly bioturbated silty mudstone strata (F2). Well 02/14-11-020-09W4/0, 965.3 m.

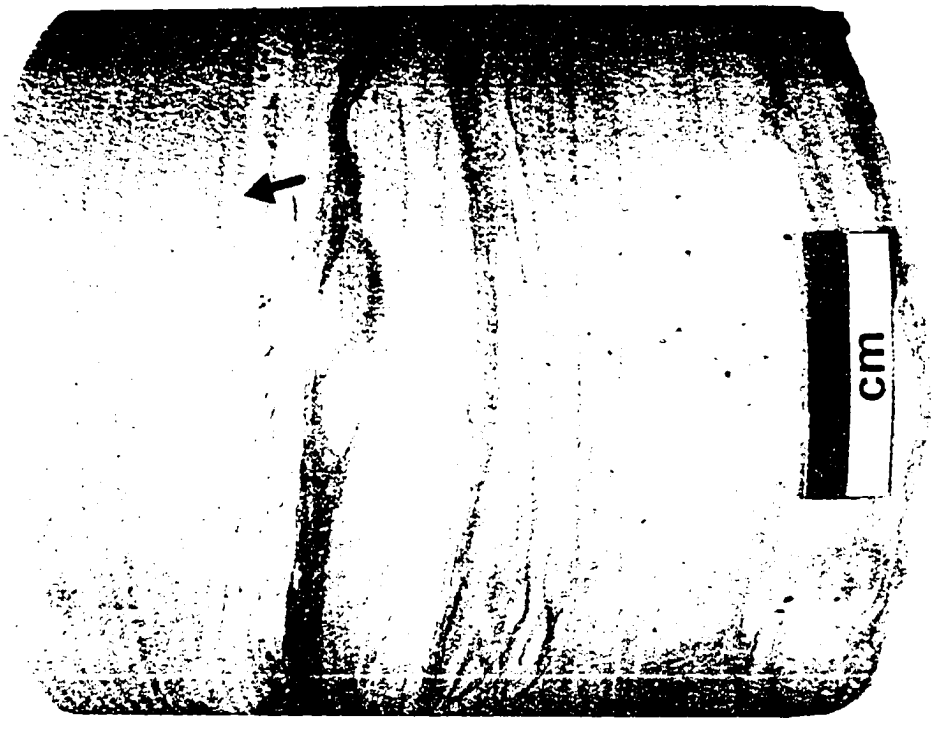

a)

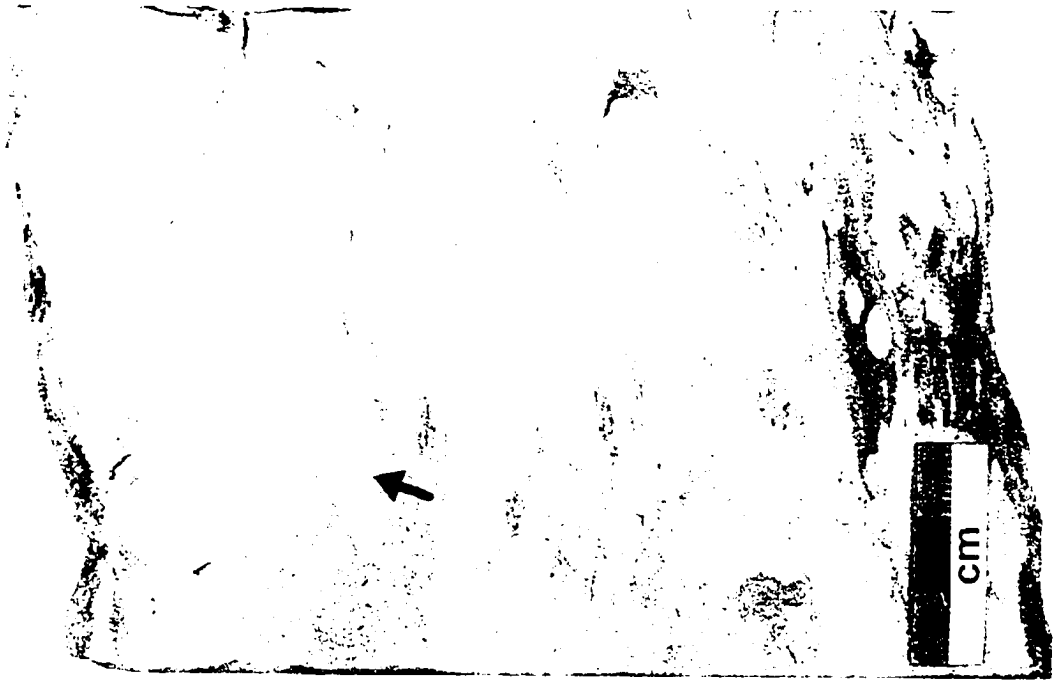

b)

Plate 2.15: Interstratified Massive Sandstone and Contorted Muddy Siltstone (F4)

a) Faint horizontal lamination within "massive" fine-grained sandstone discerned as partings (arrows) along horizons with slightly higher concentrations of coarser grains. Well 02/16-23-020-09W4/0, 949.9 m.

b) Faint low-angle cross-lamination within "massive" very fine- to fine-grained sandstone made visible by subtle variations in grain size along inclined planar laminae. Well 00/12-02-020-09W4/0, 3212'.

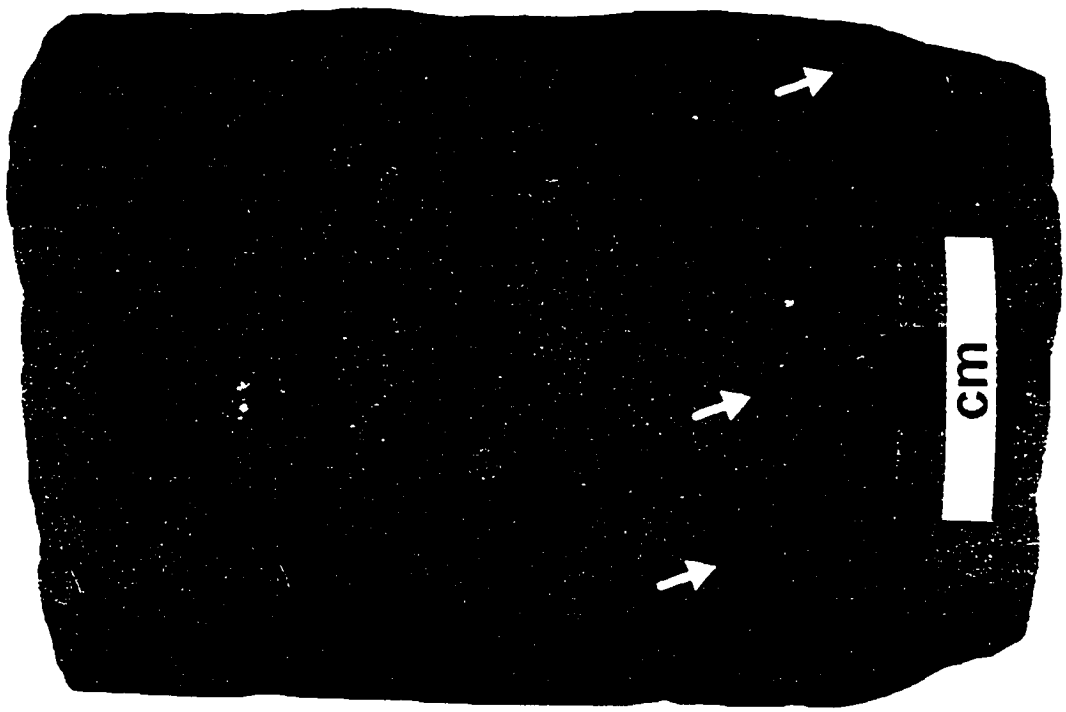

a)

b)

Plate 2.16: Interstratified Massive Sandstone and Contorted Muddy Siltstone (F4)

a) Massive fine- to medium-grained sandstone. Pervasive oil-staining has overprinted any primary sedimentary fabric. Well 00/06-34-019-09W4/0, 3278'.

b) Sharply interstratified contorted muddy siltstone and massive sandstone. Note the deformation of laminae within overlying "massive" sandstone. Well 00/01-32-019-09W4/0, 1008.1 m.

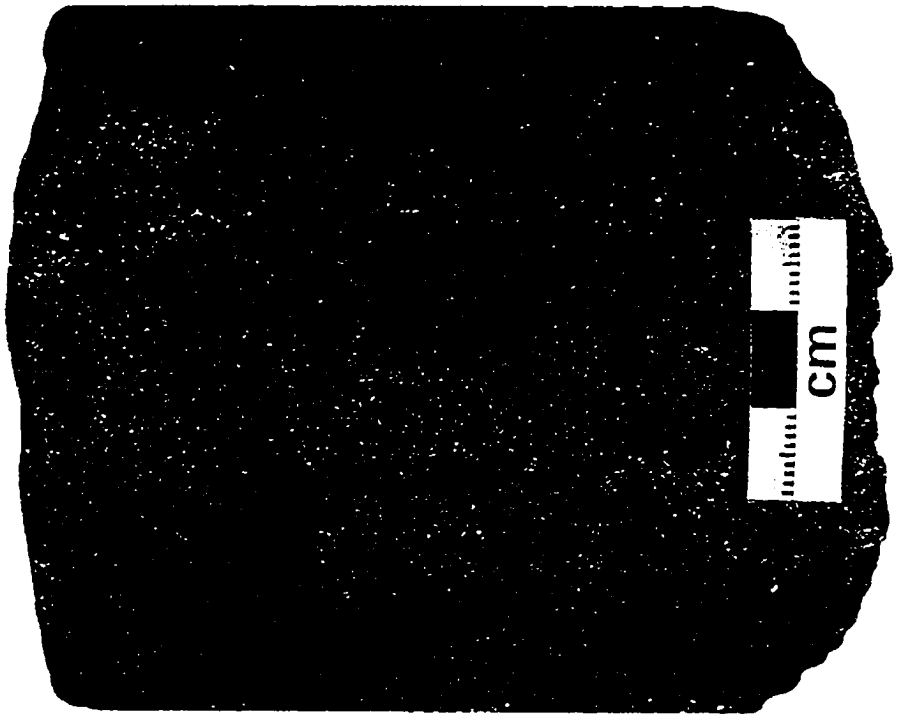

a)

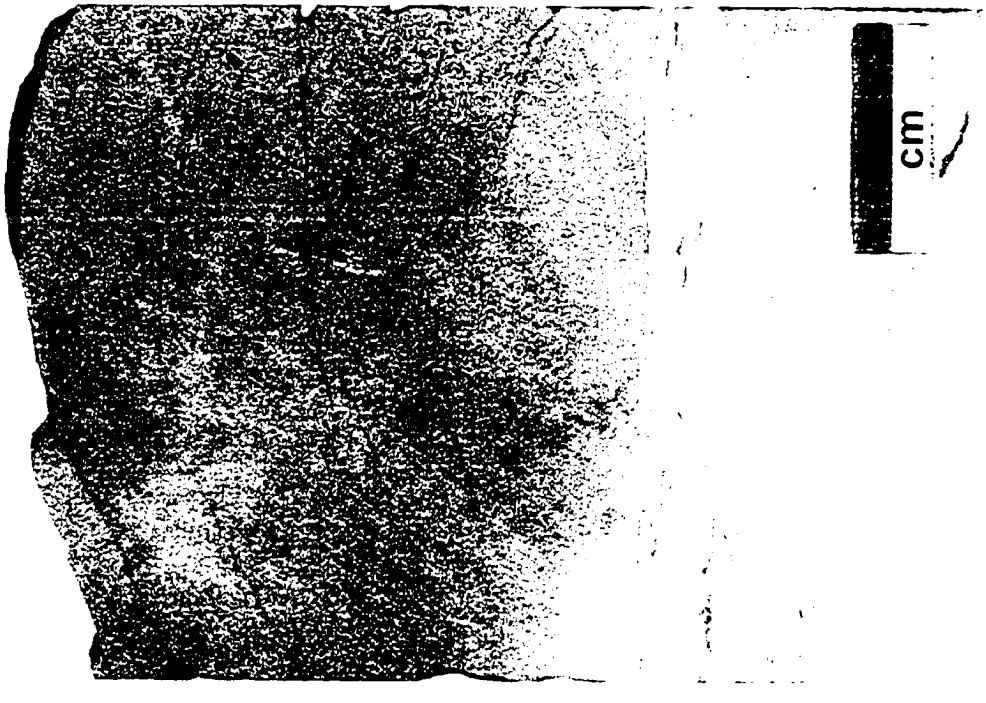

b)

material. Beds contain rare subrounded to rounded black chert pebbles, 2 mm to 3 cm in diameter, either randomly oriented or weakly aligned along internal horizontal and low-angle planar surfaces. Poorly organized coal rip-up clasts and carbonaceous mud laminae are present locally at the base of thicker beds.

Massive sandstone beds are sharp to gradationally interstratified with muddy siltstone laminae/beds; contacts separating massive sandstone and muddy siltstone are locally thoroughly bioturbated. Muddy siltstone laminae/beds are commonly associated with soft-sediment deformation structures; sandstone beds immediately adjacent to contorted muddy siltstone laminae/beds are similarly deformed (Plate 2.16b). Muddy siltstone laminae/beds contain moderate to abundant amounts of dispersed diminutive carbonaceous debris. F4 contains a low-diversity, locally moderate-abundance trace fossil assemblage consisting predominantly of horizontal structures. Trace fossils are present only in contorted muddy siltstone laminae/beds. Identified ichnotaxa include *Planolites*, *Thalassinoides*, *Skolithos*, and *Teichichnus*.

Interpretation

In the sedimentological literature, "massive" is a loosely defined term used to describe both bedding character and appearance of sandstones. Sandstones may appear massive in core due to post-depositional processes such as pedogenesis, bioturbation and diagenesis (Martin and Turner, 1998). However, massive sandstones resulting from depositional processes have been reported from many sedimentary environments including several ancient fluvial examples (e.g. McLean and Jerzykiewicz, 1978; Turner and Monro, 1987; Wizevich, 1992). The lack of clearly defined structure in massive sandstone is more consistent with deposition from laminar flow than from turbulent flows normally associated with fluvial systems (Lowe, 1982). In sediment-gravity flows, laminar flow conditions occur in highly concentrated sediment-water mixtures (Pierson and Costa, 1987). In these flows fluid turbulence is damped, which precludes traction transport and sediment is deposited directly from suspension. Arnott and Hand (1989) experimentally determined that upper-plane bed lamination formed in a fully turbulent flow ceased to form in fine sand when bed aggradation rates exceeded 6.7×10^{-4} m/s.

Thin beds of massive sandstone in F4 are incompatible with deposition from hyperconcentrated laminar or turbulent streamflow.

The interpretation of F4 is based largely on the association between beds of massive sandstone and interstratified contorted silty mudstone laminae/beds. Deformation of massive sandstone has been attributed to liquefaction of water-saturated sands followed by downslope movement (Jones and Rust, 1983). Loosely packed sand is readily liquefied, triggered by things such as seismic shock (Allen and Banks, 1972), however many other triggering mechanisms are possible (Lowe, 1976). These include sediment loading, changes in water level (Doe and Dott, 1980) and cyclical loading by waves (Dalrymple, 1979). All four mechanisms are possible, but sediment loading by bank collapse seems more likely for the massive sandstones containing randomly oriented chert pebbles and coal rip-up clasts. Failure mechanisms are controlled by factors such as sediment texture, cohesiveness, porosity, depth of the channel thalweg and flood magnitude (Laury, 1971). Bank failure due to sediment flow can occur on a large scale and is most common in cohesionless fine- to medium-grained sand (Lowe, 1976), such as that in massive beds of F4. According to Jones and Rust (1983), the parts of a river bed most sensitive to failure are the foreset slopes of major bedforms. Bank collapse and liquefaction in adjacent sand may introduce sediment into one end of a transverse scour at the toeset of a large bedform (Figure 2.7). Sediment may accumulate within the transverse scour, but some can overspill to form massive sheet sandstone. Liquefied sand flows can be highly erosive and capable of reworking underlying sediment to significant depths (Lowe, 1976). Sharp, planar-horizontal or irregular lower bounding surfaces of F4 are interpreted as the base of transverse scours and attest to the erosive nature of liquefied sand flows.

Beds of massive sandstone with faintly developed horizontal to low-angle cross-lamination provide another key to the origin of F4. The upward gradation from massive to faintly laminated sandstone indicates a related origin for both. Jones and Rust (1983) recognized faintly laminated sandstones at the base of some massive sandstone bodies in the Triassic Hawkesbury Sandstone in the Sydney Basin of New South Wales, Australia. The presence of laminae parallel to scour margins was interpreted to have formed by marginal deceleration or "frictional freezing" of a high-concentration sand flow.

Figure 2.7: Model of formation of interstratified massive sandstone and contorted muddy siltstone facies (F4). Bank collapse (A) causes loading of adjacent river bed near the crest of a large bedform (BB'). Liquefaction of the cross-stratified sand (C) generates mass flow of sand with bank-derived mud and coal clasts down the foreset slope and into one end of the transverse scour at its base. The flow partly follows the scour axis (D), generating grooves as the intraclasts are dragged along it, but also spills out to deposit a sand sheet (E), which develops faint stratification at its base as it decelerates and suddenly stops (from Jones and Rust, 1983).

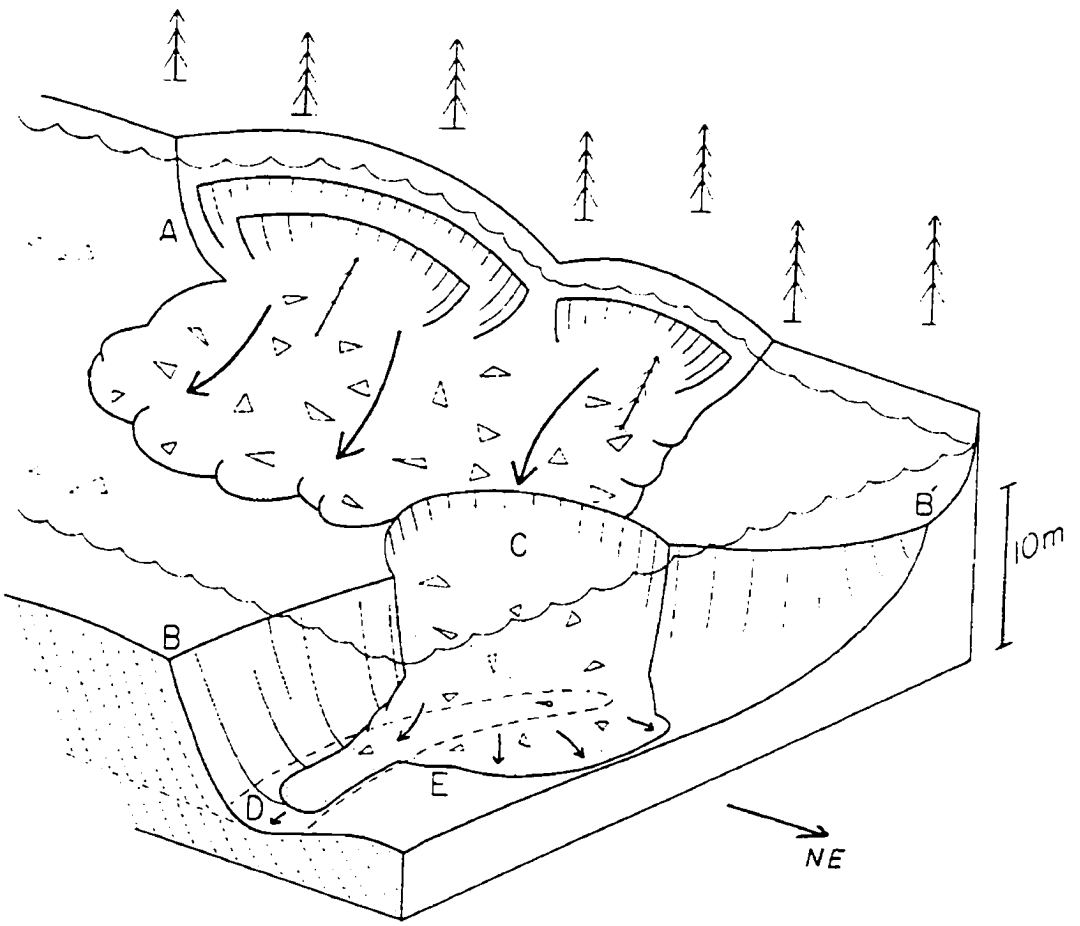
A
B
C
B'
10m
D
E
NE

Similarly, planar-lamination in sandstones interpreted by Lowe (1976) as liquefied flow deposits were attributed to a late-stage process of hydroplastic laminar shear. In both of these examples, the main liquefied sand body continued to flow while laminae accreted at its periphery due to friction at the base and sides. Rapid "freezing" of the main mass of the flow produced the overlying structureless sandstone. Faintly developed horizontal to cross-laminated horizons within massive sandstone beds of F4 are interpreted to have formed in a similar fashion.

2.6 Facies 5: Chert Pebble Conglomerate

Description

Facies 5 (F5) consists of matrix- and clast-supported chert pebble conglomerate occurring in bed sets that range from 10 cm to 1.2 m but average 20-30 cm thick. Bases of F5 are invariably sharp, planar and horizontal or inclined at angles less than 5° (Plate 2.17a). F5 sharply overlies and is sharply to gradationally overlain by strata of F3 and F4. Conglomerate is poorly to moderately sorted and is composed of rounded to well rounded clasts of varicoloured chert, rock fragments and silicified bioclasts (Appendix 2). The matrix of F5 conglomerate is a well sorted, medium- to coarse-grained quartzarenite (McBride, 1963) composed of 90-99% quartz and chert, with minor accessory rock fragments, mica, epidote and feldspar (Appendix 2). Conglomerate beds commonly fine upward with mean clast diameter ranging from 1-3 cm at the base to 2-5 mm near the top (Plate 2.17b). Graded beds also display an upward increase in the amount of sandstone matrix; texturally, conglomerates are transitional from locally clast- to matrix-supported upward within individual beds. Conglomerates show a faint moderate-angle, medium-scale cross-stratification. Cross-stratification is made visible by the alignment of elongate to ovoid 'roller' clasts along internal planar to trough cross-stratified surfaces (Plate 2.18). High-angle cross-stratified conglomerate beds, with foresets dipping beyond the angle of repose, occur locally. Rare carbonaceous material in the form of wood and coal fragments is dispersed along stratification planes within cross-bedded conglomerates. There is an absence of bioturbation within F5; no trace fossils are present

Plate 2.17: Chert Pebble Conglomerate (F5)

a) Sharp, planar and low-angle lower bounding surface (arrow) of matrix-supported chert pebble conglomerate (F5) overlying medium-scale cross-stratified sandstone (F3) with dispersed chert granules. Well 04/06-03-021-09W4/0, 952.5 m.

b) Upward-fining chert pebble conglomerate bed; clasts range from 6-8 mm in width at the base of the sample to 3-5 mm at the top. Note the upward increase in sandstone matrix. Well 04/06-03-021-09W4/0, 950.3 m.

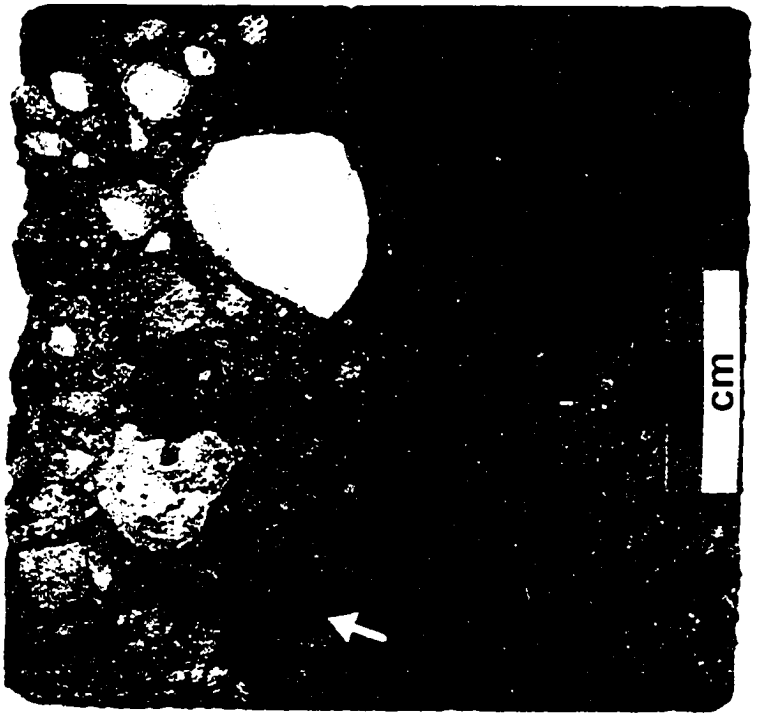

a)

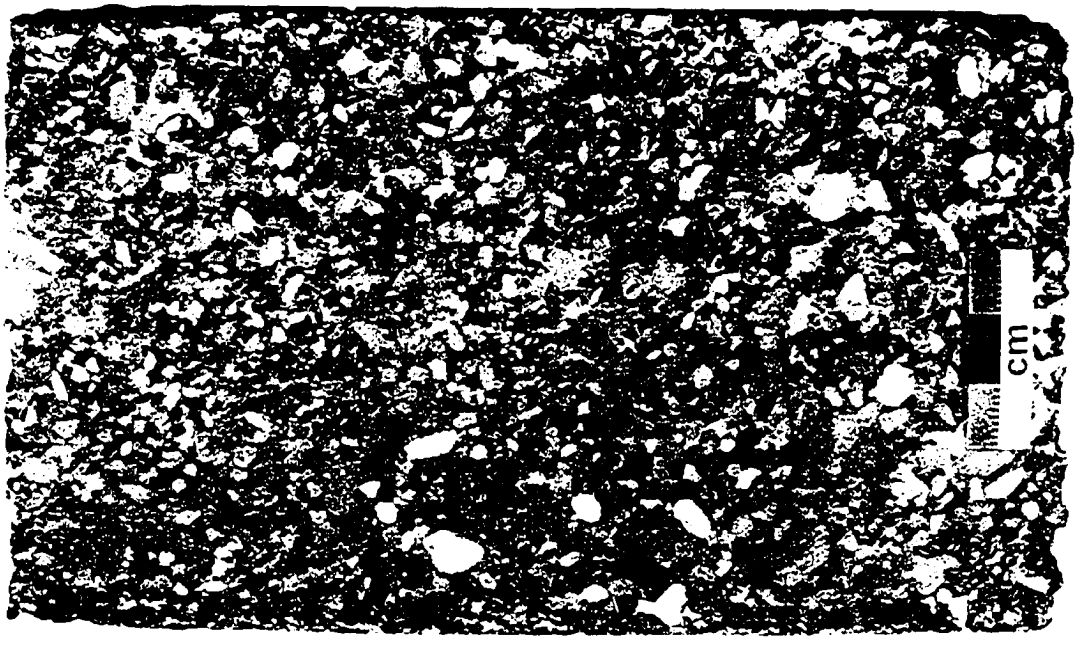

b)

Plate 2.18: Chert Pebble Conglomerate (F5)

Faint moderate-angle, medium scale cross-stratification made visible by the alignment of elongate to ovoid 'roller' clasts along internal planar cross-stratified surfaces.

a) Well 00/13-23-020-09W4/0, 947.0 m.

b) Well 02/10-23-020-09W4/0, 948.3 m.

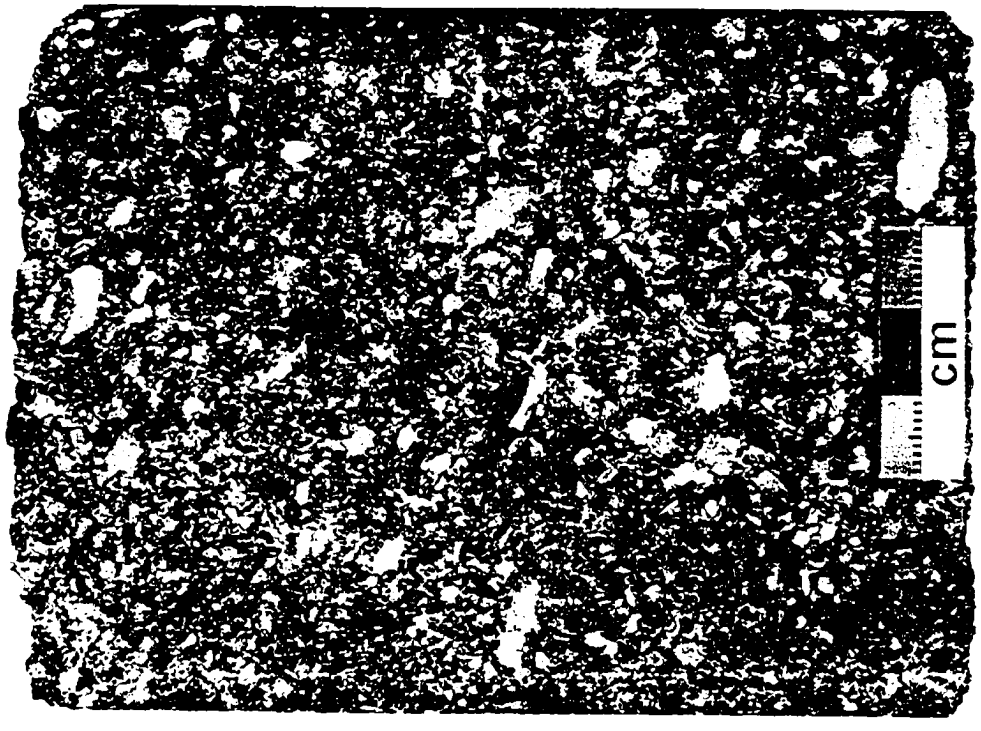

a)

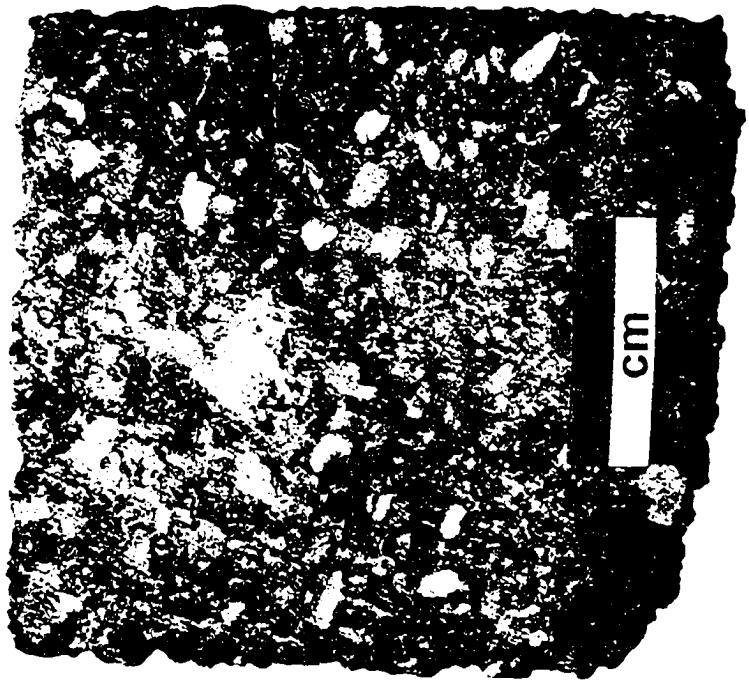

b)

within graded, faintly moderate-angle, medium-scale cross-stratified matrix- and clast-supported chert pebble conglomerate beds.

Interpretation

Graded, medium-scale cross-stratified matrix- and clast-supported chert pebble conglomerates of F5 are interpreted as the migration of subaqueous dunes in a poorly sorted sand-gravel mixture. In fluvial systems, the interactions between the coarse and fine fractions of poorly sorted material during bedload transport results in thin, migrating accumulations of sediment termed bedload sheets (Whiting *et al.*, 1988). Migration of bedload sheets is facilitated by finer sediment filling the interstices between coarser grains, which temporarily reduces the frictional resistance to flow and increases bed shear, which in turn remobilizes the coarse-grain fraction. This leads to a peristaltic movement of coarse particles in the direction of fluid flow. Flume experiments by Dietrich *et al.* (1987) showed that bedload sheets developed only when sand was added to fine gravel and emphasized the need for a poorly sorted sand-gravel mixture to generate these bedforms. Whiting *et al.* (1988) observed bedload sheets migrating up the stoss side of dunes at Muddy Creek, a 5.5-m-wide meandering channel near Boulder, Wyoming. Deposition on the slipface, and consequent dune migration, occurred by periodic arrival of bedload sheets at the brinkpoint and subsequent grain avalanching. Based on the similarity of the composition and sedimentary structures between F5 and fluvial sediments observed at Muddy Creek, it is believed that medium-scale cross-stratified chert pebble conglomerate of F5 indicate bedload sheet transport and subsequent avalanching of heterogeneous sediment on migrating subaqueous dunes in a channel. A continental or marginal-marine channel interpretation is supported by the presence of carbonaceous material. Furthermore, F5 is commonly gradationally overlain by medium-scale cross-stratified sandstone of F3, interpreted as the migration of subaqueous dunes within a tide-dominated estuarine channel system. The association, similarity of dominant sedimentary structures and gradationally interstratified nature between F5 and F3 implies a common genetic origin.

2.7 Facies 6: Interstratified Sandstone, Siltstone and Mudstone

Description

Upward-fining successions of interstratified sandstone, siltstone and mudstone characterize strata of Facies 6 (F6). F6 ranges from 25 cm to 3.5 m and averages 1.5 m in thickness. F6 gradationally overlies medium-scale cross-stratified (F3) or massive (F4) sandstone but, locally, sharply overlies thin conglomerate (F5) or coal beds (F7, see next). Where the lower bounding surface of F6 is sharp, it is overlain with clasts of material eroded from the underlying facies.

Lower successions of F6 are characterized by 40-50 cm thick flaser beds consisting of very fine- to fine-grained sandstone with carbonaceous mudstone laminae (Plate 2.19a). Sandstones are sublitharenites (McBride, 1963) composed of 70% quartz and chert, 30% rock fragments and feldspar and trace amounts of mica (Appendix 2). The comparatively high content of rock fragments and feldspar is macroscopically visible by a faint pinkish-orange colour along coarse-grained laminae. Framework grains are moderately sorted and subangular to subrounded. Up to 30% of the total volume of flaser bedded sandstone consists of fine-grained chlorite and clay-size particles infilling the pores between larger framework grains. Carbonaceous mudstone occurs as low-angle planar to undulating laminae, isolated troughs, and planar tabular to tangential or sigmoidal cross-stratified sets (Plate 2.19b). Mudstone troughs are 2-3 cm wide with tapered or flared edges. Amalgamated, cross-cutting troughs are present in localized successions 1-3 cm thick. Sets of cross-stratified mudstone laminae are 1-2 cm thick and commonly climb at angles between 5-10° (Plate 2.20a). Ichnofossil abundance and diversity in lower successions of F6 is low; bioturbation consists of *Planolites*, *Thalassinoides*, *Teichichnus* and *Zoophycos* traces that cross-cut both sandstone and mudstone lithologies (Plate 2.20b).

Flaser beds grade upwards to a wavy-bedded middle sandy siltstone and mudstone succession. Wavy-bedded successions are 25 cm to 2 m thick and average 70-80 cm. Thickness of interstratified sandy siltstone laminae/beds and mudstone laminae are 0.5-2 cm and 1-5 mm, respectively. Sandy siltstone and mudstone laminae/beds are predominantly horizontally planar-stratified to undulating and rarely low-angle planar

Plate 2.19: Interstratified Sandstone, Siltstone and Mudstone (F6)

a) Flaser-bedded very fine-grained sandstone and carbonaceous mudstone. Mudstone flasers occur as thin, paired couplets of low-angle planar laminae (lower half of photograph) and cross-cutting small-scale troughs and hummocks (upper half of photograph). Well 00/10-23-020-09W4/0, 940.8 m.

b) Flaser-bedded very fine-grained sandstone and carbonaceous mudstone. In this sample carbonaceous mudstone flasers distinguish sigmoidal cross-stratification (1), low-angle planar lamination (2) and trough cross-stratification (3). Note the shallow angle of climb of cross-stratified sets. Well 00/04-23-020-09W4/0, 959.8 m.

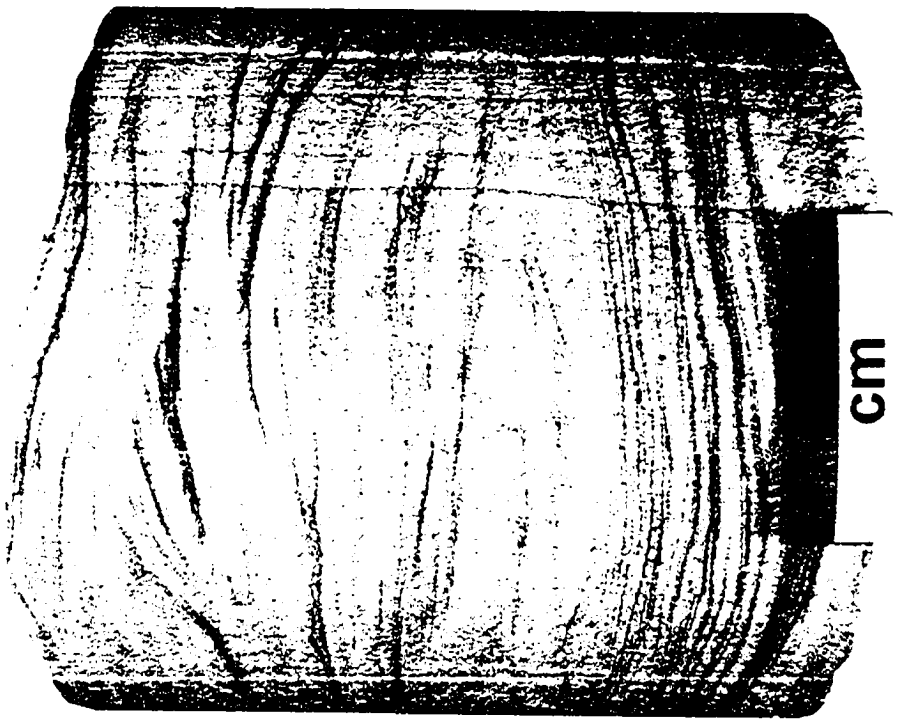

a)

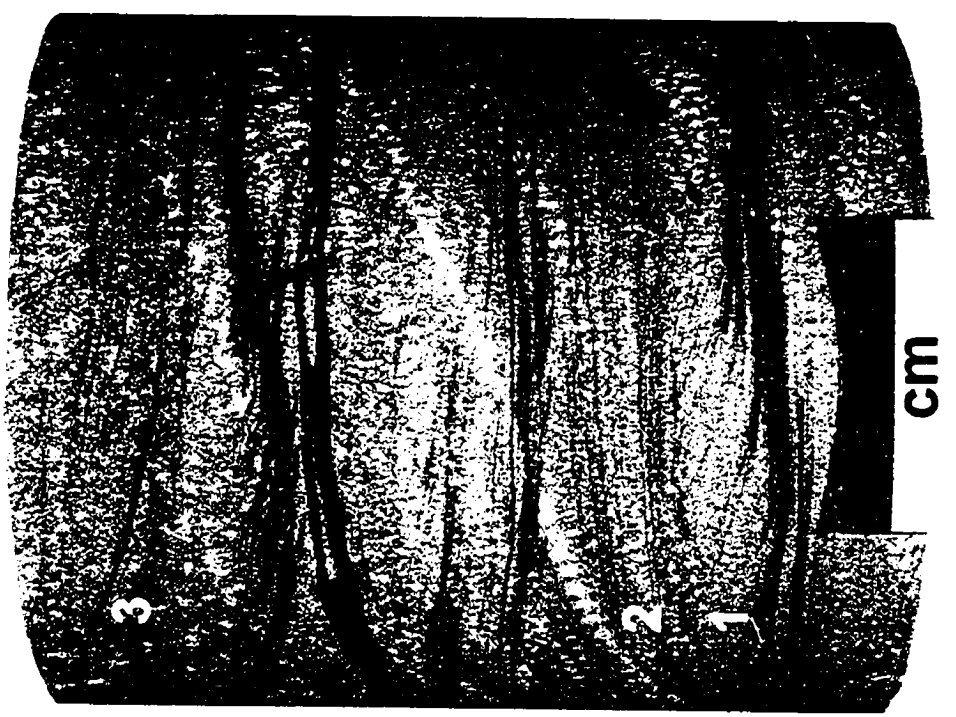

b)

Plate 2.20: Interstratified Sandstone, Siltstone and Mudstone (F6)

a) Climbing sets of cross-stratified mudstone laminae within flaser-bedded fine-grained sandstone. Note scour from overlying sandstone bed (arrow) in top right part of photograph. Well 00/06-23-020-09W4/0, 954.5 m.

b) *Planolites* (Pl), *Thalassinoides* (Th) and *Zoophycos* (Zo) trace fossil assemblage within flaser-bedded interstratified sandstone and carbonaceous mudstone. Horizontal burrow networks occur mainly within mudstone interlaminae, partially homogenizing adjacent sandstone beds into a sandy mudstone to muddy sandstone lithology. Well 02/16-17-020-09W4/0, 967.4 m.

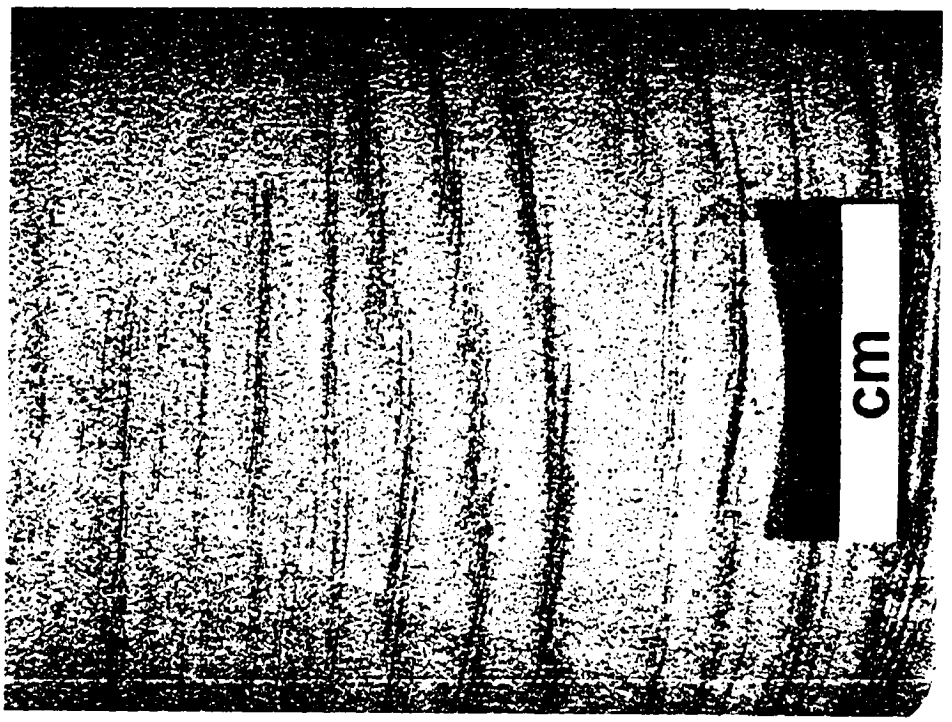

a)

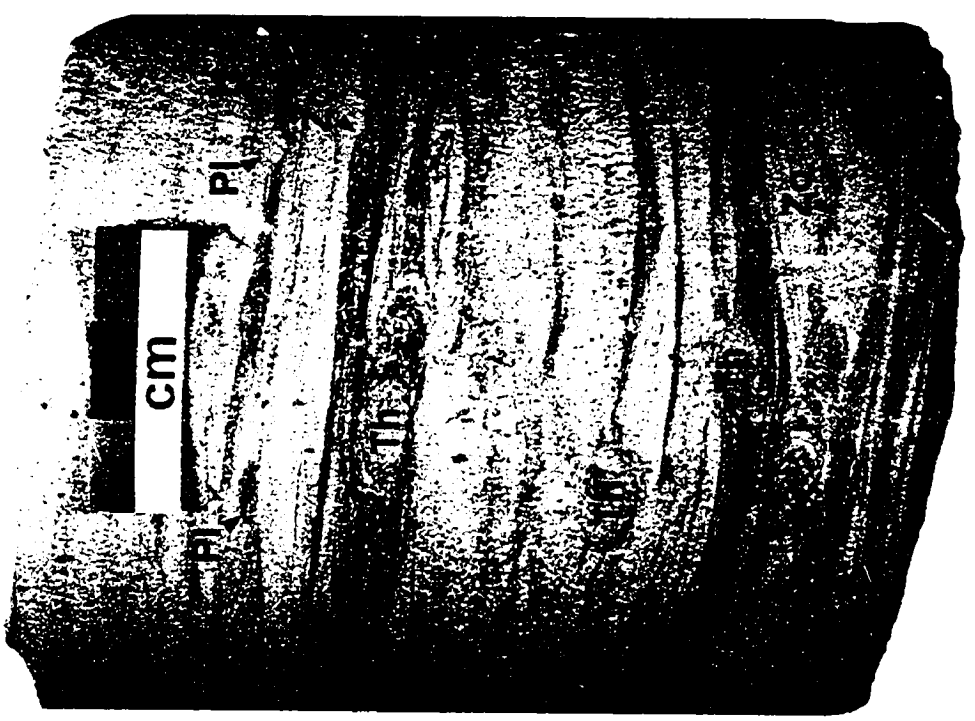

b)

cross-stratified (Plate 2.21a). Primary stratification is commonly disturbed by soft-sediment deformation and locally thinly interstratified siltstone and mudstone laminae are completely overturned. Intercalated siderite beds and lenses 2-13 cm thick occur and are uncommonly associated with vertical calcite-filled fractures a few mm wide and up to 15 cm long. Circular to ovoid pyrite nodules, up to 7 cm in diameter, are randomly dispersed within interstratified siltstone and mudstone. Carbonaceous material is commonly present within mudstone interlaminae as wood and plant fragments and rootlets. Wavy-bedded successions of F6 contain a moderate- to locally high-abundance, moderate-diversity trace fossil assemblage consisting of *Planolites*, *Cylindrichnus*, *Asterosoma*, *Teichichnus*, *Chondrites*, *Skolithos* and fugichnia (Plate 2.21b). Interstratified sandy siltstone and mudstone intervals up to 15 cm thick are locally dominated by a closely spaced, high-abundance monospecific assemblage of diminutive inclined muddy burrows (Plate 2.22a).

Wavy beds, in turn, grade upwards to lenticular beds composed of interstratified carbonaceous mudstone and siltstone that form the tops of F6 successions (Plate 2.22b). Siltstone laminae/beds are commonly a few mm thick but can be up to 2 cm and are encased in thick carbonaceous mudstone successions typically 50-60 cm thick. Siltstones have sharp bases and wavy upper contacts that commonly pinch and swell along undulating stratification planes. Siderite beds up to 12 cm thick and finely disseminated pyrite nodules are present within carbonaceous mudstone intervals. Lenticular beds contain a low-diversity, moderate-abundance trace fossil assemblage consisting of *Planolites*, *Chondrites* and *Teichichnus* with localized occurrences of *Skolithos* and *Cylindrichnus* (Plate 2.23a). Bioturbation is highly concentrated at the margins of interstratified carbonaceous mudstone and siltstone. Within thoroughly bioturbated zones, mudstone and siltstone layers are commonly mixed, producing a homogeneous silty mudstone to muddy siltstone lithology and obscuring primary stratification (Plate 2.23b).

Plate 2.21: Interstratified Sandstone, Siltstone and Mudstone (F6)

a) Wavy-bedded middle sandy siltstone and mudstone succession. Strata are horizontally planar-stratified to undulating and low-angle planar cross-stratified. Note the sparse to abundant bioturbation within interstratified siltstone and mudstone beds. Well 00/08-23-020-09W4/0, 949.0 m.

b) Moderate trace fossil diversity and abundance in wavy-bedded sandy siltstone and mudstone strata. The ichnofossil assemblage consists of diminutive varieties of *Planolites* (Pl), *Cylindrichnus* (Cy) and escape structures (esc). Thorough bioturbation in the lower part of the sample has produced a mottled texture of admixed siltstone and mudstone. Well 00/06-23-020-09W4/0, 952.2 m.

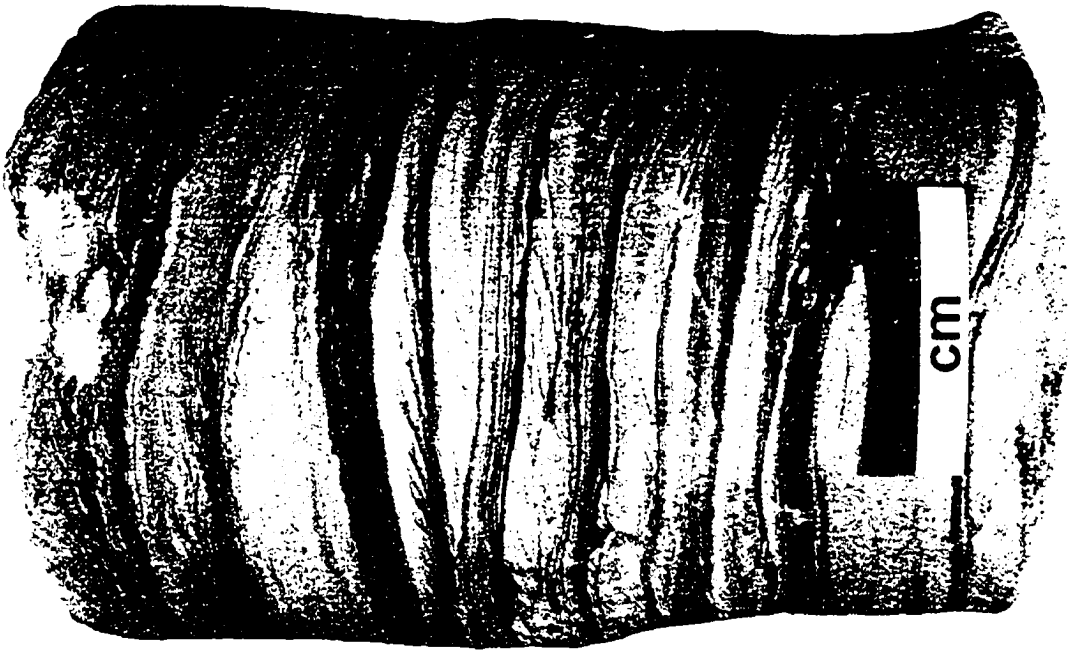

a)

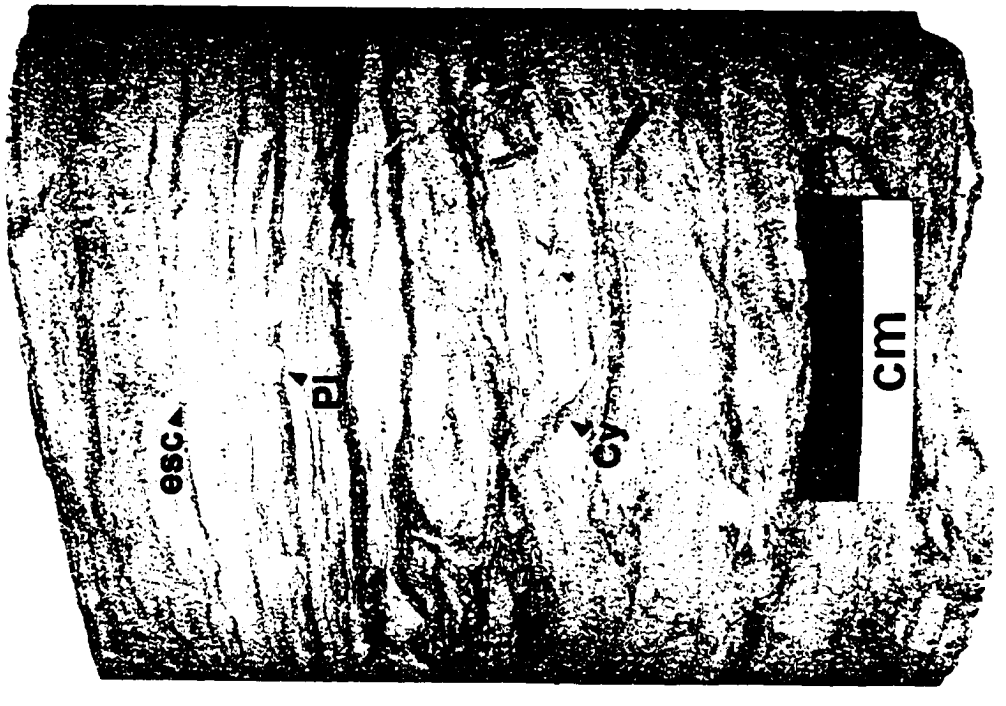

b)

Plate 2.22: Interstratified Sandstone, Siltstone and Mudstone (F6)

a) Closely spaced, high-abundance monospecific assemblage of diminutive inclined muddy burrows within interstratified sandy siltstone and mudstone. The inclined burrows have locally cross-cut a resident assemblage of horizontal, deposit-feeding structures. Note the concentrically laminated, oblate *Asterosoma* (As) burrow within a very fine-grained sandstone interbed in the lower half of the sample. Well 00/04-23-020-09W4/0, 959.0 m.

b) Lenticular bedding composed of interstratified carbonaceous mudstone and siltstone. Siltstone laminae/beds are sharp based and pinch and swell along wavy upper contacts. Interstratified within siltstone layers are thin orange-pink laminae of coarse-grained feldspar and lithic fragments. Well 00/04-23-020-09W4/0, 960.5 m.

a)

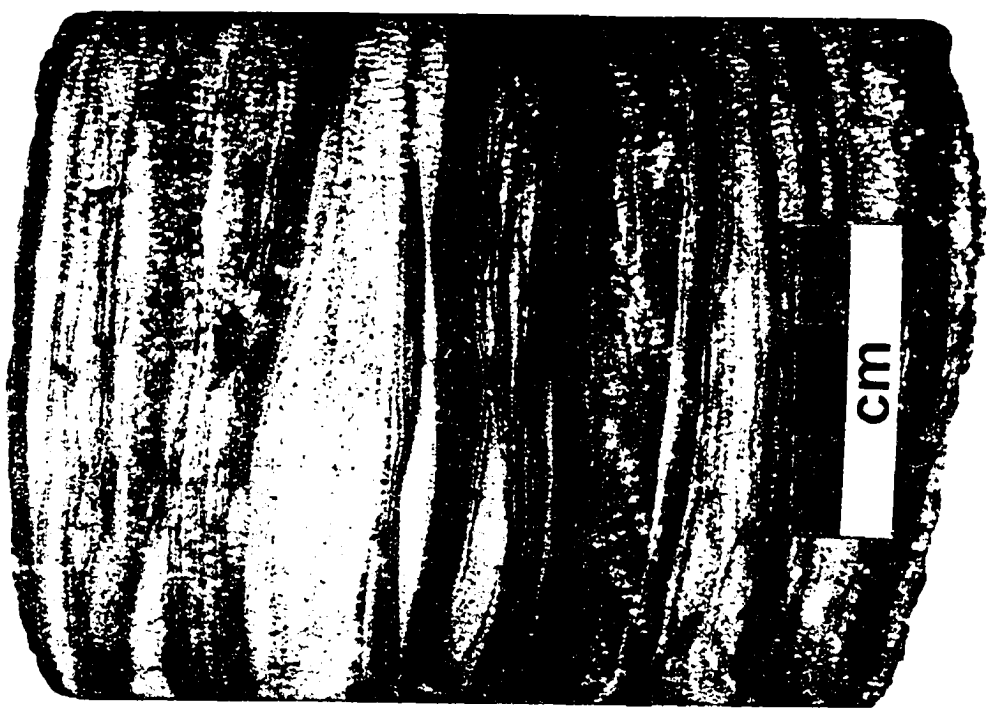

b)

Plate 2.23: Interstratified Sandstone, Siltstone and Mudstone (F6)

a) Low-diversity, moderate-abundance trace fossil assemblage composed of *Teichichnus* (Te), *Planolites* (Pl) and *Chondrites* (Ch) burrows within lenticular bed of interstratified carbonaceous mudstone and siltstone at the top of F6 succession. Well 02/14-11-020-09W4/0, 960.6 m.

b) Thoroughly bioturbated zone of interstratified carbonaceous mudstone and siltstone. Bioturbation has mixed mudstone and siltstone layers, obscuring primary stratification and homogenizing sediment at layer margins. Well 00/04-23-020-09W4/0, 960.7 m.

a)

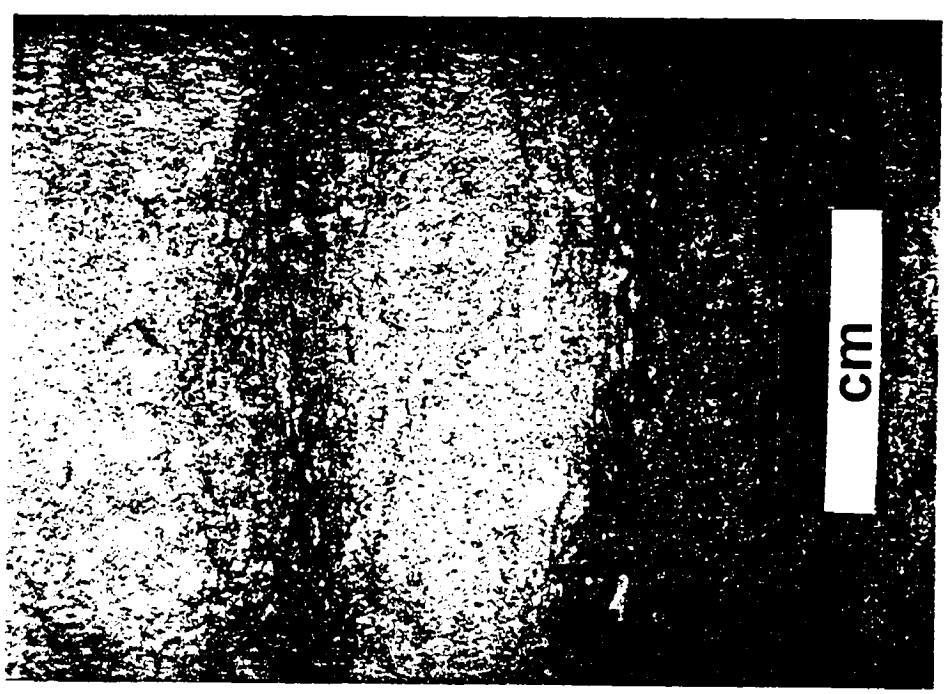

b)

Interpretation

Upward-fining successions of interstratified sandstone, siltstone and mudstone of F6 are interpreted as tidally-influenced, abandoned channel-fill deposits. The upward decrease in grain size, sand/mud ratio and scale of sedimentary structures suggests waning flow conditions associated with channel abandonment (Walker and Cant, 1984). In channel systems, meander loops can be abandoned gradually (chute cut-off) or suddenly (neck cut-off) (Allen, 1965; Figure 2.8). During chute cut-off, meander loops are gradually abandoned when a river reoccupies an old swale across a point bar. This results in gradual flow decrease in the main channel and the development of low-flow sedimentary structures such as small-scale ripple cross-lamination. Neck cut-off involves the breaching of a neck between two meanders and the permanent abandonment of the meander loop. Flow is quickly reduced to zero and results in the abrupt superposition of silt and mud dominated strata. A spectrum of sequences between chute and neck cut-off exist, depending on the length of time required for channel abandonment and the transition from active bedload transport to vertical (suspension) accretion deposition. Local variations in the thickness and lower bounding surface characteristics of F6 imply that channel abandonment was intermediate between the two end-member kinds; however, the predominantly gradational lower contact with underlying active-channel sandstones and the consistent upward transition from flaser to lenticular bedding indicates that channel abandonment was more typically by chute cut-off processes.

Flaser, wavy and lenticular bedding (Reineck and Wunderlich, 1968) observed in F6 is interpreted to reflect the alternation of bedload (sand) and suspension (silt and mud) deposition in abandoned estuarine channels. Sand was likely deposited within the abandoned channel during flooding of the active channel during extraordinary flood tides, possibly associated with spring tides. Mud, on the other hand, accumulated by vertical accretion during the more typical low-energy periods. Although flaser and lenticular bedding are not exclusive to tidally-influenced deposition (e.g. Allen, 1970a), their presence in concert with sigmoidal shaped bed sets of cross-stratified sandstone and carbonaceous mudstone, interpreted as tidal bundles (Boersma and Terwindt, 1981), suggests a tidal influence on fluvial-estuarine sedimentation. Furthermore, the low- to

Figure 2.8: Idealized stratigraphic successions produced during abandonment of channel meander loops by chute and neck cut-off processes. Old channel shown solid, new channels dashed. Chute cut-off involves reoccupation of an old swale and gradual abandonment of the main channel. The resulting succession will consist of trough cross-bedded deposits of the active channel (ACT) and a thick sequence of small-scale cross-laminated fine sand representing gradual abandonment (AB). After cut-off, the sequence is completed by vertical accretion (VA) deposits. In contrast, following neck cut-off, the meander loop is suddenly abandoned and bedload (sand) transport is abruptly diminished. Above the active channel deposits (ACT), the small-scale cross-laminated fine sand representing low-energy flow during abandonment (AB) are very thin, and most of the succession consists of fine-grained vertical accretion (VA) deposits washed into the abandoned loop in suspension during floods (from Walker and Cant, 1984).

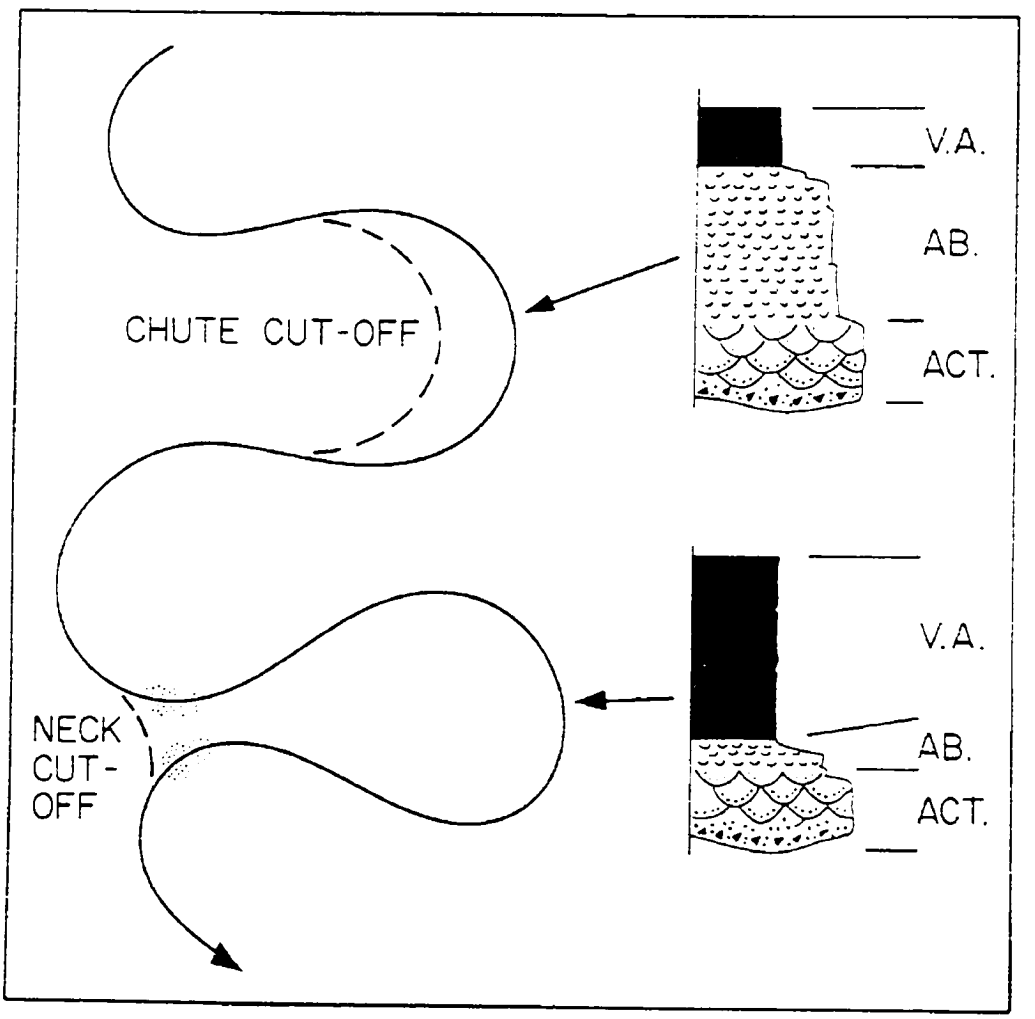
V.A.
AB.
ACT.
CHUTE CUT-OFF
V.A.
AB.
ACT.
NECK
CUT-
OFF

moderate-diversity, moderate- to locally high-abundance trace fossil assemblage dominated by a few diminutive ichnogenera is indicative of brackish water conditions such as those observed in modern and ancient estuarine settings (Wightman *et al.*, 1987; Pemberton and Wightman, 1992; Gingras *et al.*, 1999).

Over the last 15,000 years, the Holocene sea level rise has resulted in the development of extensive estuaries within drowned river valleys and the preferential development of tidally influenced facies (e.g. Campbell and Oaks, 1973; Roy *et al.*, 1980; Colman *et al.*, 1990; Ricketts, 1991). In these estuaries tides are the dominant mechanism that mixes fresh and saline waters, and the sedimentological effect of the tide can be observed well beyond the limit of saline water intrusion (e.g. Gelfenbaum, 1983; Allen, 1984, 1991; Nichols and Biggs, 1985). During reduced fluvial discharge, saline incursions may extend many tens to hundreds of km upstream and tidal processes, including slack water conditions, may occur tens to more than 300 km inland. The Chesapeake estuary on the east coast of the United States, for example, is a microtidal system in which salt water intrusion extends 290 km up the Potomac River, and slack water conditions have been recorded 330 km upstream (Gross, 1972). Tidally-influenced fluvial deposits have been documented from the Turonian to Campanian Straight Cliffs Formation exposed in the Kaiparowits Plateau of southern Utah (Shanley *et al.*, 1992). Within strata of the Straight Cliffs Formation, tidal facies are present in channel-fill strata that are encased in non-marine strata, and ~ 65 km inland from the interpreted coeval palaeoshoreline.

2.8 Facies 7: Carbonaceous Mudstone and Coal

Description

Facies 7 (F7) is composed of carbonaceous mudstone and coal. F7 successions are highly variable in thickness, ranging from 9 cm to 2.8 m and averaging 90 cm thick. Basal contacts are typically gradational with underlying cross-stratified (F3) to massive (F4) sandstone or interstratified sandstone, siltstone and mudstone (F6) (Plate 2.24a). F7 successions are commonly characterized by a 50-75 cm thick lower unit consisting of

Plate 2.24: Carbonaceous Mudstone and Coal (F7)

a) Gradational contact between very fine- to fine-grained massive sandstone (F4) and overlying carbonaceous mudstone and coal (F7). The upward facies transition is characterized by a decrease in grain size, a lowered sand/mud ratio and an increase in the amount of carbonaceous debris over a 5 cm interval. Well 02/16-23-020-09W4/0, 949.4 m.

b) Rooted and pyritized contact between medium-scale cross-stratified fine- to medium-grained sandstone (F3) and overlying bioturbated and carbonaceous silty mudstone (F7). Well 00/13-23-020-09W4/0, 942.7 m.

a)

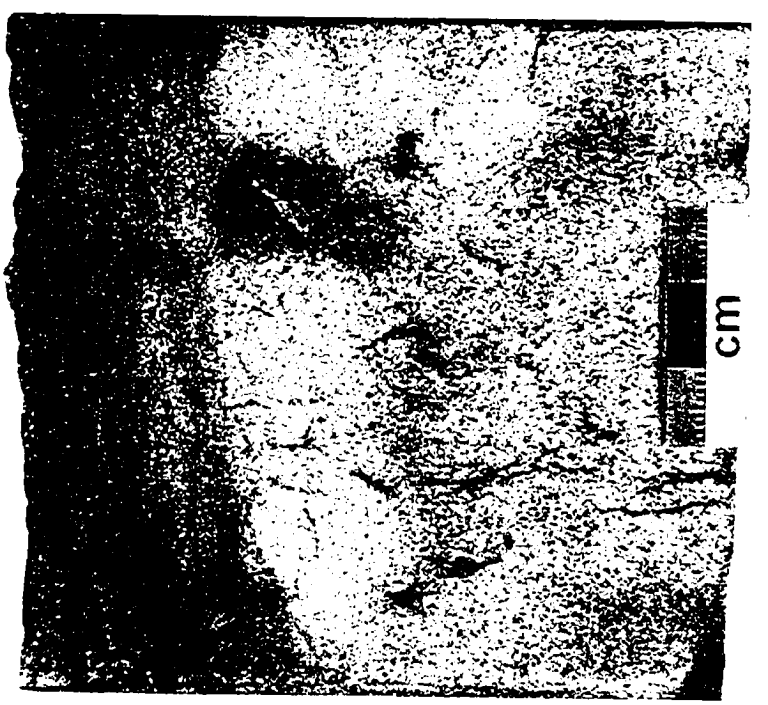

b)

blocky to finely laminated carbonaceous mudstone, sharply to gradationally overlain by a 10-15 cm thick upper unit of coal. Locally, carbonaceous mudstone is absent from F7 and a single coal horizon, up to 60 cm thick, sharply to gradationally overlies rooted sandstone beds of F3, F4 or F6 (Plate 2.24b). Coal beds are commonly erosionally overlain by fine-grained lithic sandstones of the undifferentiated Upper Mannville succession. Locally, coal beds are sharply to gradationally overlain by upward-fining successions of carbonaceous mudstone.

Mudstones are medium to dark grey but locally are tinged pale green or purple. Organic material is sparse to abundant and occurs as rootlets, coalified wood fragments and plant stems, carbonized plant leaf impressions and coal rip-up clasts (Plate 2.25a). Mudstone successions typically become more carbonaceous upward. Carbonaceous mudstones are typically characterized by a blocky textural appearance with well developed slickensides. Rarely, mudstones are fissile along weakly developed horizontal lamination. Coal beds are commonly characterized by the presence of abundant accessory nodular, finely disseminated and mouldic pyrite; nodules are commonly 1-2 cm in diameter but can be up to 10 cm. Coal rarely contains small circular to patchy yellow stained surfaces approximately 3-5 mm wide. Coaly and carbonaceous mudstone beds locally contain low- to moderate-angle cross-stratified chert granules (Plate 2.25b).

Ichnofossil diversity in mudstone beds is low. Traces are dominated by horizontal structures including *Planolites*, *Chondrites*, *Thalassinoides* and *Asterosoma*. Bioturbation intensity is generally low but localized mottled intervals of carbonaceous silty mudstone, 15-20 cm thick, contain a high-abundance trace fossil suite typically dominated by diminutive varieties of *Planolites*. Palynomorph assemblages are dominated by gymnosperm pollen with subordinate lycopod, fern and bryophyte spores, monocolpate angiosperm pollen and algae (A.R. Sweet, pers. comm., 2003; Appendix 3).

Interpretation

Carbonaceous mudstone and coal strata of F7 are interpreted as vertically accreted floodbasin deposits. Deposition of sediment in floodbasins occurs during flood stage of adjacent active stream channels when the river overtops its banks; fine-grained sediment

Plate 2.25: Carbonaceous Mudstone and Coal (F7)

a) Carbonized plant leaf impression along a silty mudstone bedding plane. Well 02/10-19-020-08W4/0, 924.6 m.

b) Moderate-angle, medium-scale cross-stratified coaly mudstone with granular to pebbly chert clasts. Well 00/04-23-020-09W4/0, 961.1 m.

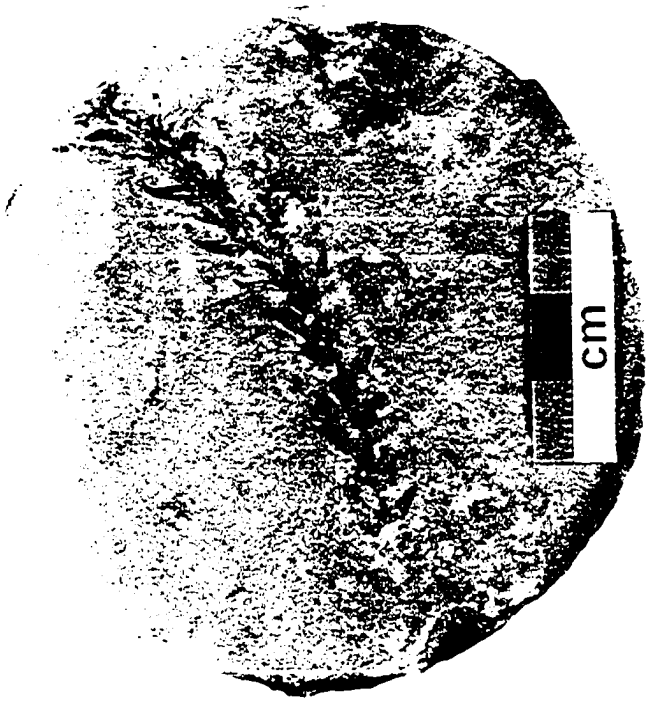

a)

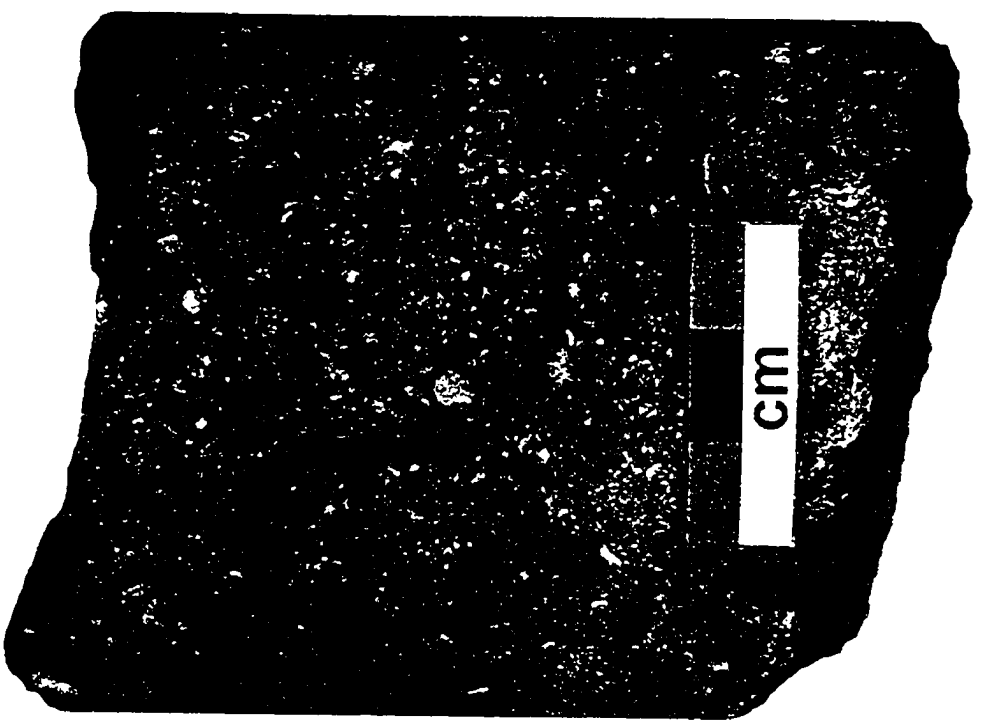

b)

settles from suspension within floodbasins after the coarser sediments have been deposited on more proximal levees and crevasse splays (Walker and Cant, 1984). Thus, blocky to finely laminated, locally upward-fining carbonaceous mudstone beds of F7 represent the accumulation of fine-grained suspended sediment within a floodbasin. Cross-stratified coaly and carbonaceous mudstone beds with chert granules are interpreted as distal crevasse splay deposits extending into the floodbasin (e.g. Hughes and Lewin, 1982). Palynomorph assemblages are mostly dominated by terrestrial, wind-blown bisaccate and Taxodiaceae/Cupressacae/Taxaceae (T/C/T) gymnosperm pollen (A.R. Sweet, pers. comm., 2003). Although consistent with deposition in a continental setting, rare to sparse occurrences of *Classopollis* and *Exesipollenites* pollen, which commonly are found in association with marine dinoflagellates in backshore and shoreface environments (Singh, 1965; Srivastava, 1976), may suggest some mixing of continental and marginal-marine conditions.

The abundance of carbonaceous material and coal horizons suggests a low, wet, thickly vegetated terrestrial environment under humid climatic conditions, such as a backswamp (Reineck and Singh, 1973). The absence of desiccation cracks, iron concretions, evaporite deposits and other features produced by subaerial exposure suggests that the floodbasin never dried out (Collinson, 1986). Swampy and waterlogged floodbasins commonly develop in coastal plain areas in the vicinity of major river confluences. For example, the Atchafalaya River Basin, Louisiana, a large backswamp bounded on two sides by river levees and along its lower end by an abandoned natural levee of the Mississippi River (Coleman, 1966), contains an assemblage of primary, secondary and post-depositional sedimentary structures similar to those observed in carbonaceous mudstone and coal strata of F7. Accordingly, F7 is interpreted to have been deposited in a brackish, waterlogged backswamp located close to a coeval marginal-marine environment.

3. FACIES ASSOCIATIONS

3.1 Introduction

The individual sedimentary facies described and interpreted in Chapter 2 have been grouped into three recurring facies associations (Table 2.1). Facies associations are "groups of facies genetically related to one another and which have some environmental significance" (Collinson, 1969, p. 207). These larger scale facies associations may be regarded as the building blocks of the various depositional systems and their recognition is fundamental to all environmental interpretation (Walker, 1992). The relationship between depositional systems in space and the resulting stratigraphic successions developed through time was first emphasized in Walther's *Law of Facies* (1894). Walther asserted that "it is a basic statement of far-reaching significance that only those facies and facies areas can be superimposed primarily which can be observed beside each other at the present time" (translation from Middleton, 1973, p. 982). Application of this law suggests that facies occurring in a conformable vertical sequence form in laterally adjacent environments. The law applies only to successions without major depositional breaks. Any break in the succession, perhaps marked by an erosive contact or surface of non-deposition, may represent the passage of any number of environments whose deposits were subsequently eroded. These bounding discontinuities are used in this study to separate stratigraphic sequences.

3.2 Facies Association 1: Prograding Shoreface to Shallow Shelf

Description

Facies Association 1 (FA1) consists of two stacked, upward-coarsening successions comprising interstratified fine siltstone to silty mudstone (F1) and cross-stratified coarse siltstone to very fine-grained sandstone (F2). FA1 ranges in thickness from 1.3-7.3 m and averages 4.3 m. It overlies the Ostracode Limestone and is overlain by Facies Associations 2 and 3 (see below) (Figure 3.1; Plate 3.1). The lower bounding surface of

Figure 3.1: Gamma-ray well log and detailed core litholog for 02/06-11-020-09W4/0. The Prograding Shoreface to Shallow Shelf Facies Association (FA1) consists of two upward-shoaling parasequences separated by a marine flooding surface. The lower parasequence begins with interstratified, planar- to wave-ripple laminated siltstone and mudstone (F1) overlain sharply by hummocky cross-stratified very fine sandstone (F2). The upper parasequence grades from bioturbated mudstone to sandy siltstone with soft-sediment deformation structures (F1). The lower parasequence is interpreted to represent storm-dominated, incised lower shoreface deposits (forced regression) overlain by prograding distal delta front deposits (normal regression). See Table 3.1 for a legend to the symbols used.

02/06-11-020-09W4/0 (Gulf et al 102 Jenner 6-1)

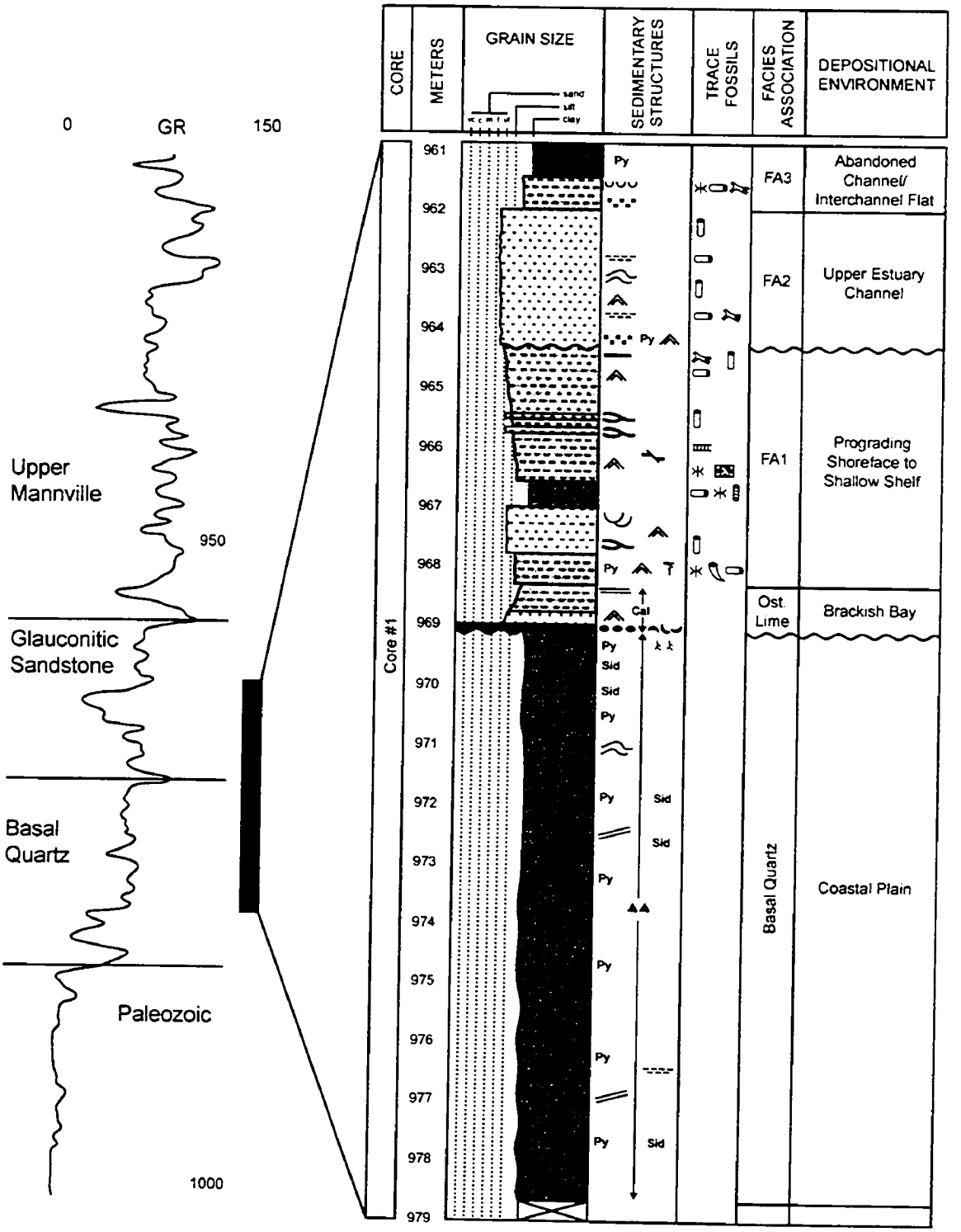

Plate 3.1: Whole core photograph of the Prograding Shoreface to Shallow Shelf Facies Association (FA1) for 02/06-11-020-09W4/0. FA1 sharply overlies calcareous strata of the Ostracode Limestone (OL) and is sharply overlain by oil-stained, fine-grained sandstone of the Upper Estuary Channel Fill Facies Association (FA2). FA1 is divisible into two distinct, upward-coarsening successions. The lower succession consists of a 40 cm thick basal unit of interstratified fine siltstone and silty mudstone (F1) overlain sharply by a 80-cm thick unit composed of hummocky cross-stratified coarse siltstone to very fine-grained sandstone (F2). The base of the overlying succession (dashed line) consists of a 25-cm thick bioturbated silty mudstone bed interpreted as a marine flooding surface. Silty mudstone grades upward into a 2.7 m-thick upward-coarsening unit of interstratified siltstone to silty sandstone (F1). Note the presence of thin, sharp-based interbeds of hummocky cross-stratified coarse siltstone to very fine-grained sandstone (F2) in the upper succession. Box length is 60 cm. Cored interval from 964.1 m to 969.0 m.

Top
FA2
FA1
OL
Bottom

FA1 is sharp, subhorizontal (<5° dip) and planar to slightly undulating; the base is identified on neutron and density porosity well-logs by an abrupt deflection. The lowermost succession is 1-1.5 m thick and begins with a 20-40 cm thick unit of interstratified, planar- to wave-ripple laminated siltstone and mudstone (F1) overlain sharply by hummocky cross-stratified very fine-grained sandstone (F2). The contact between the lower and overlying upward-coarsening successions is marked by an upward decrease in average grain size from very fine-grained sandstone to silty mudstone (Plate 2.1a). This contact is present in 21 of the 26 cores logged in the study area and is distinguished on geophysical well-logs by a (dextral) deflection of the gamma-ray curve (Figure 3.1). The upper succession ranges from 2-3.5 m thick and consists of a 5-35 cm-thick lower unit of intensely bioturbated silty mudstone that grades upward into a 1-1.5 m-thick succession of interstratified fine siltstone and silty mudstone. Interstratified siltstone and mudstone, in turn, are gradationally to sharply overlain by a 1.5-1.8 m-thick upward-coarsening succession of interbedded siltstone and silty sandstone. Sharp-based interbeds, 15-30 cm thick, of hummocky cross-stratified coarse siltstone to very fine-grained sandstone (F2) occur locally within the upper succession. FA1 is present in all wells located in the study area.

Interpretation

FA1 is interpreted as a prograding, storm-dominated shoreface to shallow shelf deposit consisting of two upward-shoaling parasequences separated by a marine flooding surface (*sensu* Van Wagoner *et al.*, 1988). The lower parasequence is interpreted to represent storm-dominated, incised lower shoreface deposits (forced regression) overlain by prograding distal delta front deposits (normal regression). Despite the extensive literature on modern coastal and continental shelf sediments and sedimentation, only a few studies provide systematic detailed descriptions of prograding shorefaces. One such example is the coast of Nayarit, located north of Rio Grande de Santiago on the western coast of Mexico (Figure 3.2). The coast of Nayarit is a broadly arcuate strandplain shoreline that has prograded 10-15 km over a strike distance of 225 km at an average rate of 3 m/y over the last 3600 years (Curray *et al.*, 1969). Well sorted fine and medium

Figure 3.2: (a) Coast of Nayarit, Mexico, showing (b) diagrammatic representation of the physiographic features of the arcuate strandplain with beach ridges and (c) schematic cross-section of the beach ridges plain. It shows a transgressive ravinement surface overlain by a transgressive littoral sand, in turn overlain by the prograding beach ridge complex (regressive shoreface sandbody) (modified from Curray *et al.*, 1969).

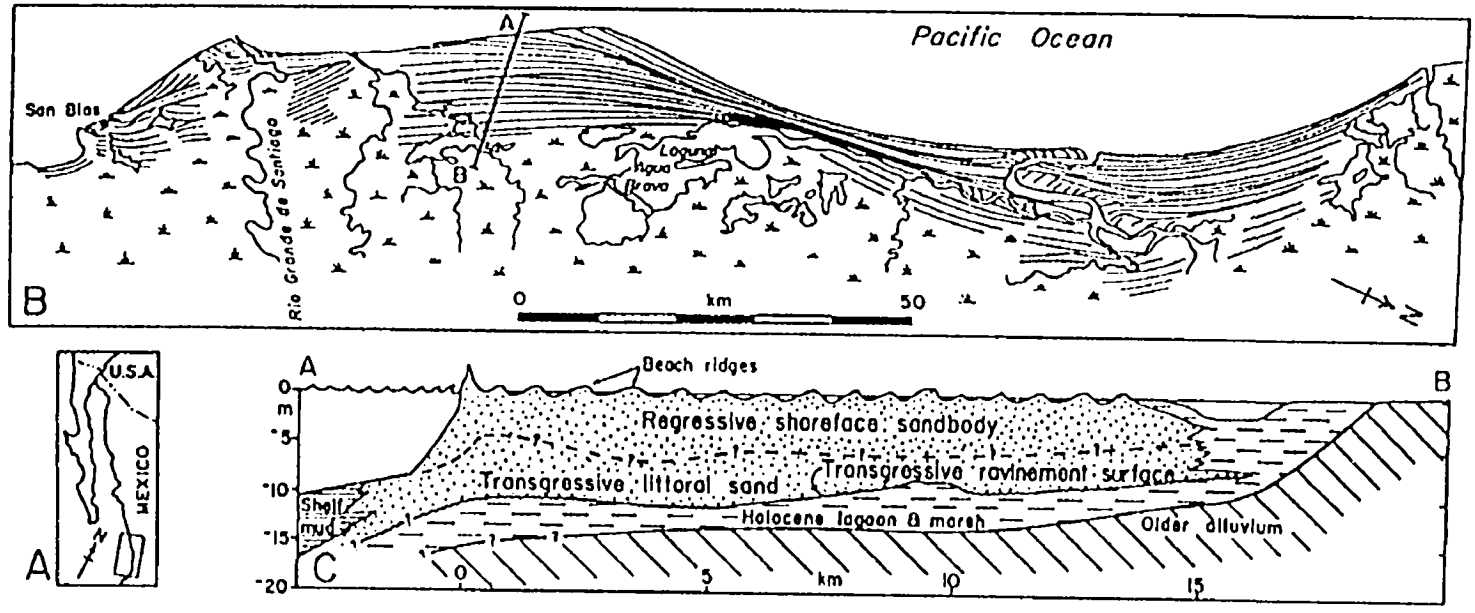
Pacific Ocean
San Blas
Río Grande de Santiago
Laguna Agua Brava
A
B
0
km
50
N
B
U.S.A.
MEXICO
A
Beach ridges
Regressive shoreface sandbody
Transgressive littoral sand
Transgressive ravinement surface
Shelf mud
Holocene lagoon & marsh
Older alluvium
0
-5
-10
-15
-20
m
C
0
5
km
10
15

sand supplied by the Rio Grande de Santiago is distributed along the coast by a powerful wave-driven longshore drift system. Shoreface sand grades seaward into silt and clay at depths ranging from 7-13 m. In addition to the lateral sequence of facies, there is also the beginning of an upward-coarsening succession of prograding shelf to shoreface deposits comparable to FA1 (Figure 3.2c). A second example is the Gulf of Gaeta, Italy, a slowly prograding coast situated north of the Gulf of Naples in the Tyrrhenian Sea. Coastline deposition is controlled by low energy summer periods with seasonal storms and high precipitation during the autumn, winter and spring (Wunderlich, 1971). Below 6 m water depth shoreface sand grades through a transition zone where sediment is silty fine sand to fine-sandy silt. Bioturbation in the transition zone is intense and biogenic structures are dominated by the "press structure" of the heart urchin *Echinocardium cordatum*, a modern equivalent of the ichnogenus *Scolicia* found in ancient marine deposits (Smith and Crimes, 1983). Further basinward, the boundary between the transition zone and shelf varies from 10-20 m water depth (Gadow, 1971). Shelf deposits consist of intensely bioturbated mud with thin, evenly laminated, weakly graded silt layers that decrease in thickness and abundance away from the coast. Silt layers are sourced mainly from sediment discharged from the Volturno delta, and to a lesser extent by sediment taken into suspension and transported away from the coast during storms (Reineck and Singh, 1971). The hypothetical progradational vertical sequence of sediments in the Gulf of Gaeta is shown in Figure 3.3.

The progradation of a clastic shoreface onto a muddy shelf forms an upward-coarsening sedimentary sequence in which sand beds become progressively thicker and more abundant upward (e.g. Tyler and Ambrose, 1986; Rosenthal and Walker, 1987; Swift *et al.*, 1987). Within the Turonian Cardium Formation of Alberta, Plint (1988) interpreted gradational- and sharp-based, upward-coarsening sandbodies as prograding, storm-dominated shoreface and shallow shelf deposits (Figure. 3.4). The lower FA1 parasequence resembles facies associations A and C of the sharp-based Cardium shoreface sequence (Figure 3.4b) and is interpreted to have developed in response to a lowering of relative sea-level that exceeded the rate of basin subsidence. The upper FA1 parasequence is similar to facies associations A and B of the gradational-based Cardium shoreface sequence (Figure 3.4a). The upward change from sharp-based, lower shoreface

Figure 3.3: Compilation of the sedimentary features of the beach-shelf mud profile off Gulf of Gaeta, Italy. The results are presented in a vertical sequence, which would develop in a prograding coast. An analogous shelf to backshore sequence is interpreted to have developed during deposition of FA1. The dashed horizontal line shows the approximate preservation limit of the FA1 succession; overlying shoreface to backshore strata were subsequently eroded due to transgressive ravinement and incision (see Chapter 4). Note the similarities between the shelf-mud, transition-zone and lower shoreface successions and FA1, including the upward-coarsening average sediment grain size, thinly laminated silty layers, hummocky cross-stratification and intensely bioturbated silty mudstone beds with abundant heart urchin traces, equivalent to *Scolicia* ichnofossils observed in F1 (modified from Reineck and Singh, 1973).

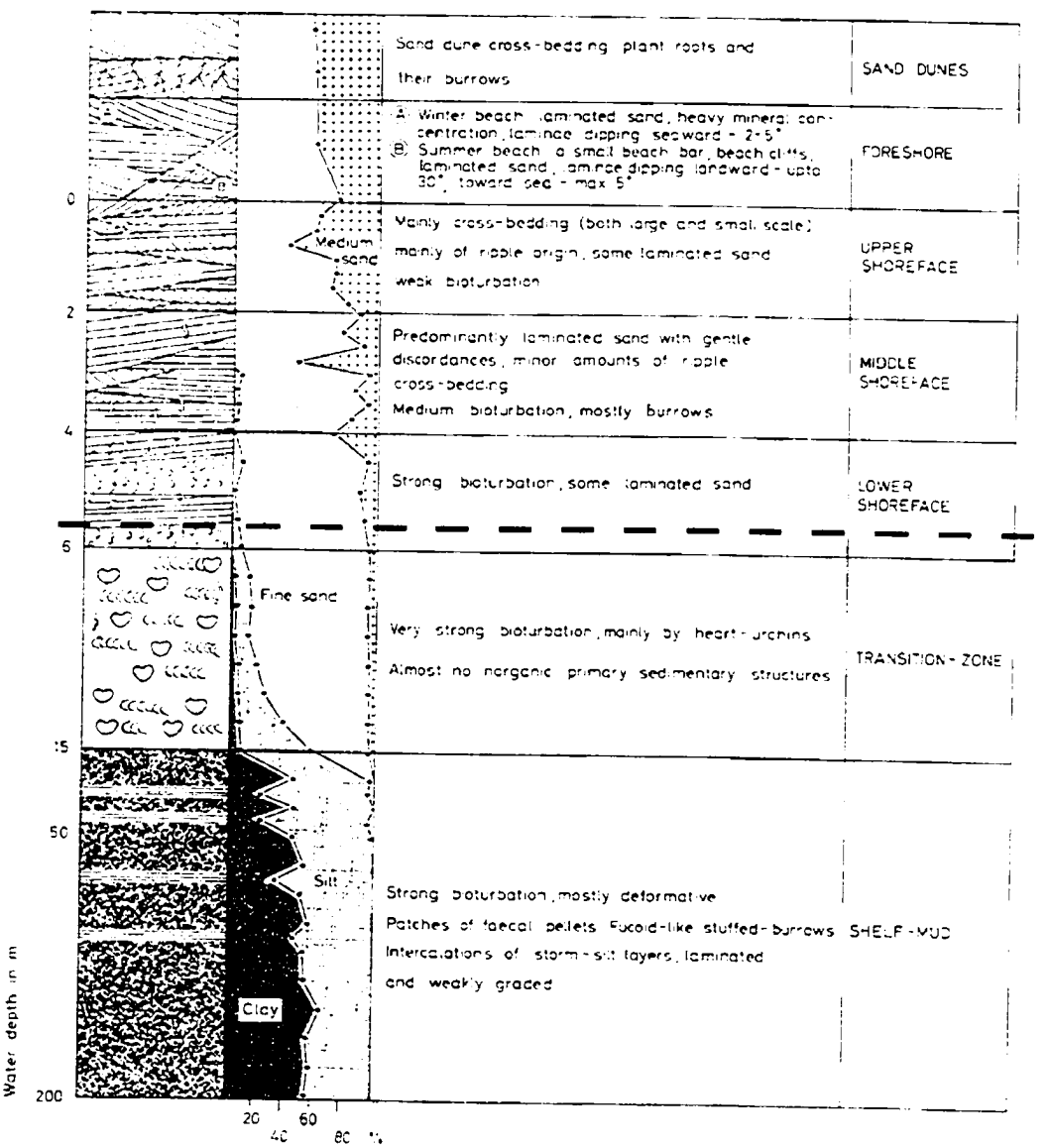
Sand dune cross-bedding, plant roots and their burrows
SAND DUNES
(A) Winter beach, laminated sand, heavy mineral concentration, laminae dipping seaward - 2-5°
(B) Summer beach, a small beach bar, beach cliffs, laminated sand, laminae dipping landward - upto 30°, toward sea - max 5°
FORESHORE
Mainly cross-bedding (both large and small scale) mainly of ripple origin, some laminated sand
weak bioturbation
Medium sand
UPPER SHOREFACE
Predominantly laminated sand with gentle discordances, minor amounts of ripple cross-bedding
Medium bioturbation, mostly burrows
MIDDLE SHOREFACE
Strong bioturbation, some laminated sand
LOWER SHOREFACE
Fine sand
Very strong bioturbation, mainly by heart-urchins
Almost no norganic primary sedimentary structures
TRANSITION-ZONE
Silt
Strong bioturbation, mostly deformative
Patches of faecal pellets, Fucoid-like stuffed-burrows
Intercalations of storm-silt layers, laminated and weakly graded
SHELF-MUD
Clay
Water depth in m
0
2
4
6
15
50
200
20
40
60
80
%

Figure 3.4: Schematic lithologs contrasting the facies sequence seen in (a) gradational and (b) sharp-based shoreface sequences of the Cardium Formation. Note the similarity between facies associations A and C of the sharp-based sequence and the lower FA1 parasequence and between facies associations A and B of the gradational-based sequence and the upper FA1 parasequence (modified from Plint, 1988).

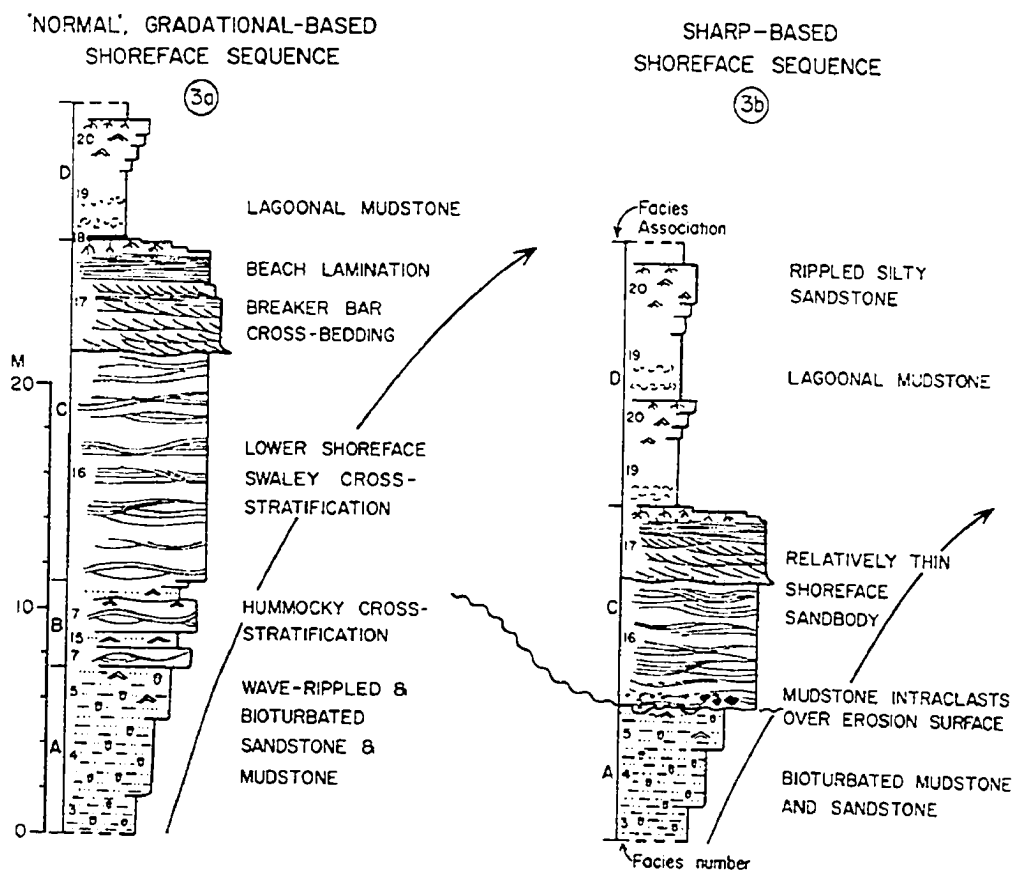
'NORMAL', GRADATIONAL-BASED
SHOREFACE SEQUENCE
3a
SHARP-BASED
SHOREFACE SEQUENCE
3b
LAGOONAL MUDSTONE
BEACH LAMINATION
BREAKER BAR
CROSS-BEDDING
LOWER SHOREFACE
SWALEY CROSS-
STRATIFICATION
HUMMOCKY CROSS-
STRATIFICATION
WAVE-RIPPLED &
BIOTURBATED
SANDSTONE &
MUDSTONE
Facies
Association
RIPPLED SILTY
SANDSTONE
LAGOONAL MUDSTONE
RELATIVELY THIN
SHOREFACE
SANDBODY
MUDSTONE INTRACLASTS
OVER EROSION SURFACE
BIOTURBATED MUDSTONE
AND SANDSTONE
Facies number
M
20
10
0
A
B
C
D

to gradationally-based, transitional offshore deposits within strata of FA1 is interpreted to have resulted from a minor deepening event during a long-term regression. Consequently, a marine flooding surface, demarcated by the 5-35 cm thick bioturbated silty mudstone bed, conformably rests between the lower and upper parasequences. Continued progradation following this temporary rise in relative sea-level is indicated by the upward-coarsening, prograding, transitional offshore and distal delta front deposits of the overlying parasequence. Thin, sharp-based interbeds of hummocky cross-stratified coarse siltstone to very fine-grained sandstone (F2) within interstratified fine siltstone and silty mudstone (F1) represent high-energy storm deposition.

Many examples of ancient prograding shorefaces have been recognized, particularly in Cretaceous strata of the Western Interior Seaway of North America (e.g. McCrory and Walker, 1986; Nummedal and Swift, 1987; Plint and Walker, 1987; Plint and Norris, 1991). For example, a complete vertical facies succession of a single upward-coarsening parasequence of the Lower Cretaceous Viking Formation in Joffre field, Alberta consists of marine shale, bioturbated silty mudstone, bioturbated sandy mudstone and bioturbated to laminated muddy sandstone (MacEachern *et al.*, 1998). Like the gradationally-based, prograding upper parasequence of FA1, middle and upper shoreface deposits are absent above the uppermost Viking parasequence. In this case, multiple incisions and subsequent transgressive ravinement have been responsible for removal of the shallow-water portion of the system. As will be discussed in Chapter 4, similar transgressive ravinement eroded middle and upper shoreface deposits of FA1; however, this transgressive surface of erosion also coincides with a sequence boundary, produced by later subaerial exposure resulting from a fall in relative sea-level, and is overlain by estuarine channel fill and interchannel deposits of Facies Associations 2 and 3.

3.3 Facies Association 2: Upper Estuary Channel Fill

Description

Facies Association 2 (FA2) comprises an upward-fining succession consisting of dune and ripple cross-stratified sandstone (F3), interstratified massive sandstone and

contorted muddy siltstone (F4) and chert pebble conglomerate (F5). Locally FA2 ranges from 1.2-9.3 m thick and averages 4.5 m thick. Throughout the study area, FA2 overlies strata of the Prograding Shoreface to Shallow Shelf Facies Association (FA1) and is overlain by the Tidally-Influenced Abandoned Channel/Interchannel Deposits Facies Association (FA3, see next) (Figure 3.5; Plate 3.2). The lower contact is commonly sharp and either planar-horizontal to slightly undulating or highly irregular. FA2 consists predominantly of fine to medium sandstone (F3 and F4) and conglomerate (F5) and is characterized on geophysical well-logs by a blocky profile on the gamma-ray curve (Figure 3.5). The vertical facies succession of FA2 is characterized by a lower unit of dune cross-stratified medium sandstone (F3), locally interbedded with conglomerate (F5), overlain by ripple cross-laminated to massive fine to medium sandstone (F3 and/or F4). FA2 is spatially restricted to a narrow N-S trending curvilinear body located between Townships 19-21, Range 9W4 (Figure 3.6). FA2 extends northward to sections 1 and 2 in Township 21, Range 9W4 where it is truncated by strata of the Jenner shoreface complex (see Chapter 1). To the south, FA2 grades into strata of Facies Association 3 in Section 23, Township 19, Range 9W4. In the Jenner Upper Mannville E Pool, the FA2 reservoir unit is approximately 10 km long and 2 km wide. There is a spatial distribution of facies comprising FA2 with a pronounced fining from north to south. The northern portion of the pool consists mainly of medium sandstone (F3) and conglomerate (F5). Wells penetrating strata of F5 are located primarily in sections 14 and 23, Township 20, Range 9W4 and are interbedded with thick F3 deposits. In contrast, the southern and central portions of the pool are dominated by intercalated sharp- or gradational-based fine to medium sandstone (F3 and F4). F3 units decrease in thickness toward the centre of the pool. FA2 successions are commonly thicker in the northern part of the pool (Figure 3.6).

Interpretation

Strata of FA2 are interpreted to represent laterally accreting point bar deposits in a tidally-influenced upper estuary meandering channel. Flow in meandering channel bends is helicoidal with a component of surface flow towards the outer bank and bottom flow

Figure 3.5: Gamma-ray well log and detailed core litholog for 02/14-11-020-09W4/0. In this well the Upper Estuary Channel Fill Facies Association (FA2) consists of dune cross-stratified sandstone (F3) and interstratified massive sandstone and contorted muddy siltstone (F4) with several bioturbated silty mudstone interbeds. See Table 3.1 for a legend to the symbols used.

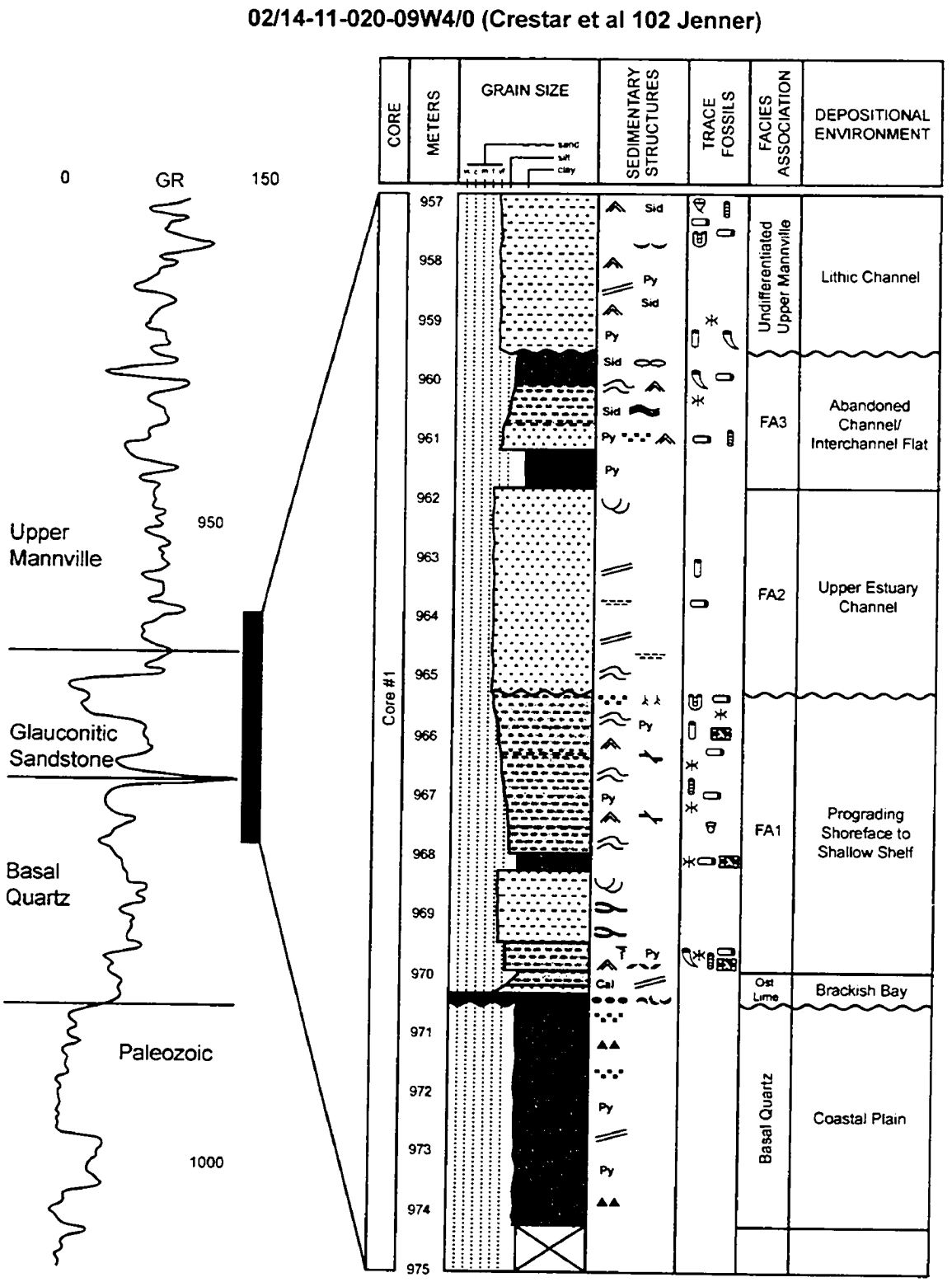
02/14-11-020-09W4/0 (Crestar et al 102 Jenner)
CORE
METERS
GRAIN SIZE
SEDIMENTARY STRUCTURES
TRACE FOSSILS
FACIES ASSOCIATION
DEPOSITIONAL ENVIRONMENT
0
GR
150
Upper Mannville
950
Glauconitic Sandstone
Basal Quartz
Paleozoic
1000
Core #1
957
958
959
960
961
962
963
964
965
966
967
968
969
970
971
972
973
974
975
Undifferentiated Upper Mannville
Lithic Channel
FA3
Abandoned Channel/ Interchannel Flat
FA2
Upper Estuary Channel
FA1
Prograding Shoreface to Shallow Shelf
Ost Lime
Brackish Bay
Basal Quartz
Coastal Plain

Plate 3.2: Whole core photograph of the Upper Estuary Channel Fill Facies Association (FA2) for 02/14-11-020-09W4/0. FA2 erosionally overlies strata of the Prograding Shoreface to Shallow Shelf Facies Association (FA1) and is sharply overlain by the Tidally-Influenced Abandoned Channel/Interchannel Deposits Facies Association (FA3). FA2 consists of an interbedded succession composed of dune cross-stratified sandstone (F3) and interstratified massive sandstone and contorted muddy siltstone (F4). Note the horizontal to inclined trace fossils in silty mudstone to muddy siltstone interbeds. Box length is 60 cm. Cored interval from 961.2 m to 965.8 m.

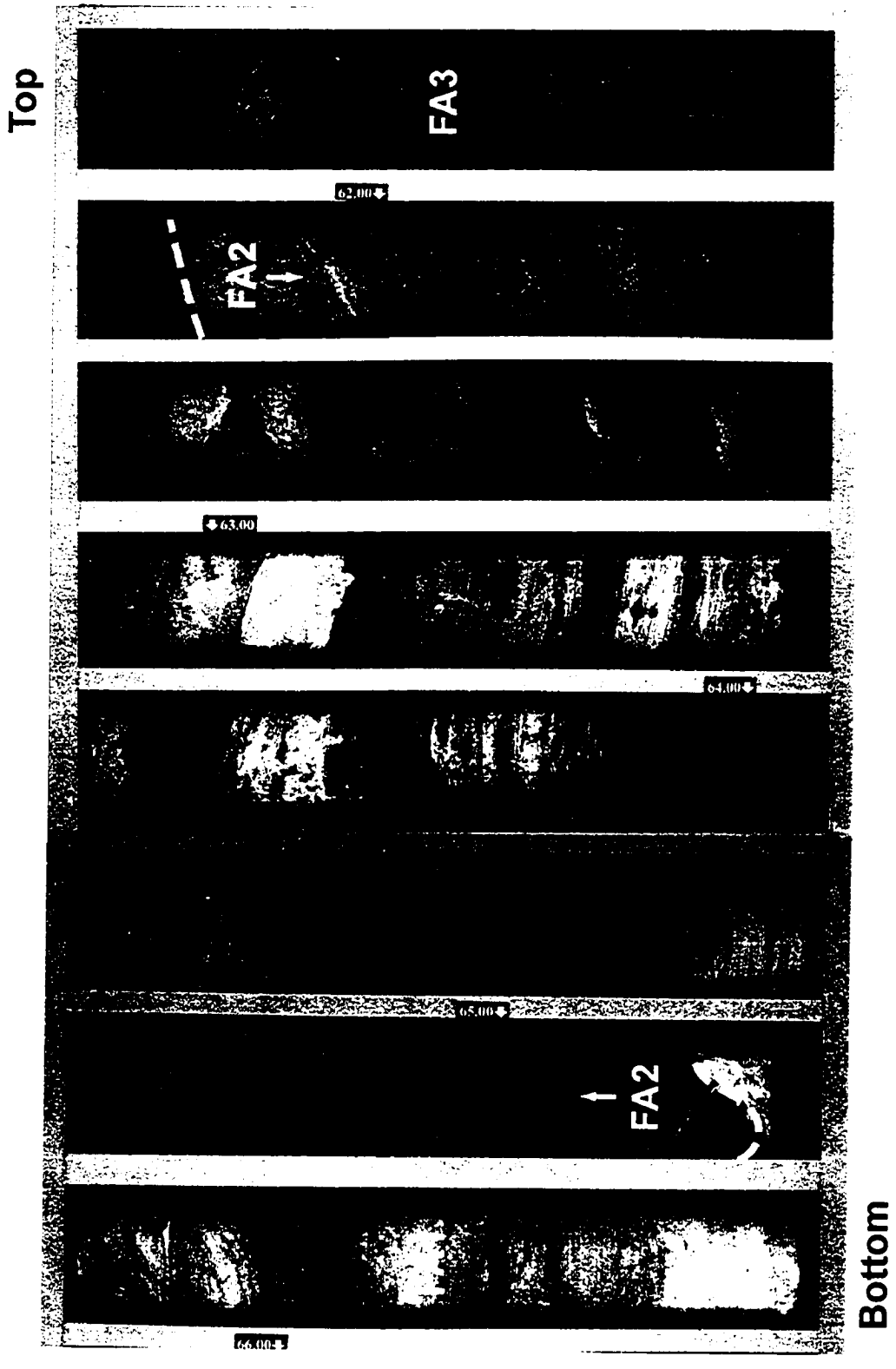
Top
FA3
62.00
FA2
63.00
64.00
65.00
FA2
66.00
Bottom

Figure 3.6: Gross sandstone isopach map for FA2. The N-S trending curvilinear geometry of the sandbody resembles a narrow channel and suggests that FA2 is the preserved remnant of an upper estuary channel fill. The FA2 reservoir is cross-cut and partially compartmentalized by impermeable lithic channels (dashed line) of the stratigraphically-younger, undifferentiated Upper Mannville succession and is truncated by strata of the Jenner shoreface complex (hatchered line) to the north. Note the thicker gross sandstone in the northern part of the study area. Contour interval is 3 m.

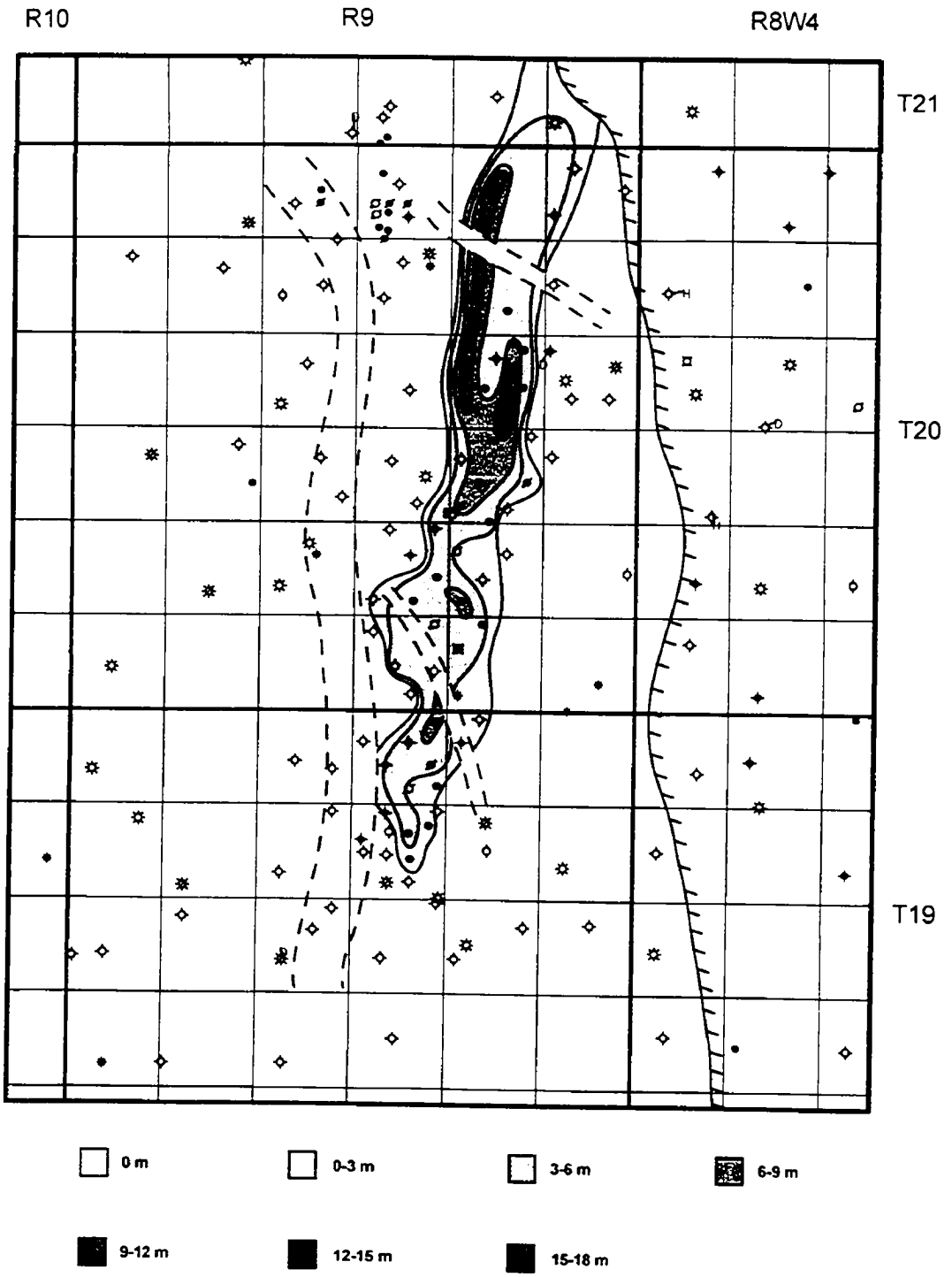
R10
R9
R8W4
T21
T20
T19
0 m
0-3 m
3-6 m
6-9 m
9-12 m
12-15 m
15-18 m

towards the inner bank (Fisk, 1947). The axis of maximum flow velocity, the thalweg, alternates from side to side of the channel as the helicoidal flow changes its sense of rotation in successive meander loops. As a result of the flow pattern, the outer concave bank is usually the site of erosion and the inner convex bank the site of deposition; the inner bank coincides with a laterally accreting point bar surface (Figure 3.7a). The point bar facies model predicts the pattern of distribution of grain size and bedforms over this surface and the vertical succession of facies produced by lateral accretion (Figure 3.7b; see Miall, 1978, 1987 for historical reviews). Lateral migration of the channel deposits a tabular sand unit overlying a near-horizontal erosion surface commonly overlain by a thin conglomerate lag. Waning flow energy, the upslope component of the secondary helicoidal flow and gravity cause the transport pathways of heterogeneous bedload sediment to diverge, resulting in the upward-fining vertical succession (Figure 3.7a inset). Bedforms also change upward, with dunes passing gradationally upward into ripples and lower plane bed (Bridge and Jarvis, 1982). The thickness of the overall sand sequence compares closely with the depth of the channel and the relative abundance and distribution of the various structures are controlled by channel size and sinuosity (Allen, 1970b). It is important to note that this well-accepted model of point bar deposition assumes bankfull discharge, fully developed helicoidal flow and uniformity of conditions along the length of the point bar surface (Collinson, 1986). Variations in the makeup of lateral accretion (point bar) deposits between and within meandering systems reflect non-uniformity and unsteadiness of flow and modification during low flow conditions. Some of the divergences from the classical model become most apparent when the bed material contains a high proportion of either gravel (bed load) or fine (suspended load) sediment. For example, Jackson (1976) demonstrated that some gravel-dominated meandering fluvial systems with little or no mud show no upward-fining trend.

The physical sedimentological processes in meandering streams, including open flow dynamics and formation of lateral accretion deposits, are similar in both fluvial and tidally-influenced channel systems. Additionally, the vertical profiles of point bar successions produced by migrating fluvial and tidal channels are similar. For example, an idealized vertical succession for tidal-inlet deposits constructed by Kumar and Sanders (1974) included the following characteristics: 1) an erosional base overlain by a

Figure 3.7: (a) Schematic illustration of a hypothetical point bar and the formation of lateral accretion deposits. Secondary helicoidal flow is deflected from high pressure on the outer bank toward low pressure on the inner bank, resulting in sediment deposition and the formation of point bars by lateral accretion. Gravitational forces are greater for larger particles than smaller particles; the net result is that coarser particles are deposited near the toe of the point bar and smaller particles are transported towards the top. The point bar facies model (b) predicts the pattern of distribution of grain size and bedforms over a single point bar surface and distinguishes between lateral and vertical accretion deposits of meandering rivers (from Walker and Cant, 1984; and Thomas *et al.*, 1987).

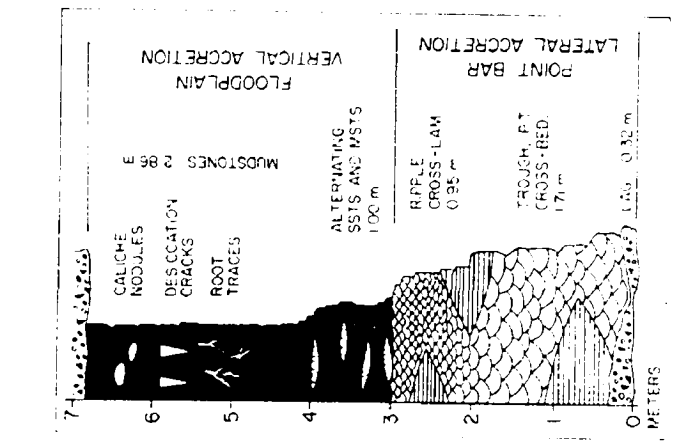
FLOODPLAIN
VERTICAL ACCRETION
POINT BAR
LATERAL ACCRETION
CALICHE NODULES
DESICCATION CRACKS
ROOT TRACES
ALTERNATING SSTS AND MSTS
RIPPLE CROSS-LAM
METERS

b)

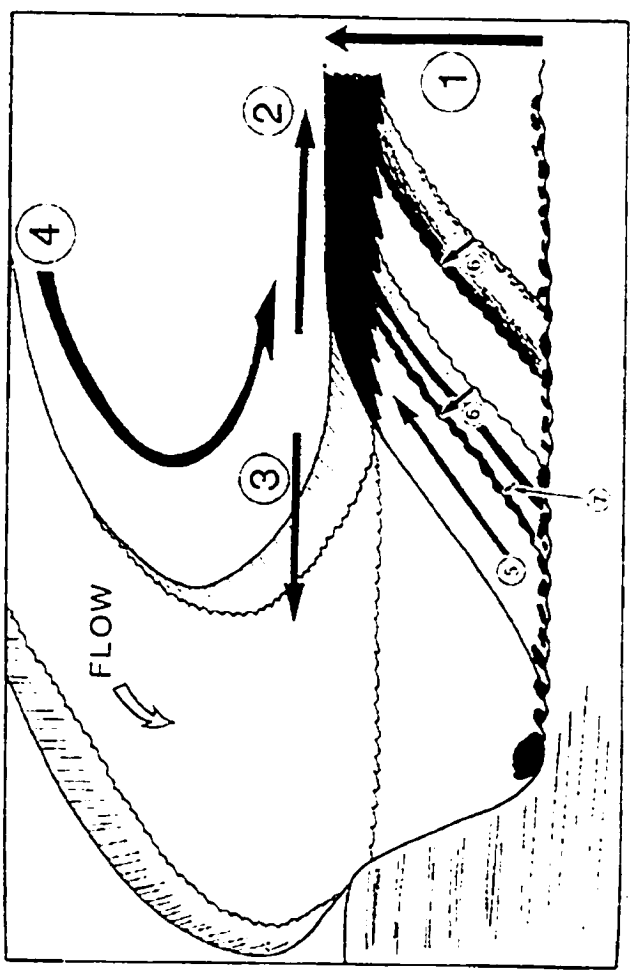
FLOW
1
2
3
4
5
6
7

a)

coarse lag deposit; 2) a deep channel facies consisting of large-scale planar to medium-scale trough cross-beds; 3) a shallow channel facies, characterized by small- to medium-scale trough cross-beds or ripple cross-laminae; and 4) upward fining in grain size and upward thinning of cross-bed thickness. Despite these broad similarities, assemblages of physical and biogenic sedimentary structures in tidally-influenced estuarine point bars are different from those of seemingly similar deposits in fluvial channel systems. The overall facies pattern of FA2 estuarine point bars is characterized by marked lateral and vertical facies changes, reflecting the variable conditions imparted by tidal processes (Clifton, 1982). Moreover, FA2 estuarine point bars commonly contain structures produced by reversing tidal currents such as bimodal cross-bedding, reactivation surfaces, rhythmic sand-mud alternations and abundant mud drapes and interbeds that produce inclined heterolithic strata (Thomas *et al.*, 1987; Smith, 1988).

Because the distribution of benthos in estuarine valleys is controlled, in part, by salinity and substrate conditions, ichnology provides a high-resolution diagnostic tool for delineating fluvial-estuarine facies transitions in the stratigraphic record (Buatois *et al.*, 1997). Trace fossil assemblages within ancient fluvial point bar deposits have traditionally been assigned to the *Scoyenia* ichnofacies (Frey *et al.*, 1984), produced by non-marine vertebrate and invertebrate tracemakers. The trace fossils are characterized by: 1) small horizontal, lined, backfilled feeding burrows; 2) curved to tortuous unlined feeding burrows; 3) sinuous crawling traces; 4) vertical cylindrical to irregular shafts; and 5) tracks and trails (Pemberton *et al.*, 1992a). Tidally-influenced estuarine point bar deposits, on the other hand, commonly contain a brackish water trace fossil assemblage - a result of the mixing of tidally-transported seawater and fluvial freshwater. In general, brackish water trace fossil suites are characterized by: 1) a low diversity ichnogenera; 2) an impoverished marine suite rather than a mixture of marine and non-marine traces; 3) simple structures constructed by trophic generalists; 4) suites that are commonly dominated by a single ichnogenus; 5) forms that are typically of a small size; 6) an admixture of vertical and horizontal ichnofossils of the *Skolithos* and *Cruziana* ichnofacies; and 7) some forms that locally occur in high density (Pemberton *et al.*, 2001). Trace fossil assemblages in FA2 strata are consistent with brackish water depositional conditions, including diminutive burrow size, simplistic morphologies, low

diversity and abundant forms of both the *Skolithos* and *Cruziana* ichnofacies (Wightman *et al.*, 1987; Pemberton and Wightman, 1992).

Upper estuary channel fill deposits of FA2 are similar to vertical and longitudinal facies sections observed in the Gironde estuary (Allen, 1991). The macrotidal Gironde estuary, located along the southwestern coast of France, was formed by the Holocene drowning of a Pleistocene incised fluvial valley and presently is being filled with a regressive wedge of fluvial sediment. Sediment and facies of the estuary are organized into a tripartite longitudinal zonation that reflects the seaward transition from fluvial, to tidal, to mixed tide-wave environments (Figure 3.8a). The fluvial channel deposits consist of a 10-15 m thick section of gravel and coarse sand point bars overlain by silty clay. Downstream, channel sediment grades from gravel to coarse sand, then to medium sand with abundant mud laminae. The fluvial-estuarine transition occurs at the upstream limit of tidal current reversal and coincides with the landward extremity of tidal estuarine facies (Figure 3.8b). Seaward of this transition, the upper estuary channels accumulate upward-fining tidal estuarine point bars comprising medium grained, cross-bedded to rippled sand, with abundant mud interbeds. Tidal estuarine point bars are differentiated from their fluvial counterparts by their smaller average sediment grain size, common mud laminae and rhythmic sand-mud bedding, and lack of alluvial flood and overbank deposits. The facies changes at the fluvial-estuarine transition result from a combination of three sedimentological processes: 1) the estuarine turbidity maximum which results in high rates of mud deposition; 2) tide current asymmetry, which blocks the downstream transport of coarse fluvial bedload; and 3) attenuation of fluvial floods in the estuary, which impedes the development of alluvial overbank deposits. By analogy, the narrow, linear geometry of FA2 suggests that the Jenner Upper Mannville E Pool consists of upper estuarine strata (Figure 3.6). Furthermore, the distribution of coarse-grained (F3 and F5) strata in the northern part of the pool and fine- to medium-grained (F3 and F4) strata in the southern part of the pool suggests that a gradational fluvial-estuarine facies transition is located approximately in the central to north-central part of the pool. It follows from this distribution of facies that paleoflow was from north to south (see discussion in Chapter 4).

Figure 3.8: (a) Morphology of the Gironde estuary, illustrating the tripartite geomorphological zonation and major depositional environments. The bathymetry datum is the lowest tide level. (b) Sediment distribution patterns and longitudinal facies section at the transition between the fluvial and estuarine channels in the upper estuary channel zone. This facies transition occurs at the upstream limit of tidal current reversal. Landward of the fluvial-estuarine facies transition the sediment is dominated by coarse sand and gravel (from Allen, 1991).

a)

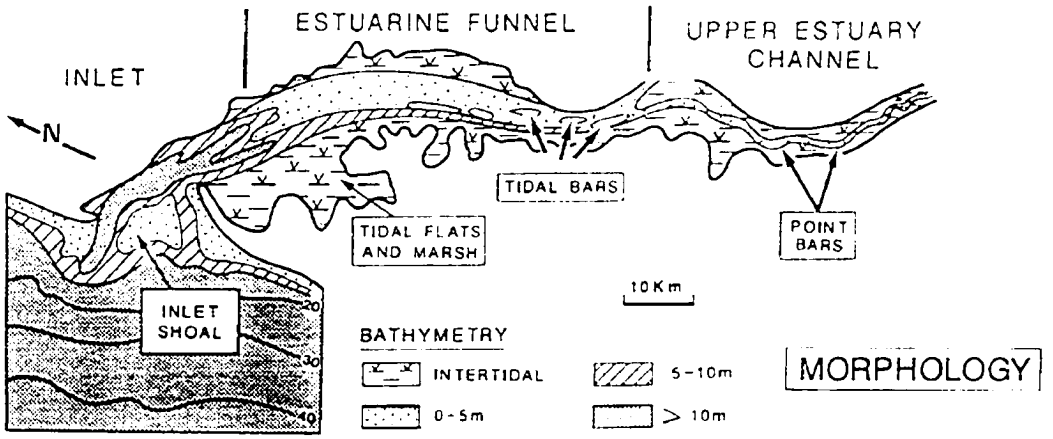
ESTUARINE FUNNEL
UPPER ESTUARY CHANNEL
INLET
N
TIDAL BARS
TIDAL FLATS AND MARSH
POINT BARS
10 Km
INLET SHOAL
BATHYMETRY
INTERTIDAL
5-10m
0-5m
> 10m
MORPHOLOGY

b)

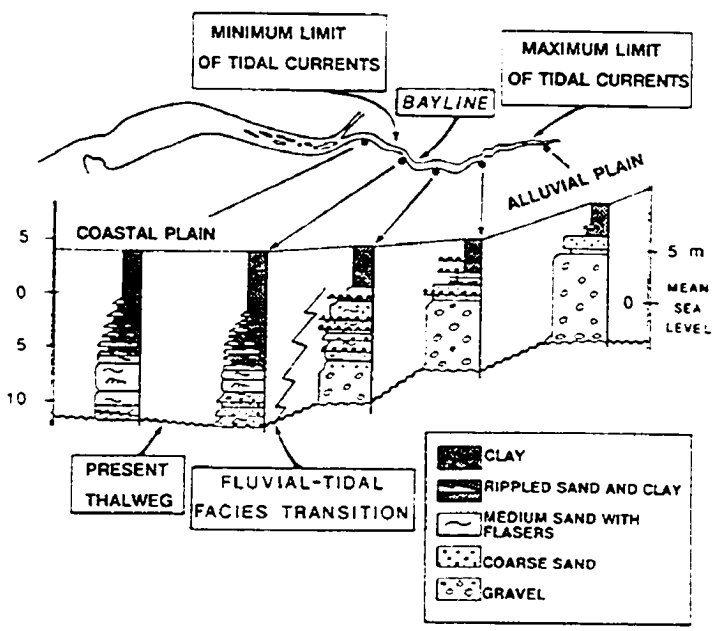
MINIMUM LIMIT OF TIDAL CURRENTS
MAXIMUM LIMIT OF TIDAL CURRENTS
BAYLINE
ALLUVIAL PLAIN
COASTAL PLAIN
5
0
5
10
5 m
0
MEAN SEA LEVEL
PRESENT THALWEG
FLUVIAL-TIDAL FACIES TRANSITION
CLAY
RIPPLED SAND AND CLAY
MEDIUM SAND WITH FLASERS
COARSE SAND
GRAVEL

From the aforementioned comparison of fluvial and tidally-influenced point bar deposits, tidally-influenced deposits of FA2 are interpreted to have been deposited seaward of the maximum tide limit in an upper estuary environment. This is suggested by: 1) abrupt lateral and vertical facies changes; 2) the distribution of coarse- and fine-grained facies at opposite ends of the pool; 3) a brackish water trace fossil assemblage; and 4) a conformable contact between FA2 and overlying tidally-influenced strata of Facies Association 3 (see next).

3.4 Facies Association 3: Tidally-Influenced Abandoned Channel/Interchannel Deposits

Description

Facies Association 3 (FA3) consists of an upward-fining vertical sequence consisting of interstratified sandstone, siltstone and mudstone (F6) and carbonaceous mudstone and coal (F7) (Figure 3.9; Plate 3.3). These strata occur throughout the study area but the composition, thickness and lower contact of the FA3 sequence varies depending on its location and on the nature of underlying strata. FA3 overlies deposits of the Prograding Shoreface to Shallow Shelf Facies Association (FA1) or the Upper Estuary Channel Fill Facies Association (FA2). Where FA3 overlies shoreface to shallow shelf strata of FA1, the lower contact is commonly sharp, horizontal and planar. Here, the FA3 sequence is dominated by interstratified sandstone, siltstone and mudstone (F6), rarely with a thin bed of carbonaceous mudstone or coal (F7) at the base. In contrast, areas where FA3 overlies upper estuarine strata of FA2 are characterized by a gradational lower surface and the FA3 sequence is composed of a lower succession consisting of carbonaceous mudstone and coal (F7) that grades upward to interstratified sandstone, siltstone and mudstone (F6). The vertical facies change from upper estuary channel fill (FA2) to abandoned channel/interchannel deposits (FA3) is abrupt, generally occurring over a stratigraphic interval of approximately 10 cm and ranging from <5-25 cm. Regionally, FA3 ranges from 55 cm to 4.6 m thick and has an average thickness of 2.3 m. Although the thickness of FA3 varies, its average thickness is typically greater where it overlies FA1 (2-3 m)

Figure 3.9: Gamma-ray well log and detailed core litholog for 0/07-27-019-09W4/0. The Tidally-Influenced Abandoned Channel/Interchannel Deposits Facies Association (FA3) consists of an upward-fining sequence composed of a lower interstratified sandstone, siltstone and mudstone (F6) succession gradationally overlain by an upper carbonaceous mudstone and coal (F7) succession. See Table 3.1 for a legend to the symbols used.

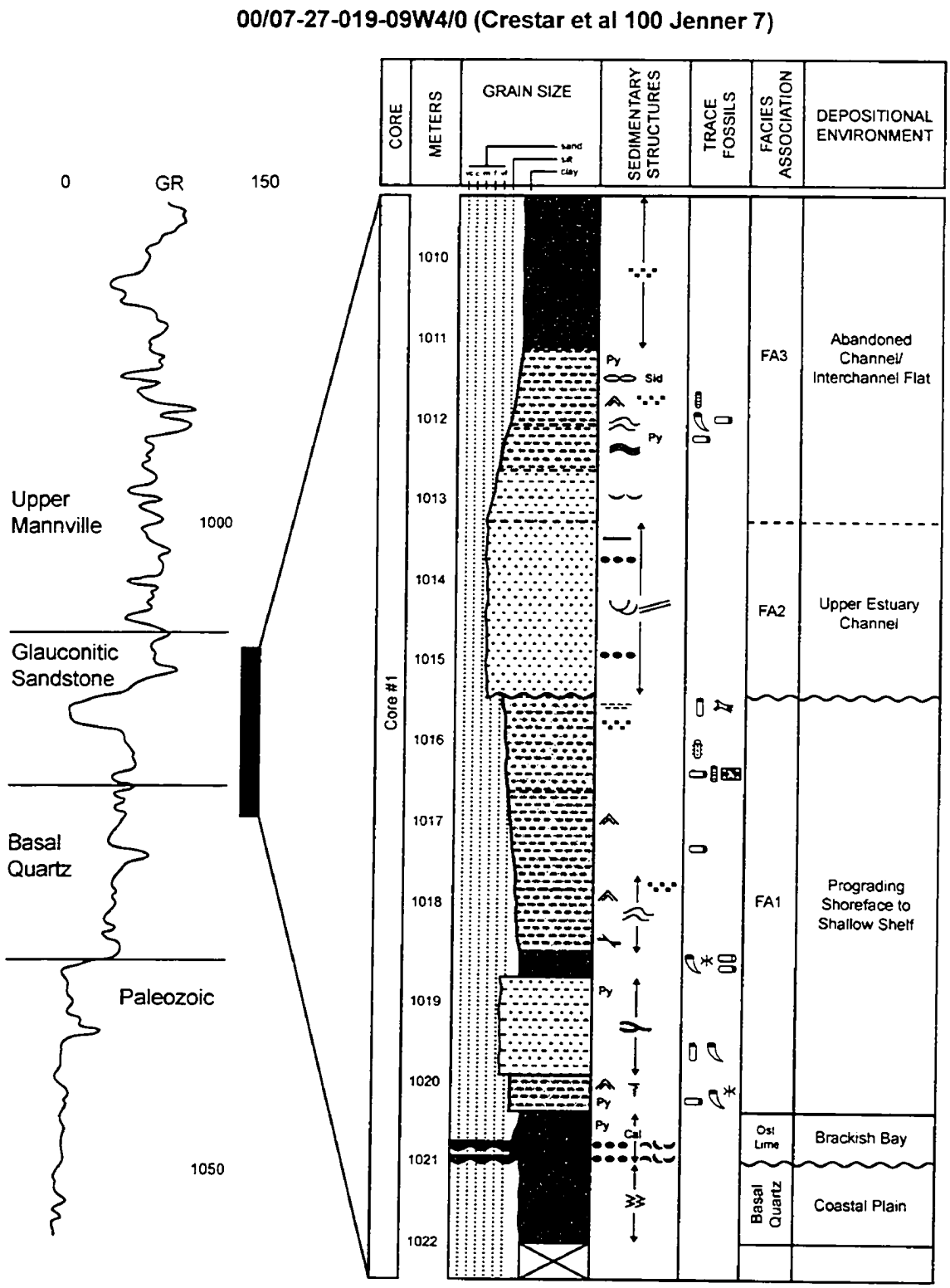
00/07-27-019-09W4/0 (Crestar et al 100 Jenner 7)
0
GR
150
Upper Mannville
1000
Glauconitic Sandstone
Basal Quartz
Paleozoic
1050
CORE
METERS
GRAIN SIZE
sand
silt
clay
SEDIMENTARY STRUCTURES
TRACE FOSSILS
FACIES ASSOCIATION
DEPOSITIONAL ENVIRONMENT
Core #1
1010
1011
1012
1013
1014
1015
1016
1017
1018
1019
1020
1021
1022
Py
Skd
Py
Py
Py
Cal
FA3
Abandoned Channel/ Interchannel Flat
FA2
Upper Estuary Channel
FA1
Prograding Shoreface to Shallow Shelf
Ost Lime
Brackish Bay
Basal Quartz
Coastal Plain

Plate 3.3: Whole core photograph of the Tidally-Influenced Abandoned Channel/Interchannel Deposits Facies Association (FA3) for 00/07-27-019-09W4/0. FA3 gradationally overlies reservoir sandstone of the Upper Estuary Channel Fill Facies Association (FA2) and consists of an upward-fining vertical sequence consisting of interstratified sandstone, siltstone and mudstone (F6) and carbonaceous mudstone and coal (F7). Box length is 60 cm. Cored interval from 1013.3 m to 1009.4 m.

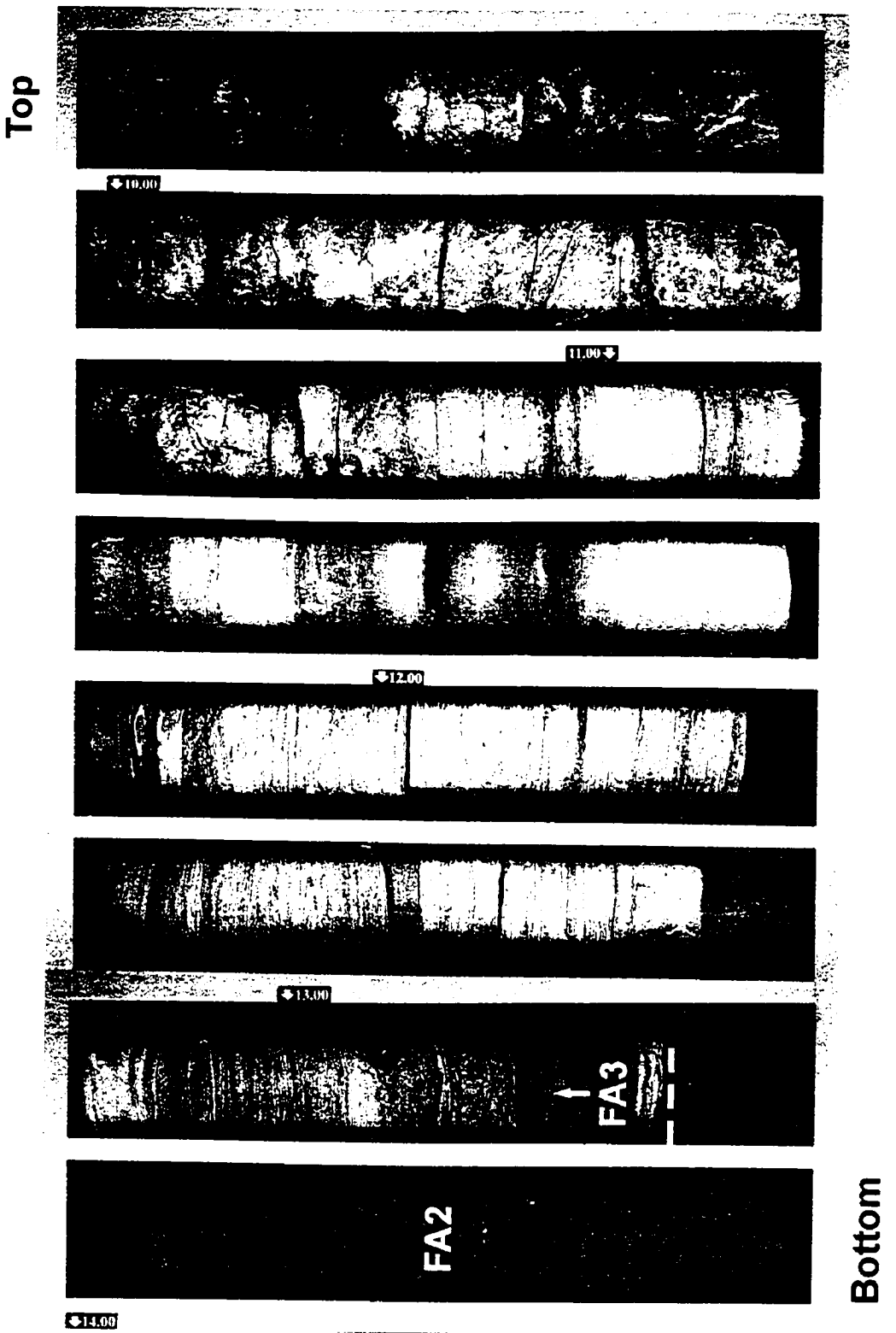
Top
10.00
11.00
12.00
13.00
FA3
FA2
14.00
Bottom

compared to FA2 (0.75-1.5 m). FA3 is erosively overlain by a sharp-based succession of very fine- to medium-grained feldspathic to lithic sandstone. The petrographic composition of the overlying sandstone succession varies depending on its location in the study area: quartz and chert range from 55-90%, feldspar grains range from tr-28%, lithic rock fragments range from 3-17% and accessory minerals make up less than 3% of the rock, by mass (Appendix 2). Because of its variable composition, the sandstone succession may be classified as sublitharenite, subarkose, lithic subarkose and lithic arkose (McBride, 1963).

Interpretation

FA3 is interpreted to be tidally-influenced, vertically-accreting, abandoned channel and interchannel deposits. Interstratified sandstone, siltstone and mudstone (F6) grading upward from tidal-channel strata (FA2) over an interval from several to tens of cm demonstrate two distinct phases of deposition within a single physiographic element: an active channel phase dominated by bedload transport overlain by an abandoned channel phase characterized by mixed bedload and suspension sedimentation. Bedload transport in the active channel was progressively replaced by suspension sedimentation as flow speeds progressively, but rapidly decreased during channel abandonment. Collectively, the interpretation of FA2 as an upper estuary channel and evidence from FA3 supporting tidally-influenced sedimentation (see Chapter 2) suggests that the channel was located downstream of the landward limit of tidal currents and verifies the continued incursion of tidally-transported seawater during and after the abandonment phase (Gingras *et al.*, 2002). An analogous succession of interbedded sandstone and mudstone to massive mudstone deposits abruptly to gradationally overlying cross-bedded channel sandstones have been similarly interpreted by Brownridge and Moslow (1991). Here, the mudstone facies is typically 1-5 m thick and contains abundant wood fragments, a low diversity ichnofossil and dinoflagellate assemblage, and little evidence of bedload transport. Similarly, a 15 m thick shale lithofacies consisting of massive mudstone, laminated mudstone and interlaminated mudstone and coarse-grained siltstone/very fine-grained sandstone was observed in stratigraphically equivalent strata at Little Bow field, southern

Alberta (Wood and Hopkins, 1989). The dominant clay to silt grain size, the presence of a low-diversity, locally high-abundance ichnofossil suite, rare syneresis cracks and the common coexistence of siderite and pyrite in the shale lithofacies supported a brackish water, abandoned estuarine channel interpretation.

Floodbasin deposits (F7) overlie and are laterally adjacent to active (FA2) and abandoned (F6) channel fill strata. This suggests that the rate of lateral accretion versus vertical aggradation progressively decreased. This, in turn, is likely due to a combination of factors, including the presence of more cohesive bank material that reduced the rate of lateral migration and/or base level rise related to rising relative sea level. In meandering fluvial systems, erosion of the concave bank is influenced by the nature of the bank material; floodplain clay with high cohesive strength resists erosion unless it is underlain by channel sand (Collinson, 1986). In the study area, accumulation of relatively thick, cohesive floodbasin sediments marginal to the active channel belt may have reduced the rate of lateral channel migration and limited the width of FA2 to approximately 2 km. Alternatively, evidence of tidally-influenced deposition in strata of F7, including a brackish water ichnofossil suite and a mixed continental and marine palynomorph assemblage, is consistent with a transgressive interpretation for the upward increase in the rate of vertical aggradation versus lateral accretion. Also, the long term tendency of fluvial channels to adjust by migrating laterally, rather than incising vertically (Yoxall, 1969), suggests that transgressive FA2 and FA3 strata may represent deposition over several hundred thousand to a few million, rather than tens of million years (Arnott *et al.*, 2002).

Interchannel strata of FA3 are thin compared to floodbasin successions in modern environments (e.g. Coleman, 1966). Thin floodbasin deposits are generally indicative of actively shifting meandering channels with high rates of lateral migration (Reineck and Singh, 1973) that result in sheet-like channel fill geometries, a condition not observed in upper estuarine channel fill strata of FA2. In the study area, thin floodbasin successions are due to post-depositional erosion; FA3 represents the uppermost stratigraphic unit of the Glauconitic Sandstone and is unconformably overlain by feldspathic to lithic sandstone of the undifferentiated Upper Mannville (Wood, 1990). These fluvial channel sandstones separate estuarine Glauconitic strata from non-marine, coal-bearing Upper

Mannville strata (Rudkin, 1964; Jackson, 1984). The framework composition of Glauconitic sandstone and Upper Mannville sandstone is very different (Appendix 2), suggesting different sediment source areas. Previous authors, for example James (1985) and Wood and Hopkins (1992), suggest that the quartzose sand of the upper estuary channel fill (FA2) was sourced from a northern paleotopographic high where little or no Lower Mannville or Glauconitic sediment was deposited. This paleotopographic high, the Kindersley Highlands, separated the Bellshill Lake-Halkirk and southern Alberta Glauconitic drainage systems (Sherwin, 1996; Figure 1.4). Feldspathic to lithic channel sandstones of the undifferentiated Upper Mannville succession, on the other hand, are interpreted to have derived from a southwestern Cordilleran source. Regional mapping shows that Upper Mannville lithic channels appear to be restricted to the southern Alberta drainage system, which is more proximal to the inferred Cordilleran source (Sherwin, 1996; Figure 1.4). Thin FA3 successions, therefore, resulted from incision by younger Upper Mannville channels and consequent erosion of previously deposited fine-grained floodbasin deposits.

Table 3.1: Legend to symbols used in Figures 3.1, 3.5 and 3.9.

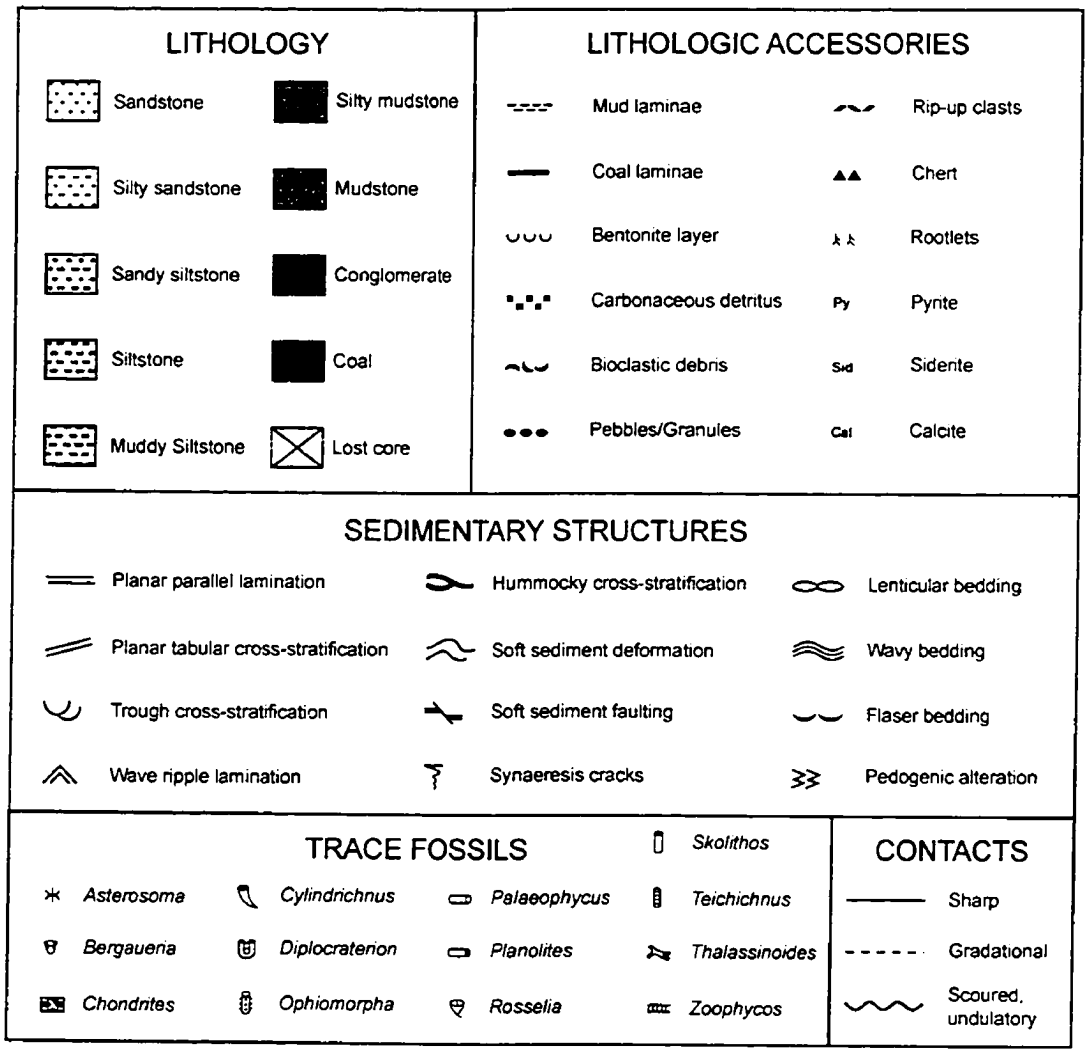
LITHOLOGY
Sandstone
Silty mudstone
Silty sandstone
Mudstone
Sandy siltstone
Conglomerate
Siltstone
Coal
Muddy Siltstone
Lost core
LITHOLOGIC ACCESSORIES
Mud laminae
Rip-up clasts
Coal laminae
Chert
Bentonite layer
Rootlets
Carbonaceous detritus
Py
Pyrite
Bioclastic debris
Sid
Siderite
Pebbles/Granules
Cal
Calcite
SEDIMENTARY STRUCTURES
Planar parallel lamination
Hummocky cross-stratification
Lenticular bedding
Planar tabular cross-stratification
Soft sediment deformation
Wavy bedding
Trough cross-stratification
Soft sediment faulting
Flaser bedding
Wave ripple lamination
Synaeresis cracks
Pedogenic alteration
TRACE FOSSILS
Asterosoma
Cylindrichnus
Palaeophycus
Skolithos
Bergaueria
Diplocraterion
Planolites
Teichichnus
Chondrites
Ophiomorpha
Rosselia
Thalassinoides
Zoophycos
CONTACTS
Sharp
Gradational
Scoured, undulatory

4. DEPOSITIONAL HISTORY

4.1 Geophysical Well-Log Characteristics

In southeastern Alberta, the Glauconitic Sandstone is characterized by a variety of geophysical well-log signatures that result from spatial variations in the composition and thickness of the three constituent facies associations (Figure 4.1). Some of these well-log signatures resemble those of sub- and superjacent strata (e.g. Basal Quartz and undifferentiated Upper Mannville), which consequently makes identifying its upper and lower boundaries problematic. Different industry-mapping databases commonly incorrectly pick the top of the Glauconitic Sandstone interval, mistaking it for either the Ostracode Limestone or a coal bed within the Upper Mannville succession. Correlating the Glauconitic Sandstone using consistently misidentified tops, therefore, will result in a distorted depositional interpretation that can lead to errors in predicting reservoir volume. As such, a discussion of geophysical well-log attributes is deemed necessary.

In the Jenner Upper Mannville E Pool, the Glauconitic Sandstone is underlain by the Ostracode Limestone, an informally recognized marker horizon in southeastern Alberta (Sherwin, 1996; Figure 1.6). Tightly cemented calcareous strata of the Ostracode Limestone have low porosity and low acoustic impedance (or, alternatively, high acoustic transmissibility). As a consequence, the Ostracode Limestone is identified principally by a sharp, rightward deflection on density porosity and sonic logs (Figure 4.1). In addition to low porosity, the Ostracode Limestone has slightly higher resistivity than sub- and superjacent strata, with an average value of 13 ohm-m. Given its lack of oil-staining in core samples, the higher average resistivity is most probably due to freshwater rather than hydrocarbon saturation. The Ostracode Limestone commonly lies stratigraphically above a 2-3 m thick 'shoulder' near the top of the underlying Basal Quartz interval. The Basal Quartz 'shoulder' is characterized by a pronounced separation between the neutron and density porosity curves and records the presence of a regionally widespread paleosol marker horizon in southeastern Alberta (Zaitlin *et al.*, 2002). Water, molecularly bound to clay minerals in the paleosol, causes the neutron porosity log to record very high porosity values. Because the density porosity curve is unaffected by the presence of

Figure 4.1: Selected geophysical well-logs illustrating the various log signatures of the Glauconitic Sandstone. (a) Sharp contact between the Prograding Shoreface to Shallow Shelf (FA1) and Upper Estuary Channel Fill (FA2) Facies Associations. (b) Prograding FA1 succession overlain by upward-fining strata of the Tidally-Influenced Abandoned Channel/Interchannel Deposits Facies Association (FA3). (c) FA2 succession characterized by a slightly upward-fining, 3 m thick homogeneous sandstone bed composed predominantly of dune cross-stratified sandstone (F3). (d) Blocky, 9 m thick FA2 succession composed of interstratified dune cross-stratified sandstone (F3) and chert pebble conglomerate (F5). Note the pronounced deflection of the density porosity curve at the stratigraphic level of the Ostracode Limestone and the upward-increase in porosity of the FA2 unit. (e) Wavy, undulating FA2 gamma-ray geophysical character produced by interstratified massive quartzose sandstone and silty mudstone (F4). (f) 20 m thick lithic channel sandstone. BQ = Basal Quartz, UM = Upper Mannville.

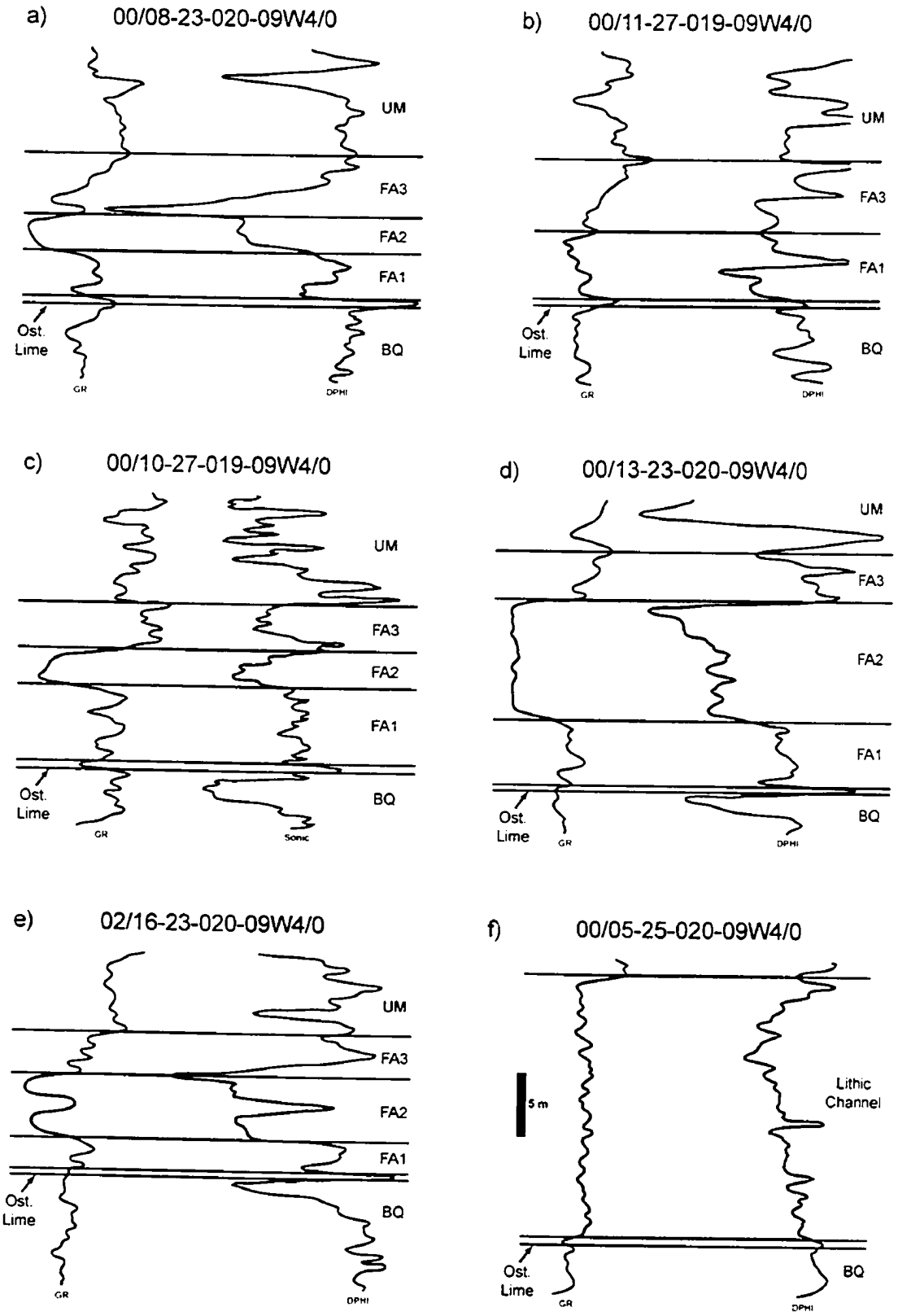
a)
00/08-23-020-09W4/0
UM
FA3
FA2
FA1
Ost.
Lime
BQ
GR
DPHI
b)
00/11-27-019-09W4/0
UM
FA3
FA1
Ost.
Lime
BQ
GR
DPHI
c)
00/10-27-019-09W4/0
UM
FA3
FA2
FA1
Ost.
Lime
BQ
GR
Sonic
d)
00/13-23-020-09W4/0
UM
FA3
FA2
FA1
Ost.
Lime
BQ
GR
DPHI
e)
02/16-23-020-09W4/0
UM
FA3
FA2
FA1
Ost.
Lime
BQ
GR
DPHI
f)
00/05-25-020-09W4/0
5 m
Lithic
Channel
Ost.
Lime
BQ
GR
DPHI

hydrogen, there is a marked separation of the neutron and density porosity logs. The curves re-approach one another and deflect to the right at the base of the overlying Ostracode Limestone.

Diagnostic geophysical well-log attributes of the three Glauconitic Sandstone facies associations can be used to correlate individual associations and map their subsurface distribution. The Prograding Shoreface to Shallow Shelf Facies Association (FA1) is characterized by a distinct upward-coarsening trend and high gamma-ray counts reflecting its high mudstone content (Figure 4.1a-e). The lower, sharp-based parasequence is represented by an abrupt decrease in gamma-ray counts above the Ostracode Limestone (Figure 4.1a). Above the lower parasequence, the gamma-ray log increases by approximately 20 API units, interpreted to indicate a marine flooding surface at the base of the overlying gradational-based parasequence. The bioturbated silty mudstone bed associated with the marine flooding surface contains abundant radioactive elements, most probably contained in clay minerals, and has lower effective porosity, causing the rightward shift of the gamma-ray and density porosity curves. This layer is then overlain by a steady decrease in gamma-ray counts that is unconformably overlain by either Facies Association 2 (Figure 4.1a, c-e) or Facies Association 3 (Figure 4.1b). Neutron and density porosity logs are fairly consistent (i.e. remain subparallel) in strata of FA1 with average values of 30% and 15% porosity, respectively. Resistivity values of FA1 consistently average 8 ohm-m.

The Upper Estuary Channel Fill Facies Association (FA2) is characterized by a sharp leftward deflection of the gamma-ray log. Average gamma-ray counts for FA2 are 30 API units, reflecting the abundance of (nonradioactive) quartz and chert. FA2 commonly displays one of three gamma-ray well-log responses: 1) a slight upward-fining, 2-3 m thick bed (Figure 4.1c); 2) a 7-9 m thick blocky unit (Figure 4.1d); and 3) a wavy, undulating unit (Figure 4.1e). FA2 strata with undulating gamma-ray well-log signatures contain one or more 30-50 cm thick silty mudstone beds interstratified with massive quartzose sandstone. Neutron and density porosity curves are closely spaced or superimposed in FA2 wells and average 24% porosity. Neutron and density porosity curves commonly cross-over in strata with blocky gamma-ray well-log signatures, especially in the upper part of the succession. Resistivity commonly increases upwards

within FA2 strata, particularly in wells with blocky gamma-ray curves. Average resistivity of FA2 successions is 35 ohm-m but can be as high as 90 ohm-m in wells with blocky gamma-ray signatures.

The Tidally-Influenced Abandoned Channel/Interchannel Deposits Facies Association (FA3) is characterized by an upward-fining, rightward deflection of the gamma-ray log associated with an upward-increase in radioactive clay and feldspar minerals and lithic rock fragments (Figure 4.1a-e). The positive gamma-ray deflection is either gradational or sharp and varies depending on the stratal composition of the FA3 succession. FA3 successions that lack coal consist of a gradationally upward-fining gamma-ray well-log signature that steadily increases in gamma-ray counts (Figure 4.1b, e). FA3 strata with coal interbeds are characterized by a sharp deflection of the gamma-ray curve at the stratigraphic position of the coal bed, followed by a steady upward-increase in API counts (Figure 4.1a). Similar to the lower FA1 succession, the neutron and density porosity curves separate widely in strata of FA3. FA3 demonstrates low average porosity on well-logs; density porosity logs record an average of 9% porosity. Similar to the gamma-ray well-log response, resistivity varies depending on the composition of the FA3 succession. FA3 successions that contain coal beds show a sharp negative deflection of the resistivity curve. In contrast, resistivity curves gradually decrease in FA3 intervals that lack coal.

Feldspathic to lithic-rich fluvial sandstones of the overlying undifferentiated Upper Mannville succession are up to 20 m thick and are characterized by a number of unique and uniform geophysical properties (Figure 4.1f). Gamma-ray values for lithic channel sandstones are consistently higher than Upper Estuary Channel Fill sandstones, reflecting a greater abundance of radioactive feldspar and clay minerals. The uniformity of the gamma-ray curve is matched by a similar trend shown by the spontaneous potential log. The neutron and density porosity logs separate significantly within lithic channels; neutron porosity values average 39% whereas density porosity values average 20%. Resistivity is consistently low with values averaging 2.5 ohm-m. It is possible to distinguish between lithic and water-wet quartzose sandstones on geophysical well-logs. Both sandstone types have resistivity values less than 10 ohm-m, but water-saturated quartzose sandstones show a slightly irregular resistivity log response that contrasts with

the straight, featureless resistivity curve in Upper Mannville feldspathic and lithic sandstones.

4.2 Lateral Facies Relationships

A grid of regional stratigraphic cross-sections (Townships 19-21, Ranges 8-10W4) was constructed using gamma-ray, neutron-density porosity or sonic, spontaneous potential and resistivity well-logs and lithological information from cored wells for stratigraphic correlation of the Glauconitic Sandstone. Four stratigraphic cross-sections were prepared using gamma-ray and density porosity logs in order to show the lateral distribution of the three facies associations in the study area (Figure 4.2).

The selection of an appropriate stratigraphic datum is important because it forms the basis for accurate and meaningful correlation. A good datum should be a regionally extensive, synchronous surface that is easily recognized on geophysical well-logs. The Ostracode Limestone, a commonly used stratigraphic horizon throughout much of southern Alberta, is locally absent where fluvial channels of the undifferentiated Upper Mannville have incised underlying strata. Considering the limited size of the study area (~ 200 km^2) and number of wells with usable geophysical logs (264), the presence of erosive Upper Mannville fluvial channels render the Ostracode Limestone an unsuitable choice of datum. In addition, the top of the Mannville Group, which represents a basin-wide transgressive surface, is an unreliable stratigraphic datum because of the significant variability in thickness of the Mannville succession (Figure 4.3). Mannville Group strata are up to 30 m thicker where they overlie areas of greater paleotopographic relief along the sub-Cretaceous unconformity surface. Also, spatial variations in post-depositional compaction create variations in the Mannville isopach. An alternative datum is a coal bed located approximately 30 m above the Glauconitic Sandstone within the undifferentiated Upper Mannville succession. The coal bed is 1-2 m thick and is recognized on geophysical well-logs by a characteristic sinistral deflection of the gamma-

Figure 4.2: Generalized facies map of the Glauconitic Sandstone showing the distribution of FA2, FA3, Upper Mannville lithic channels and the location of stratigraphic cross-sections AA'-DD'. FA1 occurs everywhere in the study area and was omitted for ease of observation. The clear region is occupied by progradational strata of the Jenner shoreface complex.

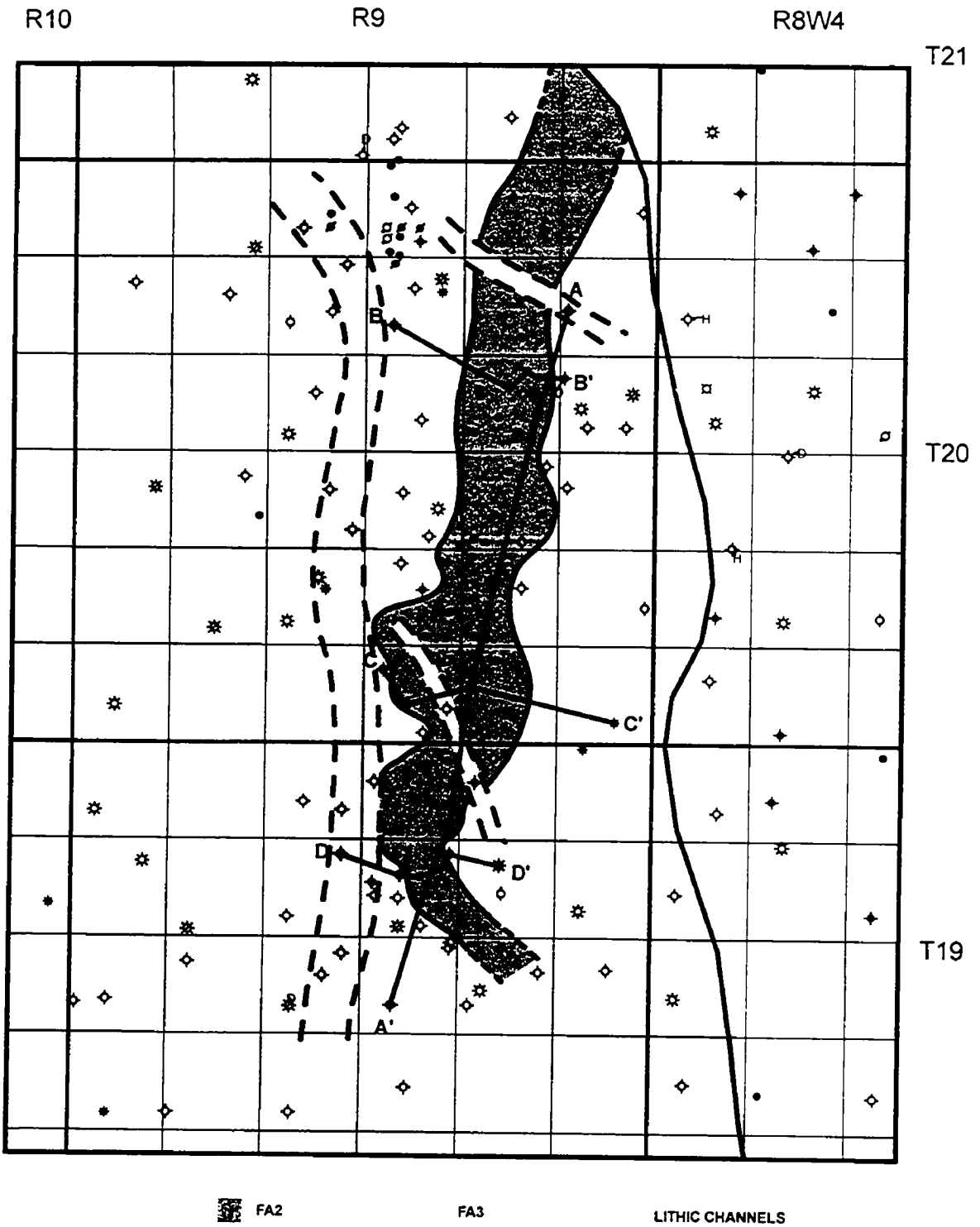
R10
R9
R8W4
T21
T20
T19
A
A'
B
B'
C
C'
D
D'
FA2
FA3
LITHIC CHANNELS

Figure 4.3: Mannville Group isopach map. The Mannville succession displays significant variability in thickness related to paleotopographic relief along the sub-Cretaceous unconformity and variations in post-depositional compaction. The top of the Mannville Group, therefore, is a poor choice of stratigraphic datum. Contour interval is 5 m.

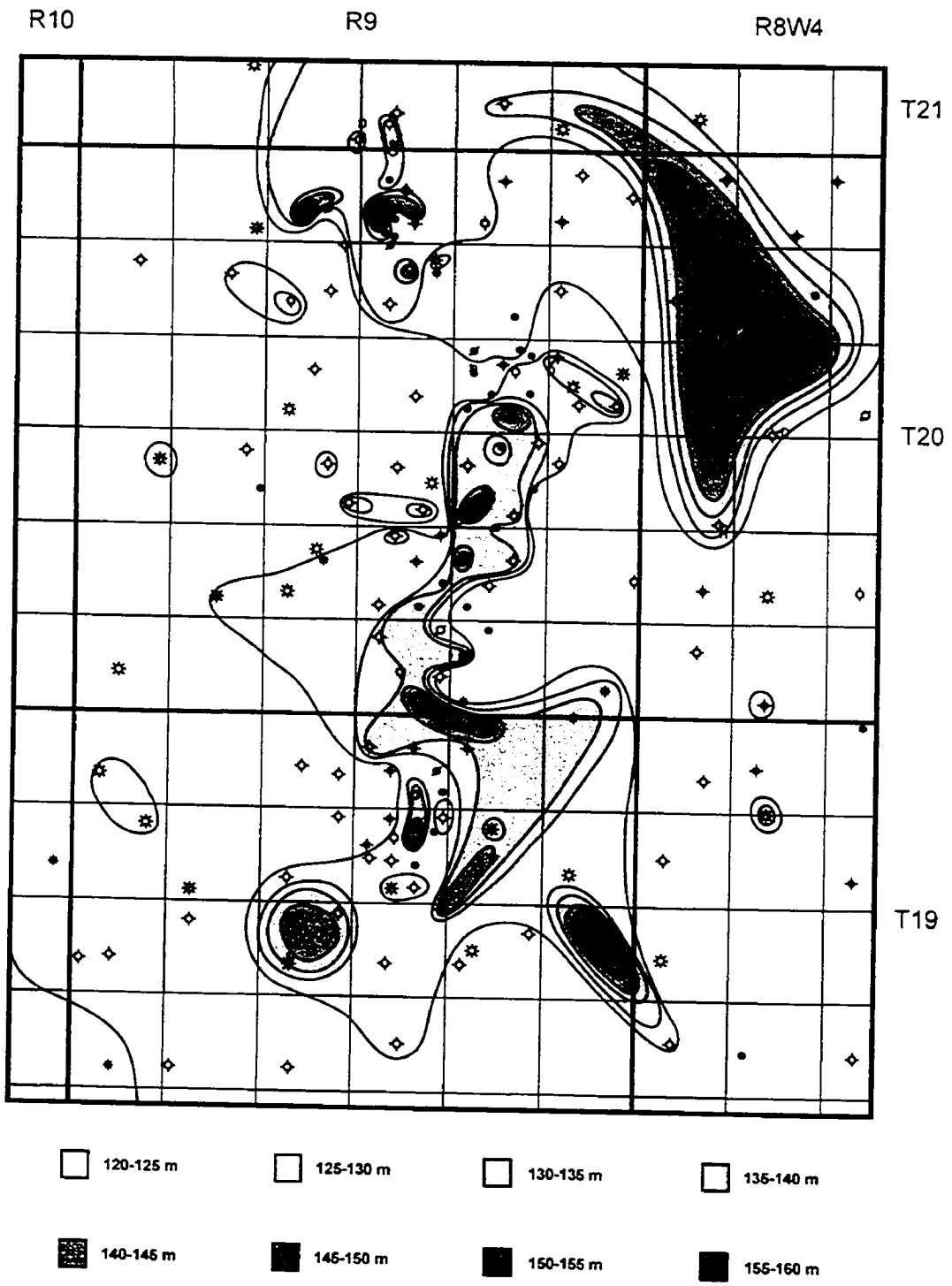
R10
R9
R8W4
T21
T20
T19
120-125 m
125-130 m
130-135 m
135-140 m
140-145 m
145-150 m
150-155 m
155-160 m

ray and neutron-density porosity curves. It is present throughout the study area and is interpreted to correlate with the Glauconite coal marker in the Medicine River area of west-central Alberta (Rosenthal, 1988). An isopach from the Upper Mannville coal bed to the Ostracode Limestone shows little variation in thickness (Figure 4.4) suggesting minimal differential compaction, relatively constant sedimentation rates between the two horizons and rapid accumulation of the coal, thus approximating a synchronous marker horizon. The Upper Mannville coal, therefore, was chosen as the stratigraphic datum in this study.

The sub-Cretaceous unconformity is an erosional surface related to a basin-wide fall in relative sea level (Cant and Stockmal, 1989). Relief on the sub-Cretaceous unconformity in the study area is locally up to 20 m (e.g. between wells 00/09-27-019-09W4/0 and 00/10-27-019-09W4/0 on cross-section DD'; Figure 4.6). Coastal plain deposits of the overlying Basal Quartz succession infilled topographic lows on the sub-Cretaceous unconformity, significantly reducing much of the surface topography before deposition of the time-transgressive Ostracode Limestone. The Prograding Shoreface to Shallow Shelf Facies Association (FA1) forms a tabular unit of relatively constant thickness (e.g. cross-sections AA', CC' and DD'; Figures 4.5, 4.6). This suggests that the irregular paleotopography along the sub-Cretaceous unconformity had been largely eliminated by deposition of the Basal Quartz. However, variations in the thickness of FA1 strata are locally present (e.g. cross-section BB'; Figure 4.5), reflecting the depositional influence of remnant surface topography produced by paleorelief along the sub-Cretaceous unconformity.

The Upper Estuary Channel Fill Facies Association (FA2) forms a laterally continuous linear sandstone unit that overlies FA1 and is laterally adjacent to and overlain by the Tidally-Influenced Abandoned Channel/Interchannel Deposits Facies Association (FA3) (Figures 4.5, 4.6). FA2 is bounded along its northern and southwestern margins by younger, impermeable Upper Mannville lithic channel sandstones and grades into silty and muddy abandoned channel/floodbasin deposits to the south (Figures 4.2, 4.5, 4.6). Stratigraphic cross-sections BB', CC' and DD' (Figures 4.5, 4.6), and the FA2 isopach map (Figure 3.6) show that strata of FA2 thin to the south by up to 10 m. This southward thinning of FA2 strata is consistent with its interpretation as

Figure 4.4: Upper Mannville coal to Ostracode Limestone isopach map. There is little variation in thickness between these two horizons. This suggests relatively constant sedimentation rates between the two horizons, minimal differential compaction and rapid accumulation of the coal. The Upper Mannville coal approximates a synchronous marker horizon and is an appropriate stratigraphic datum for subsurface correlation. The Upper Mannville coal and Ostracode Limestone are truncated by strata of the Jenner shoreface complex (hatchered line) to the north. Contour interval is 3 m.

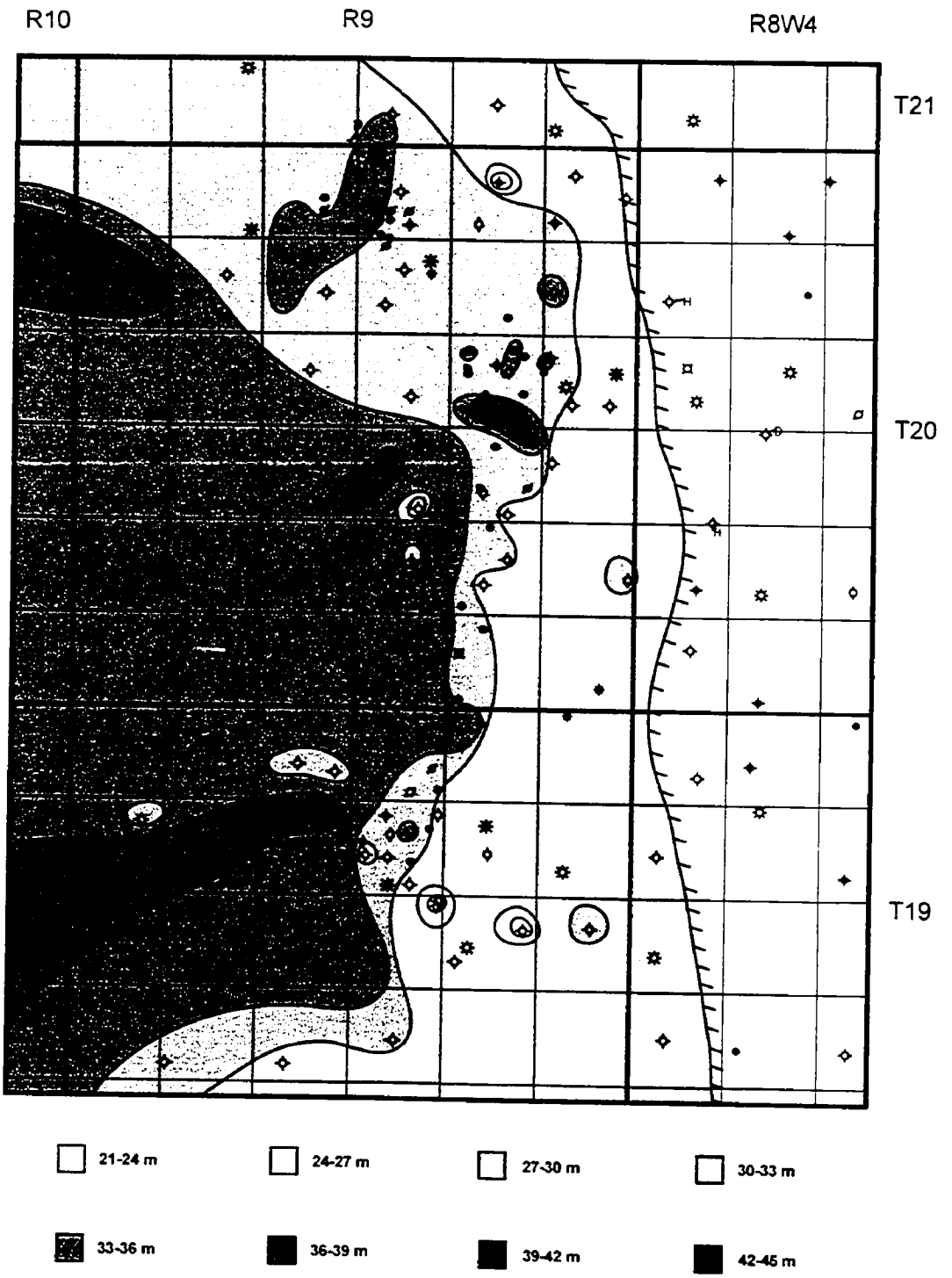
R10
R9
R8W4
T21
T20
T19
21-24 m
24-27 m
27-30 m
30-33 m
33-36 m
36-39 m
39-42 m
42-45 m

Figure 4.5: Stratigraphic cross-sections AA` and BB` illustrating the lateral relationships between major facies associations of the Glauconitic Sandstone. Geophysical well-log pairings are gamma-ray and density porosity logs (the left- and right-hand trace, respectively), except where indicated. Datum is the Upper Mannville coal. Lines of cross-sections AA` and BB` are shown in Figure 4.2.

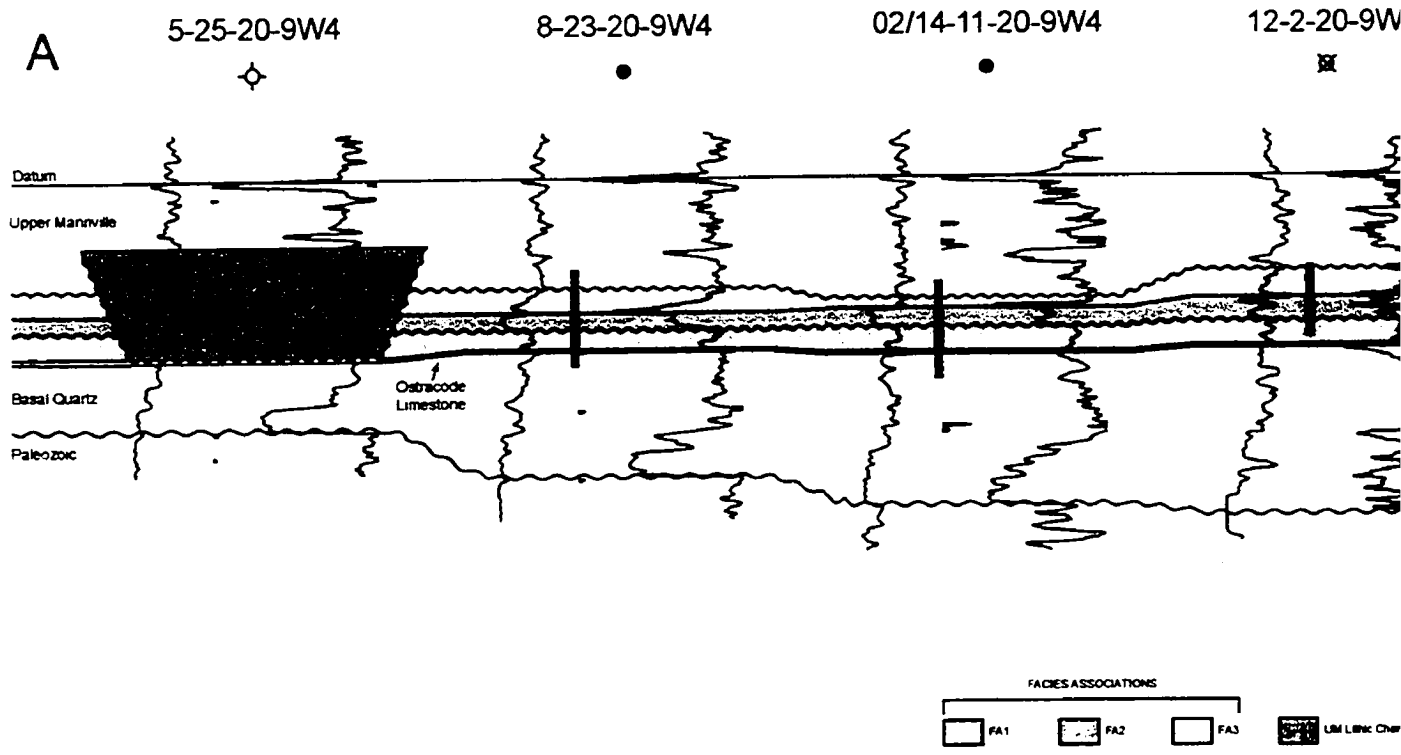
A
5-25-20-9W4
8-23-20-9W4
02/14-11-20-9W4
12-2-20-9W
Datum
Upper Mannville
Basal Quartz
Paleozoic
Ostracode Limestone
FACIES ASSOCIATIONS
FA1
FA2
FA3

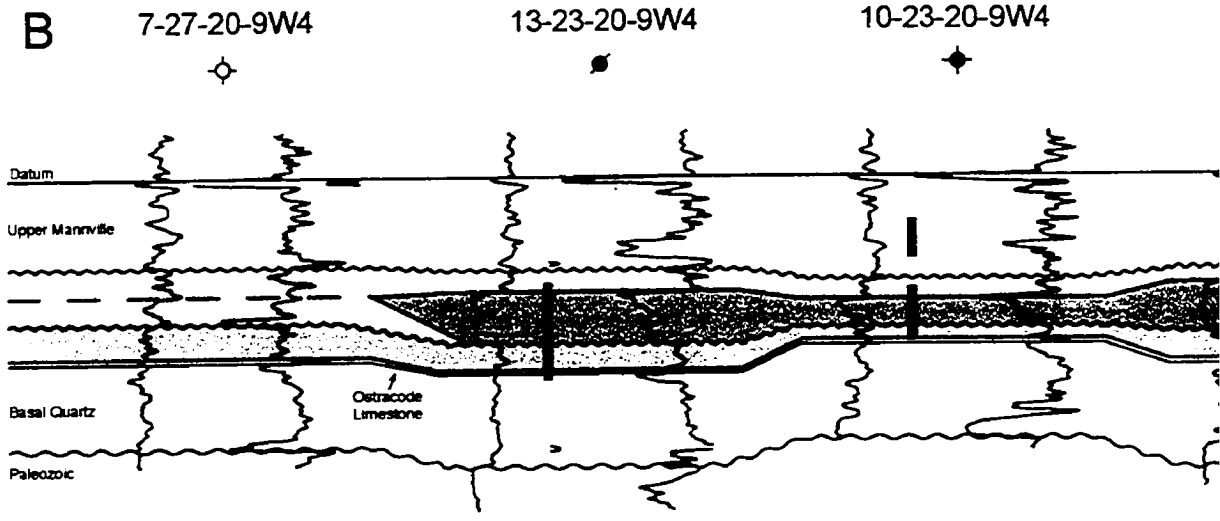
B
7-27-20-9W4
13-23-20-9W4
10-23-20-9W4
Datum
Upper Mannville
Basal Quartz
Paleozoic
Ostracode Limestone

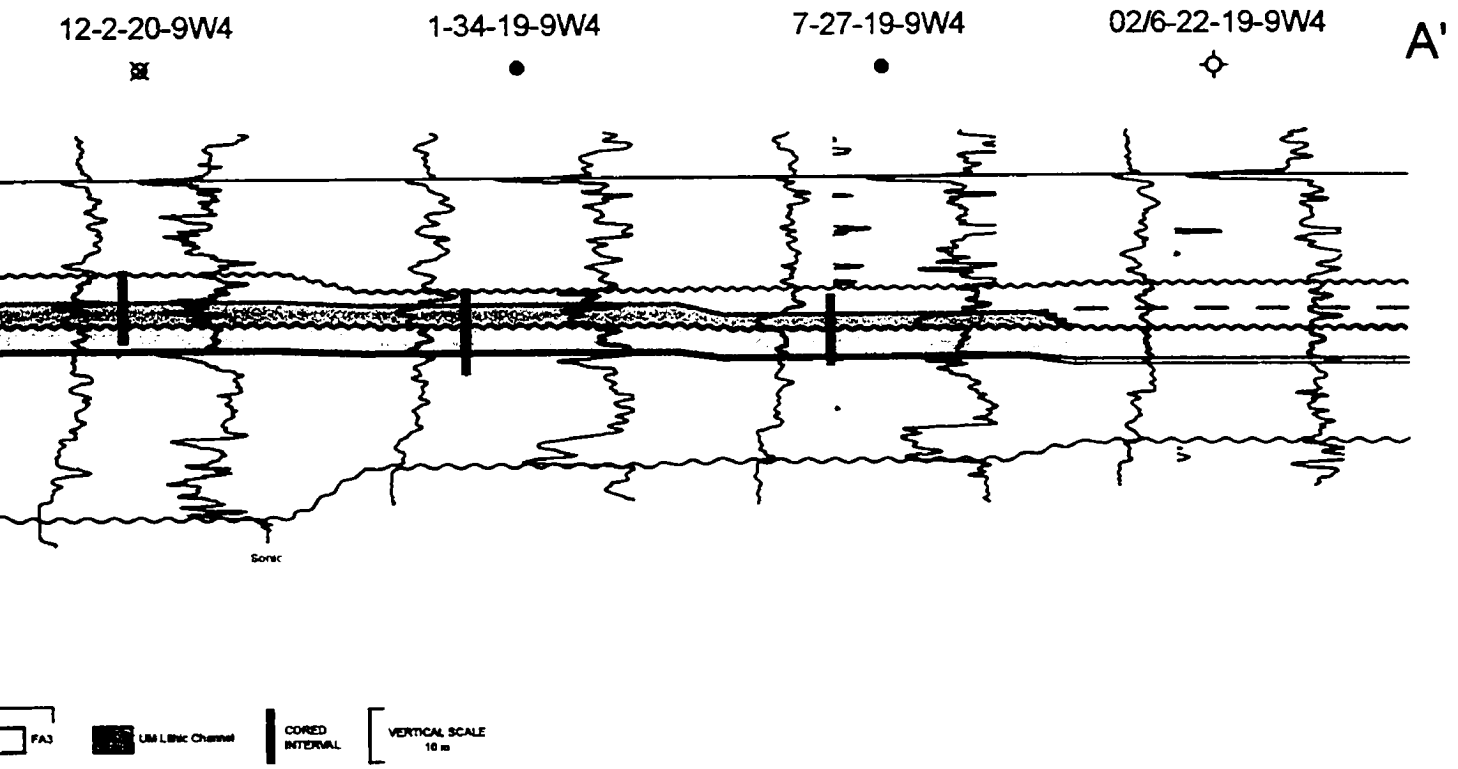
12-2-20-9W4
1-34-19-9W4
7-27-19-9W4
02/6-22-19-9W4
A'
Sonic

FA3
UM Lithic Channel
CORED INTERVAL
VERTICAL SCALE

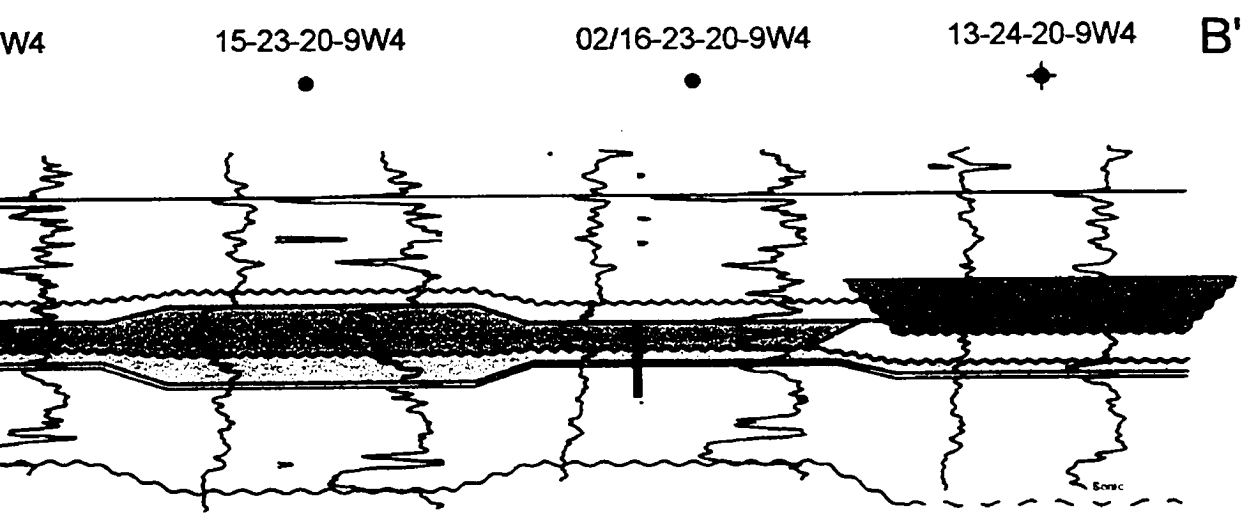
W4
15-23-20-9W4
02/16-23-20-9W4
13-24-20-9W4
B'
Sonic

Figure 4.6: Stratigraphic cross-sections CC' and DD' illustrating the lateral relationships between major facies associations of the Glauconitic Sandstone. Geophysical well-log pairings are gamma-ray and density porosity logs (the left- and right-hand trace, respectively), except where indicated. Datum is the Upper Mannville coal. Lines of cross-sections CC' and DD' are shown in Figure 4.2.

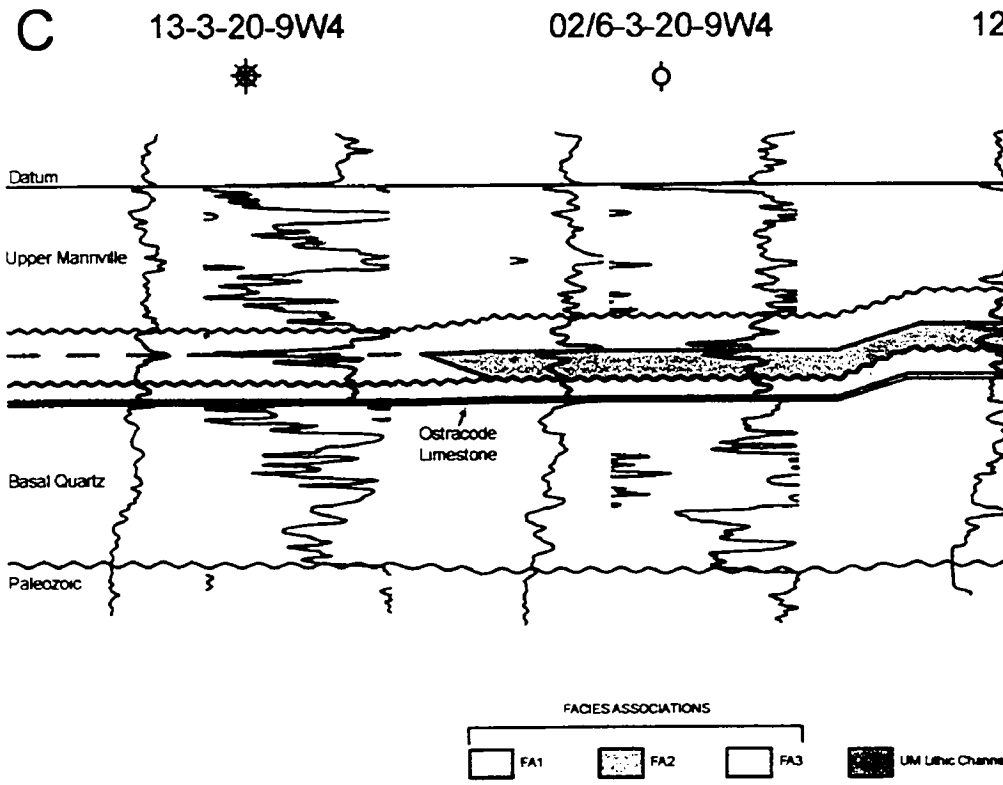
C
13-3-20-9W4
02/6-3-20-9W4
12
Datum
Upper Mannville
Ostracode
Limestone
Basal Quartz
Paleozoic
FACIES ASSOCIATIONS
FA1
FA2
FA3

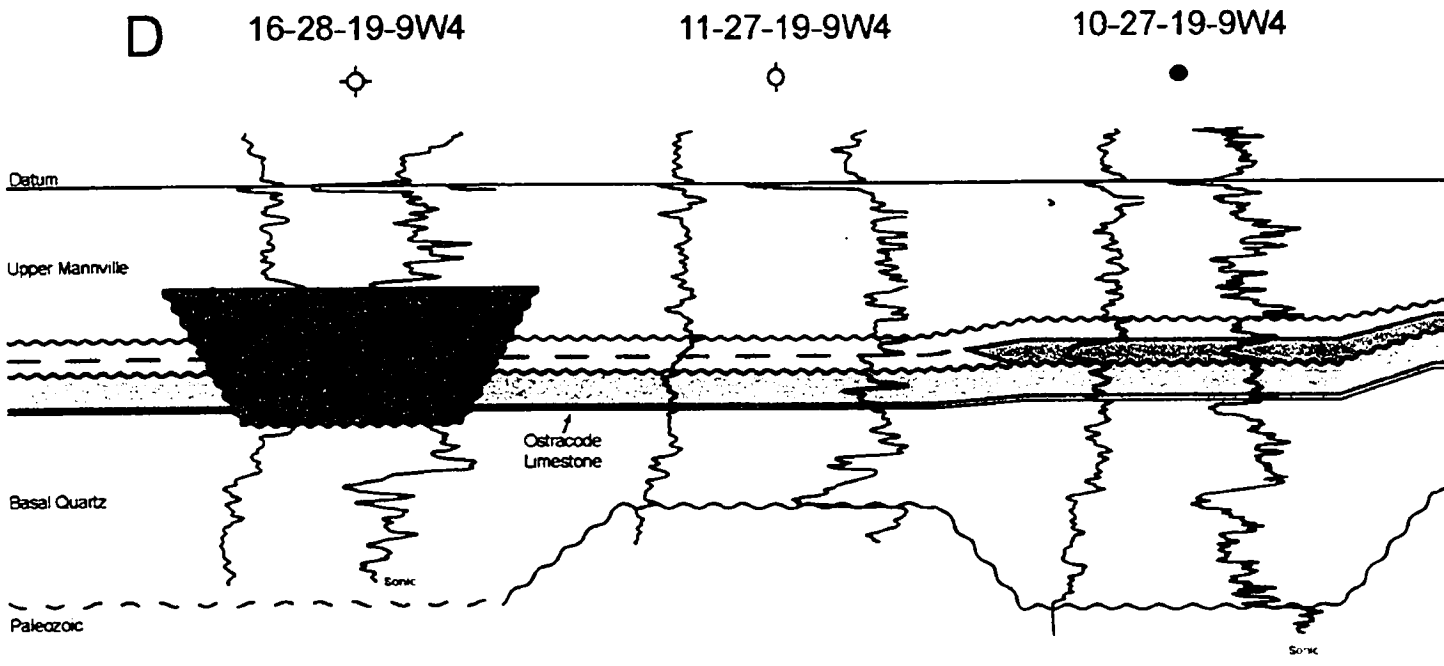
D
16-28-19-9W4
11-27-19-9W4
10-27-19-9W4
Datum
Upper Mannville
Ostracode
Limestone
Basal Quartz
Sonic
Paleozoic
Sonic

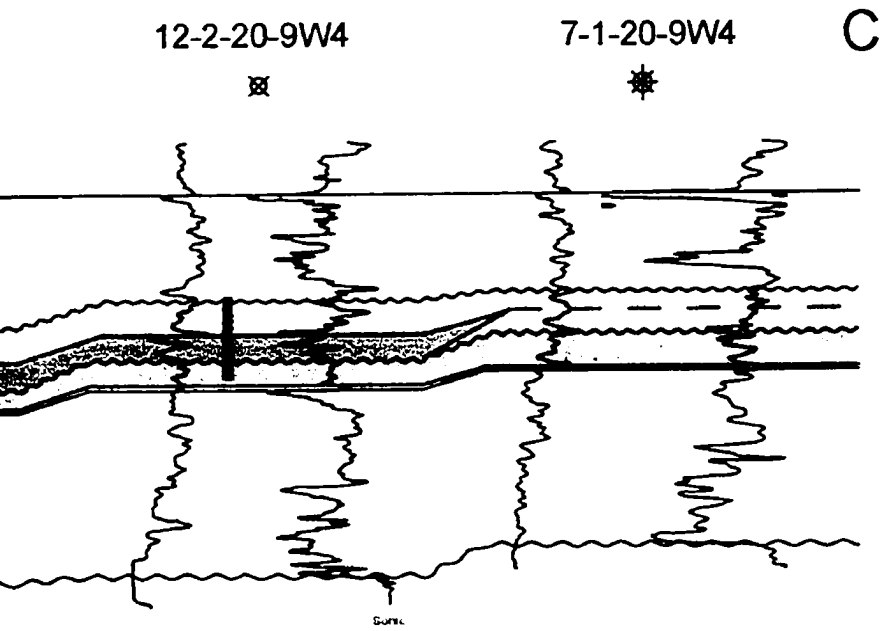
12-2-20-9W4
7-1-20-9W4
C'
Sonic


UM Lithic Channel
CORED INTERVAL
VERTICAL SCALE
10 m

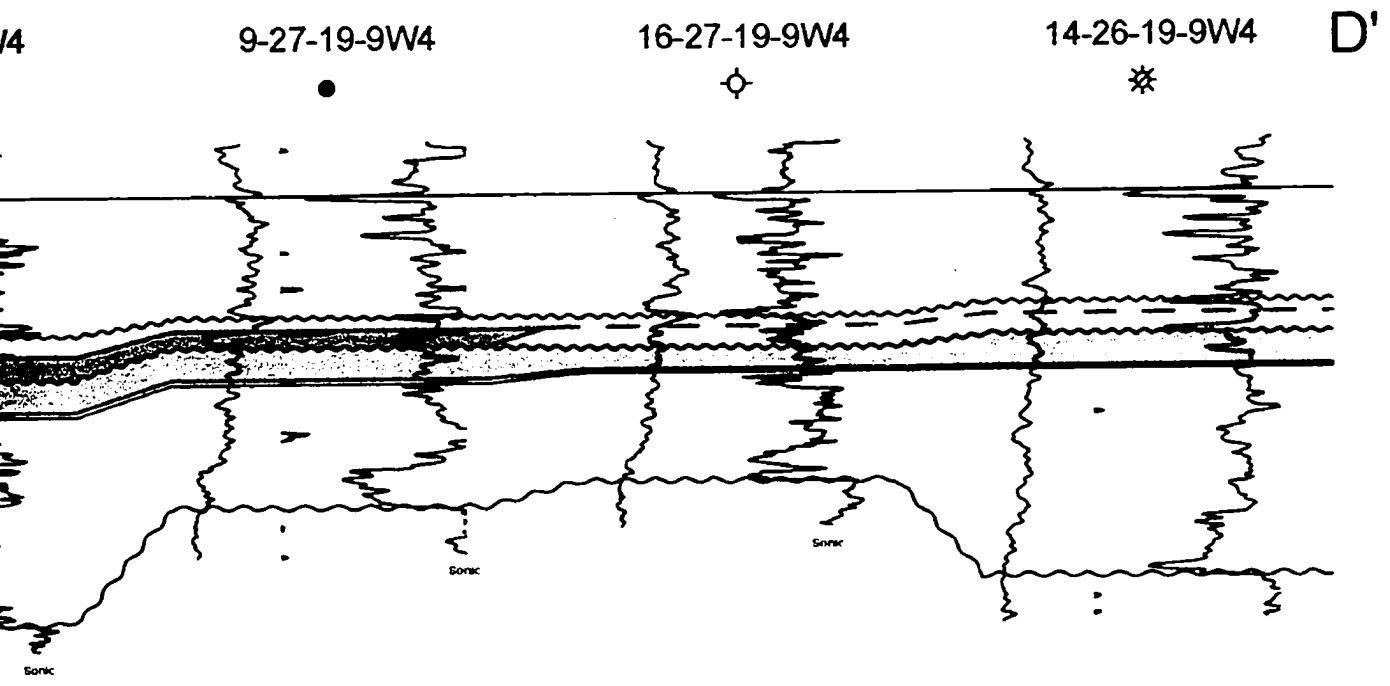
/4
9-27-19-9W4
16-27-19-9W4
14-26-19-9W4
D'
Sonic
Sonic
Sonic

the fill of a southerly-flowing upper estuary channel, wherein thicker and coarser deposits located close to the fluvial-estuarine transition grade basinward into thinner beds of finer-grained sediments toward the lower energy central basin (cf. Allen, 1991; Dalrymple *et al.*, 1992). Channel-fill sandstones and conglomerates of FA2 are thickest where negative paleotopography along the underlying sub-Cretaceous unconformity is greatest. For example, the north-south stratigraphic cross-section AA' shows that FA2 strata overlie a paleotopographic depression with up to 15 m of relief (Figure 4.5). Similarly, estuarine channel fill strata are confined to a paleolow in cross-section DD' (e.g. 00/09-27-019-09W4/0 and 00/10-27-019-09W4/0; Figure 4.6). In addition to a geographic association, there is also a direct relationship between the thickness of FA2 strata and the amount of paleorelief along the sub-Cretaceous unconformity. For example, in cross-section BB' deposits of FA2 are nearly 5 m thicker in wells where paleotopographic relief is greatest (e.g. 00/13-23-020-09W4/0 and 00/15-23-020-09W4/0; Figure 4.5). Remnant negative paleotopography is interpreted to have confined the upper estuary channel to areas of low surface relief and to have produced the stratigraphic relationship between the FA2 isopach and the elevation of the underlying sub-Cretaceous unconformity surface.

In the study area, strata of the Glauconitic Sandstone dip to the northwest by approximately 2 m/km (Figure 4.7). This structural orientation does not conform to the regional northeast dip imposed on Mannville Group strata by the Sweetgrass Arch, a tectonic element that was active during Mannville deposition, and that strongly influenced sedimentation patterns of Lower Cretaceous stratigraphy in southeastern Alberta (Hayes *et al.*, 1994). Local variations in the dip of Mannville Group strata have different origins, including salt dissolution (Handcock and Wood, 2001) and differential erosion of underlying Paleozoic carbonates (Leckie and Smith, 1992). Differential erosion of underlying Paleozoic carbonates created a regional drainage system comprising northwest-southeast trending ridges and valleys (Cant and Abrahamson, 1996). Accommodation space created by dissolution of the underlying middle Devonian Prairie Evaporite Formation, on the other hand, was much more localized. The northwest dip of the Glauconitic Sandstone in the study area, therefore, is interpreted to reflect differential erosion of underlying Paleozoic carbonates rather than salt dissolution.

Figure 4.7: Ostracode Limestone structure contour map. The top of the Ostracode Limestone is used as a proxy to determine the structural orientation of the overlying Glauconitic Sandstone. In the study area, the Glauconitic Sandstone dips to the northwest by approximately 2 m/km. This is interpreted to reflect the creation of northwest-southeast trending ridges and valleys in the WCSB through differential erosion of underlying Paleozoic carbonates. The Ostracode Limestone is truncated by strata of the Jenner shoreface complex (hatchered line) to the north. Contour interval is 4 m.

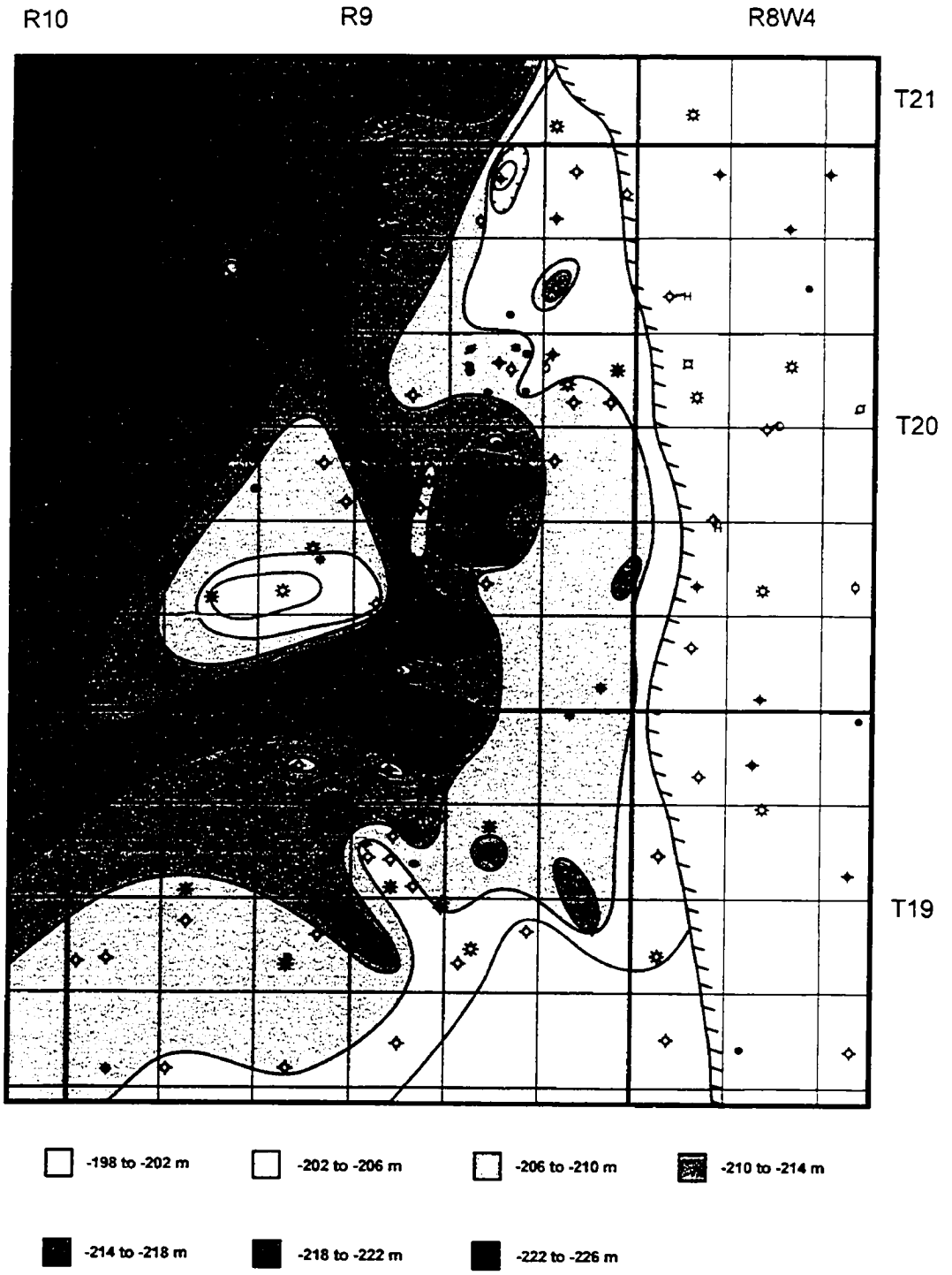
R10
R9
R8W4
T21
T20
T19
-198 to -202 m
-202 to -206 m
-206 to -210 m
-210 to -214 m
-214 to -218 m
-218 to -222 m
-222 to -226 m

The overlying undifferentiated Upper Mannville succession forms a tabular unit of relatively constant thickness until deposition of the datum coal bed (Figures 4.5, 4.6). Spatial variations in post-depositional compaction and incision by the overlying Basal Colorado Sandstone account for the irregular Upper Mannville isopach (Wilson, 1999). In addition to the two Upper Mannville lithic channels that incise FA2 at its northern and southwestern extremities, one other lithic channel incises FA2 strata in the south-central part of the E pool (Figure 4.2). Compartmentalization of the reservoir by incision of Upper Mannville lithic channels and the degree of communication across these channels is discussed in Chapter 5.

4.3 Depositional Model

A depositional model for the Glauconitic Sandstone is presented in Figure 4.8. A fall of relative sea level (SL1 to SL2) following deposition of the Basal Quartz (BQ) in southeastern Alberta resulted in progradation of a thin, lowstand shoreface (LS) across a wide regressive surface of erosion (RSE1) (Figure 4.8a). Within the study area, the lowstand shoreface is represented by the lower, sharp-based parasequence of the Prograding Shoreface to Shallow Shelf Facies Association (FA1). In general, lowstand shorefaces must prograde a long way before water depths are sufficiently deep for mud deposition in the lower shoreface/offshore transition (Walker and Wiseman, 1995). The areally extensive, thin succession of interstratified fine siltstone and silty mudstone (F1) at the base of the lowstand shoreface in the study area, therefore, suggests that it prograded several tens to a few hundreds of km from the initial shoreline position. A subsequent rise of relative sea level (SL2 to SL3) resulted in marine transgression: consequent wave ravinement (WRS) eroded the upper surface of the lowstand shoreface (Figure 4.8b). During a period of a lowered rate of relative sea level rise and/or stillstand (ITI), the shoreface became incised landward of the lowstand shoreline position. Subsequently, transgressive shoreface (TS) deposits prograded across this surface. In the study area, the transgressive shoreface is represented by distal delta front/transitional offshore deposits of the upper, gradational-based FA1 parasequence.

Figure 4.8: Wheeler diagram illustrating the depositional model for the Glauconitic Sandstone. (a) Progradation of a lowstand shoreface (LS) across a regressive surface of erosion (RSE1) following a fall of relative sea level (SL1 to SL2). (b) Wave ravinement (WRS) of the lowstand shoreface during a rise of relative sea level (SL2 to SL3). Incision of the shoreface landward of the lowstand shoreline position during a period of a lowered rate of relative sea level rise and/or stillstand (ITI) and progradation of transgressive shoreface (TS) deposits across this surface. (c) Subaerial exposure of the shoreface following a fall of relative sea level (SL3 to SL4) and generation of an incised-valley above a lowstand surface of erosion (LSE). (d) Transgression produced by a rise of relative sea level (SL4 to SL5), resulting in an amalgamated Type 1 sequence boundary/transgressive surface of erosion (SB/TSE). Firmground burrowers of the *Glossifungites* ichnofacies colonised the exhumed substrate in marginal-marine conditions during initial transgression. The incised-valley fills with backstepping estuarine deposits as transgression continues. (e) Regressive surface of erosion (RSE2) produced by a fall of relative sea level (SL5 to SL6) associated with retreat of the Boreal Sea from southeastern Alberta. Highstand incised-valley deposits eroded during lowstand time. Negative accommodation resulted in common incision of Glauconitic Sandstone strata by non-marine feldspathic to lithic-rich Upper Mannville channels (stippled pattern).

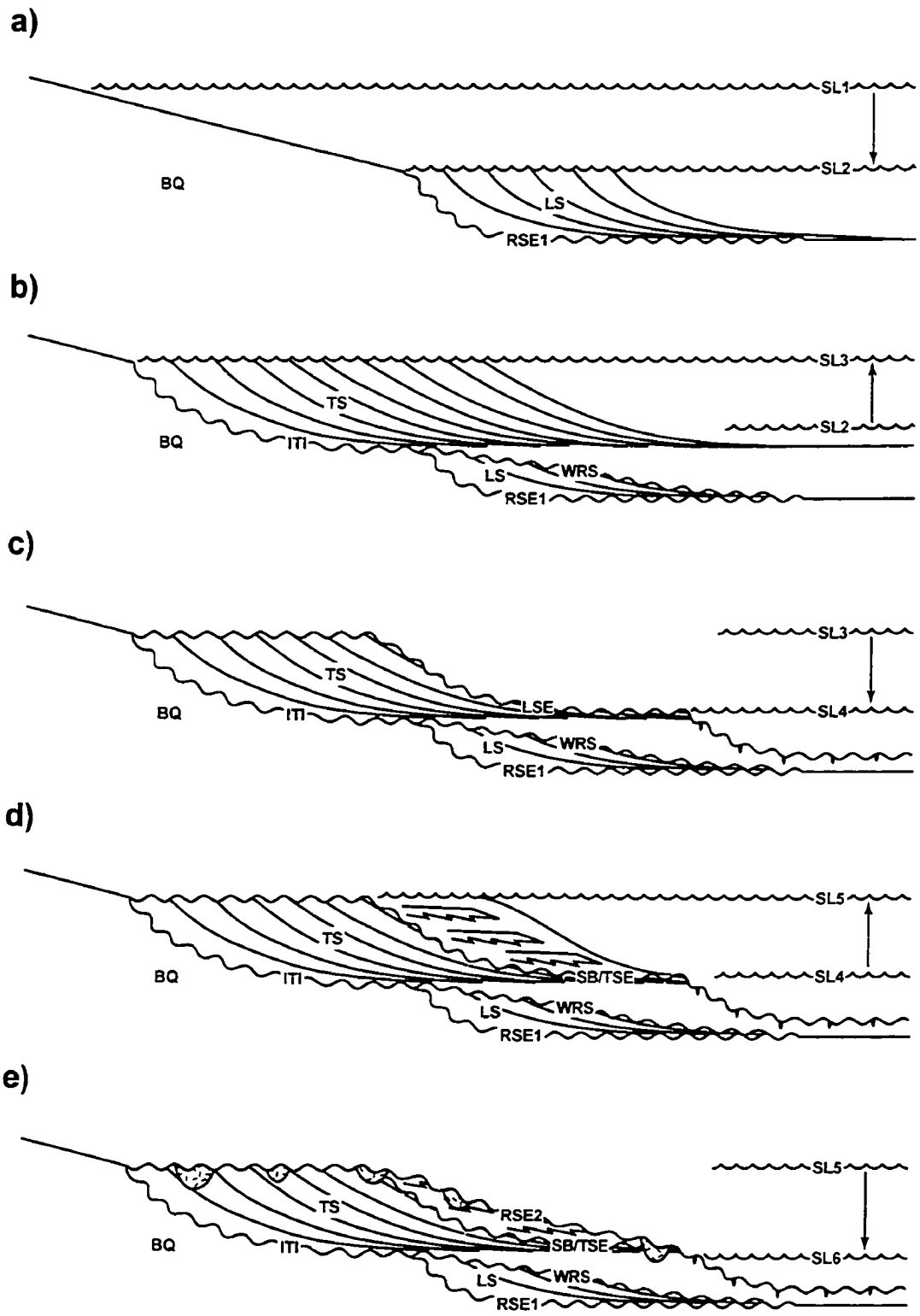
a)
SL1
SL2
BQ
LS
RSE1
b)
SL3
SL2
TS
BQ
ITI
WRS
LS
RSE1
c)
SL3
TS
LSE
SL4
BQ
ITI
WRS
LS
RSE1
d)
SL5
TS
SL4
BQ
ITI
SB/TSE
WRS
LS
RSE1
e)
SL5
TS
RSE2
SB/TSE
SL6
BQ
ITI
WRS
LS
RSE1

A second fall of relative sea level (SL3 to SL4) following deposition of FA1 resulted in subaerial exposure of the shoreface and the generation of a lowstand surface of erosion (LSE) (Figure 4.8c). The lowstand discontinuity exhibits an erosional juxtaposition of more proximal (landward) facies over more distal deposits (i.e. a basinward shift in facies) and is interpreted as a Type 1 sequence boundary (*sensu* Van Wagoner *et al.*, 1990). In the Jenner Upper Mannville E Pool, the lowstand discontinuity corresponds to an incised-valley that produced widespread firmground surfaces. An ensuing transgression (SL4 to SL5) generated a transgressive surface of erosion (TSE) that removed most or all of the lowstand deposits and exposed the discontinuity to marginal-marine conditions, permitting firmground burrowers of the *Glossifungites* ichnofacies to colonise the exhumed substrate during initial transgression (Figure 4.8d). The lowstand discontinuity, therefore, represents an amalgamated Type 1 sequence boundary/transgressive surface of erosion (SB/TSE). As transgression continued, the seaward portion of the incised valley began to fill with backstepping (late lowstand to transgressive) estuarine deposits (Upper Estuary Channel Fill (FA2) and Tidally-Influenced Abandoned Channel/Interchannel Deposits (FA3) Facies Associations) (Figure 4.8d). Estuarine channels were confined to topographic lows within the incised valley, produced by underlying paleotopographic relief along the sub-Cretaceous unconformity surface (Figures 4.5, 4.6). The distribution of FA2 strata suggests that paleoflow was toward the south (see Chapter 3). This contradicts previous regional mapping of Glauconitic Sandstone channel drainage patterns (e.g. Sherwin, 1996) that indicate a predominantly NNW direction of flow (Figure 1.5). The Kindersley Highlands, located in Townships 21-25, Ranges 5-9W4, may have created a local embayment along the northward-retreating Boreal Sea, thus permitting the southward flow of shoreline-normal estuarine and incised-valley systems (Handcock and Wood, 2001).

A third fall of relative sea level (SL5 to SL6) associated with the final retreat of the Boreal Sea from southeastern Alberta generated a regressive surface of erosion (RSE2) that overlies the preserved late lowstand to transgressive estuarine deposits of the previous transgressive systems tract (Figure 4.8e). Highstand incised-valley deposits corresponding to the time of maximum transgression are absent in the study area and are

interpreted to have been eroded during subaerial exposure at lowstand time (cf. Zaitlin *et al.*, 1994). Lowered base level associated with a fall of relative sea level resulted in negative accommodation (Johnson and Dalrymple, 2003). Accordingly, non-marine feldspathic to lithic-rich Upper Mannville channels commonly incised into the preserved upper estuarine succession, sealing and compartmentalizing reservoir-quality quartzose sandstone bodies. In addition, the marked change in mineralogy from quartzarenites of the Glauconitic Sandstone to lithic arkoses of the Upper Mannville is suggestive of a different sediment provenance resulting from Cordilleran tectonic activity. Terrestrial deposition of the undifferentiated Upper Mannville marks the termination of Glauconitic Sandstone deposition in the study area.

5. PETROLEUM GEOLOGY

5.1 Pool History/Specifications

The Jenner Upper Mannville E Pool is a 10 km long by 2 km wide north-south trending conventional oil pool located in Townships 19-20, Range 9W4 in southeastern Alberta (Figure 1.6). Since its discovery in 1963, the pool has produced 7.3 million barrels (mmbbl) of 21.1° API oil and 6.7 billion cubic feet (bcf) of gas from the Lower Cretaceous Glauconitic Sandstone. Current production averages 258 barrels per day (bbl/d) of oil and 1 million cubic feet per day (mmcf/d) of gas. The original in-place oil (OOIP) is 28.6 mmbbl and estimated remaining reserves are of the order of 700 mbbl (Alberta Energy and Utilities Board, 2003). The E pool was produced under primary depletion from discovery until November 1968, whereafter water injection and, beginning in early 1969, polymer flooding was used to maintain reservoir pressure. Polymer flooding ended in September 1973 due to poor economics and negligible improvement in waterflood efficiency (Handcock and Wood, 2001). To date, 44.6 mmbbl of water have been injected into the reservoir. Of the 39 wells drilled into the pool, 20 are currently producing and 5 are water injectors (Table 5.1).

5.2 Reservoir Characteristics

Coarse clastics of the Upper Estuary Channel Fill Facies Association (FA2) represent the main Glauconitic Sandstone reservoir and produce both oil and gas along the entire length of the deposit (see Chapters 3 and 4 for detailed discussions regarding the areal distribution of facies and facies associations in the study area). In the northern part of the pool (sections 14, 23 and 26, Township 20, Range 9W4), amalgamated coarse clastics, particularly stacked medium-scale cross-stratified sandstone (F3) and chert pebble conglomerate (F5), are common. The coarse clastics are thicker (up to 15 m thick) and less commonly interstratified with mudstone compared to the south (Figure 3.6). Unfortunately, these thicker, amalgamated intervals tend to be typically of the order of 150-200 m wide, and locally grade into interchannel mudstones over distances of less

Table 5.1: Production summary for the 39 wells drilled into the Jenner Upper Mannville E Pool and their relative location within the pool. Last Prod Avg Rate: Oil (bbl/d), Gas (mmcf/d), Water (bbl/d). Cumulative Production: Oil (mbbl), Gas (mmcf), Water (mbbl). Production data to July 31, 2003.

Well ID	Status	Production		Last Prod Avg Rate			Cumulative Production			Location
		On	Last	Oil	Gas	Water	Oil	Gas	Water	
00/07-27-019-09W4/0	Oil, Pumping	01/03	03/07	29.5	0.11	2.2	30.5	72.0	4.8	south
00/09-27-019-09W4/0	Oil, Pumping	01/09	03/07	18.5	0.06	28.5	18.2	32.7	15.0	south
00/10-27-019-09W4/0	Oil, Pumping	68/01	03/07	6.1	0.06	116.0	618.8	325.3	2588.0	south
00/14-27-019-09W4/2	Oil, Suspended	68/02	88/02	7.2	0.01	201.1	89.0	117.4	779.6	south
00/01-34-019-09W4/0	Oil, Suspended	01/11	02/07	0.6	0.02	0.9	0.7	7.4	1.6	south
00/02-34-019-09W4/0	Water, Injection	64/12	68/08	0.0	0.00	0.0	4.5	75.7	0.0	south
00/06-34-019-09W4/2	Oil, Pumping	68/02	03/07	10.4	0.03	69.7	532.6	592.7	1791.1	south
00/08-34-019-09W4/0	Oil, Suspended	65/08	90/05	7.8	<0.01	269.3	274.2	209.2	1193.9	south
00/10-34-019-09W4/0	Oil, Abandoned	64/10	90/04	10.7	0.04	352.0	198.3	102.4	334.3	south
00/16-34-019-09W4/0	Oil, Pumping	65/08	03/07	12.6	0.22	247.7	1066.6	711.7	3533.7	south
00/12-35-019-09W4/0	Oil, Abandoned	65/10	70/09	5.6	0.10	17.9	5.2	23.2	2.4	lithic channel
00/12-02-020-09W4/0	Water, Abandoned	67/12	73/09	16.2	0.05	53.5	20.9	101.9	0.5	south-central
00/14-02-020-09W4/0	Oil, Pumping	68/07	03/07	2.1	<0.01	2.8	110.7	90.7	75.1	south-central
00/16-03-020-09W4/0	Water, Injection	66/04	87/09	17.0	0.01	187.5	166.0	154.6	442.2	south-central
00/02-10-020-09W4/0	Oil, Pumping	64/11	02/11	5.8	0.01	11.4	254.9	293.8	311.3	south-central
00/08-10-020-09W4/0	Oil, Pumping	65/01	03/07	3.3	0.02	86.4	441.0	352.4	1484.7	south-central
00/10-10-020-09W4/2	Oil, Abandoned	89/06	89/08	0.6	0.00	0.0	0.1	0.0	0.2	south-central
00/16-10-020-09W4/2	Oil, Pumping	71/12	03/07	5.3	0.02	70.9	358.3	466.7	1322.1	south-central
00/04-11-020-09W4/0	Oil, Pumping	65/08	03/07	20.2	0.20	513.3	1267.3	892.8	10996.7	south-central
02/06-11-020-09W4/3	Oil, Pumping	01/09	02/10	5.1	0.00	1.5	1.7	0.0	1.7	south-central
00/12-11-020-09W4/0	Water, Injection	65/07	68/08	47.5	0.06	0.0	22.8	18.6	0.0	south-central
02/14-11-020-09W4/0	Oil, Pumping	01/02	03/07	11.6	<0.01	2.3	7.6	4.0	4.4	south-central
00/04-14-020-09W4/0	Oil, Suspended	65/07	00/04	1.3	0.01	96.3	456.2	226.2	1195.9	north
02/06-14-020-09W4/0	Stand			0.0	0.00	0.0	0.0	0.0	0.0	north
00/08-14-020-09W4/0	Oil, Suspended	65/01	99/03	8.9	0.03	100.2	242.5	122.4	737.6	north
00/10-14-020-09W4/0	Oil, Pumping	64/03	03/07	9.8	<0.01	10.6	389.6	272.0	105.2	north
00/14-14-020-09W4/0	Oil, Pumping	93/09	03/07	65.2	0.13	780.7	259.8	572.2	3097.5	north
00/02-23-020-09W4/0	Water, Injection	87/12	98/10	9.8	0.28	91.3	42.9	81.5	427.5	north
00/04-23-020-09W4/0	Oil, Pumping	88/12	03/06	9.4	0.11	485.2	75.9	583.9	758.5	north
00/06-23-020-09W4/0	Oil, Pumping	88/10	97/02	0.7	<0.01	106.8	12.4	10.2	50.0	north
00/08-23-020-09W4/0	Oil, Pumping	88/11	03/07	7.3	<0.01	43.7	59.5	36.8	51.1	north
00/10-23-020-09W4/0	Oil, Abandoned	89/01	96/11	19.0	0.02	19.7	15.9	11.4	53.1	north
02/10-23-020-09W4/2	Oil, Pumping	95/08	03/07	33.0	0.04	1190.9	241.4	217.1	1461.2	north
00/10-23-020-09W4/2	Oil, Abandoned	97/06	98/09	14.2	0.00	50.0	2.5	1.7	14.5	north
00/12-23-020-09W4/0	Oil, Pumping	96/05	03/07	21.5	0.09	101.5	24.8	133.5	66.2	north
00/13-23-020-09W4/2	Oil, Suspended	95/02	96/02	519.6	5.24	2.7	2.7	27.3	0.3	north
00/15-23-020-09W4/0	Oil, Pumping	96/06	03/07	6.4	0.05	158.1	35.1	102.1	209.5	north
02/16-23-020-09W4/0	Oil, Abandoned	83/05	83/09	7.4	<0.01	4.8	1.5	0.4	0.3	north
02/16-23-020-09W4/2	Water, Injection			0.0	0.00	0.0	0.0	0.0	0.0	north

than 1 km. Most wells located in the northern end of the pool have been on production five years less than wells in the south-central and southern parts of the pool (Table 5.1), yet they have contributed 25% of the pool's cumulative production, illustrating a direct correlation between production and facies distribution. FA2 strata in the south-central part of the pool (parts of sections 2, 3, 10 and 11, Township 20, Range 9W4) consist principally of interstratified massive sandstone and contorted muddy siltstone (F4). Here, coarse clastics of FA2 are thinner and more regularly interstratified with mudstone (Figures 3.6, 4.6). Despite this, these strata tend to be areally expansive and typically extend laterally across nearly two sections (~ 3.2 km wide), making them an easier target than the narrower clastic bodies in the northern and southern ends of the pool. FA2 strata in the southern part of the pool (sections 27 and 34, Township 19, Range 9W4 and part of Section 3, Township 20, Range 9W4) are similar to strata in the north. Specifically, they are dominated by dune cross-stratified sandstone (F3), but lack chert pebble conglomerate (F5) interbeds. FA2 strata are also much thinner in the southern part of the pool with an average thickness of ~ 3 m (Figure 3.6).

Core analyses from 220 previously collected plug samples were used in order to correlate the productive facies described in Chapter 2 (F3, F4, and F5) and reservoir quality (Figure 5.1). Porosity in medium-scale cross-stratified sandstone (F3) ranges from 7.7-28% and averages 23.4%; permeability ranges from 0.06-6401 md (K_{max}) and averages 1219 md (K_{max}). Interstratified massive sandstone and contorted muddy siltstone (F4) have porosities that range from 13.7-29.2% and average 23.0%; permeability ranges from 0.84-4120 md (K_{max}) and averages 497.6 md (K_{max}). Low porosity and permeability in this facies tend to be associated with localized mud laminae and mudstone interbeds. Although F4 has marginal reservoir quality (porosity and permeability), it constitutes the main Glauconitic Sandstone reservoir facies of FA2 because it is volumetrically large and has been penetrated by several wells that have been on production for nearly 40 years (Table 5.1). Thin chert pebble conglomerate beds (F5) have porosities ranging from 15.7-28.2% and averaging 22.1%. Permeabilities range from 309-10,240 md (K_{max}) and average 3699 md (K_{max}).

A porosity/vertical permeability cross-plot using core analyses from 151 previously collected plug samples of the three productive facies was constructed to show the effect

Figure 5.1: Porosity and maximum permeability data for Upper Estuary Channel Fill Facies Association (FA2) deposits. The plot of core analyses is based on 220 plug samples. Three main facies groups (F3, F4, and F5) are represented. Facies 3 is medium-scale cross-stratified sandstone interpreted as the migration of two- and three-dimensional subaqueous dunes. Porosity is 7.7-28%, averaging 23.4%, and permeability is 0.06-6401 md (K_{max}), averaging 1219 md (K_{max}). Facies 4 is interstratified massive sandstone and contorted muddy siltstone interpreted as the downslope movement of liquefied water-saturated sand following bank collapse. Porosity is 13.7-29.2%, averaging 23.0%, and permeability is 0.84-4120 md (K_{max}), averaging 497.6 md (K_{max}). Facies 5 is matrix- and clast-supported chert pebble conglomerate interpreted as the migration of subaqueous dunes in heterogeneous sediment. Porosity is 15.7-28.2%, averaging 22.1%, and permeability is 309-10,240 md (K_{max}), averaging 3699 md (K_{max}). Most hydrocarbon production is associated with Facies 4.

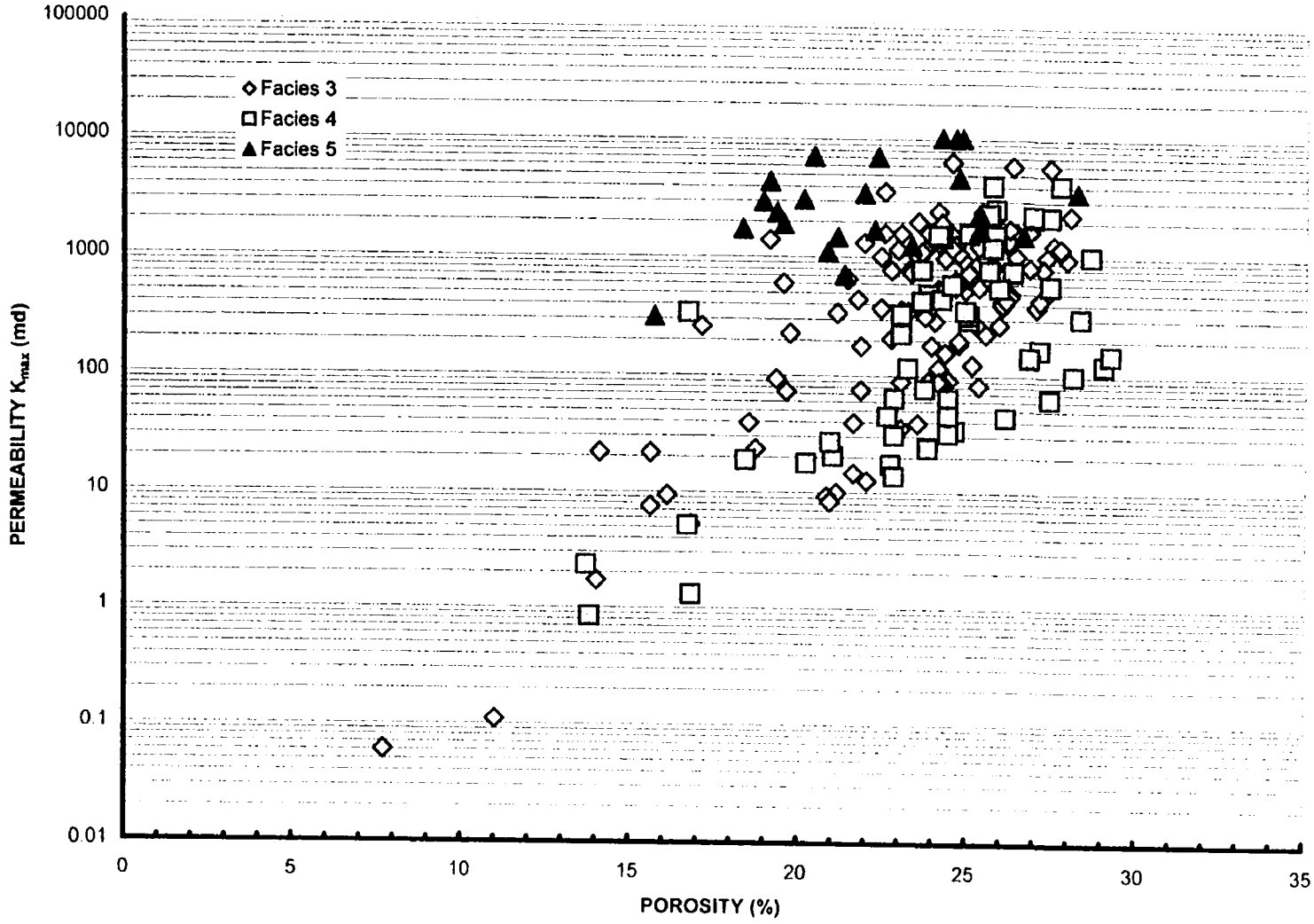
Facies 3
Facies 4
Facies 5
PERMEABILITY K_{max} (md)
100000
10000
1000
100
10
1
0.1
0.01
0
5
10
15
20
25
30
35
POROSITY (%)

of cements on reservoir quality (Figure 5.2). Porosity in medium-scale cross-stratified sandstone (F3) ranges from 14.0-27.9% and averages 23.8%; permeability ranges from 0.1-3896 md (K_{vert}) and averages 572.1 md (K_{vert}). Interstratified massive sandstone and contorted muddy siltstone (F4) have porosities ranging from 16.7-28.6% and averaging 25.4%; permeabilities range from 3.4-3350 md (K_{vert}) and average 1030 md (K_{vert}). Chert pebble conglomerate beds (F5) have porosities that range from 15.7-28.2% and average 22.1%; permeability ranges from 43.5-10,240 md (K_{vert}) and averages 2569 md (K_{vert}). F3 and F5 both show a significant reduction in average vertical versus maximum permeability. This is interpreted to represent the presence of authigenic clay minerals, derived from unstable feldspar and rock fragments during diagenesis, that impede the vertical movement of migrating fluids. Average vertical permeability of F4, on the other hand, is 500 md higher compared to average maximum permeability. This suggests a smaller amount of authigenic clay cement within sandstone of F4 compared to F3 and F5. These inferences are supported by petrographical analyses of sandstone from the productive facies that show F3 and F5 to contain more abundant lithic rock fragments and feldspar framework grains and accordingly more authigenic clay (Appendix 2). An increase in vertical versus maximum permeability in F4 further suggests that mud laminae and mudstone interbeds are ineffective barriers to vertical flow, perhaps because they are laterally discontinuous or contain abundant vertical fractures.

5.3 Reservoir Compartmentalization

Later incision by two Upper Mannville lithic channels has compartmentalized the FA2 reservoir into three separate units (Figure 4.2). The southern and central units comprise the Jenner Upper Mannville E Pool and are separated by a northwest-southeast trending lithic channel penetrated by wells 00/12-35-019-09W4/0 and 00/08-03-020-09W4/0. A major production issue is whether there is communication across this channel sandstone. Handcock and Wood (2001) argued that localized communication under the channel is suggested by the 00/04-02-020-09W4/0 well watering out in January 1984 with no gas production. They argue that the well was swept by water injected (beginning in April 1969) from the well located at 00/12-11-020-09W4/0. In this scenario the water

Figure 5.2: Porosity and vertical permeability data for Upper Estuary Channel Fill Facies Association (FA2) deposits. The plot of core analyses is based on 151 plug samples. Three main facies groups (F3, F4, and F5) are represented. F3 porosity is 14.0-27.9%, averaging 23.8%, and permeability is 0.1-3896 md (K_{vert}), averaging 572.1 md (K_{vert}). F4 porosity is 16.7-28.6%, averaging 25.4%, and permeability is 3.4-3350 md (K_{vert}), averaging 1030 md (K_{vert}). F5 porosity is 15.7-28.2%, averaging 22.1%, and permeability is 43.5-10,240 md (K_{vert}), averaging 2569 md (K_{vert}).

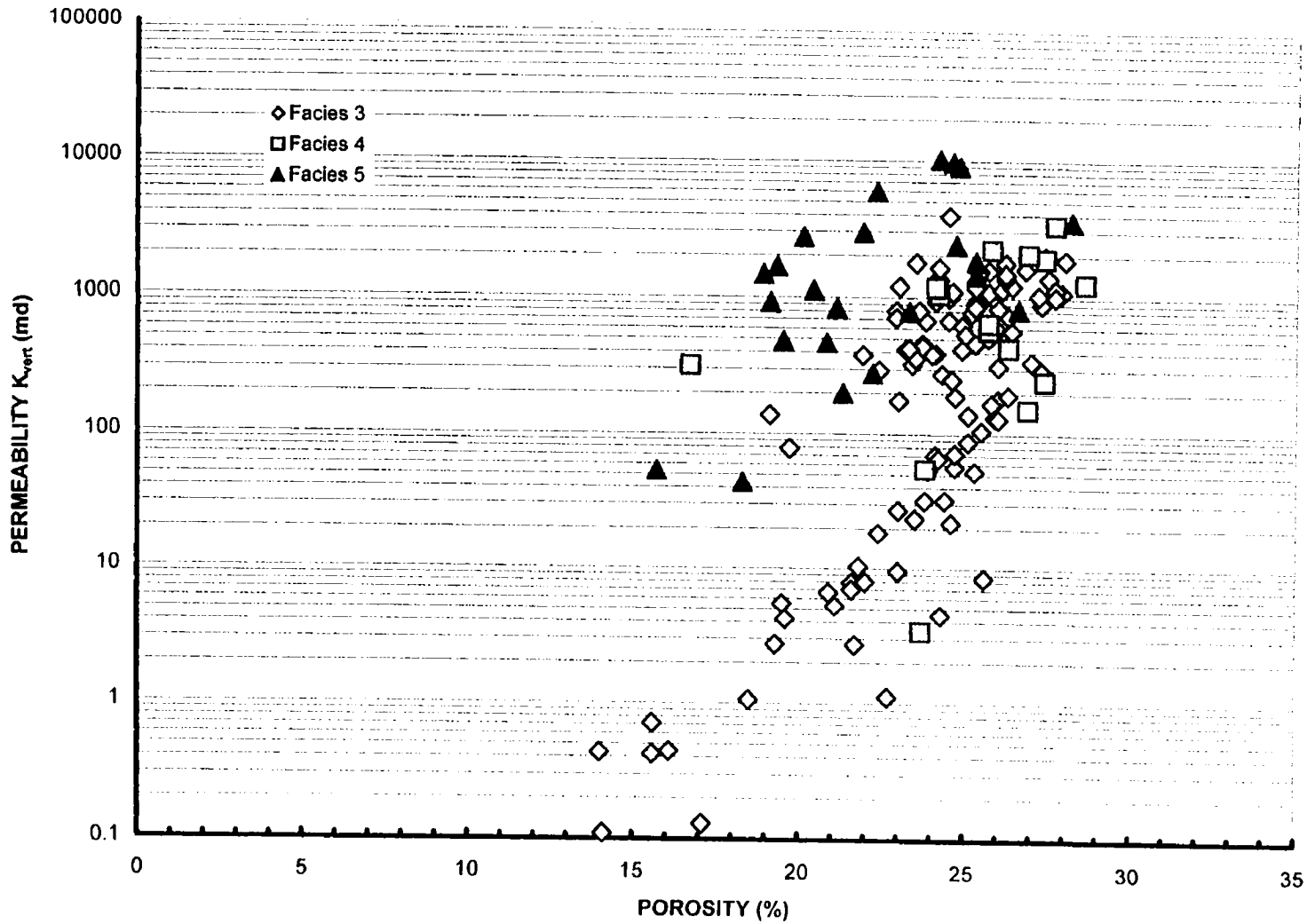
100000
10000
1000
100
10
1
0.1
PERMEABILITY K_{vert} (md)
Facies 3
Facies 4
Facies 5
0
5
10
15
20
25
30
35
POROSITY (%)

front would have migrated south sweeping past 00/04-02-020-09W4/0, indicating communication beneath the lithic channel. Pressure data from wells close to the lithic channel, however, are variable. For example, the extrapolated DST pressure at 00/12-35-019-09W4/0 was 10,814 kPa in October 1965, but subsequent datum pressures were 9331 kPa (May 1966), 10,537 kPa (June 1967), 9461 kPa (May 1968) and 9754 kPa (May 1970), respectively. Consequently, determining the communication between the south and central parts of the E pool remains equivocal.

The northern FA2 unit is penetrated by 5 wells, of which 00/03-35-020-09W4/2 and 00/04-36-020-09W4/2 have produced 2.0 bcf of gas from the Glauconitic Sandstone within the Jenner Upper Mannville XXX and B2B pools, respectively (Alberta Energy and Utilities Board, 2003). The distribution of FA2 suggests that producing wells of the E, XXX and B2B pools intersect deposits of the same upper estuary channel. This is supported by stratigraphic correlation of their similar geophysical well-log signatures. A summary of initial pool pressures and cumulative production indicates that FA2 strata are in lateral communication in the E and B2B pools, but are separated from equivalent strata in the XXX pool (Table 5.2). This may suggest partial communication across a single northwest-southeast trending lithic channel or the presence of several smaller lithic channels that have further compartmentalized the northern FA2 unit. Present well control in the northern FA2 reservoir unit is unable to resolve the occurrence of any small-scale channel forms. Furthermore, the northwest-southeast trending Upper Mannville lithic channel that separates the central and northern FA2 units is penetrated by only a single well (00/05-25-020-09W4/0) and its location in section 26 is largely inferred based on regional channel orientations. Better well and seismic control is needed to better delineate the number and position of Upper Mannville lithic channels that may further compartmentalize the FA2 reservoir. It is tentatively proposed, therefore, that wells 00/03-35-020-09W4/2 and 00/04-36-020-09W4/2 (XXX and B2B pools, respectively) be reclassified and included in the Jenner Upper Mannville E Pool.

Table 5.2: Summary of initial pressure and cumulative oil and gas production for the Jenner Upper Mannville E, B2B, and XXX pools. Production data to July 31, 2003.

Pool	Number of Wells	Initial Pressure (kPa)	Cumulative Oil (mbbl)	Cumulative Gas (mmcf)
E	39	10797.00	7352.4	7043.9
B2B	1	10420.00	0.0	24.7
XXX	2	13840.00	0.0	1956.5

5.4 Net Pay

A net pay isopach map of the FA2 reservoir sandbody was constructed using cut-offs of <45 API units gamma-ray, >15% density porosity, >30 mv spontaneous potential, >10 ohm-m resistivity and >80 ms/ft sonic (Figure 5.3). FA2 net pay corresponds closely to the gross sandstone isopach (Figure 3.6); three net pay sandbody compartments are separated by impermeable Upper Mannville lithic channels. Net pay is thickest in the northern part of the Jenner Upper Mannville E Pool and thins to the north and south.

5.5 Recommendations for Further Development

Based on current production rates, remaining reserves of the Jenner Upper Mannville E Pool will be fully exploited in approximately 7.4 years. The following recommendations are presented in order to maximize development efficiency and potentially increase the volume of remaining reserves:

1) Apply to downspace to 1 well per LSD in sections 14, 23 and 26, Township 20, Range 9W4. Amalgamated coarse clastic facies within these sections have up to 11 m of net pay and good reservoir quality. Infill drilling would more efficiently exploit the remaining reserves in the northern end of E pool.

2) Using seismic, determine the precise location of the northwest-southeast trending Upper Mannville lithic channel in sections 25 and 26, Township 20, Range 9W4. Detailed imaging of the lithic channel will reduce the risk of penetrating impermeable feldspathic and lithic-rich sandstone with development wells intended to intersect reservoir strata of the Glauconitic Sandstone.

3) Apply to extend the northern E pool boundary to the limit of the FA2 reservoir sandbody. This will increase the pool's cumulative production and remaining reserves as well as reduce confusion regarding pressure drawdown on either side of the lithic channel separating the central and northern FA2 reservoir units.

Figure 5.3: Net pay sandstone isopach map for FA2. Geophysical well-log cut-offs of <45 API units gamma-ray, >15% density porosity, >30 mv spontaneous potential, >10 ohm-m resistivity and >80 ms/ft sonic were used. The distribution of FA2 net pay matches the FA2 gross sandstone isopach (Figure 3.6). Three net pay sandbodies are separated by impermeable Upper Mannville lithic channels. FA2 is truncated by strata of the Jenner shoreface complex (hatchered line) to the north. Contour interval is 2 m.

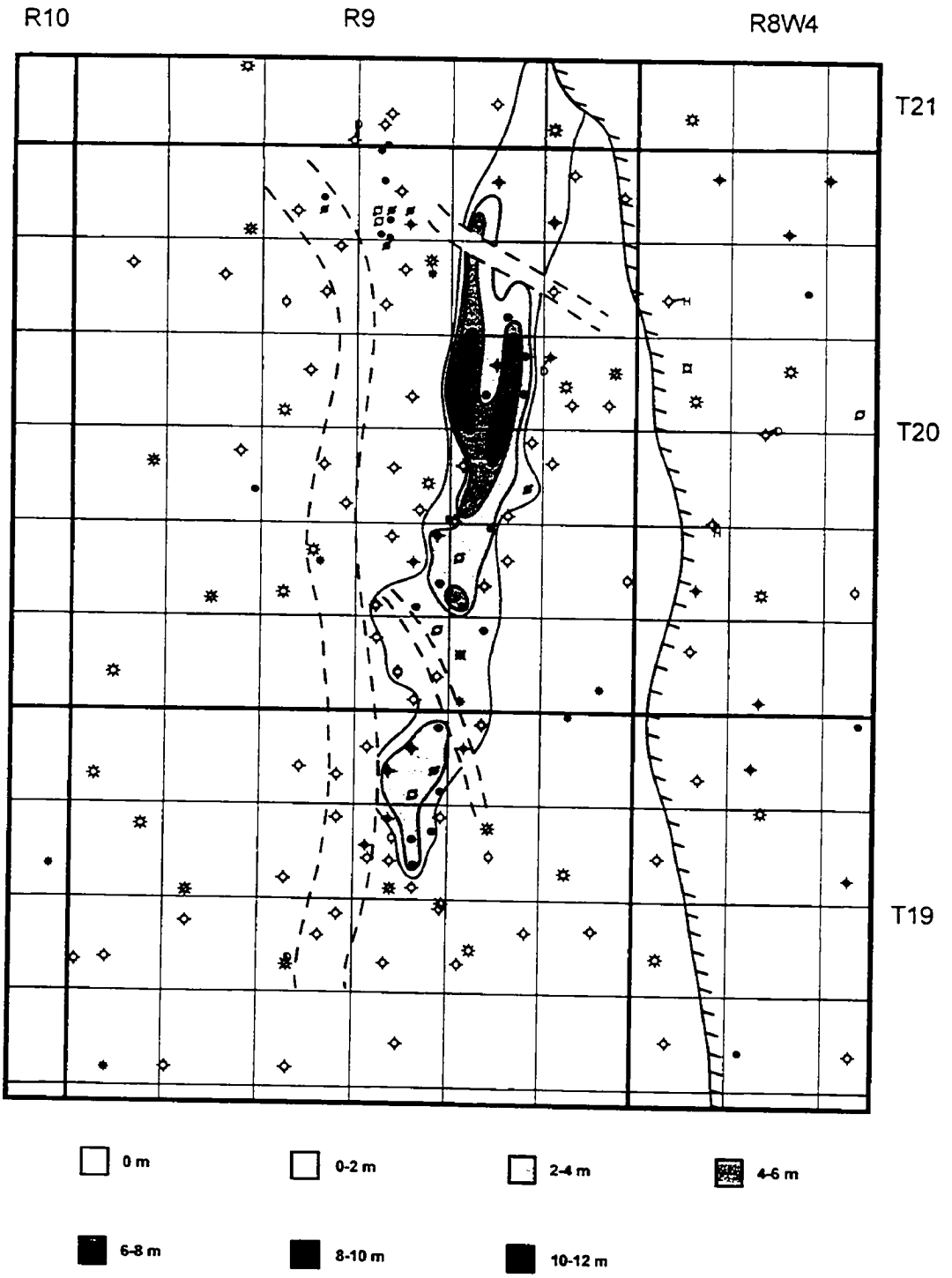
R10
R9
R8W4
T21
T20
T19
0 m
0-2 m
2-4 m
4-6 m
6-8 m
8-10 m
10-12 m

4) Drill 1 well per quarter-section in the northern FA2 reservoir unit. This unit has gas potential and is currently underdeveloped.

6. SUMMARY AND CONCLUSIONS

In the Jenner Upper Mannville E Pool of southeastern Alberta (Townships 19-20, Range 9W4), the Lower Cretaceous (Albian) Glauconitic Sandstone consists of seven sedimentary facies comprising three recurring facies associations: 1) Prograding Shoreface to Shallow Shelf (FA1); 2) Upper Estuary Channel Fill (FA2); and 3) Tidally-Influenced Abandoned Channel/Interchannel Deposits (FA3). The primary reservoir occurs in transgressive FA2 deposits.

A fall of relative sea level following deposition of the Ostracode Limestone in southeastern Alberta resulted in progradation of a thin, lowstand shoreface (lower FA1 parasequence) across a wide regressive surface of erosion. A subsequent rise of relative sea level resulted in marine transgression with attendant wave erosion. During a period of a lowered rate of relative sea level rise and/or stillstand, the shoreface became incised landward of the lowstand shoreline position. Subsequently, transgressive shoreface deposits (upper FA1 parasequence) prograded across this surface. FA1 comprises two upward-shoaling parasequences separated by a marine flooding surface. The lower parasequence consists of interstratified, planar- to wave-ripple cross-laminated siltstone and mudstone overlain sharply by hummocky cross-stratified very fine-grained sandstone and is interpreted to represent a storm-dominated, incised lower shoreface deposit (forced regression). The upper parasequence, which grades from bioturbated mudstone to silty sandstone with common soft-sediment deformation structures, is interpreted to represent the deposits of a prograding distal delta front (normal regression).

A second fall of relative sea level following deposition of FA1 resulted in subaerial exposure of the shoreface, generation of a lowstand surface of erosion (Type 1 sequence boundary), and the incision of a N-S trending incised-valley across the study area. During the early part of the ensuing transgression, marine erosion exposed the discontinuity at the base of the incised-valley and permitted firmground burrowers of the *Glossifungites* ichnofacies to colonise the exhumed substrate. As transgression continued, the seaward portion of the incised valley began to fill with backstepping estuarine deposits (FA2 and FA3). FA2 strata, which are the main reservoir strata in the study area, are composed of 3 primary facies: 1) dune cross-stratified sandstone (F3); 2)

interstratified massive sandstone and contorted muddy siltstone (F4); and 3) chert pebble conglomerate (F5). Deposits of FA2 are interpreted to have been deposited seaward of the maximum tide limit in an upper estuarine environment. This is suggested by: 1) channel morphology of the sandbody; 2) partitioning of coarse- and fine-grained facies at opposite ends of the pool; 3) thin mudstone interlaminae within sandstone channel-fill facies; 4) brackish water trace fossil assemblage; and 5) conformable contact between FA2 and overlying tidally-influenced strata of FA3. The distribution of FA2 strata suggests that paleoflow was toward the south. The Kindersley Highlands may have created a local embayment along the northward-retreating Boreal Sea, thus permitting the southward flow of shoreline-normal estuarine and incised-valley systems (Figure 1.4). FA3 consists of interstratified carbonaceous sandstone, siltstone, mudstone and coal. The grain size, sand/mud ratio and scale of sedimentary structures decrease upwards within strata of FA3 and is interpreted to represent deposition in abandoned channel and floodbasin environments. The presence of tidal sedimentary structures, a brackish water ichnofossil suite and the common coexistence of siderite and pyrite in FA3 strata supports an abandoned estuarine channel interpretation and suggests the continued influence of tides during and after the abandonment phase. FA3 represents the uppermost unit of the Glauconitic Sandstone in the study area.

A third fall of relative sea level associated with the final retreat of the Boreal Sea from southeastern Alberta generated a regressive surface of erosion that overlies the preserved estuarine deposits of the previous transgressive systems tract. Highstand deposits corresponding to the time of maximum transgression are absent in the study area and are interpreted to have been eroded during lowstand time. Lowered base level associated with a fall of relative sea level resulted in negative accommodation. Accordingly, non-marine feldspathic to lithic-rich Upper Mannville channels commonly incised into the preserved upper estuarine succession, sealing and compartmentalizing reservoir-quality quartzose sandstone bodies. The marked change in mineralogy from quartzarenite of the Glauconitic Sandstone to lithic arkose of the Upper Mannville is suggestive of a different sediment provenance resulting from Cordilleran tectonic activity. Quartzose sand of the upper estuary channel fill (FA2) was likely sourced from the Kindersley Highlands, whereas feldspathic to lithic channel sandstone of the

undifferentiated Upper Mannville succession is interpreted to have derived from a southwestern Cordilleran source. Terrestrial deposition of the undifferentiated Upper Mannville marks the termination of Glauconitic Sandstone deposition in the study area.

Two northwest-southeast trending Upper Mannville lithic channels have compartmentalized the FA2 reservoir into three separate units, of which the southern and central units comprise the Jenner Upper Mannville E Pool. Inconsistent pressure data precludes a quantitative assessment of reservoir communication across these lithic channels. However, the waterflood history of a well located near the southern lithic channel and similar initial pressures of pools on either side of the northern lithic channel suggests that there is at least some connectivity across both lithic channel sandstones. The trend of the northern Upper Mannville lithic channel is presently inferred based on its existence in a single well and knowledge of regional channel orientations. Greater well control and seismic coverage are required to better ascertain its precise location. Reservoir quality (porosity and permeability) vary between the different productive facies (F3, F4, and F5). Thin beds of chert pebble conglomerate (F5) have the highest average permeability, followed by dune cross-stratified sandstone (F3) and interstratified massive sandstone and contorted muddy siltstone (F4). The northern part of E pool is characterized by thick successions (up to 16 m thick) of interbedded F3 and F5. The south-central part of the pool consists principally of F4, where these strata tend to be areally expansive (over 3 km wide) compared to the narrower bodies in the northern and southern parts of the pool. FA2 strata in the southern part of the pool are dominated by F3 but lack F5 interbeds and are thinner (~ 3 m thick) than equivalent strata to the north. F4 is the most common facies and has been exploited for the longest time but younger development wells that have penetrated better reservoir quality F3 and F5 facies in the northern part of E pool have contributed 25% of the pool's cumulative production, illustrating a correlation between production efficiency and facies-controlled reservoir quality. Consequently, it is recommended to downspace to 1 well per LSD in sections 14, 23, and 26, Township 20, Range 9W4 in order to more efficiently exploit the pool's remaining reserves.

This thesis provides a sedimentological and stratigraphic description of the Glauconitic Sandstone in the Jenner Upper Mannville E Pool and interprets the

geomorphic processes responsible for deposition of its constituent facies associations. A sequence stratigraphic depositional model is introduced which invokes changes in relative sea level to explain the observed facies succession. In addition, the relationship between geologically controlled reservoir attributes and pool production has been identified, which should in turn help to more efficiently exploit the remaining reserves of oil and gas. It is recommended that future studies of the Glauconitic Sandstone in southeastern Alberta be conducted on a more regional scale in order to test the applicability of the conclusions made in this thesis to a broader study area.

References

Aigner, T., Reineck, H.E., 1982, Proximality trends in modern storm sands from the Helegoland Bight (North Sea) and their implications for basin analysis: Senckenbergiana Maritima, v. 14, p. 183-215.

Alberta Energy and Utilities Board, 2003, Alberta's Reserves 2002 and Supply/Demand Outlook 2003-2012: Crude Bitumen, Crude Oil, Natural Gas and Liquids, Coal, Sulphur, Statistical Series 2003-98.

Allen, G.P., 1984, Tidal processes in estuaries: a key to interpreting fluvial-tidal facies transitions. *In*: International Association of Sedimentologists, 5th European Regional Meeting, p. 23-24.

Allen, G.P., 1991, Sedimentary processes and facies in the Gironde estuary: a recent model for macrotidal estuarine systems. *In*: Clastic Tidal Sedimentology, D.G. Smith, G.E. Reinson, B.A. Zaitlin and R.A. Rahmani, eds., Canadian Society of Petroleum Geologists, Memoir 16, p. 29-40.

Allen, J.R.L., 1965, A review of the origin and characteristics of Recent alluvial sediments: Sedimentology, v.5, p. 89-191.

Allen, J.R.L., 1970a, Physical processes of sedimentation: An introduction: G. Allen & Unwin, London, 248 p.

Allen, J.R.L., 1970b, A quantitative model of grain size and sedimentary structures in lateral deposits: Journal of Geology, v. 7, p. 129-146.

Allen, J.R.L., 1982, Sedimentary Structures – Their character and physical basis: Elsevier, Amsterdam, v. 1, 593 p., v. 2, 663 p.

Allen, J.R.L., Banks, N.L., 1972, An interpretation and analysis of recumbent-folded deformed cross-bedding: Sedimentology, v. 19, p. 257-283.

Arnott, R.W.C., Hand, B.M., 1989, Bedforms, primary structures and grain fabric in the presence of suspended sediment rain: Journal of Sedimentary Petrology, v. 59, p. 1062-1069.

Arnott, R.W.C., Southard, J.B., 1990, Exploratory flow-duct experiments on combined-flow bed configurations, and some implications for interpreting storm-event stratification: Journal of Sedimentary Petrology, v. 60, p. 211-219.

Arnott, R.W.C., Zaitlin, B.A., Potocki, D.J., 2002, Stratigraphic response to sedimentation in a net-accommodation-limited setting, Lower Cretaceous Basal Quartz, south-central Alberta: Bulletin of Canadian Petroleum Geology, v. 50, p. 92-104.

Banerjee, I., 1989, Tidal structures in the Glauconitic Sandstone, Countess Field, southern Alberta, Canada. *In*: G.E. Reinson, ed., Modern and Ancient Examples of Clastic Tidal Deposits - A Core and Peel Workshop, Canadian Society of Petroleum Geologists, p. 89-97.

Banerjee, I., Davies, E.H., 1988, An integrated lithostratigraphic and palynostratigraphic study of the Ostracode zone and adjacent strata in the Edmonton embayment, central Alberta. *In*: D.P. James and D.A. Leckie, eds., Sequences, Stratigraphy, Sedimentology, Surface and Subsurface, Canadian Society of Petroleum Geologists, Memoir 15, p. 261-274.

Barwis, J.H., 1978, Sedimentology of some South Carolina tidal-creek point-bars, and a comparison with their fluvial counterparts. *In*: A.D. Miall, ed., Fluvial Sedimentology, Canadian Society of Petroleum Geologists, Memoir 5, p. 129-160.

Bhattacharya, J., Walker, R.G., 1991, Allostratigraphic subdivision of the Upper Cretaceous Dunvegan, Shaftsbury and Kaskapau formations in the northwestern Alberta subsurface: Bulletin of Canadian Petroleum Geology, v. 39, p. 145-164.

Boersma, J.R., Terwindt, J.H.J., 1981, Neap-spring tide sequences of intertidal shoal deposits in a mesotidal estuary: Sedimentology, v. 28, p. 151-170.

Bourgeois, J., 1980, A transgressive shelf sequence exhibiting hummocky stratification: The Cape Sebastian Sandstone (Upper Cretaceous), southwestern Oregon: Journal of Sedimentary Petrology, v. 50, p. 681-702.

Bridge, J.S., Jarvis, J., 1982, The dynamics of a river bend: a study in flow and sedimentary processes: Sedimentology, v. 29, p. 499-541.

Brownridge, S., Moslow, T.F., 1991, Tidal estuary and marine facies of the Glauconitic Member, Drayton Valley, central Alberta. *In*: Clastic Tidal Sedimentology, D.G. Smith, G.E. Reinson, B.A. Zaitlin and R.A. Rahmani, eds., Canadian Society of Petroleum Geologists, Memoir 16, p. 107-122.

Buatois, L.A., Mangano, M.G., Maples, C.G., Lanier, W.P., 1997, The paradox of nonmarine ichnofaunas in tidal rhythmites: integrating sedimentologic and ichnologic data from the Late Carboniferous of eastern Kansas, USA: Palaios, v. 12, p. 467-481.

Campbell, C.V., Oaks, R.Q., Jr., 1973, Estuarine sandstone filling tidal scours, Lower Cretaceous Fall River Formation, Wyoming: Journal of Sedimentary Petrology, v. 43, p. 765-778.

Cant, D.J., Abrahamson, B., 1996, Regional distribution and internal stratigraphy of the Lower Mannville: Bulletin of Canadian Petroleum Geology, v. 44, p. 508-529.

Cant, D.J., Stockmal, G.S., 1989, The Alberta foreland basin: relationship between stratigraphy and Cordilleran terrane-accretion events: Canadian Journal of Earth Sciences, v. 26, p. 1964-1975.

Chiang, K.K., 1984, The giant Hoadley gas field, south-central Alberta. *In*: J.A. Masters, ed., Elmworth, Case Study of a Deep Basin Gas Field, American Association of Petroleum Geologists, Memoir 38, p. 297-313.

Christopher, J.E., 1975, The depositional setting of the Mannville Group (Lower Cretaceous) in southwestern Saskatchewan. *In*: W.G.E. Caldwell, ed., The Cretaceous System in the Western Interior of North America, Geological Association of Canada, Special Paper 13, p. 523-552.

Clifton, H.E., 1982. Estuarine deposits. *In*: P.A. Scholle, D.R. Spearing, eds., Sandstone Depositional Environments, American Association of Petroleum Geologists, Memoir 31, p. 179-184.

Clifton, H.E., Hunter, R.E., Phillips, R.L., 1971, Depositional structures and processes in the non-barred high energy nearshore: Journal of Sedimentary Petrology, v. 41, p. 651-670.

Collinson, J.D., 1969, The sedimentology of the Grindslow Shales and the Kinderscout Grit: a deltaic complex in the Namurian of northern England: Journal of Sedimentary Petrology, v. 39, p. 194-221.

Collinson, J.D., 1986, Alluvial sediments. *In*: H.G. Reading, ed., Sedimentary Facies and Environments (second edition), Blackwell Scientific Publications, Oxford, p. 20-62.

Coleman, J.M., 1966, Ecological changes in a massive freshwater clay sequence: Transactions - Gulf Coast Association of Geological Societies, v. 16, p. 159-174.

Colman, S.M., Halka, J.P., Hobbs III, C.H., Mixon, R.B., Foster, D.S., 1990, Ancient channels of the Susquehanna River beneath Chesapeake Bay and the Delmarva Peninsula: Geological Society of America Bulletin, v. 102, p. 1268-1279.

Curray, J.R., Emmel, F.J., Crampton, P.J.S., 1969, Holocene history of a strand plain, lagoonal coast, Nayarit, Mexico. *In*: A.A. Castanares, F.B. Phleger, eds., Coastal Lagoons, a Symposium, Universidad Nacional Autónoma, Mexico, p. 63-100.

Dalrymple, R.W., 1979, Wave-induced liquefaction: A modern example from the Bay of Fundy: Sedimentology, v. 26, p. 835-844.

Dalrymple, R.W., Zaitlin, B.A., Boyd, R., 1992, Estuarine facies models: conceptual basis and stratigraphic implications: Journal of Sedimentary Petrology, v. 62, p. 1130-1146.

de Mowbray, T., 1983, The genesis of lateral accretion deposits in recent intertidal mudflat channels, Solway Firth, Scotland: Sedimentology, v. 30, p. 425-435.

de Raaf, J.F.M., Boersma, J.R., van Gelder, A., 1977, Wave-generated structures and sequences from a shallow marine succession, Lower Carboniferous, County Cork, Ireland: Sedimentology, v. 24, p. 451-483.

de Raaf, J.F.M., Reading, H.G., Walker, R.G., 1965, Cyclic sedimentation in the Lower Westphalian of North Devon, England: Sedimentology, v. 4, p. 1-52.

Dietrich, W.E., Kirchner, J., Ikeda, H., Iseya, F., 1987, The origin of the coarse surface layer in gravel-bedded streams: The role of sediment supply: Geological Society of America Abstracts with Programs, v. 19, p. 642.

Doe, T.W., Dott, R.H., Jr., 1980, Genetic significance of deformed cross-bedding: with examples from the Navajo and Weber Sandstones of Utah: Journal of Sedimentary Petrology, v. 50, p. 793-812.

Dott, R.H., Jr., 1981, Hummocky cross stratification: Yearbook of Science and Technology, McGraw-Hill, New York, p. 349-351.

Dott, R.H., Jr., 1983, Episodic sedimentation; how normal is average? How rare is rare? Does it matter?: Journal of Sedimentary Petrology, v. 53, p. 5-23.

Dott, R.H., Jr., Bourgeois, J., 1982, Hummocky stratification: Significance of its variable bedding sequences: Geological Society of America Bulletin, v. 93, p. 663-680.

Duke, W.L., 1985, Hummocky cross stratification, tropical hurricanes, and intense winter storms: Sedimentology, v. 32, p. 167-194.

Duke, W.L., Arnott, R.W.C., Cheel, R.J., 1991, Shelf sandstones and hummocky cross-stratification: New insights on a stormy debate: Geology, v. 19, p. 625-628.

Ekdale, A.A., Bromley, R.G., Pemberton, S.G., 1984, Ichnology: The use of trace fossils in sedimentology and stratigraphy: Society of Economic Paleontologists and Mineralogists, Short Course Notes No. 15, 317 p.

Farshori, M.Z., 1983, Glauconitic sandstone, Countess Field "H" pool, southern Alberta. *In*: J.R. McLean and G.E. Reinson, eds., Sedimentology of Selected Mesozoic Clastic Sequences, Canadian Society of Petroleum Geologists, p. 27-41.

Finger, K.L., 1983, Observations on the Lower Cretaceous Ostracode zone of Alberta: Bulletin of Canadian Petroleum Geology, v. 31, p. 326-337.

Fisk, H.N., 1947, Fine grained alluvial deposits and their effects on Mississippi River activity: Mississippi River Commission, Vicksburg, 82 p.

Frey, R.W., Howard, J.D., Pryor, W.A., 1978, *Ophiomorpha*; its morphologic, taxonomic, and environmental significance: Palaeogeography, Palaeoclimatology, Palaeoecology, v. 23, p. 199-229.

Frey, R.W., Pemberton, S.G., Fagerstrom, J.A., 1984, Morphological, ethological, and environmental significance of the ichnogenera *Scoyenia* and *Ancorichnus*: Journal of Paleontology, v. 58, p. 511-528.

Frey, R.W., Pemberton, S.G., Saunders, T.D.A., 1990, Ichnofacies and bathymetry: a passive relationship: Journal of Paleontology, v. 64, p. 155-158.

Frey, R.W., Seilacher, A., 1980, Uniformity in marine invertebrate ichnology: Lethaia, v. 13, p. 183-207.

Gadow, S., 1971, The Gulf of Gaeta, Tyrrhenian Sea: part 1, Sediments: Senckenbergiana Maritima, v. 3, p. 103-133.

Gelfenbaum, G., 1983, Suspended sediment response to semidiurnal and fortnightly tidal variations in a mesotidal estuary: Columbia River, U.S.A.: Marine Geology, v. 52, p. 39-57.

Gingras, M.K., MacEachern, J.A., Pemberton, S.G., 1998, A comparative analysis of the ichnology of wave- and river-dominated allomembers of the Upper Cretaceous Dunvegan Formation: Bulletin of Canadian Petroleum Geology, v. 46, p. 51-73.

Gingras, M.K., Pemberton, S.G., Saunders, T.D.A., Clifton, H.E., 1999, The ichnology of modern and Pleistocene brackish-water deposits at Willapa Bay, Washington: variability in estuarine settings: Palaios, v. 14, p. 352-374.

Gingras, M.K., Räsänen, M.E., Pemberton, S.G., Romero, L.P., 2002, Ichnology and sedimentology reveal depositional characteristics of bay-margin parasequences in the Miocene Amazonian foreland basin: Journal of Sedimentary Research, v. 72, p. 871-883.

Glaister, R.P., 1959, Lower Cretaceous of southern Alberta and adjoining areas: American Association of Petroleum Geologists Bulletin, v. 43, p. 590-640.

Glass, D.J., ed., 1990, Lexicon of Canadian Stratigraphy, Vol. 4, Western Canada, Including Eastern British Columbia, Alberta, Saskatchewan, and Southern Manitoba, Canadian Society of Petroleum Geologists, 772 p.

Gressly, A., 1838, *Observations géologiques sur le Jura soleurois*: Nouveaux mémoires de la Société Helvetique des Sciences Naturelles, Neuchâtel, v. 2, 349 p., 14 pl.

Gross, M.G., 1972, Oceanography, a View of the Earth: Prentice Hall, Englewood Cliffs, N.J., 58 p.

Handcock, P.R., Wood, J.M., 2001, Jenner Upper Mannville "E" Pool: unpublished report, Crestar Energy, 24 p.

Harms, J.C., Southard, J.B., Spearing, D.R., Walker, R.G., 1975, Depositional environments as interpreted from primary sedimentary structures and stratification sequences: Society of Economic Paleontologists and Mineralogists, Short Course No. 2, Dallas, Texas, 161 p.

Harms, J.C., Southard, J.B., Walker, R.G., 1982, Structure and Sequence in Clastic Rocks: Society of Economic Paleontologists and Mineralogists, Short Course No. 9, 249 p.

Hayes, B.J.R., Christopher, J.E., Rosenthal, L., Los, G, McKercher, B., Minkin, D., Tremblay, Y.M., Fennel, J., 1994, Cretaceous Mannville Group of the Western Canada Sedimentary Basin. *In*: G. Mossop and I. Shetsen, comps., Geological Atlas of the Western Canada Sedimentary Basin, Canadian Society of Petroleum Geologists, p. 317-334.

Herbaly, E.L., 1974, Petroleum geology of Sweetgrass arch, Alberta: American Association of Petroleum Geologists Bulletin, v. 58, p. 2227-2244.

Holmes, I.G., Rivard, Y.A., 1976, A marine barrier island bar, Jenner Field, southeastern Alberta. *In*: M.M. Lerand, ed., The Sedimentology of Selected Clastic Oil and Gas Reservoirs in Alberta, Canadian Society of Petroleum Geologists Core Conference Manual, p. 44-61.

Hopkins, J.C., Hermanson, S.W., Lawton, D.C., 1982, Morphology of channels and channel-sand bodies in the Glauconitic Sandstone Member (Upper Mannville), Little Bow area, Alberta: Bulletin of Canadian Petroleum Geology, v. 30, p. 274-285.

Howard, J.D., Frey, R.W., 1973, Characteristic physical and biogenic sedimentary structures in Georgia estuaries: American Association of Petroleum Geologists Bulletin, v. 57, p. 1169-1184.

Hradsky, M., Griffin, M., 1984, Sandstone body geometry, reservoir quality and hydrocarbon trapping mechanisms in Lower Cretaceous Mannville Group, Taber/Turin area, southern Alberta. *In*: D.F. Stott and D.J. Glass, eds., The Mesozoic of Middle North America, Canadian Society of Petroleum Geologists, Memoir 9, p. 401-411.

Hughes, D.A., Lewin, J., 1982, A small-scale flood plain: Sedimentology, v. 29, p. 891-895.

Jackson, P., 1984, Paleogeography of the Lower Cretaceous Mannville Group of Western Canada. *In*: J.A. Masters, ed., Elmworth, Case Study of a Deep Basin Gas Field, American Association of Petroleum Geologists, Memoir 38, p. 49-79.

Jackson, R.G., 1976, Depositional model of point bars in the Lower Wabash river: Journal of Sedimentary Petrology, v. 46, p. 579-594.

Jackson, R.G., 1981, Sedimentology of muddy fine-grained channel deposits in meandering streams of the American middle west: Journal of Sedimentary Petrology, v. 51, p. 1169-1192.

James, D., 1985, Stratigraphy, sedimentology and diagenesis of Upper Jurassic and Lower Cretaceous (Mannville Group) strata, southwestern Alberta, Canada: unpublished Ph.D. thesis, University of Oxford, Oxford, England, 225 p.

Johnson, M.F., Dalrymple, R.W., 2003, Negative accommodation and its influence on reservoir geometry and quality: the Lower Cretaceous Cadomin Formation of the Deep Basin Area, Alberta. *In*: Partners in a New Environment, Joint Meeting of the Canadian Society of Petroleum Geologists and Canadian Society of Exploration Geophysicists, June 2-6, 2003, Calgary, Alberta, Conference CD, 1 p.

Johnson, H.D., Baldwin, C.T., 1986, Shallow siliciclastic seas. *In*: H.G. Reading, ed., Sedimentary Facies and Environments (second edition), Blackwell Scientific Publications, Oxford, p. 229-280.

Jones, B.G., Rust, B.R., 1983, Massive sandstone facies in the Hawkesbury Sandstone, a Triassic fluvial deposit near Sydney, Australia: Journal of Sedimentary Petrology, v. 53, p. 1249-1261.

Karvonen, R.L., Pemberton, S.G., 1997, The upper Mannville Group in southeast Alberta, Canada: an example of multiple incised valley fill deposits. *In*: S.G. Pemberton and D.P. James, eds., Petroleum Geology of the Cretaceous Mannville Group, Western Canada, Canadian Society of Petroleum Geologists, Memoir 18, p. 124-139.

Krumbein, W.C., Sloss, L.L., 1963, Stratigraphy and Sedimentation: W.H. Freeman, San Francisco, 600 p.

Kumar, N., Sanders, J.E., 1974, Inlet sequence: a vertical succession of sedimentary structures and textures created by the lateral migration of tidal inlets: Sedimentology, v. 21, p. 491-532.

Laury, R.L., 1971, Stream bank failure and rotational slumping: preservation and significance in the geologic record: Geological Society of America Bulletin, v. 82, p. 1251-1266.

Layer, D.B., Geological Staff, Imperial Oil, 1949, Leduc oil field, Alberta: a Devonian coral-reef discovery: American Association of Petroleum Geologists Bulletin, v. 33, p. 572-602.

Leckie, D.A., Rosenthal, L., James, D., 1996, Sedimentology of clastic reservoirs in southern Alberta: the Blairmore-Mannville Groups and bounding strata, Geological Survey of Canada, Open File 3322, 108 p.

Leckie, D.A., Smith, D.G., 1992, Regional setting, evolution and depositional cycles of the Western Canada Foreland Basin. *In*: R.W. Macqueen and D.A. Leckie, eds., Foreland Basins and Fold Belts, American Association of Petroleum Geologists, Memoir 55, p. 9-46.

Leckie, D.A., Vanbeselaere, N.A., James, D.P., 1997, Regional sedimentology, sequence stratigraphy and petroleum geology of the Mannville Group, southwestern Saskatchewan. *In*: S.G. Pemberton and D.P. James, eds., Petroleum Geology of the Cretaceous Mannville Group, Western Canada, Canadian Society of Petroleum Geologists, Memoir 18, p. 211-262.

Leclair, S.F., 2002, Preservation of cross-strata due to the migration of subaqueous dunes: an experimental investigation: Sedimentology, v. 49, p. 1157-1180.

Lowe, D.R., 1976, Subaqueous liquefied and fluidized sediment flows and their deposits: Sedimentology, v. 23, p. 285-308.

Lowe, D.R., 1982, Sediment gravity flows: II. Depositional models with special reference to deposits of high-density turbidity currents: Journal of Sedimentary Petrology, v. 52, p. 279-297.

MacEachern, J.A., Raychaudhuri, I., Pemberton, S.G., 1992. Stratigraphic applications of the *Glossifungites* ichnofacies: delineating discontinuities in the rock record. *In*: S.G. Pemberton, ed., Applications of Ichnology to Petroleum Exploration: A Core Workshop, Society of Economic Paleontologists and Mineralogists, Core Workshop No. 17, p. 169-198.

MacEachern, J.A., Zaitlin, B.A., Pemberton, S.G., 1998. High-resolution sequence stratigraphy of early transgressive deposits, Viking Formation, Joffre Field, Alberta, Canada: American Association of Petroleum Geologists Bulletin, v. 82, p. 729-756.

Martin, C.A.L., Turner, B.R., 1998. Origins of massive-type sandstones in braided river systems: Earth-Science Reviews, v. 44, p. 15-38.

Masters, J.A., 1984. Lower Cretaceous oil and gas in western Canada. *In*: J.A. Masters, ed., Elmworth, Case Study of a Deep Basin Gas Field, American Association of Petroleum Geologists, Memoir 38, p. 1-38.

McBride, E.F., 1963. A classification of common sandstones: Journal of Sedimentary Petrology, v. 33, p. 664-669.

McCrory, V.L.C., Walker, R.G., 1986. A storm and tidally-influenced prograding shoreline: Upper Cretaceous Milk River Formation of southern Alberta, Canada: Sedimentology, v. 33, p. 47-60.

McLean, J.R., Jerzykiewicz, T., 1978. Cyclicity, tectonics and coal: Some aspects of fluvial sedimentology in the Brazeau-Paskapoo Formations, Coal Valley area, Alberta, Canada. *In*: A.D. Miall, ed., Fluvial Sedimentology, Canadian Society of Petroleum Geologists, Memoir 5, p. 441-468.

McLean, J.R., Wall, J.H., 1981. The Early Cretaceous Moosebar Sea in Alberta: Bulletin of Canadian Petroleum Geology, v. 29, p. 334-377.

Miall, A.D., 1978. Fluvial sedimentology: an historical review. *In*: A.D. Miall, ed., Fluvial Sedimentology, Canadian Society of Petroleum Geologists, Memoir 5, p. 1-47.

Miall, A.D., 1987. Recent developments in the study of fluvial facies models. *In*: F.G. Ethridge, R.M. Flores, M.D. Harvey, eds., Society of Economic Paleontologists and Mineralogists, Special Publication 39, p. 1-9.

Middleton, G.V., 1973, Johannes Walther's law of correlation of facies: Geological Society of America Bulletin, v. 84, p. 979-988.

Middleton, G.V., 1978, Facies. *In*: R.W. Fairbridge and J. Bourgeois, eds., Encyclopedia of sedimentology: Stroudsburg, Pennsylvania, Dowden, Hutchinson and Ross, p. 323-325.

Monger, J.W.H., Price, R.A., Templeman-Kluit, D.J., 1982, Tectonic accretion and the origin of the two major metamorphic and plutonic belts in the Canadian Cordillera: Geology, v. 10, p. 70-75.

Moslow, T.F., Pemberton, S.G., 1988, An integrated approach to the sedimentological analysis of some Lower Cretaceous shoreface and delta front sandstone sequences. *In*: D.P. James and D.A. Leckie, eds., Sequences, Stratigraphy, Sedimentology: Surface and Subsurface, Canadian Society of Petroleum Geologists, Memoir 15, p. 373-386.

Nichols, M.M., Biggs, R.B., 1985, Estuaries. *In*: R.A. Davis Jr., ed., Coastal Sedimentary Environments, 2nd Edition, Springer-Verlag, New York, p. 77-186.

Nummedal, D., Swift, D.J.P., 1987, Transgressive stratigraphy at sequence-bounding unconformities: some principles derived from Holocene and Cretaceous examples. *In*: D. Nummedal, O.H. Pilkey, J.D. Howard, eds., Sea-level fluctuation and coastal evolution, Society of Economic Paleontologists and Mineralogists, Special Publication 41, p. 241-260.

Paik, I.S., Kim, H.J., 1998, Subaerial lenticular cracks in Cretaceous lacustrine deposits, Korea: Journal of Sedimentary Research, Section A: Sedimentary Petrology and Processes, v. 68, p. 80-87.

Pemberton, S.G., Frey, R.W., 1984, Ichnology of storm-influenced shallow marine sequences: Cardium Formation (Upper Cretaceous) at Seebe, Alberta. *In*: D.F. Stott and D.L. Glass, eds., The Mesozoic of Middle North America, Canadian Society of Petroleum Geologists, Memoir 9, p. 281-304.

Pemberton, S.G., Frey, R.W., 1985, The *Glossifungites* ichnofacies: modern examples from the Georgia coast, USA. *In*: H.A. Curran, ed., Biogenic Structures: Their Use in Interpreting Depositional Environments, Society of Economic Paleontologists and Mineralogists, Special Publication No. 35, p. 237-259.

Pemberton, S.G., MacEachern, J.A., 1995. The sequence stratigraphic significance of trace fossils: examples from the Cretaceous foreland basin of Alberta, Canada. *In*: J.C. Van Wagoner and G. Bertram, eds., Sequence stratigraphy of foreland basin deposits–outcrop and subsurface examples from the Cretaceous of North America. Society of Economic Paleontologists and Mineralogists, Memoir 64, p. 429-475.

Pemberton, S.G., MacEachern, J.A., Frey, R.W., 1992a. Trace fossil facies models: environmental and allostratigraphic significance. *In*: R.G. Walker and N.P. James, eds., Facies Models: Response to Sea Level Change, Geological Association of Canada, Geotext 1, p. 47-72.

Pemberton, S.G., MacEachern, J.A., Ranger, M.J., 1992b. Ichnology and event stratigraphy: The use of trace fossils in recognizing tempestites. *In*: S.G. Pemberton, ed., Applications of Ichnology to Petroleum Exploration: A Core Workshop, Society of Economic Paleontologists and Mineralogists, Core Workshop No. 17, p. 85-117.

Pemberton, S.G., Spila, M., Pulham, A.J., Saunders, T.D.A., MacEachern, J.A., Robbins, D.J.C., Sinclair, I.K., 2001. Ichnology and Sedimentology of Shallow to Marginal Marine Systems: Ben Nevis and Avalon Reservoirs, Jeanne D'arc Basin: Geological Association of Canada, Short Course Notes v. 15, 343 p.

Pemberton, S.G., Van Wagoner, J.C., Wach, G.D., 1992c. Ichnofacies of a wave-dominated shoreline. *In*: S.G. Pemberton, ed., Applications of Ichnology to Petroleum Exploration: A Core Workshop, Society of Economic Paleontologists and Mineralogists, Core Workshop No. 17, p. 339-382.

Pemberton, S.G., Wightman, D.M., 1992. Ichnological characteristics of brackish water deposits. *In*: S.G. Pemberton, ed., Applications of Ichnology to Petroleum Exploration: A Core Workshop, Society of Economic Paleontologists and Mineralogists, Core Workshop No. 17, p. 141-167.

Pierson, T.C., Costa, J.E., 1987. A rheologic classification of subaerial sediment-water flows. *In*: J.E. Costa and G.F. Wieczorek, eds., Debris Flows/Avalanches: Processes, Recognition and Mitigation, Geological Society of America Reviews in Engineering Geology, v. 7, p. 1-12.

Plint, A.G., 1988, Sharp-based shoreface sequences and "offshore bars" in the Cardium Formation of Alberta: their relationship to relative changes in sea level. *In*: C.K. Wilgus, B.S. Hastings, C.G.St.C. Kendall, H. Posamentier, C.A. Ross, J.C. Van Wagoner, eds., Sea-Level Changes: An Integrated Approach, Society of Economic Paleontologists and Mineralogists, Special Publication 42, p. 357-370.

Plint, A.G., Norris, B., 1991, Anatomy of a ramp margin sequence: facies successions, paleogeography, and sediment dispersal patterns in the Muskiki and Marshybank formations, Alberta Foreland Basin: Bulletin of Canadian Petroleum Geology, v. 39, p. 18-42.

Plint, A.G., Walker, R.G., 1987, Cardium Formation 8, facies and environments of the Cardium shoreline and coastal plain in the Kakwa Field and adjacent areas, northwestern Alberta: Bulletin of Canadian Petroleum Geology, v. 35, p. 48-64.

Podruski, J.A., 1988, Contrasting character of the Peace River and Sweetgrass arches, Western Canada Sedimentary Basin, Canada: Geoscience Canada, v. 15, p. 94-97.

Price, R.A., 1981, The Cordilleran foreland thrust and fold belt in the southern Canadian Rocky Mountains. *In*: K. R. McClay and N.J. Price, eds., Thrust and nappe tectonics, Geological Society of London, Special Publication 9, p. 427-448.

Reading, H.G., 1986, Facies. *In*: H.G. Reading, ed., Sedimentary Facies and Environments (second edition), Blackwell Scientific Publications, Oxford, p. 4-19.

Reineck, H.E., Singh, I.B., 1971, The Gulf of Gaeta, Tyrrhenian Sea: part 3, Fabrics of foreshore and shelf sediments: Senckenbergiana Maritima, v. 3, p. 185-194.

Reineck, H.E., Singh, I.B., 1972, Genesis of laminated sand and graded rhythmites in storm-sand layers of shelf mud: Sedimentology, v. 18, p. 123-128.

Reineck, H.E., Singh, I.B., 1973, Depositional Sedimentary Environments: With Reference to Terrigenous Clastics: Springer-Verlag, Berlin, 439 p.

Reineck, H.E., Wunderlich, F., 1968, Classification and origin of flaser and lenticular bedding: Sedimentology, v. 11, p. 99-104.

Reinson, G.E., 1989, Tide-influenced channel deposits in the Lower Cretaceous Glauconitic member, southern Alberta, Canada. *In*: G.E. Reinson, ed., Modern and Ancient Examples of Clastic Tidal Deposits - A Core and Peel Workshop, Canadian Society of Petroleum Geologists, p. 98-104.

Ricketts, B.D., 1991, Lower Paleocene drowned valley and barred estuaries, Canadian Arctic Islands: aspects of their geomorphological and sedimentological evolution. *In*: Clastic Tidal Sedimentology, D.G. Smith, G.E. Reinson, B.A. Zaitlin and R.A. Rahmani, eds., Canadian Society of Petroleum Geologists, Memoir 16, p. 91-106.

Rosenthal, L., 1988, Wave dominated shorelines and incised channel trends: Lower Cretaceous Glauconite Formation, west-central Alberta. *In*: D.P. James and D.A. Leckie, eds., Sequences, Stratigraphy, Sedimentology: Surface and Subsurface, Canadian Society of Petroleum Geologists, Memoir 15, p. 207-220.

Rosenthal, L., Walker, R.G., 1987, Lateral and vertical facies sequences in the Upper Cretaceous Chungo Member, Wapiabi Formation, southern Alberta: Canadian Journal of Earth Sciences, v. 24, p. 771-783.

Roy, P.S., Thom, B.G., Wright, L.D., 1980, Holocene sequences on an embayed high-energy coast: an evolutionary model: Sedimentary Geology, v. 26, p. 1-19.

Rudkin, R.A., 1964, Chapter 11 – Lower Cretaceous. *In*: R.G. McCrossan, R.P. Glaister, eds., Geological History of Western Canada, Alberta Society of Petroleum Geologists, p. 156-169.

Savrda, C.E., 1991, Ichnology in sequence stratigraphic studies: an example from the lower Paleocene of Alabama: Palaios, v. 6, p. 39-53.

Shanley, K.W., McCabe, P.J., Hettinger, R.D., 1992, Tidal influence in Cretaceous fluvial strata from Utah, USA: a key to sequence stratigraphic interpretation: Sedimentology, v. 39, p. 905-930.

Sherwin, M.D., 1996, Channel trends in the Glauconitic Member, southern Alberta: Bulletin of Canadian Petroleum Geology, v. 44, p. 530-540.

Singh, C., 1965, Palynology of the Mannville Group (Lower Cretaceous), central Alberta: Bulletin of Canadian Petroleum Geology, v. 13, p. 538-539.

Smith, A.B., Crimes, T.P., 1983, Trace fossils formed by heart urchins: a study of *Scolicia* and related traces: Lethaia, v. 16, p. 79-92.

Smith, D.G., 1988, Modern point bar deposits analogous to the Athabasca Oil Sands, Alberta, Canada. *In*: P.L. de Boer, A. van Gelder, S.D. Nio, eds., Tide-Influenced Sedimentary Environments and Facies, D. Reidel Publishing Company, Dordrecht, p. 417-432.

Southard, J.B., Lambie, J.M., Federico, D.C., Pile, H.T., Weidman, C.R., 1990, Experiments on bed configurations in fine sands under bidirectional purely oscillatory flow, and the origin of hummocky cross-stratification: Journal of Sedimentary Petrology, v. 60, p. 1-17.

Srivastava, S.K., 1976, The fossil pollen genus Classopollis: Lethaia, v. 9, p. 437-457.

Stockmal, G.S., Cant, D.J., Bell, J.S., 1992, Relationship of the stratigraphy of the Western Canada foreland basin to Cordilleran tectonics: insights from geodynamic models. *In*: R.W. Macqueen and D.A. Leckie, eds., Foreland Basins and Fold Belts, American Association of Petroleum Geologists, Memoir 55, p. 107-124.

Strobl, R.S., 1988, The effects of sea-level fluctuations on prograding shorelines and estuarine valley-fill sequences in the Glauconitic Member, Medicine River field and adjacent areas. *In*: D.P. James and D.A. Leckie, eds., Sequences, Stratigraphy, Sedimentology: Surface and Subsurface, Canadian Society of Petroleum Geologists, Memoir 15, p. 221-236.

Swift, D.J.P., Hudelson, P.M., Brenner, R.L., Thompson, P., 1987, Shelf construction in a foreland basin: storm beds, shelf sandbodies, and shelf-slope depositional sequences in the Upper Cretaceous Mesaverde Group, Book Cliffs, Utah: Sedimentology, v. 34, p. 423-457.

Teichert, C., 1958, Concept of Facies: American Association of Petroleum Geologists Bulletin, v. 42, p. 2718-2744.

Thomas, R.C., Smith, D.G., Wood, J.M., Visser, J., Calverley-Range, E.A., Koster, E.H., 1987, Inclined heterolithic stratification: terminology, description, interpretation and significance: Sedimentary Geology, v. 53, p. 123-179.

Tilley, B.J., Longstaffe, F.J., 1984, Controls on hydrocarbon accumulation in Glauconitic sandstone, Suffield heavy oil sands, southern Alberta: American Association of Petroleum Geologists Bulletin, v. 68, p. 1004-1023.

Tovell, W.M., 1958, The development of the Sweetgrass Arch, southern Alberta: Geological Association of Canada Proceedings, v. 10, p. 19-30.

Turner, B.R., Monro, M., 1987, Channel formation and migration by mass-flow processes in the Lower Carboniferous fluviatile Fell Sandstone Group, north-east England: Sedimentology, v. 34, p. 1107-1122.

Tyler, N., Ambrose, W.A., 1986, Facies architecture and production characteristics of strand-plain reservoirs in North Markham-North Bay City Field, Frio Formation, Texas: American Association of Petroleum Geologists Bulletin, v. 70, p. 809-829.

Van Wagoner, J.C., Mitchum, R.M., Campion, K.M., Rahmanian, V.D., 1990, Siliciclastic sequence stratigraphy in well logs, cores, and outcrops: concepts for high resolution correlation of time and facies: American Association of Petroleum Geologists, Methods in Exploration Series, No. 7, 55 p.

Van Wagoner, J.C., Posamentier, H.W., Mitchum, R.M., Jr., Vail, P.R., Sarg, J.F., Loutit, T.S., Hardenbol, J., 1988, An overview of the fundamentals of sequence stratigraphy and key definitions. *In*: C.K. Wilgus, B.S. Hastings, C.G.St.C. Kendall, H.W. Posamentier, C.A. Ross and J.C. Van Wagoner, eds., Sea-level changes: An integrated approach, Society of Economic Paleontologists and Mineralogists, Special Publication No. 42, p. 39-45.

Walker, R.G., 1992, Facies, facies models and modern stratigraphic concepts. *In*: R.G. Walker and N.P. James, eds., Facies Models: Response to Sea Level Change, Geological Association of Canada, Geotext 1, p. 1-14.

Walker, R.G., Cant, D.J., 1984, Sandy fluvial systems. *In*: R.G. Walker, ed., Facies Models, Second Edition, Geological Association of Canada, Geoscience Canada, Reprint Series 1, p. 71-90.

Walker, R.G., Duke, W.L., Leckie, D.A., Dott, R.H., Jr., Bourgeois, J., 1983, Hummocky stratification: Significance of its variable bedding sequences: Discussion and reply: Geological Society of America Bulletin, v. 94, p. 1245-1251.

Walker, R.G., Plint, A.G., 1992, Wave- and storm-dominated shallow marine systems. *In*: R.G. Walker and N.P. James, eds., Facies Models: Response to Sea Level Change, Geological Association of Canada, Geotext 1, p. 219-238.

Walker, R.G., Wiseman, T.R., 1995, Lowstand shorefaces, transgressive incised shorefaces, and forced regressions: examples from the Viking Formation, Joarcam area, Alberta: Journal of Sedimentary Research, v. 65, p. 132-141.

Walther, J., 1894, *Einleitung in die Geologie als Historische Wissenschaft*: Lithogenesis der Gegenwart: Fischer Verlag, Jena, p. 535-1055.

Whiting, P.J., Dietrich, W.E., Leopold, L.B., Drake, T.G., Shreve, R.L., 1988, Bedload sheets in heterogeneous sediment: Geology, v. 16, p. 105-108.

Wightman, D.M., Pemberton, S.G., Singh, C., 1987, Depositional modeling of the Upper Mannville (Lower Cretaceous), east-central Alberta: implications for the recognition of brackish water deposits. *In*: R.W. Tillman and K.J. Weber, eds., Reservoir Sedimentology, Society of Economic Paleontologists and Mineralogists, Special Publication 40, p. 189-220.

Williams, G.D., 1963, The Mannville Group (Lower Cretaceous) of central Alberta: Bulletin of Canadian Petroleum Geology, v. 11, p. 350-368.

Williams, G.D., Stelck, C.R., 1975, Speculations on the Cretaceous paleogeography of North America. *In*: Caldwell, W.G.E., ed., The Cretaceous System in the Western Interior of North America, Geological Association of Canada, Special Paper 13, p. 1-20.

Wilson, M.E., 1999, Sedimentology and sequence stratigraphy of the Basal Colorado Sandstone, Lower Cretaceous, southern Alberta, Canada: unpublished M.Sc. thesis, University of Aberdeen, Aberdeen, Scotland, 301 p.

Wizevich, M.C., 1992, Sedimentology of Pennsylvanian quartzose sandstones of the Lee Formation, Central Appalachian Basin: fluvial interpretation based on lateral profile analysis: Sedimentary Geology, v. 78, p. 1-47.

Wood, J.M., 1990, Sequence stratigraphy, sedimentology and petroleum geology of the Glauconitic member and adjacent strata, Lower Cretaceous Mannville Group, southern Alberta: unpublished Ph.D. thesis, University of Calgary, Calgary, Alberta, Canada, 355 p.

Wood, J.M., 1994, Sequence stratigraphic and sedimentological model for estuarine reservoirs in the Lower Cretaceous Glauconitic member, southern Alberta: Bulletin of Canadian Petroleum Geology, v. 42, p. 332-351.

Wood, J.M., Hopkins, J.C., 1989, Reservoir sandstone bodies in estuarine valley fill: Lower Cretaceous Glauconitic Member, Little Bow Field, Alberta, Canada: American Association of Petroleum Geologists Bulletin, v. 73, p. 1361-1382.

Wood, J.M., Hopkins, J.C., 1992, Traps associated with paleovalleys and interfluves in an unconformity bounded sequence: Lower Cretaceous Glauconitic Member, southern Alberta, Canada: American Association of Petroleum Geologists Bulletin, v. 76, p. 904-926.

Workman, L.E., 1958, Glauconitic sandstone in southern Alberta: Journal of the Alberta Society of Petroleum Geologists, v. 6, p. 237-245.

Wright, G.N., McMechan, M.E., Potter, D.E.G., 1994, Structure and architecture of the Western Canada Sedimentary Basin. *In*: G. Mossop and I. Shetsen, comps., Geological Atlas of the Western Canada Sedimentary Basin, Canadian Society of Petroleum Geologists, p. 25-40.

Wunderlich, F., 1971, The Gulf of Gaeta, Tyrrhenian Sea: part 2, Beach structures and dynamics: Senckenbergiana Maritima, v. 3, p. 135-169.

Yoxall, W.H., 1969, The relationship between falling base level and lateral erosion in experimental streams: Geological Society of America Bulletin, v. 80, p. 1379-1384.

Zaitlin, B.A., Dalrymple, R.W., Boyd, R., 1994, The stratigraphic organization of incised-valley systems associated with relative sea-level change. *In*: R.W. Dalrymple, R. Boyd and B.A. Zaitlin, eds., Incised-Valley Systems: Origin and Sedimentary Sequences, Society of Economic Paleontologists and Mineralogists, Special Publication 51, p. 45-60.

Zaitlin, B.A., Warren, M.J., Potocki, D.J., Rosenthal, L., Boyd, R., 2002, Depositional styles in a low accommodation foreland basin setting: an example from the Basal Quartz (Lower Cretaceous), southern Alberta: Bulletin of Canadian Petroleum Geology, v. 50, p. 31-72.

Appendix 1

Core Descriptions

Well ID	Cored Interval	Length (m)
00/11-18-019-08W4/0	970.0-988.0 m	18.0
03/06-19-019-09W4/0	1002.0-1018.0 m	16.0
00/10-24-019-09W4/0	3248-3278'	9.1
00/07-27-019-09W4/0	1009.4-1022.6 m	13.2
00/16-30-019-09W4/0	1016.8-1034.0 m	17.2
00/01-34-019-09W4/0	1004.0-1019.8 m	15.8
00/06-34-01909W4/2	3257-3308'	15.6
02/10-19-020-08W4/0	922.0-940.0 m	18.0
00/12-02-020-09W4/0	3185-3225'	12.2
02/06-11-020-09W4/0	961.0-979.0 m	18.0
02/14-11-020-09W4/0	957.2-975.2 m	18.0
02/16-17-020-09W4/0	963.0-978.2 m	15.2
00/02-23-020-09W4/0	972.0-985.0 m	13.0
00/04-23-020-09W4/0	954.8-975.1 m	20.3
00/06-23-020-09W4/0	946.5-964.5 m	18.0
00/08-23-020-09W4/0	944.0-962.0 m	18.0
00/10-23-020-09W4/0	937.5-959.3 m	21.8
02/10-23-020-09W4/2	948.0-960.3 m	12.3
00/13-23-020-09W4/2	940.0-958.0 m	18.0
02/16-23-020-09W4/0	946.0-959.5 m	13.5
02/16-27-020-09W4/0	955.0-973.0 m	18.0
00/11-34-020-09W4/0	970.0-986.5 m	16.5
02/13-34-020-09W4/0	954.0-969.2 m	15.2
04/06-03-021-09W4/0	945.5-963.5 m	18.0
00/16-08-021-09W4/0	931.0-947.3 m	16.3
00/05-10-021-09W4/0	950.0-965.0 m	15.0

Table A1.1: List of cores logged in this study. See Figure 1.6 for location of cored wells.

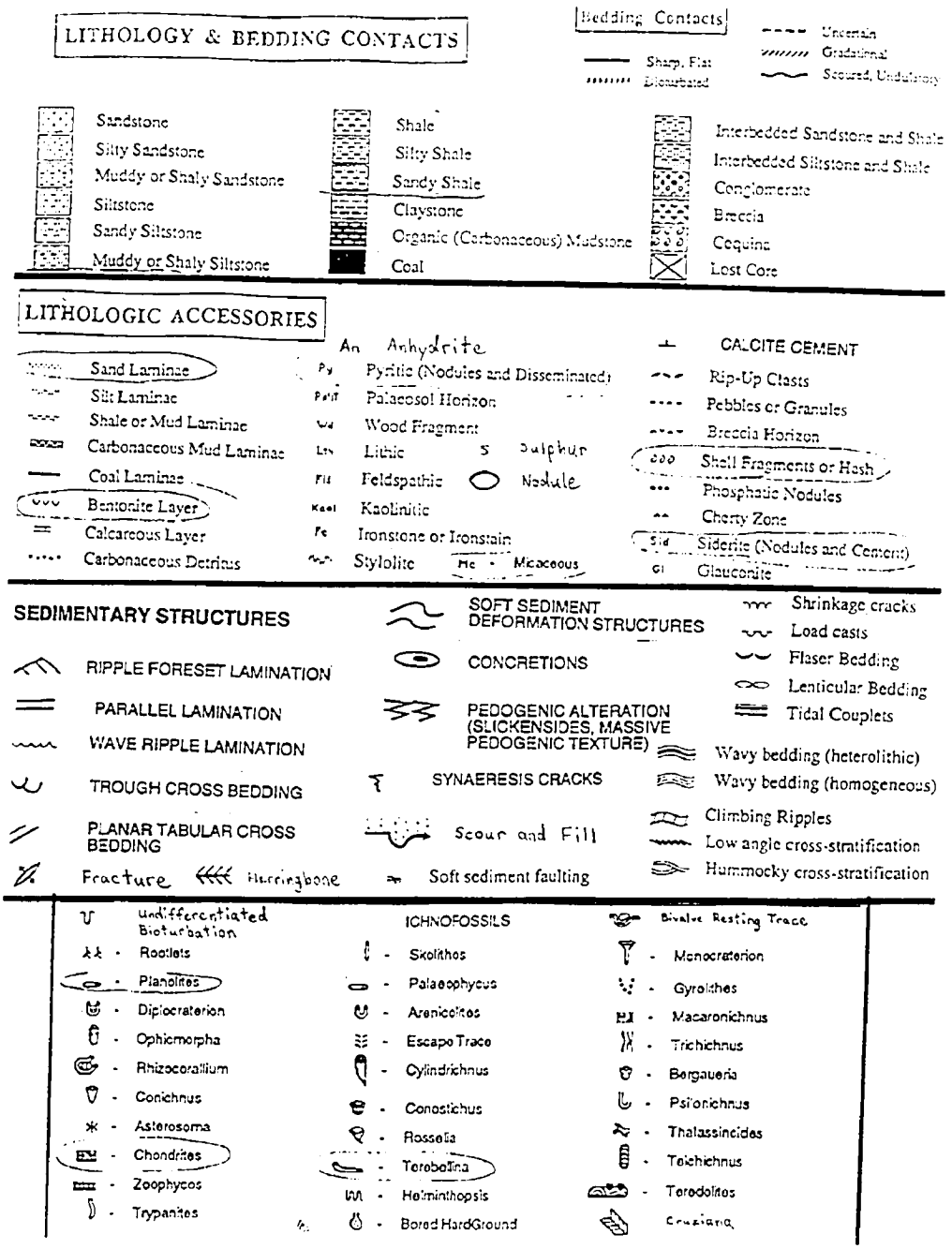

Table A1.2: Legend to symbols used in Appendix 1.

25/07/02

CRESTAR ENERGY

CARBONATE CORE LOG

Location 20/11-18-019-08W4/0 Interval 970.00 - 988.00m ☒ Core ☐ Chips 1 of 1

Formation | Facies | Depth | Lithology | Sedimentary and Structural Features | Biogenic Components | Classification | Matrix Type | Porosity Type | Effective Reservoir | Petrophysical Log / Core Analysis — Description / Comments

970
971
972
973
974
975
976
977
978
979
980
981
982
983
984
985
986

- carbonaceous Mudstone
- light grey
- massive
- pyritic

971.5 — Fining-upward vf-sst. -up through shaly siltstone/silty shale, gradationally through to full-blown, carbonaceous mudstone
- ~~low-angle plane laminated~~
- light - m. grey

974.4 — Fining-upward vf-sst. silty shale
- unidirectional current ripples, pyrite
- profuse Teichichnus
- low-angle plane laminated

975.2 — Sharp-based, low-angle cross-laminated fining-upward vf-m-L → grey siltstone/shale
- huge scoured cross-cutting contact through shaly siltstone @ 975.5m
- abundant Teichichnus

976.4 — Interbedded vf-m-L lithic sandstone/mudclast breccia
- breccia matrix is consistent with clean sandstone
- sandstone contains siderite/feldspar grain, dark chert, kaolinitic clay cement
- mudclasts in brecciated horizons are parallel, wavy-laminated; clasts range in size from <1mm to >8cm; imbrication of clasts parallel to sandstone stratification is sometimes present; mud clasts are sometimes cross-laminated internally
- breccia is matrix-supported
- fine-grained pyrite sparsely dispersed throughout sandstone
- unidirectional current ripples marked by organic laminae @ 979.9m
- calcite-cemented from 980.9-978.9m (grey colour, less brown tinge than underlying and overlying sandstone units) => could mark separate channel incision events
- slight decrease in grain size to vf-? near top
- low-angle to horizontal planar laminations above uppermost breccia:
  - mud rip-ups, unidirectional current ripples (1-2cm thick)

982.9 — Silty Mudstone
- light-dark grey
- nodular, radiating pyrite growths (replaced plants/roots)
- mottled colouration due to interlaminated silt stringers + bioturbation
- carbonaceous material (diminutive plant debris)
- conspicuous, bulbous trace: dark lining, internal spreite → Diplo/Rhizo/escape trace? (picture)
- 10cm thick pyrite bed @ 983m

CRESTAR ENERGY Name: Canhunter Jenner

CARBONATE CORE LOG

Location 03/06-19-019-09W4/0 Interval 1002.00 - 1018.00 m ☒ Core ☐ Chips 1 of 1

Formation	Facies	Depth	Lithology	Sedimentary and Structural Features	Biogenic Components	Classification	Matrix Type	Porosity Type	Effective Reservoir	Petrophysical Log / Core Analysis — Description/Comments
	1	1002								Carbonaceous/argillaceous greenish-grey mudstone - branched, black rootlets along bedding planes (picture) - cmoly interbed @ 1003.4m
	2	1004		massive						large-scale cross-stratified, well sorted lithic sandstone - dark chert, brown/orange feldspar/siderite, quartz - carbonaceous mud laminae - mt-mu grain size - siderite particles are wt-vcu grain size - porosity is almost entirely occluded by a whitish clay mineral (diagenetic kaolinite?) - cross-stratification is uniform in appearance and dip - stratification is fuzzy → cryptic bioturbation? (picture) - stratification defined by segregation of quartz chert/siderite/carbonaceous muds into discrete laminae - from 1006.8-1007m, large + abundant siderite blebs, carb. mud laminae and coal clasts. - low-angle cross-lamination @ 1005.2m - increase in mud laminae, overall decrease in grain size @ ~1006m - bioturbated silty shale interbed @ 1004.2-1004.4m
	3	1005								
	4	1006		Fld s/st Chert						
	5	1007		s/st						
	6	1008								
	7	1009		s/st						Lenticular (mainly) to wavy-bedded silty mudstone - thinly, horizontal plane-wavy laminated - siderite beds, 0.5-5cm thick - nodular pyrite ~ 5cm across - 9cm thick muddy sandstone bed with chert granules @ 1010.40m - dark grey-black shale with bedding-parallel pyrite nodules - carbonaceous plant stems/fragments @ 1012.6m - 1.5-2cm thick pyrite bed @ 1013.55m - coal clast, bidirectional current ripples, coarse-s pyritic lag, mud or sand rip-up casts (hollow impressions) @ 1013.4m - increase in silt content @ ~ 1013.4m - abundant carbonaceous plant material in shale fraction - diminutive Cylindrichnus + Skolithos trace fossil starting @ 1013.2m - silty current ripple laminations persist in calcite lenticular-wavy bedded fraction - 6cm thick siderite bed w calcite-filled fractures @ 1011.4m - horizontal, unlined burrow with sparrish @ 1010.1m - low-angle (7°) inclination in laminated strata @ 1009.95m
	8	1010		s/st Py						
	9	1011		Py s/st Burr						
	10	1012		s/st						
	11	1013		s/st						
	12	1014		Py						
		1015								Lost/missing core
		1016								
		1017								
		1018								

26/07/02

CRESTAR ENERGY Name. Westcoast AEC Suffield

CARBONATE CORE LOG

Location 00/10-24-019-09W4/0 Interval 3248 - 3278ft ☒ Core ☐ Chips _____ of 1

Formation	Facies	Depth	Lithology	Sedimentary and Structural Features	Biogenic Components	Classification	Matrix Type	Porosity Type	Effective Reservoir	Petrophysical Log / Core Analysis Comments / Description
		3248								Flaser-bedded Muddy Siltstone - 2.5cm thick siderite beds - light-brown colouration throughout => siderite/Fe staining - small, mud-filled vertical to inclined burrows: Skolithos/Trichichnus/Anconichnus/Arenicolites ?
1		3251								3250.7 Silty mudstone - carbonaceous detritus, dark-light grey - abundant bioturbation - silty wavy ripple laminations
2		3254								3253.5 3253.2 Pyritic Coal Black carbonaceous mudstone/shale - Skolithos trace at base of unit
		3257	vfl-vfu							3255.2 Muddy Siltstone - flaser bedding - significantly bioturbated - low-angle cross-lamination
3		3260					7°			- siderite-cemented, 6cm thick fl-fu sandstone bed @ 3259.7 - CACL double mud-drapes (?) @ - sandier-upwards - pyritized Rosselia (?) at very top of facies - discontinuously calcite-cemented
		3263					9°			3262.2 Black carbonaceous mudstone/shale - 10cm thick coal - nodular pyrite - 15cm thick sideritized bed: internally, contains large pyrite nodules and bioturbation - silter-upwards heavy bioturbation
4		3266								
										3267.2 Interbedded muddy siltstone/silty mudstone - prolific bioturbation/soft-sediment deformation - Teichichnus/Taenidium horizon 1.5' thick - carbonaceous near upper, undulatory contact
5		3269								
		3272					7°			3270.8 Moderate-high angle cross-laminated muddy siltstone - thin (<1-1cm) fining-upward wavy lamination - soft sediment deformation, faulting - pyritized root traces w reaction rings/halos
6							10°			3272.8 well-sorted clean, low-angle medium scale cross-laminated siltstone - tan-light brown
		3275					12°			- tiny, nodular pyrite crystals - dark mud/organic rip-up clasts along bedding planes
7		3278					13°			- pyritized Terebellina - medium-scale cross-cutting, wave-ripple lamination, trough-cross-stratification - silty laminations muddy calcareous

?/05/02

CRESTAR ENERGY Name: Crestar ETAL 100 Jenner

CARBONATE CORE LOG

Location 00/07-27-019-09W4/0 Interval 1009.40 - [illegible] m ☑ Core ☐ Chips [illegible] of [illegible]

Formation	Facies	Depth	Lithology	Sedimentary and Structural Features	Biogenic Components	Description/Comments
		1009				
1	Pedogenic Mudstone	1010				Medium grey - light green - brownish red mudstone - ~~somewhat fissile and blocky~~ - carbonaceous
2	Wavy Bedded Siltstone	1011	FUS	sid Py		wavy bedded sandstone - ~~subequal amounts of sand and mud~~ base grading up to muds at top
3	Wavy Bedded Siltstone	1012		Py	Cy? Pl	- carbonaceous detritus
		1013		sid		
4	Clean Sandstone					lower contact interbedded with lower unit fU - mL quartz arenite (> 90% qtz) - excellent porosity, very little fines/ clay particles plugging up pores
5	Clean Sandstone	1014				- high angle foreset laminations marked by coarser, mafic material w/ occasional pebble stringers
		1015				- oil staining is ~~discontinuous~~ but pervasive where present - ~~1-1.5 cm thick current ripple/cobbles~~ ← No! (AK 25/10/02)
6		1016	mudstone	vug	Pl Th	Rhythmically interbedded v.f. sandstone and siltstone. ~100% sand at base of subunits, grading up to lenticularly bedded shaly siltstones
7		1017				- wave ripple laminations - bioturbation
8		1018				- ~~planar tabular~~ - swaly cross-bedding - pyrite nodules up to 2 cm (w/ siderite nodules)
9		1019				- syneresis cracks - *Planolites*, *Teichichnus* - roots (minor) - angled, tapering, lined burrows ~ 1-3 cm long [illegible] ?
10	Pedogenic Calcareous Shale	1020	shell frags.	Pyr, calcareous (calcite cemented)		- tan - light brown (sandstone) -> light grey (shaly siltstone) chert pebble conglomeratic lag at base
11	Pedogenic Mudstone	1021				Massive, pedogenic mudstone - very friable, rubbly - medium grey
12		1022				Lost/missing core
		1023				

CRESTAR ENERGY

CARBONATE CORE LOG

Location _____ Interval _____ ☐ Core ☐ Chips _____ of _____

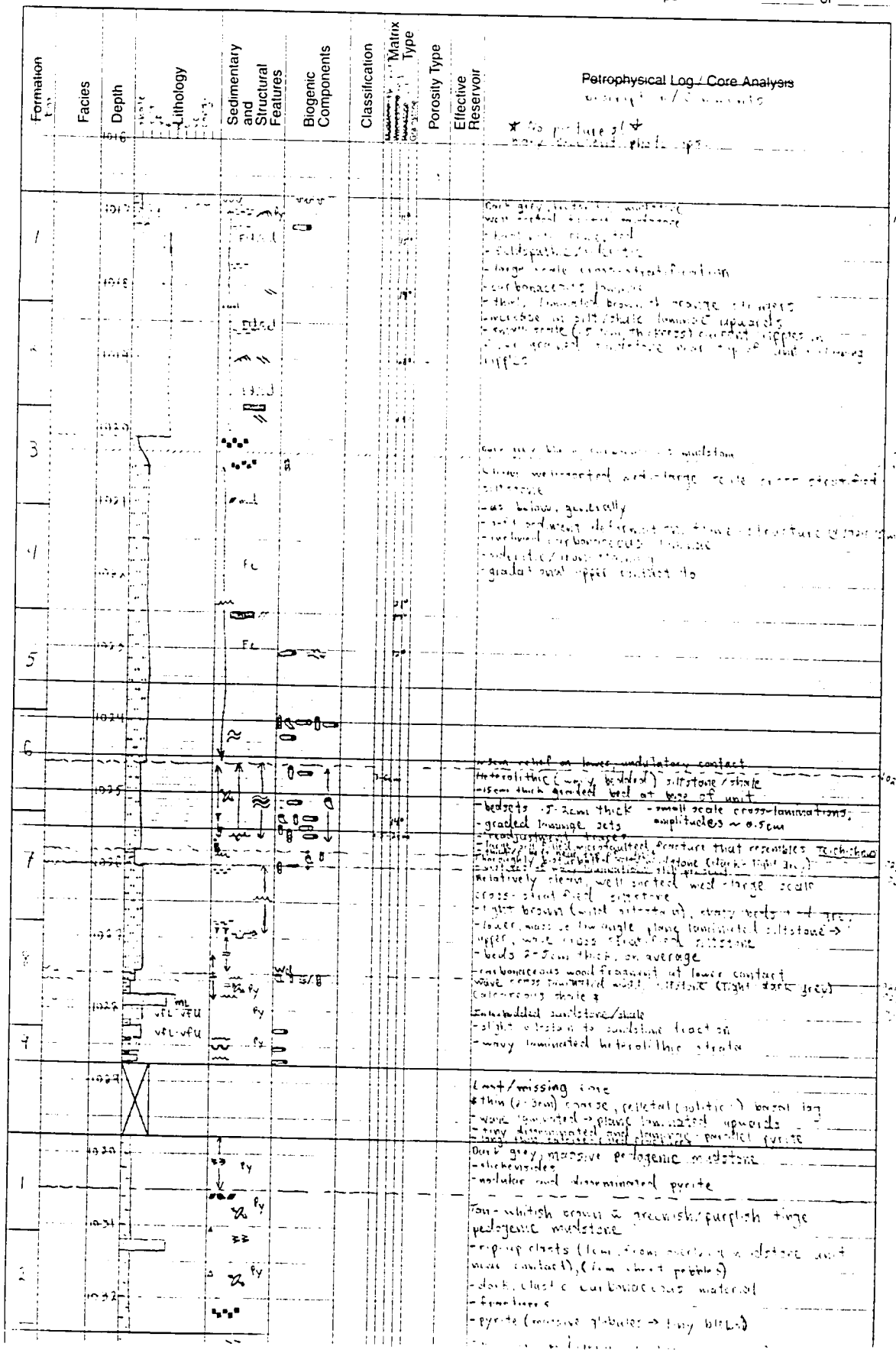

23/05/02

CRESTAR ENERGY Gulf et al 100 Jenner 1-3

CARBONATE CORE LOG

Location 00/01-34-019-09W4/0 Interval 1004.00-1019.80 m ☑ Core (slabbed) ☐ Chips 1 of 1

Formation / Fm	Facies	Depth	Lithology	Sedimentary and Structural Features	Biogenic Components	Fractures (~~Classification~~)	~~Φ Matrix~~ Type / Samples (~~Porosity Type~~)	Effective Reservoir	~~Petrophysical Log / Core Analysis~~ Description / Comments
	Coal	1004		Py					... thick coal
1	Fining-Upward Sst./Siltst. → Mdst.	1005	FUS						Fining up to grey mudstone - rubbly and friable for top 50cm - highly carbonaceous, abundant coal fragments
2		1006		sid, Brecc, coal	Pl., Pl., Pl., escape?, Pl., Te., Cy., Pl., Pa., Ch.				light grey siltstone - v.f. sandstone ≈ shale stringers - light oil staining - abundant Planolites in shaly fractions - escape traces - dark grey muddy siltstone
3	Kaolinitic Sandstone	1007			Th. Pl. or Te.				Reservoir sandstone unit - brown (stained) - pale tan/cream white v.f. - m. sandstone. - much kaolinite / fines in between pores of unstained sections. - minor siltstone stringers
4		1008							- parallel and cross-bedded laminations marked by dark organic matter - sand-on-sand contact @ 1006.5m
5	Bioturbated Sandstone / Siltstone / Mudstone	1009		carbonaceous	Te.				Interbedded mudstone / siltstone / v.f. sandstone - extremely bioturbated and reworked - fractures, micro-faults, convolute bedding / soft sediment deformation, large scour mark / gutter cast
6		1010		oil stain	Pl. Te. Cy. Ch. Th. Sk. Pl. Sk.				- some oil staining near top - excellent Teichichnus at top
7		1011	CUS	(~35cm) Py	Pl., Cy. Te., Pl. Pa.				- trough cross stratification - slightly carbonaceous - stained gr. silts cross-cut by robust Teichichnus burrows
8	Wave Ripple Laminated Siltstone	1012			Sk. Pl.				Fantastically cross-laminated siltstone light-medium grey ← pic opportunity wave ripple laminated - bottom 10cm is calcite cemented
9	Calcareous Siltstone	1013							Massive calcite-cemented siltstone - scoured upper contact
		1014							shale ripup clast at base
	Calcareous Siltstone / ...			frac. calcareous					Silty shale to silty v.f. sandstone, limy - calcite filled fractures
10	Limy Breccia	1015		calcareous					Breccia with limy grey mud matrix and tan-cream white limestone clasts - thin (5cm) calcareous conglomerate ≈ chert pebbles
11	Fining-Upward Siltstone → Mudstone	1016							Massive tan-light grey siltstone grading to blocky/rubbly mudstone - mottled grey/tan colouration in siltstone due to reworking by bioturbators
12		1017							
13				Py, frac.					
		1018							Lost / Missing Core
		1019							
		1020							

CRESTAR ENERGY Empire [illegible]

CARBONATE CORE LOG

Location [illegible] Interval [illegible] ☑ Core ☐ Chips 1 of 1

Facies No.	Depth	Description / Comments
1	3256–3260	Stacked fining-upward [illegible] from v.f. sandstone [illegible] to interlaminated sandstone/shale [illegible] to [illegible] dark grey shales
2	3262–3268	- sandstones are massive, [illegible] wave ripple laminated, [illegible] and shales contain [illegible] pyrite - sandstones are carbonaceous with large ([illegible]) wood chips, chert pebble [illegible] in [illegible] interior [illegible]
3	3268–3270	silty [illegible]; wavy bedded siltstone/shale [illegible] fining-upwards to black mudstone + coal
4	3270–3274	- light-dark grey → black - pyritized [illegible] burrows at base - pedogenic alteration of mudstone
5	3274–3280	chert pebble conglomerate w̄ large wood/coal frags v.f.-f. sandstone, [illegible] % [illegible] fragments significant proportion of fines/clay particles filling up pores. - light-dark brown (heavily oil stained) - massive, save for faint planar laminations and minor chert pebbles
	3282	Lost/missing core
6	3284–3286	
7	3286–3290	Low angle parallel to wavy ripple cross-laminated silty sandstone - deformed/convolute bedding - micro-faulting - bioturbation - v.f. sandstone interbeds w̄ F→G porosity, oil-stained
8	3292–3294	- calcite-cemented near base associated with pinkish-orange colouration [illegible] ripple foreset laminae ([illegible] or feldspar? [illegible] oil-staining) - some picture-perfect traces here
9	3296–3300	
10	3302–3304	
11	3304–3308	erosional, scoured contact marked by cubic pyrite and globular chert granules Rooted tan/cream, slightly calcareous mudstone with chert pebble conglomerate horizons

Facies (vertical labels): Cross-Laminated Silty Sandstone; Calcareous Conglomeratic Mudstone

^6/07/02

CRESTAR ENERGY Name: Crestor 102 Jenner

CARBONATE CORE LOG

Location 02/10-19-020-08w4/0 Interval 922.00 - 949.00m ☑ Core ☐ Chips 1 of 1

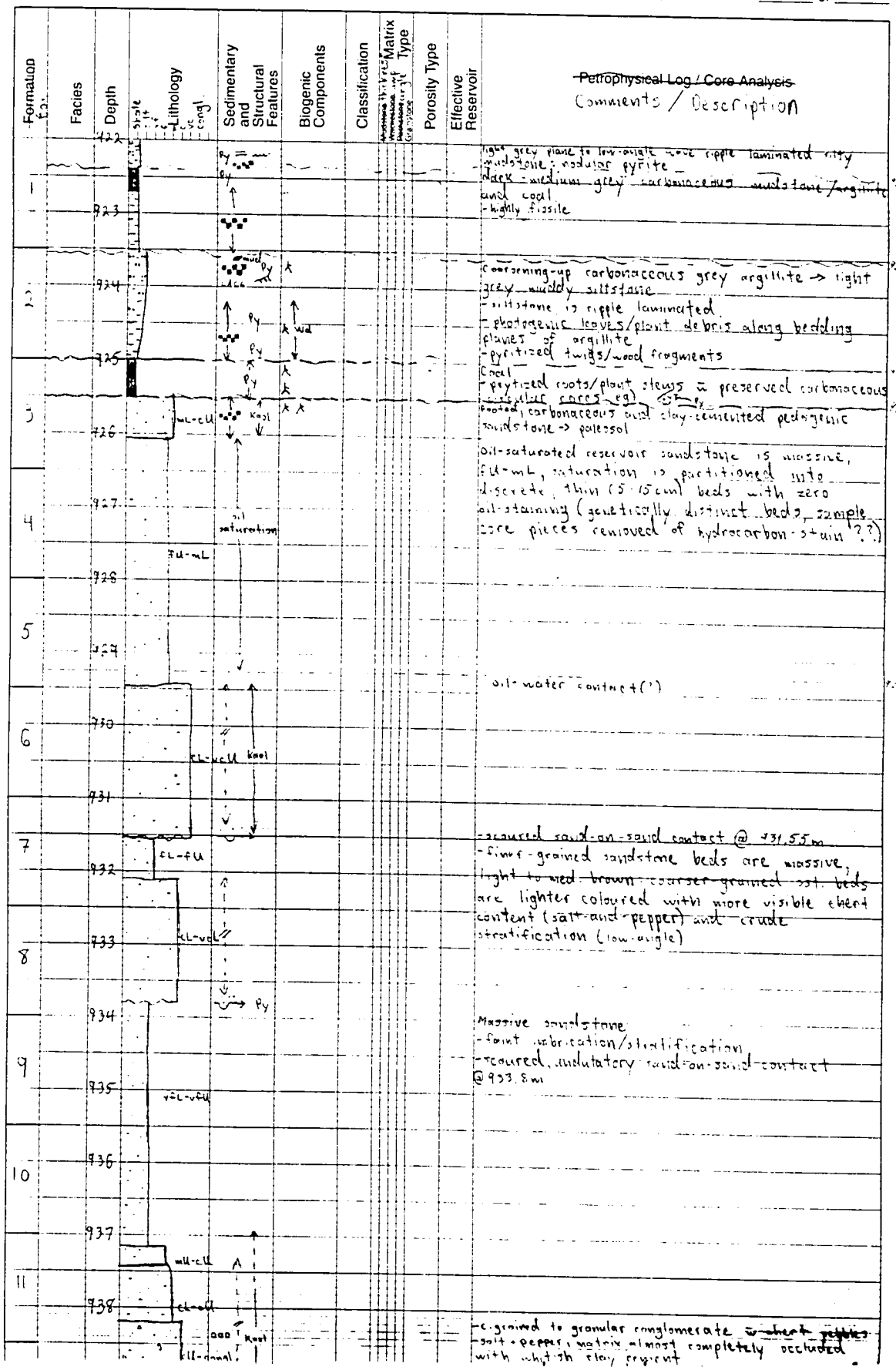

02/08/02

CRESTAR ENERGY Name: Amoco Jenner 12-20-7

CARBONATE CORE LOG

Location 12-20-7 Interval 3185' - 3225' ☑ Core ☐ Chips 1 of 1

Formation	Facies	Depth (ft)	Lithology	Sedimentary and Structural Features	Biogenic Components	Classification	Matrix Type	Porosity Type	Effective Reservoir	Petrophysical Log / Core Analysis
	1	3187								Sandy Mudstone - Glossy surface at 3187' - Diplo ? @ 3189.4' - 12cm thick bentonite at top of facies - carbonaceous coal bed (2-3cm thick) below bentonite
	2	3190	slstn.-vfL							Interbedded f. sandstone - silty mudstone - small, subvertical mud-filled burrows in silty mudstone (Teichichnus?) - Pyrite-replaced Rx. @ 3191.3'? - wispy siderite mud chip laminae (smeary facies)
		3193	fL-cU	LACL						
	3	3196	fL-fU							med to large scale cross-laminated lithic sandstone - angular cross-lamination - sweeping width of core - siderite mud chips defining laminations - tightly cemented - trace carbonaceous material - mud rip-up clasts - rhythmic light/dark (fine/coarse) laminations ~ 1cm thick (beds?)
		3199	fL-fU							
		3202	cL-fU							
	4	3205	fL-fU	sulphur wtl						Carbonaceous mudstone → coal - slickensides in mudstone - wood debris in coal - yellowish (sulphur) stain in coal well sorted, various wL-mU sandstone - heavy oil stain - chert granules
		3208	ch	Py						Carbonaceous grey siltstone/coal/bentonitic mudstone - carbonaceous coal clasts are imbricated in siltstone, aligning themselves parallel to moderate angle planar strata - sandy chert bed @ pl. @ 3205.5'
	5	3211		Py LACL						Massive, heavily oil-stained wL-vfL sandstone - large (5cm) pyrite nodule at top of facies - LACL
	6	3214								Med-scale wavy cross-laminated sandy siltstone - stratification highlighted by faint oil-staining - shaly, bioturbated bed near top of facies
		3217	siltstn.-vfL							
	7	3220	slstn.-vfL	Sid Sid						Carbonaceous silty mudstone - siltstones small-scale wr - larger pl. traces - low angle dip to all strata Interbedded siderite sandy siltstones/bioturbated mudstones - flame structure at base Bioturbated wave ripple laminated silty mudstone/muddy siltstone (carbonaceous material) - low diversity/high abundance of trace fossils at base (lower 10-20cm) of facies, degree of bioturbation decreases upwards - small scale low-angle cross-lamination, ripple wls 0.5-1cm thick - soft-sediment deformation, micro-faulting - med-high angle cross-laminated sandy siltstone - trough cross-stratification(?) medium-scale
	8	3223	slstn.-vfL							
		3226								

Note: Sample numbers that are out of sequence were changed on core boxes.

Note: Core was laid out in boxes opposite to how they are normally laid out (i.e., bottom is lower right, top is upper left, as opposed to the other way around the standard orientation). Core was properly relogged on 02/08/02.

CRESTAR ENERGY

CARBONATE CORE LOG

Location [illegible] Interval [illegible] ☑ Core ☐ Chips 1 of 1

Formation	Facies	Depth (m)	Lithology	Sedimentary and Structural Features	Biogenic Components	~~Classification~~	Φ ~~Matrix~~ Type	~~Porosity Type~~	Effective Reservoir	Petrophysical Log / ~~Core Analysis~~
1	silty mudstone / coal	961.5		Py						[illegible] silty sandstone – heavily bioturbated
	coal									Coal w/ large (up to ~10cm) pyrite nodules
2	Silty Shale-type	963					1, 3, 4			silty, wavy/bioturbated v.f. grained sandstone – [illegible] siltstone is heavily [illegible] out of reservoir quality
3				Py			5, 6			
	silty mudstone	964.5								[illegible] calcareous silty mudstone – bentonitic
4	cross-stratified silty siltstone									[illegible] and cross-laminated muddy siltstone – [illegible] of wave ripple laminated siltstone are up to 3cm thick (typically) 0.5-1cm and grade to mudstone
5		966								– trough (+ hummocky ?) cross-laminated beds
6		967.5								[illegible] hydrocarbon staining – robust [illegible] @ 965.69m
7	calcareous mudstone	969								Calcareous mudstone with conglomerate [illegible] – chert clasts of underlying unit [illegible]
8	Green Mudstone			Py						Green Mudstone Matrix supported Conglomerate w/ white-cream, angular chert clasts up to 3.5cm large
9		970.5		Fe, Py						– framboidal and disseminated (tiny balls) pyrite – some cryptic, moderate angle stratification
10		972								– green mudstone admixed with l. brown-tan argillite @ ~ 976.75 m
11		973.5		Py, Fe						– chert clasts are silicified fossils; some have retained their original morphology (e.g. brachiopod (?) shell @ 975.90 m), others have been leached out leaving vugs with calcareous linings.
12				Fe, Py						– 45cm thick chert bed @ ~ 974.8 m: fossiliferous (bivalves, bryozoa, [illegible] shell fragments) extremely vuggy / porous
13		975								– mudstone grades to a buff/tan colour toward the top of the section
14		976.5		Py						– root traces @ 967.70m – erosive contact w/ overlying unit; ripped up clasts of overlying material incorporated into mudstone matrix
15				Argillite						
16		978		Py Fe						– iron staining (halos)
										missing/lost core
		979.5								Recovered 17.65m
		981								

13/06/02

CRESTAR ENERGY Name: Crestar et al 102 Sounding

CARBONATE CORE LOG

Location 02/14-11-035-09W4/0 Interval 957.25 - 975.20 m ☑ Core ☐ Chips 1 of 1

(957.25 - 970.31 m)

Box	Facies	Depth (m)	Lithology	Sedimentary and Structural Features	Biogenic Components	Matrix Type	Porosity Type	Effective Reservoir	Description / minerals
		955							
1	Coarsening-up silty siltstone	957.5		sid			1P		Thinly laminated coarsening-up shaly siltstone - coal rip-up clasts above erosional contact - more mud than stratigraphically lower muddy siltstone
2		959		Py; sid; Py			2P, 3P		- siderite bands/lenses (≈ 2cm thick) common - slight increase in silt/sand ratio up-section - large (7cm) pyrite nodule at ≈ 958.76m
3		960.5		sid					- Glass-like surface @ 959.20m - slickensides @ 958.96 m - combined flow ripples(?) @ 958.06m
4				Py					- pyritized Zoophycos at top of core - Siphonichnus(?) (1-80K) @ 957.00m
	Coal			Py					Coal w abundant nodular pyrite
5	Silty v.f.-grained sandstone	962					4P		Relatively massive siltstone - v.f.-grained sandstone - prolific hydrocarbon staining
6		963.5		Py			5P, 6P, 7P		- dark-light brown/tan-light grey (stained) (unstained) - sandstone fraction is dune-cross stratified
7		965					8P, 9P, 10P		- oil-staining is patchy (not continuous); may be related to porosity or sampling - plugs are salt and pepper v.f.-grained sst. - silty fractions are ripple laminated and bioturbated
8	Cross-laminated muddy siltstone	966.5		Py					wave ripple laminated/bioturbated muddy siltstone - laminated/trough cross-laminated beds demarcated by oil-staining
9				Py					- oil-stained wave ripple cross-laminated bed sets are restricted to ≈ the lower 1.5m; at 966.5m, an erosional break separates cross-laminated siltstones and more massive, bioturbated muddy siltstones above.
10		968					11P		- nodular pyrite near top - highly irregular upper contact with abundant Planolites traces
11		969.5					12P, 13P		- rootlets may indicate presence of nonmarine conditions (plus increase in dark organic matter) near top of facies. (M. Hearn)
	calcareous grey mudstone			coal					Calcareous grey mudstone ≈ sandy [illegible]
12	Massive Mudstone	971							Massive mudstone - [illegible] colour - nodular pyrite
13									
14		972.5		Py; Py					- silica cemented granular siltstone - v.f. grained sandstone at bottom 20cm - faintly high-angle bedded - organic detritus
15		974							- mudstone becomes highly friable for top 1.5m
									Lost/missing core
		975.5							

CRESTAR ENERGY

CARBONATE CORE LOG

Location _____ Interval _____ ☒ Core ☐ Chips 1 of 1

Formation	Facies	Depth	Lithology	Sedimentary and Structural Features	Biogenic Components	Classification	Matrix Type	Porosity Type	Effective Reservoir	~~Petrophysical Log / Core Analysis~~
1		764								fining-upward silty mudstone - pyritized root traces and/or shell shards - degree of pedogenesis increases upwards - 5cm thick sandy bed @ 764.2m
										★ No pictures from this core! ★
2		765								
		766								wavy bedded siltstone/shale - low-mod angle laminations Carbonaceous well-sorted fine sandstone
3										pyritic grey mudstone - cm-scale globular/framboidal pyrite nodules lenticular to flaser bedded siltstone/shale - Teichichnus / Taenidium (Rhizocorallium) burrows - coarser sandy laminations
		767								
4		768								Pyritic grey mudstone/shale - tubular pyrite may be replaced burrows - silty siltstone - coal laminations
										Carbonaceous + pyritic shale → coal - slickenside surfaces
5		769								
		770								muddy oil-saturated vf-grained carbonaceous sandstone
6		771								low angle, plane-laminated muddy vf-med sandstone
7		772								low angle, low amplitude, med-large scale, broadly cross-stratified silty mudstone/muddy siltstone - light-dark grey - several sharp-based, fining-upward beds (storm deposits) - contacts may be at high-angle (eg 2m)
8		773								- thick beds to 5cm
		774								Cross-stratified muddy siltstone - as below - laminae sets from ~0.5-2.5cm thick ∧
9		775								wave-ripple laminated, bioturbated silty mudstone - laminae sets .5-1cm thick - bioturbation tough to make out - pyritized root traces - upper 12cm is low angle plane laminated siltstone
10		776								small-medium scale cross-stratified muddy siltstone - light-dark grey - lowermost 20-30cm is moderately-heavily bioturbated - inclined fracture (sweeps across core) @ ~775.95m [many such fractures] Non-calcareous Mudstone ∧ Rubby Pedogenic Mudstone - tannish white - light brown - rhizomal burrows
		777								Lost/missing core
		778								∧ lower contact is brecciated with large (up to ~15cm across) clasts containing fossil fragments (ammonites, bivalves) - entire unit is non-calcareous
										- organic debris, tiny pyrite nodules, plane → finely wavy laminated ∧ mudstone/shale
										★ Paleophycus, Asterosoma trace fossils are probably all the same (Cylindrichnus) cut at different angles Across stratified foresets appear to have a unidirectional

18/06/02

CRESTAR ENERGY Name: HEC [illegible] 2 [illegible] 20-9

CARBONATE CORE LOG

Location [illegible]-22-25-020-07W4/0 Interval 772.0 - 785.0m

☑ Core ☐ Chips

Formation	Facies	Depth	Lithology	Sedimentary and Structural Features	Biogenic Components	Classification	Matrix Type	Porosity Type	Effective Reservoir	Petrophysical Log / Core Analysis
1	Coarsening-up cross stratified sandstone	773								[illegible] cross stratified, coarsening-up sandstone - relatively clean, quartz arenite composition - major features: - low angle laminations (marked either by dark organic matter or contrasting grain size) that sweeps across length of core - coal clasts aligned parallel to planar laminations - ~~thin silty shale beds with Thalassinoides burrows~~ - ~~lamination plane parallel and chaotically~~ oriented pyrite veins/bands - ~~[illegible] @ [illegible]m~~ - cross-stratified pyrite laminations @ 777.15m - vc-granular = chert pebbles/granules at top ~1.2 [illegible] of core
2		774								
3		775								
		776								
4		777								
		778		Py, Py				NA		
5		779		Mc?, Py						
		780								Lost/missing core
1		781			coal					
2	Heavily bioturbated, silty mudstone	782		Py						Heavily bioturbated and deformed silty mudstone - pyritized roots - rare preservation of primary stratification (plane and wave ripple laminated)
3	Cross-stratified and bioturbated sandstone	783		Py						Cross-stratified and bioturbated [illegible] siltstone - [illegible] cross [illegible] - [illegible] overlain by bioturbated silty mudstone facies -> observed in other core but not broken up into distinct facies, probably should be - shale rip-up clasts - [illegible] @ 783.7m
4		784								- [illegible] - [illegible] dark grey - Lost/missing core
		785								Note: [illegible] Map [illegible] [illegible] [illegible] [illegible] 757-7 [illegible]m N.B. well is deviated

18/06/02

CARBONATE CORE LOG

CRESTAR ENERGY Name: PEC Jenner 4-5-30-4

Location: [illegible] Interval: 954.75 – 975.10 m ☑ Core ☐ Chips 1 of 1

Formation	Facies	Depth	Lithology	Sedimentary and Structural Features	Biogenic Components	~~Classification~~	~~Matrix~~ Type	~~Porosity Type~~ Sample	Effective Reservoir	~~Petrophysical Log / Core Analysis~~ Description/Comments
		954								
1		955.5								Greenish-grey / argillaceous mudstone → pedogenic finely laminated silty mudstone coarsening and cleaning up to a lithic [illegible] ss.
2		957								
3		958.5								~~Block missing~~ -large soft-sediment deformation structure @ ~ [illegible] -pyritized roots -coal rip-ups
4		960		Py						Cleaning upwards [illegible] sideritic [illegible] grained sandstone -10cm thick siderite bed @ ~ 959.1m ~~[illegible]~~ fraction -rooted horizon @ ~ 959.1m
5				Py						
6		961.5								Rhythmically stacked fining-upward coarse grained sandstones -commonly with a coarse conglomerate lag -reservoir unit, significantly oil stained -[illegible] sandstone fraction is [illegible]
7		963								
										~~Lost/missing core~~
1		964.5								
2		966								
3		967.5								
		969								Lost/missing core
		970.5								
		972								
1	[illegible] siltstone	973.5		Py						Thinly laminated muddy siltstone -~~minor interbedded oil stained siltstones~~ -combined flow ripple laminations
2	Calc. Mudstone	975		Py						Calcareous mudstone with conglomerate lag -pyrite-filled fractures + [illegible] cracks -need core analysis to verify sample locations
		976.5								

CRESTAR ENERGY Well: AEC Jenner E 23-29-9

19/06/32

CARBONATE CORE LOG

Location [illegible] Interval 746.50 - 764.50m ☑ Core ☐ Chips 1 of 1

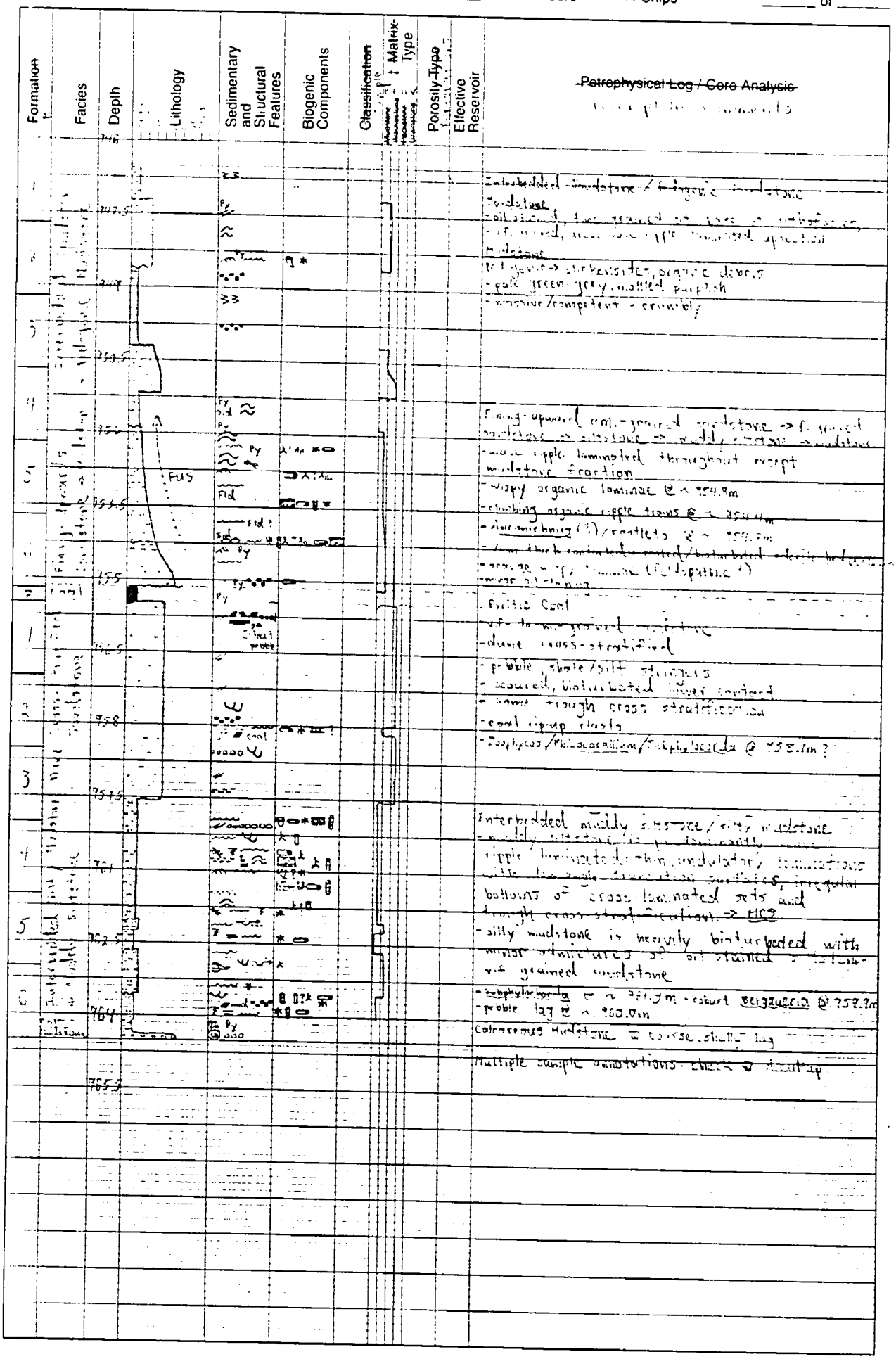

CRESTAR ENERGY

CARBONATE CORE LOG

Location [illegible] Interval [illegible] ☑ Core ☐ Chips [illegible] of [illegible]

Formation	Facies	Depth	Lithology	Sedimentary and Structural Features	Biogenic Components	Classification	Matrix Type	Porosity Type	Effective Reservoir	Petrophysical Log / ~~Core Analysis~~
	1									pedogenic mudstone - greenish-purplish - organic debris - sandstone beds/lenses
	2									
	3		FUS							fining upwards - sandstone → siltstone → mudstone - feldspathic sandstone : [illegible] - 3cm thick [illegible] bed @ [illegible]m - coal laminae and rip-ups - [illegible] pyritized laminations (pyritized [illegible]) @ [illegible] - pedogenic mudstone bed @ [illegible]m
										Lost/missing core
	1									fine-grained sandstone [illegible] (laminated) [illegible] Interbedded [illegible] mudstone/muddy [illegible]stone - bedding plane view of [illegible] @ 75[illegible].9m
	2									
	3									
	4	[illegible]stone								[illegible] calcareous mudstone with [illegible] [illegible] massive [illegible] - minor chert pebbles/granules - abundant roots - discrete slickensides - mottled/patchy dark spots (organic, phosphatic?)
	5									
										Lost/missing core
										Multiple sample annotations

Name: AEC Jenner 10-33-20-9

CRESTAR ENERGY

(1) 137.55 - 144.70 m

CARBONATE CORE LOG

Location 00/10-33-020-09W4/0 Interval (2) 750.00 - 757.25 m ☑ Core ☐ Chips 1 of 1

Formation	Facies	Depth	Lithology	Sedimentary and Structural Features	Biogenic Components	Classification	Matrix Type	Porosity Type	Effective Reservoir	Comments / Description
	1	138								Pedogenic mudstone -increase in carbonaceous matter upwards ~~-pyrite nodule @ ...~~ -rounded shale contact @ 138.5m -cubic pyrite crystal @ 137.7m -13cm thick siderite bed w/ calcite-filled open fractures
	2	139, 140	vfU-fL, fL-fU							Fining-upwards vf-f grained sandstone → carbonaceous mdstn. -sandy beds thin upwards from 10-1cm ~~-large scale contact at base of vfU-fL sandstone~~ -pyritized roots + reaction halos → Retallack "Soils of the Past" - paleosol reference (M Johnson) ~~other side lamina mark ripple foresets~~
	3	141	fL-fU, fL-mL							climbing ripples/wavy faces in top 15cm Small scale ripple laminated siltstone - f grained sandstone -predominantly current ripple laminated w/ some wave-ripple stratification -current ripple foresets commonly have tangential bases ~~-two 2mm pyrite nodules @ 141.15m~~ -ripple set thicknesses from .5-2cm Shaly coal/carbonaceous shale
	4	142, 143	fU-mL							Massive pedogenic mudstone -slickensides, organic material ~~-red clays bleeding out of slickensided mudstone~~ -colour range/variability from reddish brown-tan/buff-~~grey-greenish grey-purplish red (red beds)~~ -coarser grained sandy laminations and beds. ~~-texture ranges from massive, intact mudstone + sandy~~ beds to rubbly/friable muddy shales with abundant organic detritus
	5	144	fU-mL, vfL-fU							-burrowers have piped down fU-mL sand into underlying mudstone @ 143.9m -small-scale, imbricated vugs in fU-mL sand interbed @ 143.9m -mudstones faintly, thinly planar laminated -small rip-up in 12cm thick, small scale cross stratified fU-mL sandstone bed
		145								
	1	750, 751	fL-fU, vfU-fL							Small-scale current ripple laminated fL-fU sandstone -carbonaceous detritus ~~-pyrite nodules, wavy ripple stratification in discontinuous~~ bands -porosity well occluded w/ fines/clay cement -faint low-angle cross-lamination -small-scale current ripples climbing up the backs of larger, low-angle cross-stratified structures -well sorted, current
	2	752								Pedogenic mudstone + 25cm thick coal -coal clasts in mudstone -desiccation/shrinkage crack @ ~752.25m
	3	753, 754	mL-mU, fU, fU-fL							~~well sorted, large scale cross-stratified fL-mU sandstone~~ -lower, undulatory contact is mL-mU atop vfL sand; contact is conspicuously marked with dark chert pebbles and granules ~~-vertical burrowers have piped in sand into underlying vf sand firmground~~ ~~-m sands are medium-large scale cross-stratified~~ ~~-chert pebble/granule stringer @ 753.0m; tangential foresets~~ downlapping onto pebbly lamina -chert granules found in cross-stratified sands -wave ripple laminated coated vfU sand @ 754.7m
	4	755	vfU-fL, fL-mU							-well rounded chert pebbles @ 754.85m: largest clast is 2.3cm long and 0.5cm wide -25cm thick muddy siltstone - vfL sandstone bed @ ~754.3m: contains both carbonaceous, coal laminae and ... sand stringers -nodular pyrite lamina @ 756.10m
	5	756	siltstn.-vfL, siltstn.-vfL, fU-mL, vfL-vfU							Bioturbated + crumbled muddy siltstone -carbonaceous debris in muddy fractions -carbonaceous shale stringers -pyritized rootlets -vf sandstone rip-up clasts at base well sorted, large-scale cross-stratified fL-fU sandstone -heavily oil-stained -undulatory + partially bioturbated basal contact -few thick mudstone bed @ 756.65m w/ 3kolithos + synaeresis cracks -mud clasts
	6	757, 758	siltstn.-vfL, siltstn.				1-2cm amplitude			Bioturbated small- to medium-scale cross laminated muddy siltstone -tiny pyritized 3kolithos @ 757.2m -ripple laminae sets ~1.3cm thick, on average -symmetrical, sharp based, fining-upwards wave ripples -slightly coarser fractions mildly oil-stained -3D wave ripple x-strat. @ 757.25m

Right margin depths: 139.0, 140.35(?), 141.25, 141.45, 752.60, 752.35, 755.25, 756.15, 756.75, 757.1

CRESTAR ENERGY

CARBONATE CORE LOG

Location _____ Interval _____ ☐ Core ☐ Chips _____ of _____

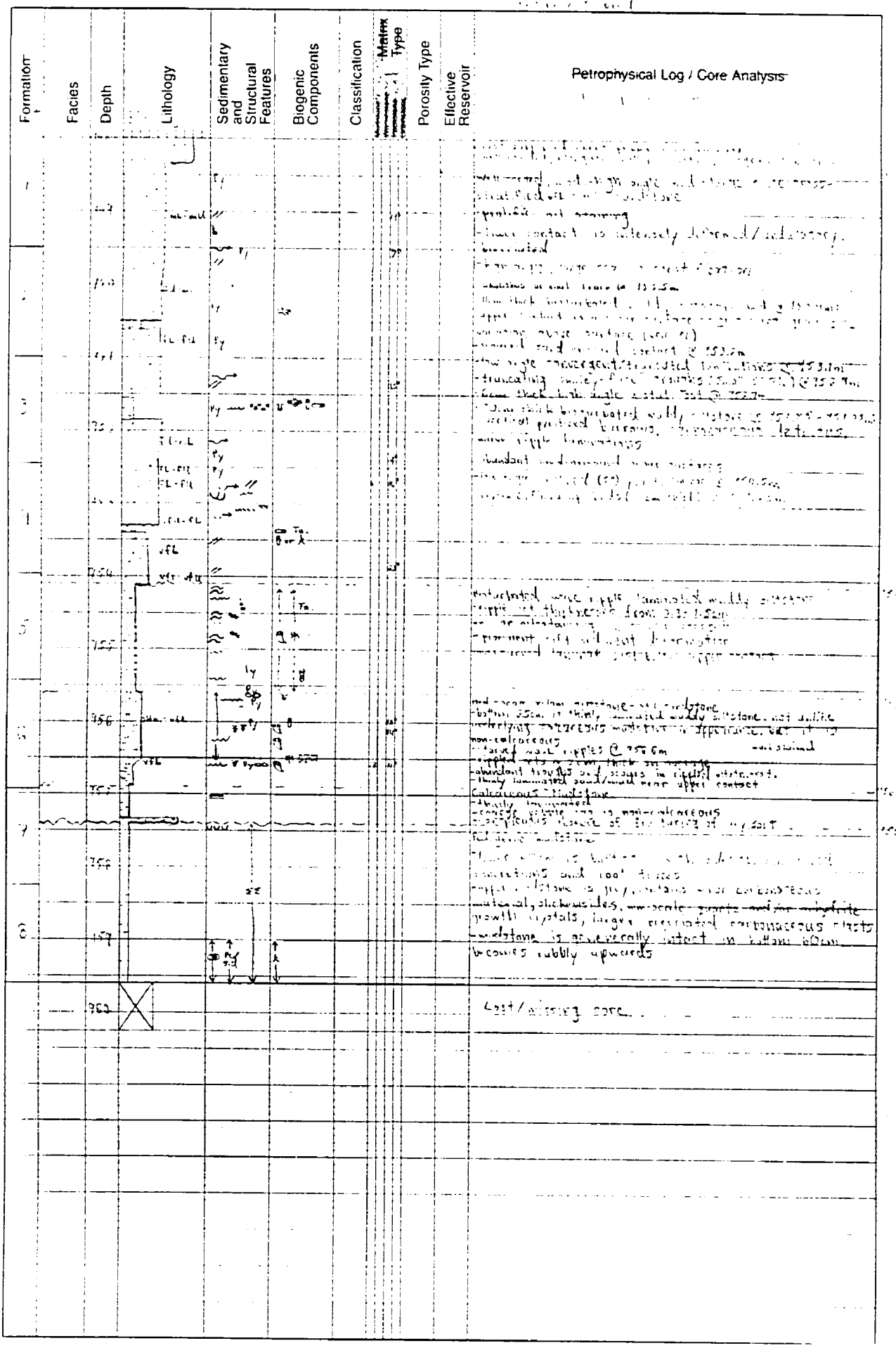

04/07/02

CRESTAR ENERGY Nomura AEC [illegible]

CARBONATE CORE LOG

Location 10/13-23-020-29W4/0 Interval 940.90-956.10m

☑ Core ☐ Chips

~~Formation~~ Facies	Depth	Lithology	Sedimentary and Structural Features	Biogenic Components	Classification	~~Matrix~~ Type	Porosity Type	Effective Reservoir	~~Petrophysical Log / Core Analysis~~ Comments / Description
	940								
1	941								Black Mudstone -10cm thick siderite bed @ 940.? m Lenticular bedded siltstone/shale -abundant Teichichnus traces -carbonaceous debris/root traces -distinct wave and current ripple laminations -pyrite nodules & root traces
2	942								feldspathic/lithic vf-fU sandstone -wave cross-stratification -~~flaser bedding~~ Bioturbated silty mudstone ?cm thick siderite bed @ 9?? ?m
3	943								well sorted fU-mL sandstone -~~lower contact with underlying conglomerate~~ conspicuously included at a high angle -~~massive, faintly low angle stratified sandstone~~ -pyritized/carbonaceous roots at top of facies, ~~porosity plugged up w/ clay cement → paleosol~~ development
4	944 / 945								
5	946								
6	947								Difficult unit to classify. Possibilities: -well matrix-supported chert pebble conglomerate -~~clast supported granular conglomerate~~ -pebbly well sandstone ~~Explanation~~ ~~[illegible]~~ - ~30% clasts >2mm (conglomerates are 30% >2mm by definition)
	948								Sandstone, as below ~~-faint inclined stratification~~ (947.65)
7									
	949								Sharp-based, clast supported chert pebble conglomerate (948.52) -coarse-grained matrix -~~faint high angle stratification~~
8		fU-mU							Moderately sorted fU-mL sandstone (949.0) -abundant pebble stringers/clasts -dominantly horizontal to low angle plane laminated with some high-angle cross-laminae & truncated upper boundaries
	950								-mud rip up clast @ 951.15m
9	951								-rhythmically bedded, wave ripple laminated coarse/fine sets @ 951.2m -stratified inclined cross-bedding: likely sorting during avalanching down dune slip faces -pebbles up to 1.5cm long
10	952								Med-scale x-strat muddy siltstone - fL sst. (951.77) -prolific cross-laminated wave ripples -carbonaceous root traces
11	953	vfU / vfL-vfU							-near horizontal plane laminated siltstone steepens upwards for 35cm (laminations dip @ ~5° at top) where it is truncated by a set of med scale x-strat. siltstn - vfL sst → Hummocky cross-stratification -cross-laminae have tangential bottomsets
	954								-ripple set thicknesses highly variable from ~0.5-25cm -swaly cross-stratification?
12	955								Coarsening-upwards silty mudstone/muddy siltstone (954.5) -35cm thick interbedded silts/muds with abundant Thalassinoides & Planolites -increase in ripple set thickness upwards -inclined, cross laminated wave ripple sets
13	956	vfL-vfU / vfL							-heavily bioturbated 25cm thick muddy interval 15cm above lower contact -combined flow ripples -~~finely laminated silty mudstone~~ Med-scale x-strat. muddy siltstone (956.05) -lower 30cm is significantly bioturbated -laminations [illegible]

CRESTAR ENERGY

15/07/02

CARBONATE CORE LOG

Location 02/16-23-020-09W4/0 Interval 946.00 - 959.50m ☑ Core ☐ Chips

Formation	Facies	Depth	Lithology	Sedimentary and Structural Features	Biogenic Components	Classification	Matrix Type	Porosity Type	Effective Reservoir	Comments / Description
	1	946, 947	fL-fU, fU	Py						Reservoir mudstone - [illegible], relatively massive, faint stratification - undulatory [illegible] contact w no [illegible] - rooted/carbonaceous just below coal at very top [illegible] of core
	2	948, 949	silt - vfL							Moderately bioturbated interbedded siltstone/mudstone 948.5 - 10cm shaly coal at base - pervasive soft sediment deformation - coal fragments, laminae - burrows in silty/sandy fractions - carbonaceous mudstones
	3	950	vfL - fU							Reservoir Sandstone 949.1 * check porosity/permeability on core analysis vs. ϕ/k of sst. above coal/mudstone. Could separate/distinguish two different sands - relatively massive, faint stratification, difficult to make out because of oil-staining - [illegible]
	4	951								Cross laminated siltstone 950.5 - muddier upwards Silty Mudstone 950.85 - lenticular - wavy laminated - fining-upward wavy laminated beds. - laminae sets thin upwards, then thicken - wave ripple laminated [illegible]
	5	952, 953	silt - vfL							Muddy Siltstone 951.6 - 3D wave ripple laminated (~5-10cm thick) - 22cm thick bioturbated horizon - low-angle planar to slightly undulatory laminated at base - faintly planar laminated at top Calcareous Mudstone 952.8 - thinly laminated, fining-upwards - lamination-parallel pyritic laminae - fractured, pyritized root traces *
	6	954								Pedogenic mudstone 953.45 - crumbly/rubbly reddish/grey mdstn. w slickensides, chert pebble
		955, 956								Lost / missing core
	7, 8	957, 958, 959, 960		Py, sid						Pedogenic mudstone - tan w pink/green/grey tinges - spherulitic siderite (tiny dots/blebs) - rooted, carbonaceous - fractured - high-angle (~30°) crude, deformed stratification - chert + pyrite rip-up clasts with sulphurous residue - lithic (volcanic?) fragments/clasts ~ 1-2cm [illegible] - spherulitic siderite blebs and opaque, dull white quartz/chert crystals formed penecontemporaneously (in close association with one another) - slickensides - large vugs with infilled/precipitated siderite or pyrite in pinkish mudstone @ 957.35m * fenestral/birdseye textural porosity from dissolution of small, horizontally oriented mud/carbonaceous clasts (Rhizoconcretions?) - erosional/scoured upper contact - cm scale chert pebbles above pyritized roots * tangential, downlapping bottomsets of wave ripple troughs.

CRESTAR ENERGY

CARBONATE CORE LOG

Location [illegible] Interval [illegible] ☒ Core ☐ Chips ____ of ____

Formation	Facies	Depth	Lithology	Sedimentary and Structural Features	Biogenic Components	Classification	Matrix Type	Porosity Type	Effective Reservoir	Petrophysical Log / Core Analysis — Description / Comments
		755								interbedded mudstone/siltstone/sandstone
1										bioturbated mudstone
		756								FL-Pd sandstone as below
										fining-upward wavy bedded sandstone/mudstone → dark grey mudstone
										-bioturbated
2		757								FL-Pd Sandstone -relatively massive
										-carbonaceous (coal clasts, carb laminae) -lower 60cm are poorly sorted
		758		Pd/sid						-cross-laminations of coarse, dark (lithic/chert) and orange (K-feldspar/siderite) material
	2									
3		759								Sandy Mudstone -soft sediment deformation -carbonaceous detritus -sideritic nodules (sand filled in mud matrix)
4		760		fy Py wd fy						Coal / Carbonaceous mudstone -pedogenic nodules at bottom (5cm) -pyrite nodules and beds (up to 4cm thick) -wood fragments in coal beds
		761								
5				Py Py						Massive to faintly cross-stratified vf-f sandstone -Planolites, Thalassinoides -pyrite nodules -siderite/feldspar orange coloration
		762		Py						-coated, carbonaceous at top
6		763								Bioturbated and ripple cross-laminated silty mudstone / muddy siltstone. -pinstripe silt/mud laminations
7		764								-fining-upward ripple laminated beds ~ 0.5-1cm thick @ ~ 765.2m -oil staining in coarser, cleaner siltstone beds
1		765								
2		766								
		767								Calcareous mudstone -coarse pebbly/granular log -small white clasts & dark, reactionary halos
										Pedogenic mudstone
3		768								-high angle (~25°) stratification, spherulitic siderite in lower 1m, chert clasts -portions of lower 2m are pedoturbated (Arnott) granular silt/sandstones with whitish clay material occluding pore space
4		769								-upper 3.5 m is massive grey mudstone with carbonaceous material
		770								
5		771		wd						

CRESTAR ENERGY

6/07/02

CARBONATE CORE LOG

Location 13/11-34-020-09W1/0 Interval 970.00 - 986.50m ☒ Core ☐ Chips 1 of 1

Formation	Facies	Depth	Lithology	Sedimentary and Structural Features	Biogenic Components	Classification	Matrix Type	Porosity Type	Effective Reservoir	Petrophysical Log / Core Analysis
		970		fy						bioturbated and wave ripple laminated muddy siltstone/silty mudstone - synsedpositional faulting - wave sets are ~1-2cm thick
		971								
		972								pyritic mudstone? pelagenic mudstone - slickensides - soft-sediment deformation - spherulitic siderite - pyrite - high-angle stratification - coarse sand beds -@ 976m, mudstone replaced by pedogenically altered mudstone. - fractured/brecciated
		973								
		974								
		975								
		976								* - only ~5cm is calcareous - coarse chert/pyrite lag - pyritized roots/burrows/fractures
		977								
		978								
		979								
		980								
		981								
		982								
		983								
		984								
		985		fy						
		986								

CRESTAR ENERGY

CARBONATE CORE LOG

Location [illegible] Interval 754.0 - [illegible] m ☑ Core ☐ Chips [illegible] of [illegible]

Formation-Unit	Facies	Depth	Lithology	Sedimentary and Structural Features	Biogenic Components	Classification	Matrix Type	Porosity Type	Effective Reservoir	~~Petrophysical Log / Core Analysis~~ Comments / Description
1		754		py						convolute laminated [illegible]
										[illegible]
										[illegible] wave ripple laminations
		755		py						
2				py						Pinstripe laminated siltstone
										- pyritic, carbonaceous
										- sandy interbeds
										- [illegible] lamination
		756		py						Wavy, bioturbated silty mudstone
				py						~~Tight, low-angle cross-laminated pyritic siltstone - [illegible]~~
										- carbonaceous, coal clasts
3		757								Med. - coarse scale cross-stratified fL - mU sandstone
		758								- salt and pepper colour where not pervasively oil-saturated
4										- many granular-pebbly interbeds
										- sand-on-sand scour surfaces
		759								- well-rounded ovoid-elongate chert pebble stringers, beds, and isolated clasts
5										- sands above and below pebble beds are not identical: different colour, oil-saturation, grain size, etc.
		760								- oil-saturation tends to be preferentially located in well sorted sandstone beds. oil-staining is negligible in [illegible] sandstone - granular / pebbly interbeds
6		761								- carbonaceous silty interbed with wispy coal laminae @ 761.[illegible]
										- 4 cm thick coal at top of unit
		762								
7										
		763								
8		764								
		765								
9										
		766								
10			shale-fill							[illegible] cross-stratified muddy [illegible]
		767								- moderate bioturbation (Cylindrichnus, Asterosoma, Skolithos, Teichichnus)
										- [illegible] cm thick plane laminated mudstone beds
										- grain size up to fU sst.
11			mottly shale	py						- wave ripple laminations replaced by plane bed laminae @ 768.5 m
		768								
		769								Lost/missing core

CRESTAR ENERGY Name: Crestar [illegible] Jenner

11/03/02

CARBONATE CORE LOG

Location [illegible]-23-021-09 W4/0 Interval 745.50 - 7[illegible].50 m

☑ Core ☐ Chips — slabbed [illegible] — 1 of 1

Formation	Facies	Depth	Lithology	Sedimentary and Structural Features	Biogenic Components	Classification	Matrix Type	Porosity Type	Effective Reservoir	~~Petrophysical Log / Core Analysis~~ Description / [illegible]
1		745.5 – 746								well-sorted, vfL-vfU sandstone - low-high angle, large scale cross-stratification - [illegible] - salt and pepper -> light-> grey-brown colour - ~~[illegible]~~ - carbonaceous mudstone beds
2		747								- high angle x-strat. in alternating vfL vfU -> mL mU sands - devoid of trace fossils in sst., planolites in muddy interbeds - [illegible] fill [illegible] clasts + pyrite @ 745.45 m
3		748								
4		749 – 750	fU-mL							[illegible] sandstone - large scale cross stratified vfL - vcU sst. - large chert pebbles + granules occurring in well sorted conglomeratic beds, [illegible] stringers [illegible] one clast thick, and randomly dispersed in a sandstone matrix*
5		751	fu-mL							- granular/pebbly beds are conspicuously less oil-stained than well-sorted sandstone matrix * and thin (~5cm thick) fining-upward beds, usually grading from granules -> mL sand
6		752								- minor, small scale wave ripples in sandstone
7		753	mL							
8		754								
9		755	fL-fU vfL-vfU							
10		756	vfL-vfU	Py						Interbedded sandstone/siltstone/shale - sandstone is vfL vfU, planar to slightly wave-laminated, brown (oil stained) - distinctly different trace fossil assemblage (Planolites, [illegible], [illegible]) - silts/muds are plane-laminated, [illegible] = pyrite - load structures at upper contact
11		757		Py						Med scale cross-stratified, brown siltstone - wave ripple laminations - Cylindrichnus, Asterosoma - ~~disseminated pyrite~~
12		758		Py						Small-med. scale cross-stratified light-dark grey siltstone/mudstone - zonation into lowest, thinly bedded, fining-upward muddy siltstone beds, contorted zone of soft-sediment deformation and microfaulting, pinstripe wave ripple laminated muddy siltstone, highly bioturbated and contorted wave ripple laminated siltstone
13		759								- flame structures @ 757.8 m
14		760		Py						Med. scale cross-laminated muddy(?) siltstone (brown) - very little if any mud in facies: mud restricted to infilling burrows and fractures, isolated stringers, and finer grained ripple foreset laminae - ~~lowest [illegible] is inclined to ~[illegible], above which~~ ~ 30cm* calcareous mudstone*
15		761 – 762		Py						Tan-greenish grey pedogenic mudstone - disseminated pyrite - ~~clastic chert fragments~~ - massive pedogenic texture, slickensides rare

Right margin depth marks: 756.95, 757.6, 759.6, 760.65, 760.4

CRESTAR ENERGY

CARBONATE CORE LOG

Location [illegible] Interval [illegible] ☑ Core ☐ Chips [illegible] of [illegible]

Formation	Facies	Depth	Lithology	Sedimentary and Structural Features	Biogenic Components	Classification	Matrix Type	Porosity Type	Effective Reservoir	~~Petrophysical Log / Core Analysis~~ Description/Comments
1		931		Py, Fe, sid						Carbonaceous grey Mudstone - lower contact is interbedded with underlying silty [illegible] grey mudstone [illegible] in a silty/sand matrix - iron-staining
		932		sid, SS, Fe, Py						- siderite bed @ 932.4m w/ slickensides + calcite-filled fractures - pyrite nodules with dark reaction halos - coal clasts - microfault @ 931.6m
2		933		Py, SS			25°			Silty sandstone - high-angle bedding in lower 22cm - slickensides at basal silty mudstone ~~[illegible] wave-ripple laminations~~ Pyritic Coal
		934								Lost / missing core
1		935								Pedogenic Mudstone - dark-light grey, greenish- to purplish-grey - siderite beds/intraclasts - massive from lower 1.5m, otherwise rubbly - slickensides, massive pedogenic texture - organic carbonaceous debris
2		936		SS						- 13cm thick siderite bed at base - large (~5-10cm) siderite clasts in bentonitic mudstone matrix
		937								
3		938		sid						
4		939		sid, Py						Silty Mudstone - primary wave laminated fabric almost completely wiped out by burrowers and soft-sediment deformation
		940		sid, Py						Brown-light grey muddy siltstone - potential Glossifungites surface at bottom of unit - small-scale current laminations, ~1cm thick sets
5										Silty Mudstone
		941								Feldspathic / siderite [illegible] sandstone - 2.2cm thick siderite bed at top of unit
6		942	FL	Fld/Sid						- small-medium scale wave cross-laminations ~.5cm thick - calcite filled fractures in siderite bed
										Pyritic Coal
7		943								Massive, bentonitic, slightly carbonaceous mudstone - light grey
		944								
8		945								Interbedded wavy laminated muddy siltstone/silty mudstone - climbing current ripples @ 946.35m
9		946		sid, Py						- ripple set (not amplitude) thicknesses range from 3mm -> 6mm - globular pyrite bed 5.5cm thick @ 946m - 6cm thick siderite bed @ 945.45m - thin Cylindrichnus from 946.1 - 945.5m
10		947								

CRESTAR ENERGY Name: Pinnacle et al Jones

CARBONATE CORE LOG

Location _____ Interval _____ ↗ Core ↰ Chips ____ of ____

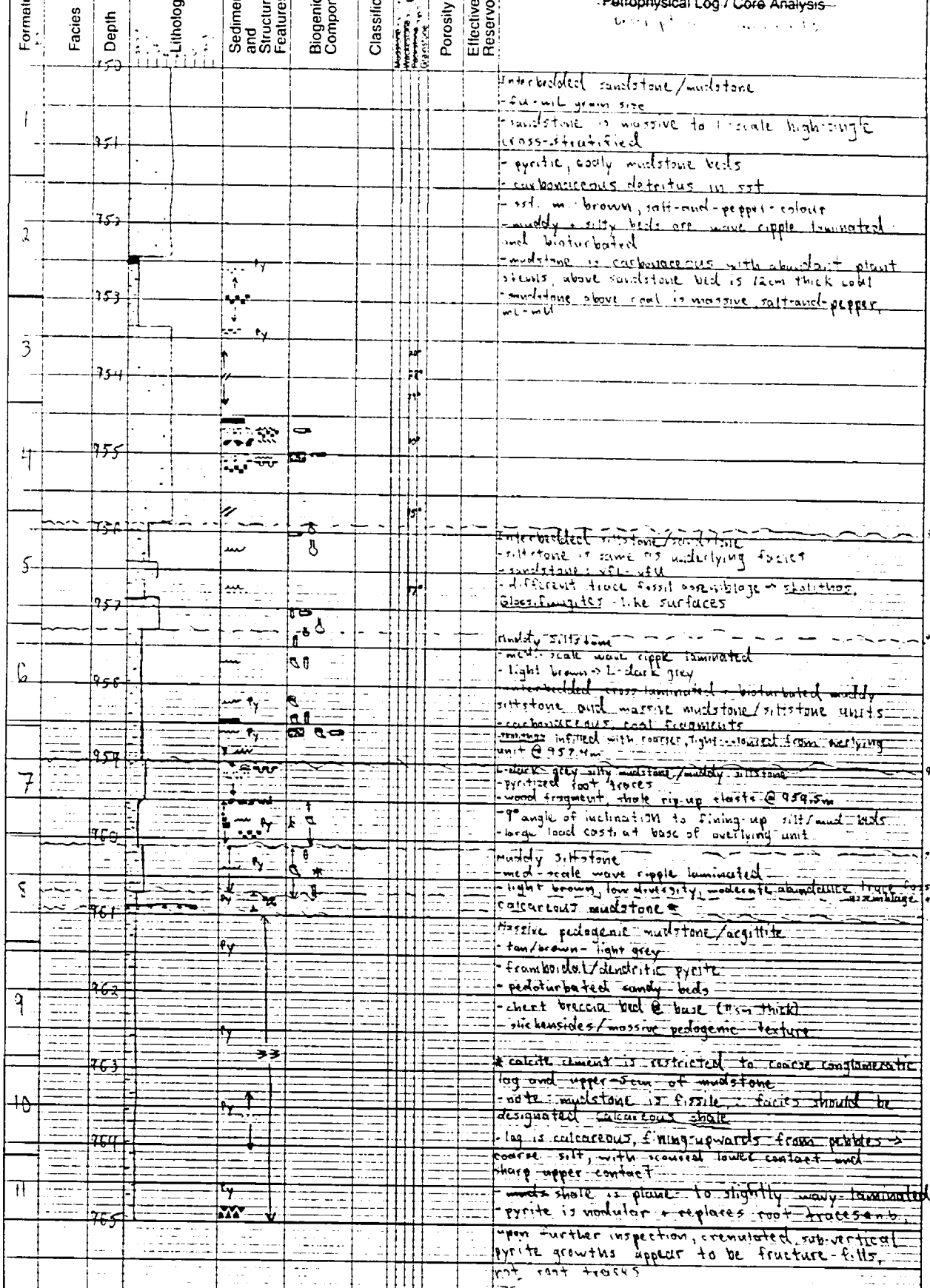

Appendix 2

Petrology

Well ID	Depth (m)	Approximate % of framework grains													Rock name	Facies
		quartz	chert	rock fragments	feldspar	bioclasts	muscovite	biotite	epidote	chlorite	calcite	chalcedony	siderite	pyrite		
03/06-19-019-09W4/0	1004.0	35	45	3	7		tr		tr	tr			10		subarkose	lithic ch.
03/06-19-019-09W4/0	1006.9	23	25	2	tr		tr						48	2	mudstone conglomerate	F5
00/07-27-019-09W4/0	1014.3	90	5	3	tr		1		1			tr			quartzarenite	F3
00/16-30-019-09W4/0	1018.5	45	45	10	tr										sublitharenite	lithic ch.
00/16-30-019-09W4/0	1027.8	75	22	3			tr	tr				tr			quartzarenite	Ost Lime
00/01-34-019-09W4/0	1007.8	85	14		tr		tr		1						quartzarenite	F4
00/06-34-019-09W4/0	993.0	35	30	15	20		tr	tr	tr			tr			lithic subarkose	lithic ch.
00/06-34-019-09W4/0	998.2	37	43	13		7	tr		tr						chert conglomerate	F5
00/12-02-020-09W4/0	974.1	35	45	8	12		tr			tr					subarkose	lithic ch.
00/12-02-020-09W4/0	976.5	70	27	3								tr			quartzarenite	F4
00/12-02-020-09W4/0	978.7	92	8		tr			tr	tr						quartzarenite	F4
00/04-23-020-09W4/0	956.1	30	25	17	28		tr								lithic arkose	lithic ch.
00/04-23-020-09W4/0	965.2	30	53	12		4						1			chert conglomerate	F5
00/06-23-020-09W4/0	954.8	35	35	22	8		tr			tr					sublitharenite	F6
00/10-23-020-09W4/0	940.4	50	30	15	4		tr			tr	1				sublitharenite	lithic ch.
00/10-23-020-09W4/0	950.5	50	30	10	7		3		tr	tr					sublitharenite	lithic ch.
00/10-23-020-09W4/0	953.0	80	15	4					1						quartzarenite	F3
02/10-23-020-09W4/0	948.0	36	34	25	tr	5			tr						chert conglomerate	F5
02/10-23-020-09W4/0	949.9	75	21	3	1		tr								quartzarenite	F3
00/13-23-020-09W4/0	941.9	50	30	13	7		tr								sublitharenite	lithic ch.
02/16-23-020-09W4/0	946.5	70	30		tr				tr						quartzarenite	F4
02/16-23-020-09W4/0	948.1	60	40				tr		tr	tr					siltstone	F4
02/16-23-020-09W4/0	948.8	70	15	5	10							tr			siltstone	F4
02/16-23-020-09W4/0	949.3	80	15	4					1						quartzarenite	F4
02/16-27-020-09W4/0	956.7	42	42	15	1		tr	tr		tr					sublitharenite	lithic ch.
04/06-03-021-09W4/0	948.4	35	45	15	5		tr								sublitharenite	lithic ch.
04/06-03-021-09W4/0	950.9	67	23	10					tr			tr			sublitharenite	F3
04/06-03-021-09W4/0	954.7	26	39	30		5						tr			lithic conglomerate	F5
04/06-03-021-09W4/0	960.5	100	tr							tr					siltstone	F1

Table A2.1: Summary of petrographical analysis. Ost Lime: Ostracode Limestone, F1: interstratified fine siltstone and silty mudstone, F3: medium-scale cross-stratified sandstone, F4: interstratified massive sandstone and contorted muddy siltstone, F5: chert pebble conglomerate, F6: interstratified sandstone, siltstone, and mudstone, lithic ch.: Upper Mannville lithic channel sandstone.

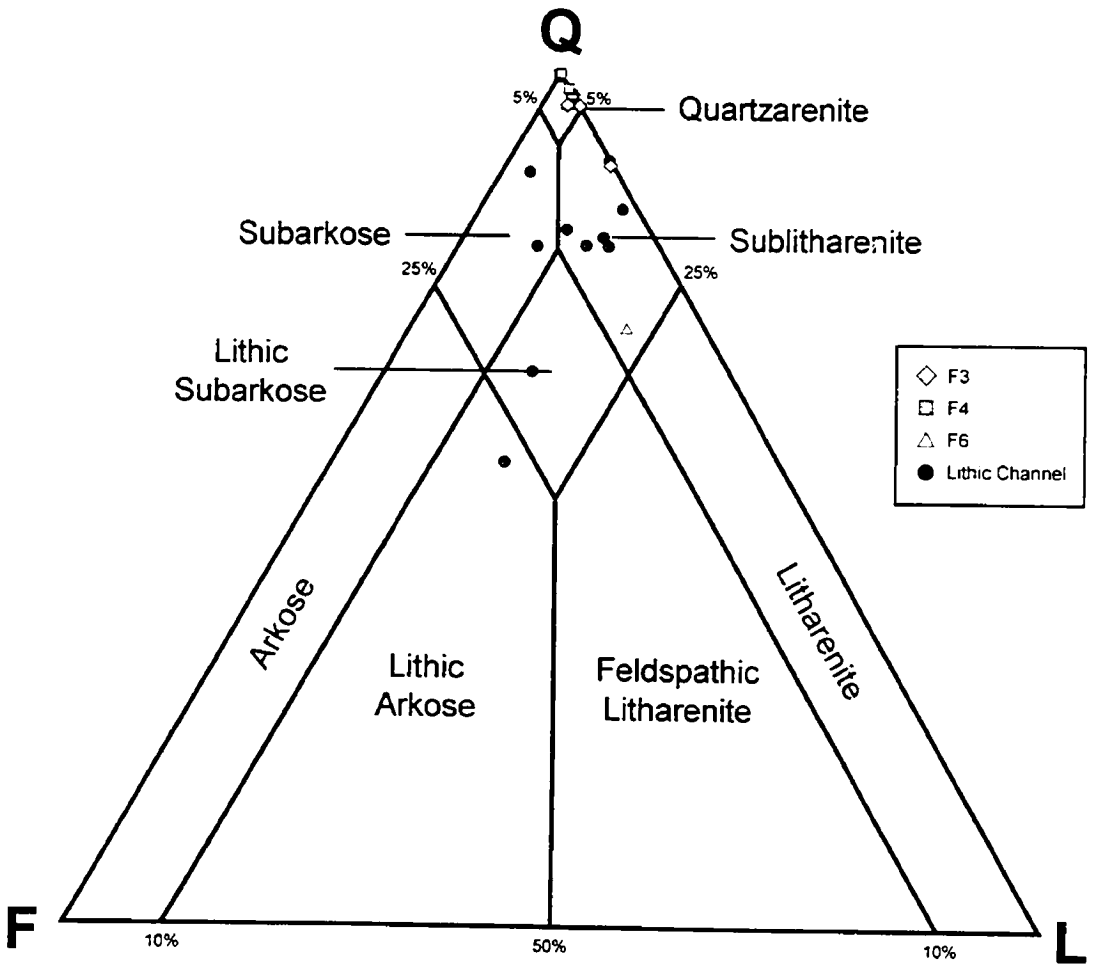

Figure A2.1: QFL ternary diagram. The Q pole comprises quartz, quartzite and chert, the F pole includes potassium feldspar and plagioclase, and the L pole comprises lithic rock fragments including granite and gneiss (modified from McBride, 1963).

Plate A2.1: Thin section photomicrograph of medium-scale cross-stratified fine-grained quartzarenite (F3). Sample is composed of quartz (Q), chert (C), lithic rock fragments (L), and trace muscovite (M). Note the curved muscovite grain, indicative of post-depositional compaction. Well 02/10-23-020-09W4/0, 949.9 m. Scale bar is 0.5 mm.

a) Plane-polarized light.

b) Cross-polarized light.

a)

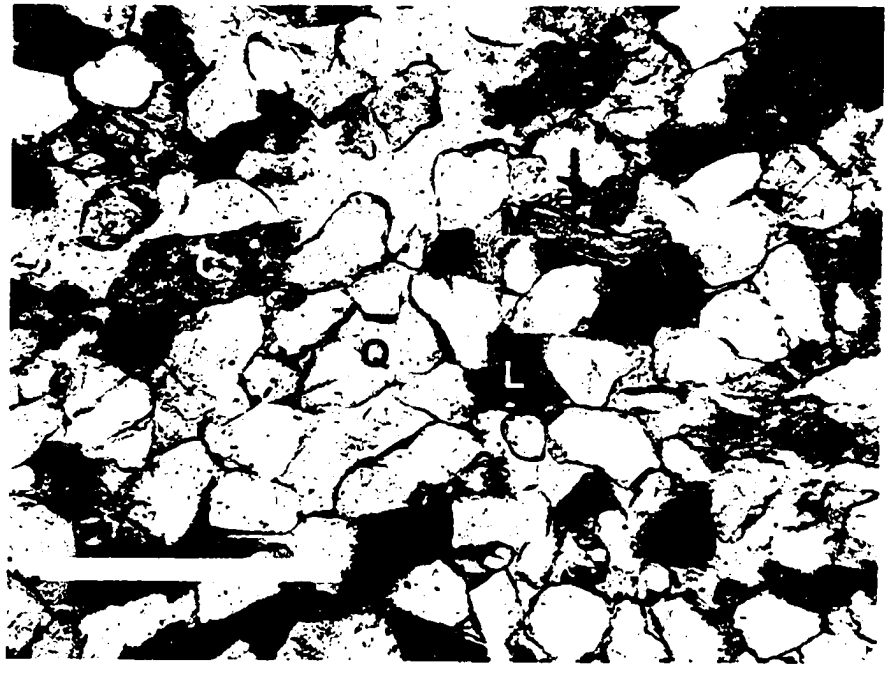

b)

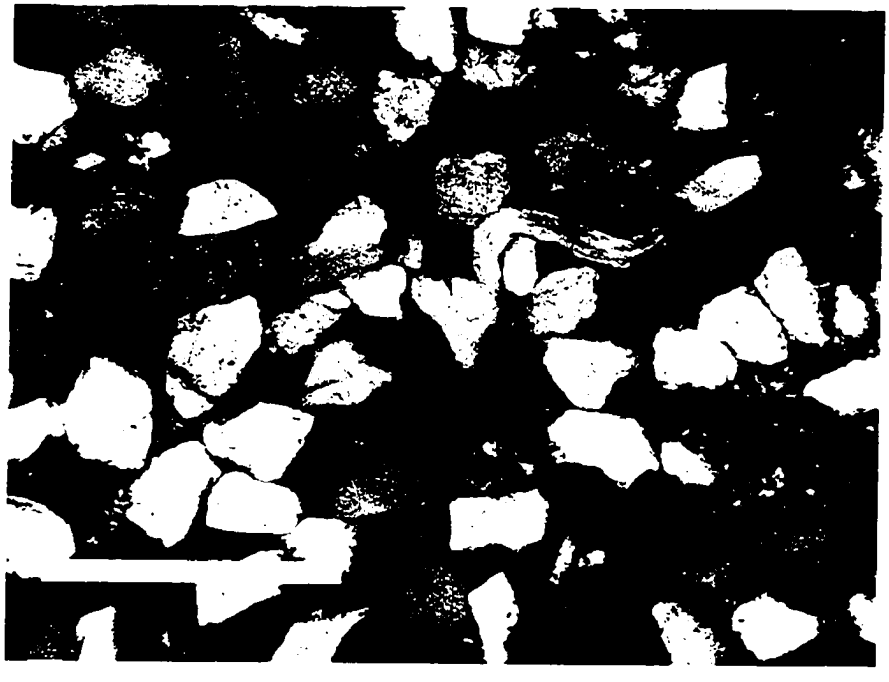

Plate A2.2: Thin section photomicrograph of massive medium-grained quartzarenite (F4). Sample is composed almost exclusively of quartz (Q) and chert (C). Note authigenic syntaxial overgrowth around centre quartz grain. Well 00/12-02-020-09W4/0, 3203.7'. Scale bar is 0.5 mm.

a) Plane-polarized light.

b) Cross-polarized light.

a)

b)

Plate A2.3: Thin section photomicrograph of matrix-supported chert pebble conglomerate (F5). Framework clasts are composed of chert (C), lithic rock fragments (L), and bioclasts (B). Matrix is composed mainly of quartz (Q) and chert. Well 00/06-34-019-09W4/0, 3275'. Scale bar is 1.0 mm.

a) Plane-polarized light.

b) Cross-polarized light.

a)

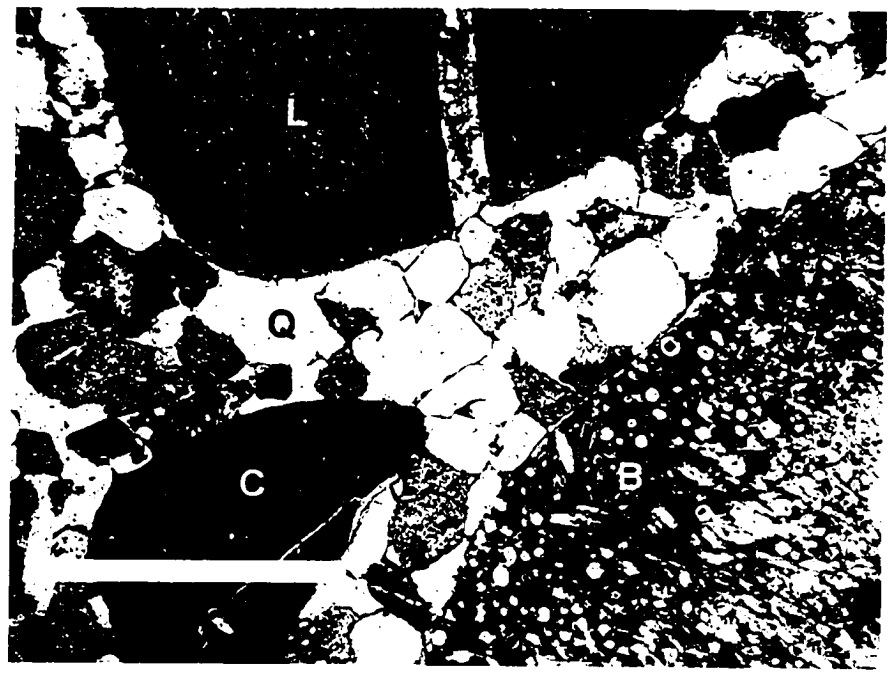

b)

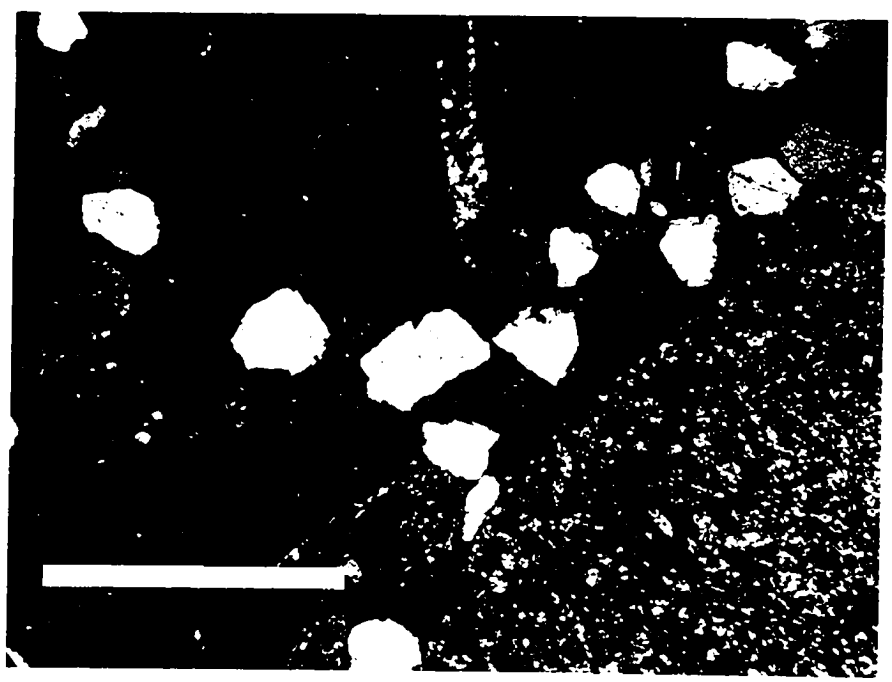

Plate A2.4: Thin section photomicrograph of Upper Mannville lithic channel sublitharenite. Framework clasts are mainly quartz (Q) and chert (C) with minor epidote (E). Note the abundance of authigenic pore-filling cement, derived from the breakdown of unstable lithic fragments and feldspar grains. Well 00/10-23-020-09W4/0, 950.5 m. Scale bar is 0.5 mm.

a) Plane-polarized light.

b) Cross-polarized light.

a)

b)

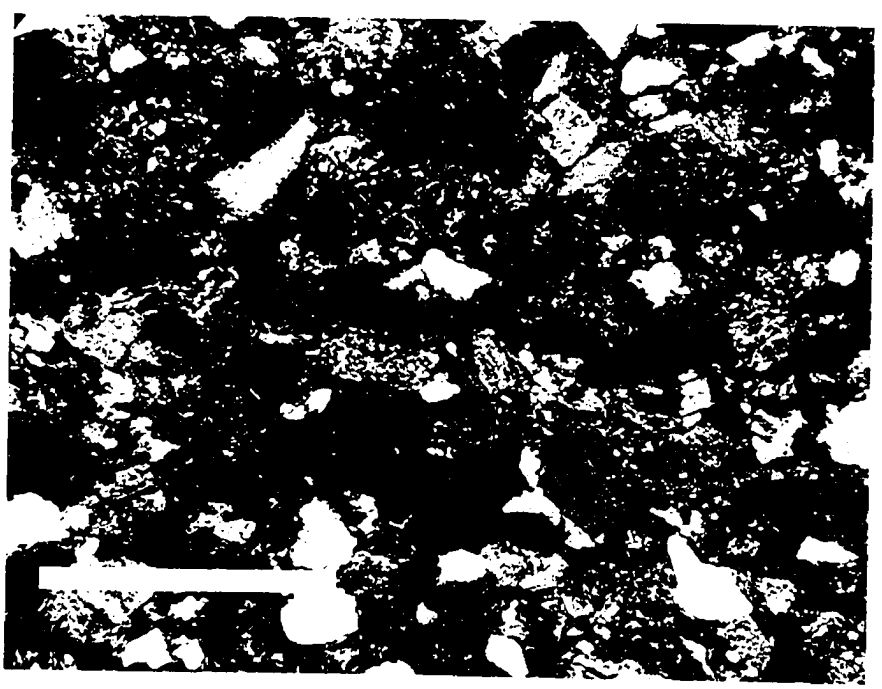

Appendix 3

Palynology

Table A3.1: Relative abundances of taxa based on primary counts of between 200-300 specimens and qualitative occurrence records from mudstone and shale samples of the Glauconitic Sandstone. The qualitative R (rare, 1-2 specimens), S (scarce, 3-5 specimens), C (common, 6-9 specimens), and A (abundant, >10 specimens) indicates the number of specimens seen outside of the area of the primary count. It is estimated that the slides scanned to arrive at the qualitative estimate of the relative abundance contained between at least 20,000-40,000 specimens. Analysis courtesy of Dr. A.R. Sweet, Geological Survey of Canada. BQ: Basal Quartz, Ost Lime: Ostracode Limestone, F1: interstratified fine siltstone and silty mudstone, F7: carbonaceous mudstone and coal, lithic ch.: Upper Mannville lithic channel sandstone.

Well ID	Depth (m)	*Aequitriradites* spp.	*Appendicisporites potomacensis*	*A. problematicus*	*Arecellites* sp.	*Cicatricosisporites australiensis*	*C. hughesi*	*C. mohrioides*	*Cicatricosisporites* spp.	*Concavissimisporites punctatus*	*Coronatispora valdensis*	*Cyathidites/Deltoidospora* spp.	*Echinatisporis* sp.	*Foraminisporis asymmetricus*	*F. dailyi*	*F. wonthaggiensis*	*Gleicheniidites senonicus*	*Impardecispora apiverrucata*	*I. tribotrys*	*I. trioreticulosa*	*Kraeuselisporites hastilobatus*	*Klukisporites granulatus*
		Selected lycopod, fern and bryophyte spores																				
03/06-19-019-09-W4/0	1003.0				R							10			R		45			2?		
03/06-19-019-09-W4/0	1011.0		R			R	R	R		R	R	10	R	R	R		3					R
00/07-27-019-09-W4/0	1009.7	Effectively barren																				
00/07-27-019-09-W4/0	1010.0											R					S					
00/07-27-019-09-W4/0	1022.3	Effectively barren																				
00/16-30-019-09-W4/0	1027.8								2			8					2					
00/16-30-019-09-W4/0	1030.0	Effectively barren																				
00/01-34-019-09-W4/0	1004.6		C				R		3	R		7					1					
00/01-34-019-09-W4/0	1009.0			R		11	1		12			41					12					
00/01-34-019-09-W4/0	1011.7	R	R			1	R			S		10		1						S		S
00/01-34-019-09-W4/0	1014.6					2	R		2			2					2					
00/01-34-019-09-W4/0	1015.8								1			17							99			
00/10-23-020-09-W4/0	952.3					5	1			R		18					2					
02/10-23-020-09-W4/0	957.3											1	R				1					
02/10-23-020-09-W4/0	958.2	No records																				
02/10-23-020-09-W4/0	959.5	Effectively barren																				
02/16-23-020-09-W4/0	953.3	Effectively barren																				
02/16-23-020-09-W4/0	959.5											R					R					
02/16-27-020-09-W4/0	958.6	S		S		2				R		2	R				2	R		R	C	S
02/16-27-020-09-W4/0	959.7	S		R		2	R			S			R	R	R	R						R

Well ID	Depth (m)	*K. pseudoreticulatus*	*K. areolatus*	*Laevigatosporites* sp.	*Leptolepidites proxigranulatus*	*Leptolepidites* sp.	*Lycopodiumsporites* spp.	*Matonisporites* sp.	*Microreticulatisporites uniformis*	*Osmundacidites* sp.	*Pilifera* sp.	*Plicatella* spp.	*Pilosisporites trichopapillosus*	*Psilatriletes radiatus*	*Reticulatasporites duplexinous*	*Taurocusporites* sp.	*Tigrisporites reticulatus*	*Tigrisporites scurrandus*	*Trilobosporites* sp. cf. *T. canadensis*	*Trilobosporites humilis*	*Trilobosporites trireticulosus*	*Zlivisporis* spp.
03/06-19-019-09-W4/0	1003.0			7							R											
03/06-19-019-09-W4/0	1011.0			2			R		R				R	R						R	r	R
00/07-27-019-09-W4/0	1009.7	Effectively barren																				
00/07-27-019-09-W4/0	1010.0																					
00/07-27-019-09-W4/0	1022.3	Effectively barren																				
00/16-30-019-09-W4/0	1027.8																					
00/16-30-019-09-W4/0	1030.0	Effectively barren																				
00/01-34-019-09-W4/0	1004.6			2																		
00/01-34-019-09-W4/0	1009.0	R		5					R	1						R	R					
00/01-34-019-09-W4/0	1011.7			4		R	1	R				R							R			1
00/01-34-019-09-W4/0	1014.6				R			1	1	1		R					R	R				
00/01-34-019-09-W4/0	1015.8			3						1												
00/10-23-020-09-W4/0	952.3								2													
02/10-23-020-09-W4/0	957.3						1										R					
02/10-23-020-09-W4/0	958.2	No records																				
02/10-23-020-09-W4/0	959.5	Effectively barren																				
02/16-23-020-09-W4/0	953.3	Effectively barren																				
02/16-23-020-09-W4/0	959.5			R																		
02/16-27-020-09-W4/0	958.6		R	1						2			C		C	R					S	
02/16-27-020-09-W4/0	959.7					R			R			R	R						R			

Well ID	Depth (m)	Marine-Algae-Nonmarine						Gymnosperm pollen										Angiosperms			Total count	Facies
		acritarchs	dinoflagellates	*Gonyaulacysta*	*Exesipollenites tumulus*	*Januaspontes spiniferus*	*Schizosporis reticulatus*	*Araucariacites* sp.	bisaccate pollen	*Callialasporites dampieri*	*C. trilobatus*	*Cerebropollenites mesozoicus*	*Classopollis classoides*	*Eucommiidites minor*	*Scadopitysporites* sp.	T/C/T	*Vitreisporites pallidus*	*Clavatipollenites hughesii*	*Retimonocolpites* sp.	*Stellatopollis* sp.		
03/06-19-019-09-W4/0	1003.0								43	2?		4	32			5	1				85	F7
03/06-19-019-09-W4/0	1011.0			C	R	R	R	4	12	R	R	R	4	C	S	228		S			248	F1
00/07-27-019-09-W4/0	1009.7	Effectively barren																				F7
00/07-27-019-09-W4/0	1010.0								R				R									F7
00/07-27-019-09-W4/0	1022.3	Effectively barren																				BQ
00/16-30-019-09-W4/0	1027.8	R							113		R	2	26			66					207	Ost Lime
00/16-30-019-09-W4/0	1030.0	Effectively barren																				BQ
00/01-34-019-09-W4/0	1004.6								11					R		206	1				218	F7
00/01-34-019-09-W4/0	1009.0								14				9		R	120	2		R		145	F1
00/01-34-019-09-W4/0	1011.7					R		19	36			R	3		2	143		R		R	203	F1
00/01-34-019-09-W4/0	1014.6		R	R	R		R		118			1	71		1	82					273	Ost Lime
00/01-34-019-09-W4/0	1015.8								69			1	2		3	27		1		R	103	BQ
00/10-23-020-09-W4/0	952.3				1.0		r		24			1	4		2	184		1		R?	217	F7
02/10-23-020-09-W4/0	957.3		R?					5	45			1	20		1	150					222	Ost Lime
02/10-23-020-09-W4/0	958.2	No records																				BQ
02/10-23-020-09-W4/0	959.5	Effectively barren																				BQ
02/16-23-020-09-W4/0	953.3	Effectively barren																				Ost Lime
02/16-23-020-09-W4/0	959.5												R									BQ
02/16-27-020-09-W4/0	958.6				R	R		1	12			R	1	R		207		R			221	lithic ch.
02/16-27-020-09-W4/0	959.7					R	S		14						3	210		1		R?	228	F7